

# **The role of the intramembrane protease SPPL2a and its substrate CD74 in development and function of dendritic cells**

Dissertation in partial fulfilment of the requirement  
for the degree “Dr. rer. nat.” at the Faculty of Mathematics  
and Natural Sciences at Kiel University

submitted by  
**Ann-Christine Gradtke**

Kiel, May 2018



Referee: Prof. Dr. Paul Saftig

Co-referee: Prof. Dr. Thomas Roeder

Date of oral presentation: 12.07.2018

Approved for publication: 12.07.2018

The dean



## Table of Contents

<b>Abbreviations</b>	<b>IX</b>
<b>1 Introduction</b>	<b>1</b>
1.1 Regulated intramembrane proteolysis (RIP)	1
1.1.1 Intramembrane–cleaving proteases (I–CLiPs)	2
1.1.2 SPPL2 proteases	5
1.1.3 <i>In vitro</i> substrates of SPPL2 proteases	6
1.2 The role of the SPPL2a substrate CD74 in the immune system	7
1.3 The SPPL2 knockout mouse models	8
1.4 Differentiation and function of DCs in mice	10
1.4.1 <i>In vivo</i> and <i>in vitro</i> differentiation of DCs and marker for murine DCs	10
1.4.2 Pattern–recognition receptor (PRR) families	12
1.4.2.1 C–type lectin receptors (CTLRs)	12
1.4.2.2 Toll–like receptors (TLRs)	15
1.4.3 T cell induction by DCs	15
1.4.4 Modulations of immune responses by cytokines	17
1.5 The role of SPPL2a in human patients	18
1.5.1 Mendelian susceptibility to mycobacterial disease in SPPL2a–deficient patients	19
1.6 Aim of the study	19
<b>2 Material &amp; Methods</b>	<b>21</b>
2.1 Material	21
2.1.1 Chemicals	21
2.1.2 Animals	21
2.1.3 Antibodies	21
2.1.4 Pattern recognition receptor ligands	24
2.2 Methods	25
2.2.1 Cell biological methods	25
2.2.1.1 Analysis of DC populations in mice	25
2.2.1.2 Generation of bone marrow–derived immune cells	26
2.2.1.3 Co–culture of BMDCs with <i>Mycobacterium bovis</i> Bacille Calmette–Guérin	28
2.2.1.4 Stimulation of immune cells with different PRR ligands	28

## TABLE OF CONTENTS

---

2.2.1.5	Indirect immunofluorescence . . . . .	29
2.2.1.6	Flow cytometric analysis of BMDCs . . . . .	30
2.2.2	Biochemical methods . . . . .	30
2.2.2.1	Preparation of protein extracts . . . . .	30
2.2.2.2	Determination of protein concentration . . . . .	32
2.2.2.3	Biotinylation of BMDC surface proteins . . . . .	32
2.2.2.4	Glycine–SDS PAGE . . . . .	33
2.2.2.5	Tricine–SDS PAGE . . . . .	34
2.2.2.6	Western Blotting . . . . .	35
2.2.2.7	Immunodetection . . . . .	36
2.2.2.8	Measurement of secreted cytokines in conditioned media by ELISA . . . . .	36
2.2.2.9	Lactate dehydrogenase cytotoxicity assay . . . . .	38
2.2.3	Molecular biology methods . . . . .	38
2.2.3.1	Genotyping of <i>SPPL2a</i> <sup>-/-</sup> and <i>CD74</i> <sup>-/-</sup> mice . . . . .	38
2.2.3.2	Agarose gel electrophoresis . . . . .	39
2.2.3.3	RNA isolation . . . . .	40
2.2.3.4	Complementary DNA synthesis . . . . .	40
2.2.3.5	Expression analysis by quantitative real–time PCR . . . . .	40
<b>3</b>	<b>Results</b>	<b>43</b>
3.1	Absence of SPPL2a leads to reduced DC numbers <i>in vivo</i> , but not <i>in vitro</i> . . . . .	43
3.1.1	Conventional DC2 population is reduced in spleens of <i>SPPL2a</i> <sup>-/-</sup> mice . . . . .	43
3.1.2	BMDCs as a model system for functional analysis . . . . .	44
3.1.3	Analysis of cell marker surface expression reveals comparable differentiation of <i>wt</i> and <i>SPPL2a</i> <sup>-/-</sup> BMDCs . . . . .	45
3.2	Functional analysis of <i>in vitro</i> differentiated DCs in response to pattern recognition receptor stimuli . . . . .	47
3.2.1	Altered response to Dectin–1 stimulation in <i>SPPL2a</i> <sup>-/-</sup> BMDCs . . . . .	47
3.2.2	Increased TLR response in the absence of SPPL2a . . . . .	49
3.3	Cytokine response towards mycobacteria in <i>SPPL2a</i> <sup>-/-</sup> immune cells . . . . .	51
3.3.1	Analysis of cytokine response of BMDCs to heat–killed <i>Mycobacterium tuberculosis</i> . . . . .	51
3.3.2	Alterations in IL-1 $\beta$ expression and release are direct effects of SPPL2a deficiency . . . . .	53
3.3.3	IL–12 cytokine release from <i>wt</i> and <i>SPPL2a</i> <sup>-/-</sup> BMDCs . . . . .	56
3.3.4	Analysis of BMDC cytokine responses upon BCG co–culture . . . . .	58

3.3.5	Macrophage responses to mycobacterial stimuli are not altered by SPPL2a deficiency . . . . .	61
3.4	CD74 protein abundance plays a major role in effects of SPPL2a knockout . . . .	62
3.4.1	Lower CD74 protein levels and NTF accumulation in BMDMs compared to BMDCs . . . . .	62
3.4.2	Cathepsin S knockout BMDCs show milder phenotype than <i>SPPL2a</i> <sup>-/-</sup> BMDCs . . . . .	63
3.4.3	Cytokine responses can be rescued by additional ablation of CD74 . . . . .	65
3.5	Altered receptor surface expression leads to differential cytokine response in <i>SPPL2a</i> <sup>-/-</sup> BMDCs . . . . .	67
3.5.1	Comparison of <i>wt</i> and <i>SPPL2a</i> <sup>-/-</sup> BMDC cytokine responses upon stimulation of different receptors . . . . .	67
3.5.2	Alterations of Dectin-1 receptor function and distribution in <i>SPPL2a</i> <sup>-/-</sup> BMDCs . . . . .	68
3.5.3	Increase of TLR4 surface levels and expression in <i>SPPL2a</i> <sup>-/-</sup> BMDCs . . . . .	73
<b>4</b>	<b>Discussion</b>	<b>75</b>
4.1	The CD74 NTF accumulation is causative for altered <i>SPPL2a</i> <sup>-/-</sup> DC development <i>in vivo</i> and <i>SPPL2a</i> <sup>-/-</sup> BMDC function <i>in vitro</i> . . . . .	76
4.2	Potential role of further <i>SPPL2a</i> <sup>-/-</sup> substrates in the <i>SPPL2a</i> <sup>-/-</sup> DC phenotype . . . . .	77
4.3	How could the CD74 NTF accumulation cause the observed DC phenotype? . . . . .	78
4.3.1	Possible CD74-dependent mechanisms for altered Dectin-1 and TLR4 surface levels . . . . .	81
4.4	The role of SPPL2a in DC development <i>in vivo</i> and differentiation <i>in vitro</i> . . . . .	83
4.4.1	Known factors in DC differentiation and homeostasis . . . . .	84
4.5	Can the altered Dectin-1 and TLR4 surface levels and Dectin-1 signalling explain cytokine differences between <i>wt</i> and <i>SPPL2a</i> <sup>-/-</sup> BMDCs? . . . . .	86
4.5.1	The impact of altered PRR levels on Mycobacteria detection . . . . .	89
4.6	The physiological relevance of SPPL2a deficiency in infections . . . . .	90
4.7	Outlook . . . . .	93
<b>5</b>	<b>Summary</b>	<b>95</b>
<b>6</b>	<b>Zusammenfassung</b>	<b>97</b>
	<b>References</b>	<b>99</b>

TABLE OF CONTENTS

---

<b>Supplement</b>	<b>XIII</b>
List of figures . . . . .	XIV
List of tables . . . . .	XV
List of publications . . . . .	XVII
Statutory Declarations . . . . .	XIX
Acknowledgements . . . . .	XXI
Scientific Career . . . . .	XXIII



## Abbreviations

2a	SPPL2a
ADAM	A Disintegrin And Metalloproteases
ANG	Angiotensin
APC	Allophycocyanin
APH-1	Anterior pharynx defective-1
APP	Amyloid precursor protein
APS	Ammonium persulfate
ASC	Apoptosis-associated speck-like protein containing a caspase recruitment domain
ATP	Adenosine triphosphate
BACE	$\beta$ -site Amyloid precursor protein cleaving enzyme
BCA	Bicinchoninic acid
BCG	<i>Mycobacterium bovis</i> Bacille Calmette-Guérin
Bcl10	B cell lymphoma/ leukemia 10
BCR	B cell receptor
BSA	Bovine serum albumin
Bst2	Bone marrow stromal antigen 2
BMDC	Bone marrow-derived dendritic cell
BMDM	Bone marrow-derived macrophage
CARD9	Caspase recruitment domain-containing protein 9
CatS	Cathepsin S
CCR9	C-C chemokine receptor type 9
CD	Cluster of differentiation
CD74	Cluster of differentiation CD74, invariant chain, li
cDC1 / 2	Conventional / myeloid / classical dendritic cell type 1 / 2
cDNA	Complementary DNA
CDP	Common dendritic cell progenitor
CHI3L1	Chitinase-3-like protein 1
CLN5	Ceroid-lipofuscinosis neuronal protein 5
CS	Cover slips
CTF	C-terminal fragment
CLIP	Class II-associated invariant chain peptide
CTL	Cytotoxic T cell
CTLD	C-type lectin domain
CTLR	C-type lectin receptor
CXCR4	C-X-C chemokine receptor type 4
CX3CR1	C-X3-C chemokine receptor type 1
DAMP	Danger-associated pattern
DAPI	4-,6-diamidino-2-phenylindole
DCAR	Dendritic cell activating immunoreceptor
DCIR	Dendritic cell immunoreceptor
DC	Dendritic cell
Dectin	Dendritic cell-associated C-type lectin
Dkk	Dickkopf
DKO	SPPL2a-CD74 double knockout
DMSO	Dimethyl sulfoxide
DNA	Deoxyribonucleic acid
dZym	Depleted Zymosan
EBI2	Epstein-Barr virus-induced gene 2
EDTA	Ethylene diamine tetra acetic acid
ELISA	Enzyme-linked immunosorbent assay
ENU	N-ethyl-N-nitrosourea
ER	Endoplasmic reticulum
ERAD	Endoplasmic reticulum-associated degradation
ERK	Extracellular signal-regulated kinase
ESCRT	Endosomal sorting complex required for transport

## ABBREVIATIONS

---

FACS	Fluorescence-activated cell sorting
FAM	Fluorescein amidite
FasL	First apoptosis signal ligand
FC	Flow cytometry
FcR $\gamma$	Fragment crystallizable receptor $\gamma$ chain
Fc $\gamma$ RI	Fragment crystallizable $\gamma$ receptor I
Fc $\epsilon$ RI	Fragment crystallizable $\epsilon$ receptor I
FCS	Fetal calf serum
FITC	Fluorescein isothiocyanate
FL	Full length
FLT3L	Fms like tyrosine kinase 3 ligand
FSC	Forward-scattered light
FVenv	Foamy virus envelope protein
Fw	forward
GAPDH	Glyceraldehyde 3-phosphate dehydrogenase
GM-CSF	Granulocyte-macrophage colony-stimulating factor
GM-CSFR	Granulocyte-macrophage colony-stimulating factor receptor
GOI	Gene of interest
h	Hour
HKMT	Heat-killed <i>Mycobacterium tuberculosis</i>
HPRT	Hypoxanthine-guanine phosphoribosyltransferase
HRP	Horseradish peroxidase
ICAM-1	Immune cell adhesion molecule-1
ICD	Intracellular domain
I-CLiP	Intramembrane-cleaving protease
IF	Immunofluorescence
IFN	Interferon
IL	Interleukin
IRF	Interferon regulatory factor
ITAM	Immunoreceptor tyrosine-based activation motif
ITIM	Immunoreceptor tyrosine-based inhibitory motif
Ko	Knockout
LAM	Lipoarabinomannan
LAMP-2	Lysosome-associated membrane protein 2
LDH	Lactate dehydrogenase
LIF	leukemia inhibitory factor
LPS	Lipopolysaccharides
Ly6C	Lymphocyte antigen 6C
MIIC	MHC class II compartment
MACS	Magnetic activated cell sorting
MALT-1	Mucosa-associated lymphoid tissue lymphoma translocation protein 1
MCP	Monocyte chemoattractant protein
M-CSF	Macrophage colony-stimulating factor
MDP	Macrophage and dendritic cell progenitor
MerTK	Mer receptor tyrosine kinase
MFI	Mean fluorescence intensities
MHCI / MHCII	Major histocompatibility complex I / II
MIF	Macrophage migration inhibitory factor
MIP	Macrophage inflammatory protein
Min	Minute
Mincle	Macrophage-inducible C-type lectin
MMP	Matrix metalloproteinase
moDC	monocyte-derived DC
MOI	Multiplicity of infection
MPO	Myeloperoxidase
MR	Mannose receptor
mRNA	Messenger RNA
MSMD	Mendelian susceptibility to mycobacterial disease
MVB	Multivesicular body

M $\Phi$	Macrophage
NFAT	Nuclear factor of activated T cells
NF $\kappa$ B	Nuclear factor 'kappa-light-chain-enhancer' of activated B cells
NK	Natural killer cells
NLR	Nucleotide-binding oligomerization domain-like receptor
NLRP3	Nucleotide-binding domain, leucine-rich-containing family, pyrin domain-containing-3
NTF	N-terminal fragment
OADC	Oleic albumin dextrose catalase
OD	Optical density
OPN	Osteopontin
PAGE	Polyacrylamide gel electrophoresis
PAMP	Pathogen-associated pattern
PARL	Presenilins-associated rhomboid-like protein, mitochondrial
PBS	Phosphate buffered saline
PCR	Polymerase chain reaction
PCSK9	Proprotein convertase subtilisin/kexin type 9
pDC	Plasmacytoid DC
PEN-2	Presenilin enhancer-2
PFA	Paraformaldehyde
PKC	Protein kinase C
PLC $\gamma$	Phospholipase C $\gamma$
pre-cDC	Conventional dendritic cell precursor
PRR	Pattern recognition receptor
PS	Presenilin
PTX	Pentraxin
qRT-PCR	Quantitative real-time PCR
Raf-1	Rapidly accelerated fibrosarcoma-1
Rv	Reverse
RHBDL	Rhomboid-like
RNATES	Regulated on activation, normal T cell expressed and secreted
RIP	Regulated intramembrane proteolysis
RNA	Ribonucleic acid
ROS	Reactive oxygen species
RT	Room temperature
S1P	Site 1 protease
S2P	Site 2 protease
Sca-1	Stem cells antigen-1
SD	Standard deviation
SDH	Succinate dehydrogenase
SDS	Sodium dodecyl sulfate
SFRP2	Secreted frizzled-related protein 2
SH2	Src-homology domain 2
SHP	Src-homology domain 2-containing cytoplasmic tyrosine phosphatase
SiglecH	Sialic acid binding Ig-like lectin H
SIRP $\alpha$	Signal regulatory protein $\alpha$
SPP	Signal peptide peptidase
SPPL	Signal peptide peptidase-like
Sra1	Scavenger receptor 1
SREBP	Sterol-regulatory element-binding proteins
SSC	Side-scattered light
Syk	Spleen tyrosine kinase
T1/ T2	Transitional 1/ transitional 2
TACE	Tumour necrosis factor $\alpha$ converting enzyme
TAF $_{II}$ 105	Transcription initiation factor TFIID 105
TARC	Thymus- and activation-regulated chemokine
TBS	Tris buffered saline
TBS-T	Tris buffered saline with 0.1% Tween 20
TCR	T cell receptor
TDB	Trehalose-6,6-dibehenate

## ABBREVIATIONS

---

TDM	Trehalose–6,6–dimycolate, cord factor
TEMED	N, N, N', N'–tetramethylethylenediamine
T <sub>H</sub> 1 / 2 / 17	T helper cell type 1 / 2 / 17
TGF $\beta$	Transforming growth factor $\beta$
TLR	Toll–like receptor
TMB	3,3',5,5'–Tetramethylbenzidin
TMD	Transmembrane domain
TNF $\alpha$	Tumour necrosis factor $\alpha$
T <sub>reg</sub>	Regulatory T cell
TRIS	Tris(hydroxymethyl)–Aminomethan
WB	Western Blotting
Wt	Wild type
XCR1	X–C Motif Chemokine Receptor 1

# 1 Introduction

## 1.1 Regulated intramembrane proteolysis (RIP)

Proteolysis is a post-translational modification. The enzymatic hydrolysis of peptide bonds is irreversible. It plays a role in the regulation of cellular processes as for example in transcription and cell signalling, but it is also involved in degradation of proteins. Most proteases cleave in an aqueous environment. A subgroup of proteases is specialised in cleaving substrates even within the hydrophobic bilayer of biological membranes. These enzymes are called intramembrane-cleaving proteases (I-CLiPs; Wolfe *et al.*, 1999).

I-CLiPs are involved in a process referred to as regulated intramembrane proteolysis (RIP), which describes sequential cleavage of single pass transmembrane proteins. Substrates of RIP are type I or type II integral proteins, which are classified by their orientation within the membrane. Type I orientated proteins harbour their C-terminus within the cytosol, while type II orientated proteins show an opposite topology. Apart from releasing proteins from the membrane, RIP is also involved in regulation of cellular functions.

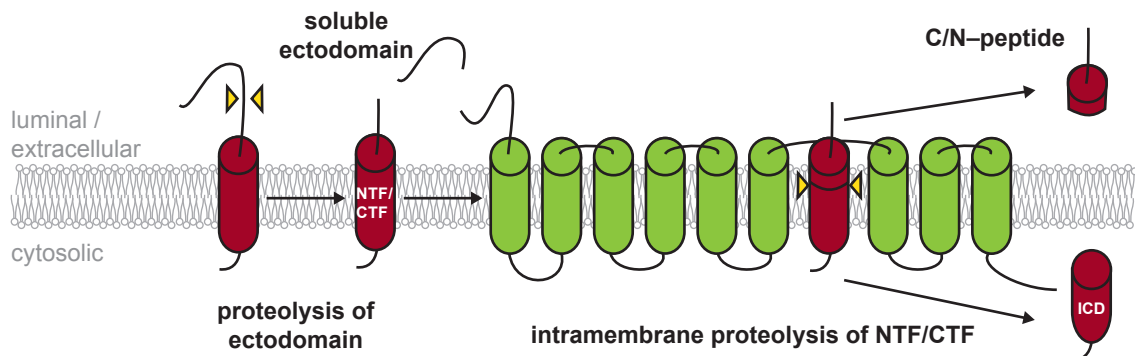


**Figure 1: Scheme of regulated intramembrane proteolysis.** A membrane bound substrate is shortened by regulated ectodomain shedding. The remaining N- or C-terminal fragment (NTF/CTF) undergoes intramembrane proteolysis. This leads to the release of a C- or N-peptide, respectively. An intracellular domain (ICD) is released to the cytoplasm and may function as transcriptional regulator, signalling molecule or is further degraded.

The process itself works as follows (see figure 1). First, a transmembrane substrate is cleaved close to the membrane by a protease, releasing the ectodomain. At the plasma membrane, the proteolysis is called shedding and releases the soluble ectodomain into the extracellular space. The proteolysis of the ectodomain is tightly regulated and performed for example by family members of the A Disintegrin And Metalloproteases (ADAMs), matrix metallo proteases (MMPs),  $\beta$ -site APP cleaving enzymes (BACEs), neutrophil-derived proteases or cysteine proteases (Lal and Caplan 2011, McCarthy *et al.*, 2017, Becker-Herman *et al.*, 2005). After ectodomain shedding, the remaining N-terminal (type II integral protein) or C-terminal (type I

integral protein) fragment (NTF/CTF) is cleaved within the membrane by an I-CLiP (Wolfe *et al.*, 1999). A luminal C/N-peptide and an intracellular domain (ICD) is thereby released from the membrane. The ICD can regulate transcription, cell signalling or is further degraded (McCarthy *et al.*, 2017).

### 1.1.1 Intramembrane-cleaving proteases (I-CLiPs)

Proteases can be defined by their catalytic centres. According to this classification, I-CLiPs of four different families are described so far, namely, metallo proteases, serine proteases, aspartyl proteases and glutamate proteases (McCarthy *et al.*, 2017). I-CLiPs are not only involved in the RIP process, but can also cleave transmembrane proteins which harbour a short ectodomain, such as tail-anchored proteins (Boname *et al.*, 2014, Bergbold and Lemberg 2013, Laurent *et al.*, 2015). Furthermore, it was shown that also a type III transmembrane protein, a protein with two transmembrane domains (TMDs) harbouring N- and C-terminus within the cytosol, can be a direct substrate for intramembrane cleavage (Voss *et al.*, 2012). An overview of the I-CLiP families is shown in table 2 and figure 2.

**Table 2: Overview of intramembrane cleaving protease families.**

Signal peptide peptidase (SPP); SPP like (SPPL); transmembrane domain (TMD).

Modified from Weihofen and Martoglio 2003, Beel and Sanders 2008 and Mentrup *et al.*, 2017a.

Protease family	I-CLiP	Number of TMD	Catalytic motif	Essential co-factors	Substrate topology
Metallo-proteases	Site 2 protease	6	HExxH (TMD 2) LDG (TMD 4)	No	Type II
Serine proteases	Rhomboid-like	7	GxSG (TMD 4) H (TMD 6)	No	Type I
Glutamate protease	Ras converting enzyme 1	8	E (TMD 4) H (TMD 5) HxxxN (TMD 7)	No	Type II
Aspartyl proteases	Presenilin-1/2	9	YD (TMD 6) GxGD (TMD 7)	APH-1a/b Nicastrin PEN2	Type I
	SPP	9	YD (TMD 6) GxGD (TMD 7)	No	Type II tail anchored
	SPPL2a/b/c	9	F/YD (TMD 6) GxGD (TMD 7)	No	Type II
	SPPL3	9	YD (TMD 6) GxGD (TMD 7)	No	Type II Type III

The process of intramembrane cleavage was first linked to the sterol-regulatory element-binding proteins (SREBPs) SREBP-1 and SREBP-2 (Sakai *et al.*, 1996). The responsible I-CLiP was identified one year later as the golgi residual zinc metalloprotease site-2 protease (S2P; Rawson *et al.*, 1997, Rawson 2013). The type III transmembrane protein SREBP-2 is first cleaved

within the loop between the two TMDs by the site-1 protease (S1P). The resulting fragment with the type II orientated TMD is then proteolysed by S2P (Rawson 2013). The released SREBP-2 fragment regulates expression of genes involved in lipid metabolism (Sakai *et al.*, 1996). Proteolysis of S2P substrates is regulated by protein trafficking. Under steady-state conditions substrates reside within the endoplasmic reticulum (ER), but re-localise to the golgi apparatus, where the protease S1P and S2P are localised, in a regulatory manner (Rawson 2013).

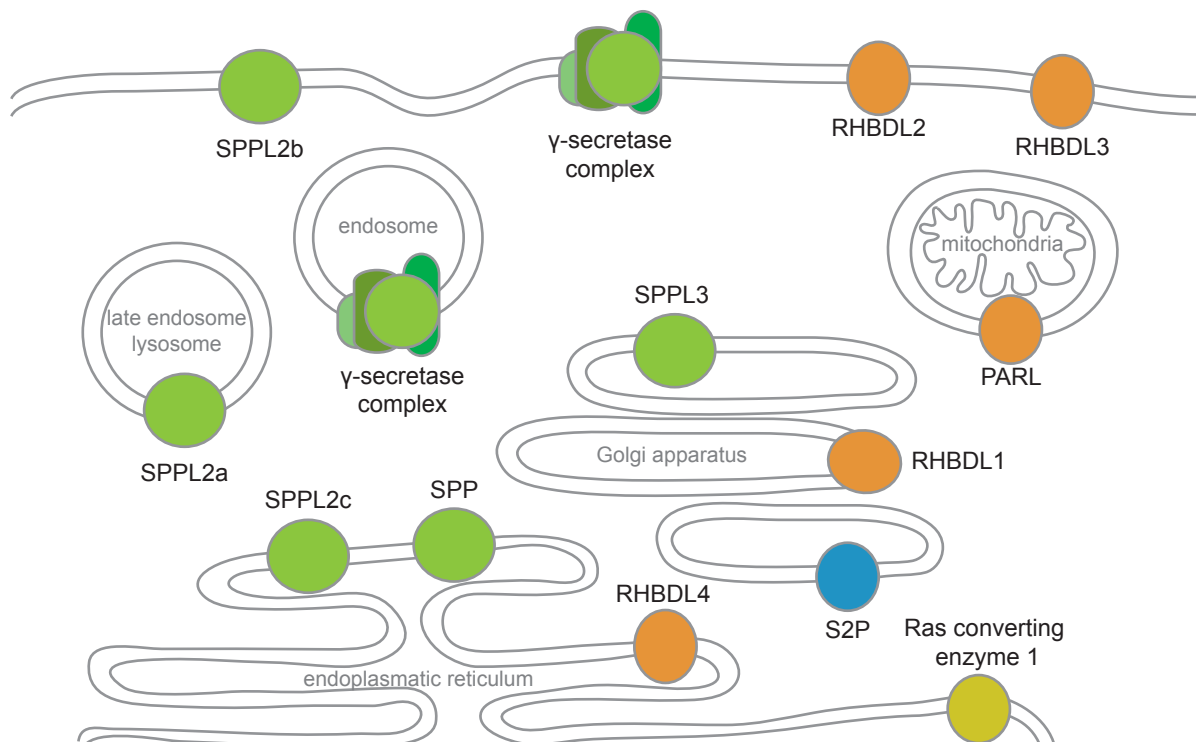


**Figure 2: Subcellular localisation of I-CLiPs.** Schematic overview of subcellular localisation of rhomboid-like (RHBDL) serine proteases (orange) including presenilins-associated rhomboid-like protein, mitochondrial (PARL), metallo protease site-2 protease (S2P; blue), glutamate proteases (yellow) and aspartyl proteases (green) of the signal peptide peptidase (SPP) / SPP-like (SPPL) family and presenilins within  $\gamma$ -secretase complex. Adapted from Urban 2016.

The serine protease family of rhomboids was first described in *Drosophila melanogaster*. There, rhomboid-1 cleaves spitz, the ligand for the epidermal growth factor receptor. The ablation of the protease in *Drosophila melanogaster* drives abnormal rhomboid-shaped head skeleton and led to the name of the protease family. Based on sequence homology, Rhomboid-like (RHBDL) proteases were discovered in all kingdoms of life, also in mammals. Members are localised to the ER, golgi, mitochondria and plasma membrane (Freeman 2008). Substrates of Rhomboid-like proteases are type I orientated. Since the family members are localised within the cell in different compartments, they have a diverse substrate spectrum. For example, the plasma membrane localised mammalian RHBDL2 releases the epidermal growth factor and is involved in growth regulation (Adrain *et al.*, 2011).

The most recently described family of I-CLiPs is formed by a glutamate protease called ras converting enzyme 1 (Manolaridis *et al.*, 2013). The protease is conserved in pro- and eukaryotes. In eukaryotic organisms it localises to the ER and its prenylated type II orientated substrates are involved in cell signalling processes (Hampton *et al.*, 2018).

Presenilins were the first members discovered in the aspartyl protease family. The conserved catalytic center between TMD six and seven is formed by a YD - GxGD motif (Steiner *et al.*, 2000, Yamasaki *et al.*, 2006). Based on sequence homology to the presenilins and conservation of the catalytic motifs, the signal peptide peptidase (SPP) / SPP-like (SPPL) family was identified (Weihofen *et al.*, 2002, Ponting *et al.*, 2002, Grigorenko *et al.*, 2002). Presenilins were identified in search of proteases involved in cleavage of the amyloid precursor protein (APP) participating in Alzheimer's disease (De Strooper *et al.*, 1999, Wolfe *et al.*, 1999, Haass and Steiner 2002). Later on, it was found that the cleavage is performed by a complex comprising the catalytic subunits presenilin-1 (PS1) or PS2 with the co-factors anterior pharynx defective-1 (APH-1), presenilin enhancer-2 (PEN-2) and nicastrin (Francis *et al.*, 2002, Lee *et al.*, 2002, Gu *et al.*, 2003). Six  $\gamma$ -secretase complexes of different compositions are assumed due to isoforms of PS1 and PS2 as well as APH-1a and APH-1b. The different complexes show distinct affinity for their over 80 known type I substrates (Haapasalo and Kovacs 2011). Besides APP, the Notch-receptor is one of the *in vivo* validated substrates. The Notch ICD released by  $\gamma$ -secretase was shown to play a role in regulation of transcription (De Strooper *et al.*, 1999, Jorissen and De Strooper 2010).

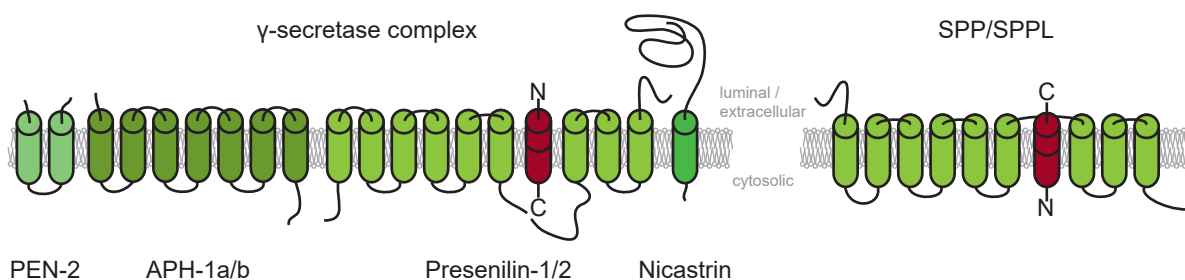


**Figure 3: Comparison of aspartyl proteases.** Presenilins require the co-factors anterior pharynx defective-1 (APH-1), presenilin enhancer-2 (PEN-2) and nicastrin for proteolytical activity, forming the  $\gamma$ -secretase complex. In contrast, SPP/SPPL-family members do not need accessory proteins, according to current models. The topology of both protease families are inverted to each other, as well as the topology of their substrates (depicted in red). Presenilins cleave type I orientated proteins, while SPP/SPPLs show specificity to type II orientated substrates. Adapted from Haapasalo and Kovacs 2011 and Voss *et al.*, 2013

The mammalian SPP/SPPL family is constituted of five members, namely, SPP, SPPL2a, SPPL2b, SPPL2c and SPPL3. In comparison to presenilins, membrane topology of SPP/SPPL family proteases is inverted. Based on the different orientation of the catalytic center, substrate



topology within the membrane is also inverted, as they are type II orientated in the case of SPP/SPPL family proteases (Friedmann *et al.*, 2004). In contrast to presenilins, no co-factors are described so far for SPP and SPPLs (see figure 3; Nyborg *et al.*, 2004, Voss *et al.*, 2013).

The protease SPP localises to the ER where it cleaves signal peptides (Mentrup *et al.*, 2017a). The substrate spectrum of SPP does also include other type II orientated fragments of proteins than signal peptides (see table 2; Mentrup *et al.*, 2017a). For example, SPP can be involved in ER-associated protein degradation (ERAD; Avci and Lemberg 2015). SPP can also proteolyse tail-anchored proteins without premature shedding (Boname *et al.*, 2014, Mentrup *et al.*, 2017a).

SPPL3 cleaves proteins with large ectodomains directly without preceding cleavage by other proteases (Mentrup *et al.*, 2017a). It localises to the golgi apparatus where it cleaves and thereby inactivates glycan-modifying enzymes and other proteins involved in glycosylation (Voss *et al.*, 2014, Kuhn *et al.*, 2015). It can also directly cleave the type III foamy virus envelope protein (FVenv) derived from a zoonotic retrovirus (Voss *et al.*, 2012). In addition to its proteolytic activity, SPPL3 also harbours a protease-independent function by mediating protein-protein interactions (Makowski *et al.*, 2015).

### 1.1.2 SPPL2 proteases

SPPL proteases contain nine TMDs, exposing the C-terminus to the cytoplasm (Voss *et al.*, 2013). A signal sequence at their N-terminus leads to insertion into the ER membrane during protein synthesis, which is cleaved off afterwards (Friedmann *et al.*, 2004). All SPPLs are glycosylated, while SPPL2a harbours the highest degree of glycosylation (Friedmann *et al.*, 2004). The catalytical center is formed by a YD motif in TMD six of SPPL2a and SPPL2b or by a FD motif in TMD six of SPPL2c together with a GFGD sequence in TMD seven of all three proteases. Additionally, they contain a PALL motif within their ninth TMD (Krawitz *et al.*, 2005, Voss *et al.*, 2013, Mentrup *et al.*, 2017a). Even though SPPL2c harbours catalytic motifs, proteolytic activity of SPPL2c has not been demonstrated yet (Mentrup *et al.*, 2017a).

SPPL2c stays within the ER after its synthesis (Friedmann *et al.*, 2006), while SPPL2a and SPPL2b exit the ER. SPPL2a localises to the endolysosomal system due to a YXXØ sorting motif (Friedmann *et al.*, 2006, Behnke *et al.*, 2011). This motif is lacking in the plasma membrane-localised SPPL2b protease (Friedmann *et al.*, 2006, Behnke *et al.*, 2011). By overexpression studies, SPPL2b was also found to localise in the Golgi and to lysosomes (Martin *et al.*, 2008, Krawitz *et al.*, 2005). In overexpression experiments, minor amounts of SPPL2a were also found at the plasma membrane (Behnke *et al.*, 2011). However, only its lysosomal localisation was confirmed *in vivo* (Schröder *et al.*, 2007, Schneppenheim *et al.*, 2014b).

Besides their differences in intracellular localisation, the expression profiles within tissues vary. SPPL2a protein is ubiquitously expressed throughout the murine organism with lower levels observed in brain tissue (Schneppenheim *et al.*, 2014b). In contrast, SPPL2b protein shows highest expression within the brain and in bone marrow. Low amounts of SPPL2b protein can be detected in other organs (Schneppenheim *et al.*, 2014b). No protein expression data for SPPL2c are described. SPPL2c messenger ribonucleic acid (mRNA) can be detected in murine brain, heart, skin and testis (Friedmann *et al.*, 2004).

### 1.1.3 *In vitro* substrates of SPPL2 proteases

In contrast to the large number of substrates for presenilins, only a few proteins are known to be cleaved by SPPLs. Evidence for majority of substrates was obtained by overexpression systems. CD74 is the only *in vivo* validated substrate so far, while the function of cleavage of the other substrates *in vivo* are not well defined (see table 3; Schneppenheim *et al.*, 2013, Beisner *et al.*, 2013, Bergmann *et al.*, 2013, Schneppenheim *et al.*, 2014a, Mentrup 2018).

**Table 3: SPPL family member substrates.** *In vivo* validated substrate CD74 is written in bold. FVenv abbreviates foamy virus envelope protein, NRG1 abbreviates neuregulin 1, CLN5 abbreviates ceroid-lipofuscinosis neuronal protein 5. Adapted from Mentrup *et al.*, 2017a.

Protease	Substrate type	Substrate	Reference	
SPPL2a	Type II protein	TNF $\alpha$	Fluhrer <i>et al.</i> , 2006, Friedmann <i>et al.</i> , 2006	
		FasL	Kirkin <i>et al.</i> , 2007	
		ITM2B	Martin <i>et al.</i> , 2008	
		<b>CD74</b>	Schneppenheim <i>et al.</i> , 2013, Beisner <i>et al.</i> , 2013, Bergmann <i>et al.</i> , 2013, Schneppenheim <i>et al.</i> , 2014a	
		TMEM106B	Brady <i>et al.</i> , 2014	
SPPL2b	Type III protein	NRG1	Fleck <i>et al.</i> , 2016	
	Type II protein	FVenv (viral)	Voss <i>et al.</i> , 2012	
		TNF $\alpha$	Fluhrer <i>et al.</i> , 2006, Friedmann <i>et al.</i> , 2006	
SPPL2c	-	ITM2B	Martin <i>et al.</i> , 2008	
		Transferrin receptor	Zahn <i>et al.</i> , 2013	
		CLN5	Jules <i>et al.</i> , 2017	
		Type III protein	NRG1	Fleck <i>et al.</i> , 2016
		FVenv (viral)	Voss <i>et al.</i> , 2012	

The pro-inflammatory cytokine tumor necrosis factor $\alpha$  (TNF $\alpha$ ) was the first substrate described for SPPL2a and SPPL2b (Fluhrer *et al.*, 2006). TNF $\alpha$  converting enzyme (TACE / ADAM17) is involved in the shedding of the type II orientated TNF $\alpha$  from the cell membrane, releasing a soluble TNF $\alpha$  ectodomain and a intramembranous NTF (Black *et al.*, 1997, Moss *et al.*, 1997,

Zheng *et al.*, 2004). The NTF is further degraded by SPPL2a and SPPL2b (Fluhrer *et al.*, 2006, Friedmann *et al.*, 2006). Thereby, an ICD is released, which was shown to induce Interleukin–12 (IL–12) expression, as this was reduced in activated human dendritic cells (DCs) after protease knockdown or inhibition (Friedmann *et al.*, 2006).

Another member of the TNF–family, the first apoptosis signal ligand (FasL), was also discovered as a SPPL2 substrate. Soluble FasL is shed from the plasma membrane by ADAM10 (Schulte *et al.*, 2007, Kirkin *et al.*, 2007). The membrane bound NTF is a substrate for SPPL2 proteases (Kirkin *et al.*, 2007). The released FasL ICD translocates to the nucleus, where it might exert a role in regulation of transcription (Kirkin *et al.*, 2007). The Fas ligand (FasL) is expressed on T cells and natural killer (NK) cells. Binding of the membrane bound FasL to its receptor leads to induction of cell death, while the soluble form leads to survival within the Fas expressing cell. The Fas/FasL system is involved in homeostasis of T cells, but also in mediating killing of viral infected cells and tumour cells (Yamada *et al.*, 2017).

## 1.2 The role of the SPPL2a substrate CD74 in the immune system

The NTF of the invariant chain (CD74, li) is the only *in vivo* validated substrate for SPPL2a (Schneppenheim *et al.*, 2013, Beisner *et al.*, 2013, Bergmann *et al.*, 2013, Schneppenheim *et al.*, 2014a). Even though SPPL2b can cleave CD74 in overexpression experiments, it plays no apparent role in CD74 NTF proteolysis *in vivo* (Schneppenheim *et al.*, 2014b).

CD74 serves as a chaperone for major histocompatibility complex II (MHCII). It is involved in endosomal trafficking, cell migration and macrophage migration inhibitory factor (MIF) signalling (see figure 4; Schröder 2016). Under steady–state conditions, CD74 is expressed in cells of the immune system, specifically in B cells, macrophages and DCs (Momburg *et al.*, 1986).

CD74 plays an important role in antigen presentation towards T cells, as it serves as a chaperone for MHCII alpha and beta chain assembly and correct folding within the ER. The luminal class II–associated invariant chain peptide (CLIP) of the CD74 protein binds to the MHCII complex within its peptide binding groove, thereby blocking this binding site (Bijlmakers *et al.*, 1994). The complex enters the trans Golgi network and reaches the endolysosomal compartment either directly or via the plasma membrane and endocytosis (Broeke *et al.*, 2013, Schröder 2016). Within specialised lysosomes, the MHC class II compartment (MIIC), the luminal part of CD74 is trimmed by proteases (Matza *et al.*, 2003). CLIP is separated from the membrane bound part of CD74 by cathepsin S (CatS)–mediated proteolysis in DCs, B cells and epithelial cells (Driessen *et al.*, 1999, Nakagawa *et al.*, 1999, Beers *et al.*, 2005). The CLIP segment within the MHCII peptide binding groove can be exchanged with antigenic peptides. After peptide acquisition, MHCII translocates to the plasma membrane, presenting the peptide to T cells (Broeke

*et al.*, 2013). The remaining CD74 membrane bound part is the NTF of CD74. This is the substrate for SPPL2a intramembrane proteolysis, releasing an CD74 ICD (Schneppenheim *et al.*, 2013, Beisner *et al.*, 2013, Bergmann *et al.*, 2013, Schneppenheim *et al.*, 2014a). This small CD74 fragment can enter the nucleus, where it may activate transcription of secreted frizzled-related protein 2 (SFRP2; Mentrup *et al.*, 2015). Furthermore, the CD74 NTF proteolysis is associated with B cell maturation and survival, as it may activate transcription via the transcription initiation factor TFIIID 105–nuclear factor 'kappa-light-chain-enhancer' of activated B cells (TAF<sub>II</sub>105–NF $\kappa$ B) complex (Shachar and Flavell 1996, Matza *et al.*, 2001, Matza *et al.*, 2002a, Matza *et al.*, 2002b).

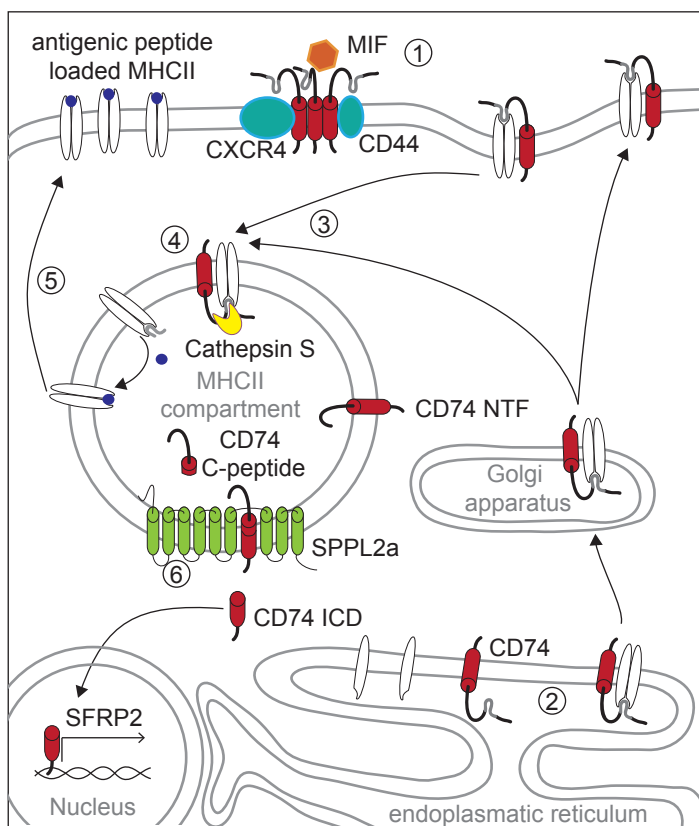


**Figure 4: CD74 in antigen presentation and MIF signalling.** ① CD74 homotrimers bind to the cytokine MIF at the cell surface. The subsequent signalling relies on the co-factors CD44 or CXCR4 and induces B cell survival. ② Within the endoplasmic reticulum, CD74 serves as MHCII chaperone. ③ The complex reaches specialised lysosomes, the MHCII compartment, either directly or via endocytosis from the plasma membrane. ④ CD74 luminal domain is shortened by endosomal proteases within the MHCII compartment. MHCII is released upon CD74 cleavage by Cathepsin S. ⑤ Peptide loaded MHCII translocates to the plasma membrane for antigen presentation. ⑥ The CD74 N-terminal fragment (NTF) is the substrate of SPPL2a, releasing CD74 intracellular domain (ICD) into the cytoplasm. It can enter the nucleus and may activate transcription. Scheme adapted from Schröder 2016.

CD74 is also present at the cell surface (Koch *et al.*, 1982), where it serves as a receptor for the pro-inflammatory cytokine MIF (Leng *et al.*, 2003). The co-receptors CD44 or C–X–C chemokine receptor type 4 (CXCR4) are indispensable for receptor endocytosis and activation of signalling cascades (Shi *et al.*, 2006, Schwartz *et al.*, 2009, Schröder 2016). MIF is an important cytokine for B cell survival and activation in healthy and leukemic B cells (Binsky *et al.*, 2007, Gore *et al.*, 2008, Sapoznikov *et al.*, 2008).

### 1.3 The SPPL2 knockout mouse models

Knockout mouse models for SPPL2a and SPPL2b were generated to study the physiological role of both proteases. While the SPPL2a-deficient mice exhibit striking immunological B cell

defects, for *SPPL2b*<sup>-/-</sup> mice no obvious phenotype was described so far (Schneppenheim *et al.*, 2013, Beisner *et al.*, 2013, Bergmann *et al.*, 2013, Schneppenheim *et al.*, 2014b). Furthermore, the *SPPL2a*<sup>-/-</sup>*SPPL2b*<sup>-/-</sup> double knockout mouse does not display a more severe immunological phenotype than the *SPPL2a*<sup>-/-</sup> mouse, leaving the physiological role of SPPL2b unknown until now (Schneppenheim *et al.*, 2014b).

Three independent SPPL2a knockout mouse strains were generated by two different approaches. Beisner *et al.*, 2013 and Bergmann *et al.*, 2013 aimed to identify novel genes involved in immune function and therefore both used the mutagen N-ethyl-N-nitrosourea (ENU) to induce random mutations in the mouse genome. Among the generated mutants, the *SPPL2a*<sup>mut/mut</sup> mice were identified by decreased numbers of blood B cells in both studies (Beisner *et al.*, 2013, Bergmann *et al.*, 2013). The *SPPL2a*<sup>-/-</sup> mouse by Schneppenheim *et al.*, 2013 was generated by targeted insertion of a neomycin-cassette into intron 2 of the *SPPL2a* gene.

In all three SPPL2a-deficient strains a maturation block of B cells is observed at splenic transitional stage 1 (T1; Schneppenheim *et al.*, 2013, Beisner *et al.*, 2013, Bergmann *et al.*, 2013). DCs are also reduced in number in lymphatic tissues of *SPPL2a*<sup>-/-</sup> and *SPPL2a*<sup>mut/mut</sup> mice, while T cell numbers remain normal (Schneppenheim *et al.*, 2013, Beisner *et al.*, 2013, Bergmann *et al.*, 2013).

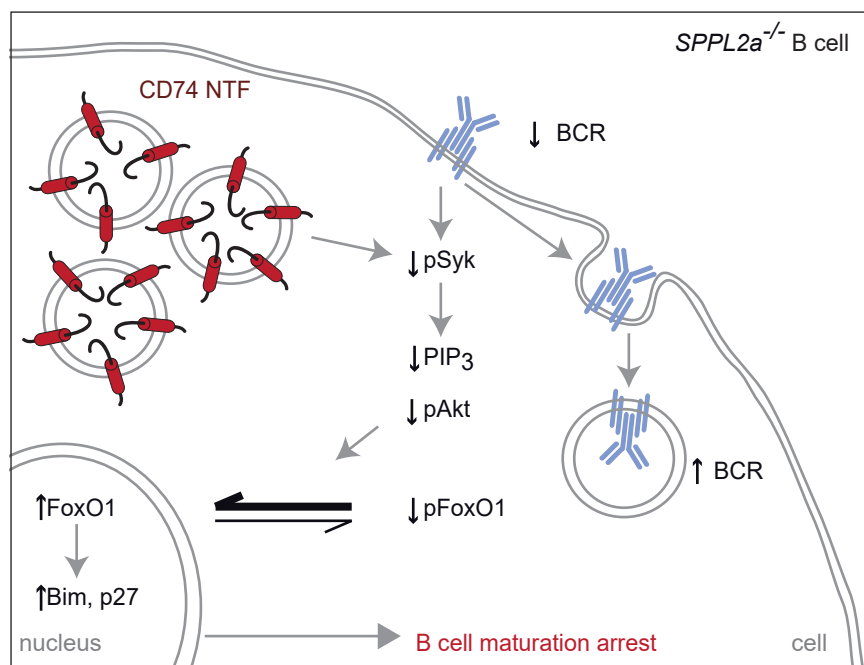


**Figure 5: Influence of the CD74 NTF accumulation on B cell development.** The NTF of CD74 accumulates in endosomal compartments of SPPL2a-deficient B cells. This leads to increased numbers of endosome-derived vacuoles. The surface levels of the B cell receptor (BCR, IgM) are reduced due to increased endocytosis. Subsequently, BCR signalling via spleen tyrosine kinase (Syk) is diminished, leading to increased activity of the transcription factor FoxO1. Transcription of proapoptotic Bim and cell cycle inhibitor p27 is enhanced by FoxO1, leading to arrest of B cell maturation. Adapted from Hüttl 2015 and Schröder 2016.

The residual B cells in SPPL2a-deficient mice show compromised function. In the serum of SPPL2a-deficient mice, antibody titers are significantly reduced. A detailed analysis of the remaining cells revealed that the CD74 NTF accumulates in lysosome-associated membrane protein 2 (LAMP-2) positive endosomes in B cells as well as in DCs of *SPPL2a*<sup>-/-</sup> mice (Schneppenheim *et al.*, 2013, Beisner *et al.*, 2013, Bergmann *et al.*, 2013, Schneppenheim *et al.*, 2014b, Hüttl 2015). *SPPL2a*<sup>-/-</sup> B cells show an accumulation of endosome-derived vacuoles (Schneppenheim *et al.*, 2013, Schneppenheim *et al.*, 2017). In addition, the endocytic trafficking within *SPPL2a*<sup>-/-</sup> B cells is reduced, while the endocytosis of the B cell receptor (BCR, IgM) is enhanced. This leads to reduced surface BCR levels and subsequent signalling, as observed by decreased activation of spleen tyrosine kinase (Syk), Akt and of the NF $\kappa$ b pathway (see figure 5; Hüttl *et al.*, 2015). In contrast to that, extracellular signal-regulated kinase (ERK) is activated normally in *SPPL2a*<sup>-/-</sup> B cells upon BCR ligation. The altered signalling capacity of the BCR on *SPPL2a*<sup>-/-</sup> B cells leads to induction of proapoptotic gene expression and thus may lead to cell death of developing B cells. Furthermore, the calcium flux is reduced after activation of the BCR (Schneppenheim *et al.*, 2013).

It could be shown that the described phenotype in all three SPPL2a-deficient mouse strains is caused by accumulation of the CD74 NTF. Additional ablation of CD74 (SPPL2a-CD74-double knockout mouse) leads to a rescue of B cell numbers and function to the degree of the CD74 single knockout mouse as well as to a rescue of DC frequencies (Schneppenheim *et al.*, 2013, Beisner *et al.*, 2013, Hüttl *et al.*, 2015).

### 1.4 Differentiation and function of DCs in mice

DCs are professional antigen presenting cells with surveillance function, as they continuously process antigens and present them on MHCI and MHCII (Macri *et al.*, 2017). Extracellular antigens can be taken up by DCs and are presented on MHCII complexes, while intracellular antigens are presented on MHCI complexes. Sensing of intracellular and extracellular danger- and pathogen-associated patterns (DAMPs and PAMPs) by innate immune cells is mediated by pattern recognition receptors (PRR). Sensing of the ligand by these receptors initiates signalling cascades leading to maturation and activation of DCs. They increase antigen processing and MHC expression, migrate into the T cell zones of lymphoid organs and stimulate T cells (Heuzé *et al.*, 2013). Thereby DCs connect the innate and the adaptive immune system.

#### 1.4.1 *In vivo* and *in vitro* differentiation of DCs and marker for murine DCs

Two major subtypes of DCs are formed by conventional DCs (cDCs), also called myeloid or classical, and plasmacytoid DCs (pDCs). The shape of cDCs led to the name of the cell type,

as they harbour “processes of varying length and width” (Steinman and Cohn 1973). The pDCs were described later due to their capacity to produce large amounts of type I interferons (IFNs; Macri *et al.*, 2017). DCs develop from hematopoietic stem cells, which give rise to the macrophage and DC progenitor (MDP) within the bone marrow (Figure 6; Geissmann *et al.*, 2010, Tussiwand and Gautier 2015). MDPs are precursors for monocytes and the common DC progenitor (CDP). The latter differentiate into pDCs or cDC precursors (pre-cDCs). These leave the bone marrow into blood vessels from where they colonise peripheral lymphoid or non-lymphoid organs. Two types of cDCs (cDC1 and cDC2) develop from pre-cDCs thereafter. A further type of monocyte-derived DCs (moDCs) can emerge in peripheral tissues from monocytes during inflammation (Geissmann *et al.*, 2010, Tussiwand and Gautier 2015, Macri *et al.*, 2017). DC subsets can be defined by their expression of different compositions of surface markers, listed in table 4.

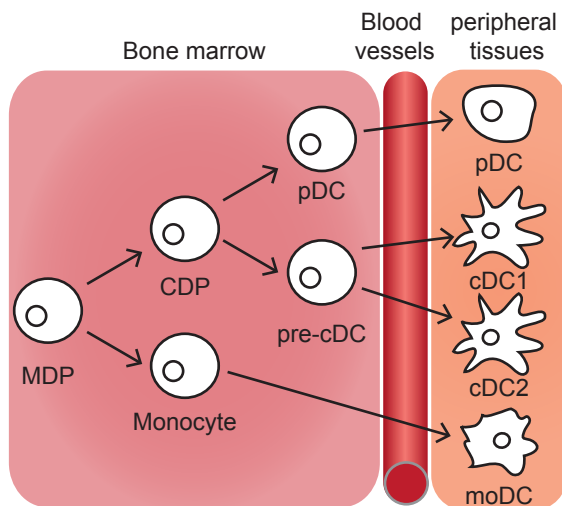


**Figure 6: Development of DCs.** The macrophage DC progenitor (MDP) derives from hematopoietic stem cells within the bone marrow. MDP give rise to monocytes and the common DC progenitor (CDP). Plasmacytoid DCs (pDCs) develop within the bone marrow from CDP and settle peripheral organs via the blood stream. Conventional DCs (cDCs) differentiate within the peripheral tissue after the pre-cDCs developed from CDP and left the bone marrow. Under inflammatory conditions, monocytes can give rise to monocyte-derived DCs (moDCs). Scheme modified from Geissmann *et al.*, 2010 and Tussiwand and Gautier 2015.

**Table 4: Markers defining DC populations.** Markers in brackets display a low expression on indicated population. Adapted from León *et al.*, 2007, Merad *et al.*, 2013, Shortman *et al.*, 2013, Segura and Amigorena 2013, Durai and Murphy 2016.

Population	Marker
pDC	(CD11c), (MHCII), B220, Sra1, SiglecH, Bst2, CCR9
cDC1	CD11c, MHCII, CD8, CD24, XCR1
cDC2	CD11c, MHCII, CD4, SIRP $\alpha$
moDC	CD11c, MHCII, CD11b, F4/80, Ly6C, GM-CSFR, LAMP-2, Fc $\epsilon$ RI, Fc $\gamma$ RI

For characterisation of DC function, *in vitro* culture systems have been developed as these cells are of low abundance in murine tissues. These culture systems are realised by application of the granulocyte-macrophage colony-stimulating factor (GM-CSF) or fms like tyrosine kinase 3 ligand (FLT3L) to bone marrow cultures.

The generation of DCs in culture was first described for GM-CSF, leading to a heterogeneous composition of DCs, macrophages and granulocytes (Inaba *et al.*, 1992, Lutz *et al.*, 1999). The

latter were shown to be reduced by longer culture period (Lutz *et al.*, 1999). The origin and phenotype of these DCs are a matter of debate. It was shown that GM-CSF cultures lead to inflammatory moDCs and macrophages (Xu *et al.*, 2007, Rogers *et al.*, 2017). However, it was also demonstrated that the DCs in this culture arise from CDP (Helft *et al.*, 2015). In another study, the presence of pDCs was excluded in these cultures and cells are comparable to cDC2s (Scheicher *et al.*, 1992).

The culture of bone marrow cells with FLT3L leads to generation of DCs, which show high similarity to pDCs, cDC1s and cDC2s (Brasel *et al.*, 2000, Naik *et al.*, 2005, Xu *et al.*, 2007).

### 1.4.2 Pattern-recognition receptor (PRR) families

As described above, PAMPs and DAMPs are sensed by PRR on DCs. The ligation of the receptors induces signalling cascades within DCs, leading to their activation and qualifying them for T cell maturation induction. The two families of membrane bound PRR are C-type lectin receptors (CTLR) and Toll-like receptors (TLR).

#### 1.4.2.1 C-type lectin receptors (CTLRs)

CTLRs are single-pass transmembrane proteins. They all harbour at least one C-type lectin-like domain (CTLD) in their extracellular part, which mediates binding of carbohydrates (Dambuza and Brown 2015, Brown and Crocker 2016). Furthermore, they can also recognise lipids and proteins. CTLR can bind to fungi as well as bacteria, viruses, dead cells and tumour cells (see figure 7). With few exceptions, like DC-associated C-type lectin-1 (Dectin-1), ligand binding by these receptors is  $Ca^{2+}$ -dependent. The activation of intracellular signalling pathways is mediated by immunoreceptor tyrosine-based activation motifs (ITAMs). Dectin-1 harbours a ITAM-like sequence within their cytoplasmic tail. Macrophage-inducible C-type lectin (Mincle), Dectin-2 and Dectin-3 (also called MCL) have to associate with the ITAM-containing adaptor molecule Fc Receptor  $\gamma$ -chain (FcR $\gamma$ ). The interacting protein of the mannose receptor (MR), required for signalling, is unknown (Dambuza and Brown 2015, Brown and Crocker 2016).

The canonical CTLR signalling is mediated by activation of the kinase Syk. Subsequently, protein kinase C (PKC) activates ERK and NF $\kappa$ B. Transcription factors of the NF $\kappa$ B pathway, but also the nuclear factor of activated T cells (NFAT) and interferon regulatory factor (IRF) translocate to the nucleus and regulate gene transcription (Brown and Crocker 2016). A Syk-independent signalling pathway was lately found for Dectin-1 mediated by rapidly accelerated fibrosarcoma-1 (Raf-1), which leads to activation of NF $\kappa$ B (Gringhuis *et al.*, 2009, Dambuza and Brown 2015).



The CTLRs myeloid inhibitory C-type lectin-like receptor (MCL) and DC immunoreceptor (DCIR) comprise a tyrosine-based inhibition motif (ITIM) within their cytoplasmic tail, activating the phosphatases Src-homology domain 2 (SH2)-containing cytoplasmic tyrosine phosphatase 1 (SHP-1) and SHP-2. These dephosphorylate and thus inactivate Syk among other kinases. Endogenous ligands derived from dead cells can bind to MCL, thereby regulating immunity (Brown and Crocker 2016, Redelinghuys and Brown 2011).

Dectin-1 plays a pivotal role in anti-fungal immunity by recognition of fungal  $\beta$ -glucans as the yeast cell wall glucan Zymosan (Brown and Gordon 2001). The important role of Syk-mediated Dectin-1 signalling is supported by the failure of Syk-deficient DCs to release IL-10 and IL-2 upon co-culture with yeast (Rogers *et al.*, 2005). Dectin-1 ligation induces T helper cell type 1 ( $T_H1$ ) and  $T_H17$  differentiation mediated by DCs (LeibundGut-Landmann *et al.*, 2007). The recognition of Zymosan is enhanced by the interaction of Dectin-1 with TLR2 (Gantner *et al.*, 2003). These two receptors can also interact in the recognition of mycobacteria species (Yadav and Schorey 2006). Furthermore, Dectin-1 was shown to be an important receptor in detection of *Mycobacterium bovis* Bacille Calmette-Guérin (BCG) in macrophages and to be required for IL-12p40 release in co-culture of splenic DCs with *Mycobacterium tuberculosis* (Yadav and Schorey 2006, Rothfuchs *et al.*, 2007).

Dectin-2 is also involved in fungal and bacterial recognition. Dectin-2 heterodimerises with Dectin-3 to bind structures with high mannose content. Fungal recognition by Dectin-2 from DCs drives  $T_H1$  and  $T_H17$  development (Kerscher *et al.*, 2013). The recognition of mycobacteria species is mediated by binding of Dectin-2 to Lipoarabinomannan (LAM; Yonekawa *et al.*, 2014). LAM can be also recognised by the MR (Schlesinger *et al.*, 1994). Due to its different domains, MR can recognise a broad range of ligands. Thereby the MR can induce immune responses towards fungi, bacteria, helminths, viruses and also endogenous ligands. The induction of MR-mediated immunity leads to  $T_H17$  differentiation, but due to its broad range of ligands it also plays a role in homeostasis (Brown and Crocker 2016).

The CTLR Mincle is associated with the adaptor molecule FcR $\gamma$  and Dectin-3. The latter is involved in regulating surface expression of Mincle, which can be induced by inflammatory stimuli, as for example lipopolysaccharides (LPS), mycobacteria species or TNF $\alpha$  (Kerscher *et al.*, 2013, Brown and Crocker 2016, Patin *et al.*, 2017). Mincle primarily binds to microbial glycolipids, like trehalose-6,6'-dimycolate (TDM; cord factor) from mycobacteria (Ishikawa *et al.*, 2009). Furthermore, it can bind to glycerol monomycolate from mycobacteria, but also components from other bacteria and fungi and even from damaged cells (Patin *et al.*, 2017). Mincle and MCL promote  $T_H1$  and  $T_H17$  development. However, Mincle can also inhibit Dectin-1 mediated IL-12p70 release leading to  $T_H2$  development (Wevers *et al.*, 2014).

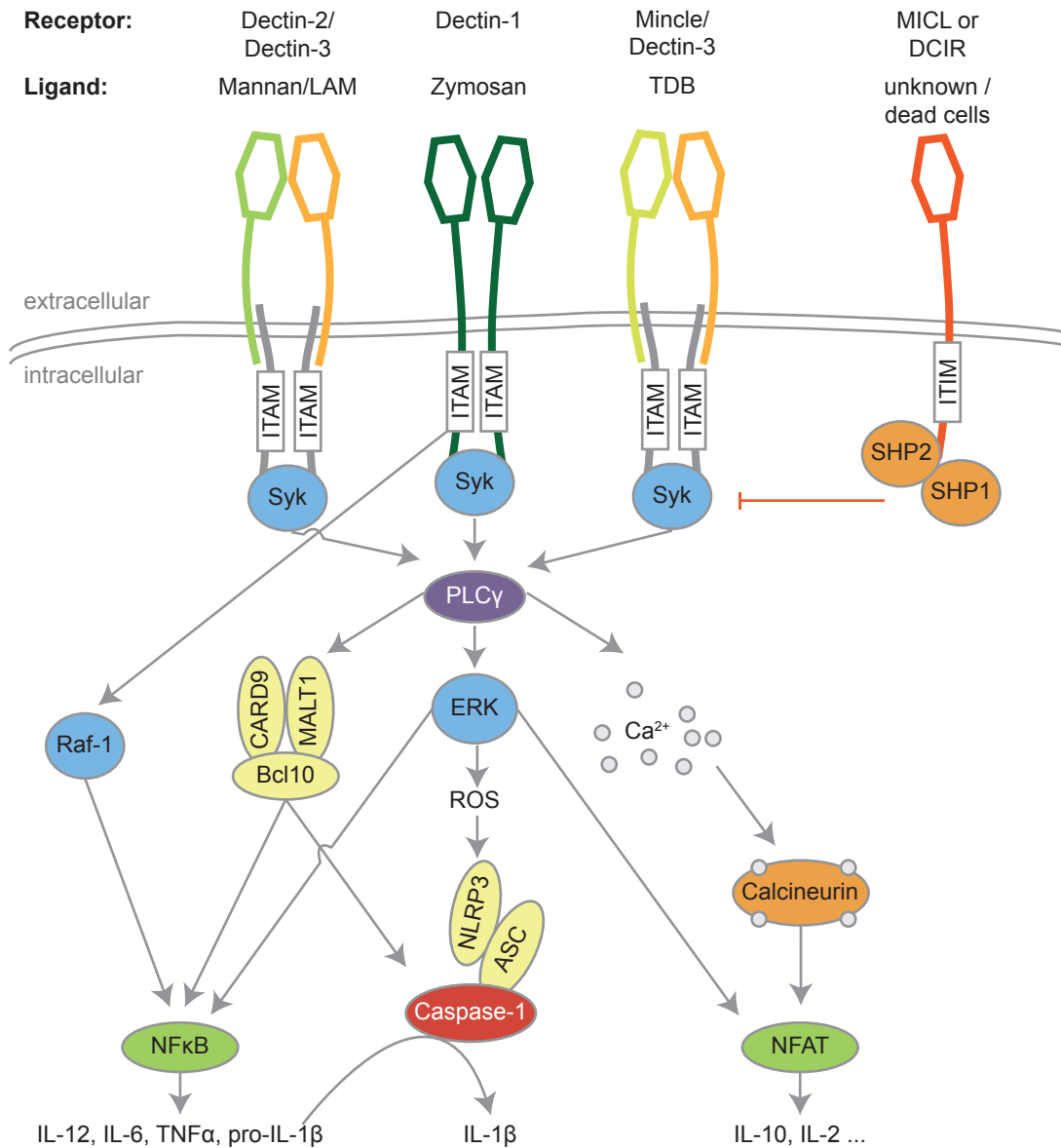


**Figure 7: Signalling by receptors of the CTLR family.** Receptors of the C-type lectin receptor (CTLR) family harbour at least one C-type lectin domain (CTLD) within their extracellular domain for recognition of indicated ligands. Subsequent signalling of immunoreceptor tyrosine-based activation motif (ITAM)-containing or -associated CTLR is mediated by spleen tyrosine kinase (Syk) activation. Immunoreceptor tyrosine-based inhibitory motif (ITIM)-containing receptors activate SH2-containing cytoplasmic tyrosine phosphatase (SHP) phosphatases, which inhibit Syk. Syk triggers phospholipase C $\gamma$  (PLC $\gamma$ ). This leads to calcium release, extracellular signal-regulated kinase (ERK) activation and assembly of the CARD9-MALT1-Bcl10 complex. The calcium is bound by calcineurin, which activates nuclear factor of activated T cells (NFAT)-dependent interleukin-10 (IL-10) and IL-2 transcription. ERK activates NFAT, as well. Furthermore, the NF $\kappa$ B-mediated transcription is induced by ERK as well as the CARD9-complex leading to expression of IL-12 family members, pro-IL-1 $\beta$  and further pro-inflammatory cytokines. The ERK induced production of reactive oxygen species (ROS) induces the inflammasome comprising of NLRP3, ASC and Caspase-1. The inflammasome cleaves pro-IL-1 $\beta$ . A Syk-independent activation of NF $\kappa$ B is mediated by Dectin-1 via rapidly accelerated fibrosarcoma-1 (Raf-1). Kinases depicted in blue, phosphatases in red, transcription factors in green, accessory protein in yellow. Adapted from Drummond and Brown 2011 and Brown and Crocker 2016.

### 1.4.2.2 Toll-like receptors (TLRs)

Another family of membrane bound PRR are the TLRs. They are important for detection of and immunity against bacterial, viral, fungal, and protozoan PAMPs. Extracellular pathogens are detected by TLR1, TLR2, TLR4, TLR5, TLR6 and TLR11, while the endosomal localised TLR3, TLR7, TLR8, TLR9 and TLR13 are sensing nucleotides from host, bacteria and viruses (O'Neill *et al.*, 2013, West *et al.*, 2006).

All TLRs contain a Toll/IL-1 receptor homology (TIR) domain within their cytoplasmic tail, which recruits myeloid differentiation primary-response protein 88 (MYD88) or TIR-domain-containing adaptor protein inducing IFN $\beta$  (TRIF) upon ligand binding. The plasma membrane-resident TLRs all induce MYD88 association upon ligand recognition. The subsequent signalling cascade includes p38, JNK and NF- $\kappa$ B, leading to translocation of the transcription factors CREB, AP1 and NF- $\kappa$ B to the nucleus, where they induce expression of pro-inflammatory cytokines, including TNF $\alpha$  and IL-1 $\beta$ . Endosomally localised TLRs either bind to TRIF or MYD88, inducing translocation of transcription factors of the IRF family and induce expression of type I IFNs. In addition, they do activate p38, JNK and NF- $\kappa$ B, as described for the plasma membrane TLRs. TLR4 can signal from the plasma membrane, as described above, but upon receptor endocytosis it induces TRIF-mediated type I IFN release and a late-phase NF- $\kappa$ B activation (West *et al.*, 2006, O'Neill *et al.*, 2013).

The best studied TLR ligand is the TLR4 ligand LPS from the outer membrane of gram-negative bacteria. TLR4 signalling is supported by LPS binding to the soluble LPS-binding protein, which delivers LPS to CD14 at the cell surface of innate immune cells. CD14 then transfers LPS to the TLR4, which mediates the subsequent signalling (O'Neill *et al.*, 2013).

TLR2 forms heterodimers with either TLR1 or TLR6. As recognition of some TLR2 ligands are neither dependent on TLR1 nor TLR6, TLR2 might also heterodimerize with non-TLRs. The TLR2/1 complex recognises triacylated lipoproteins from bacteria and additional lipoproteins, derived from mycobacteria or meningococci (Akira and Takeda 2004, West *et al.*, 2006). Detection of fungi, but also bacteria and diacylated lipoproteins from mycoplasma is the task of the TLR2/6 complex (Akira and Takeda 2004, West *et al.*, 2006).

### 1.4.3 T cell induction by DCs

Induction of effector T cells is mediated by DCs by three signals. The antigenic peptides are presented on MHC complexes, as described above, costimulatory molecules on DCs bind to receptors on T cells and cytokines, released by DCs, bind cytokine receptors on T cells (Reis e Sousa 2006, Merad *et al.*, 2013). The complex network of cytokines, released by DCs and their effector functions are depicted in figure 8.

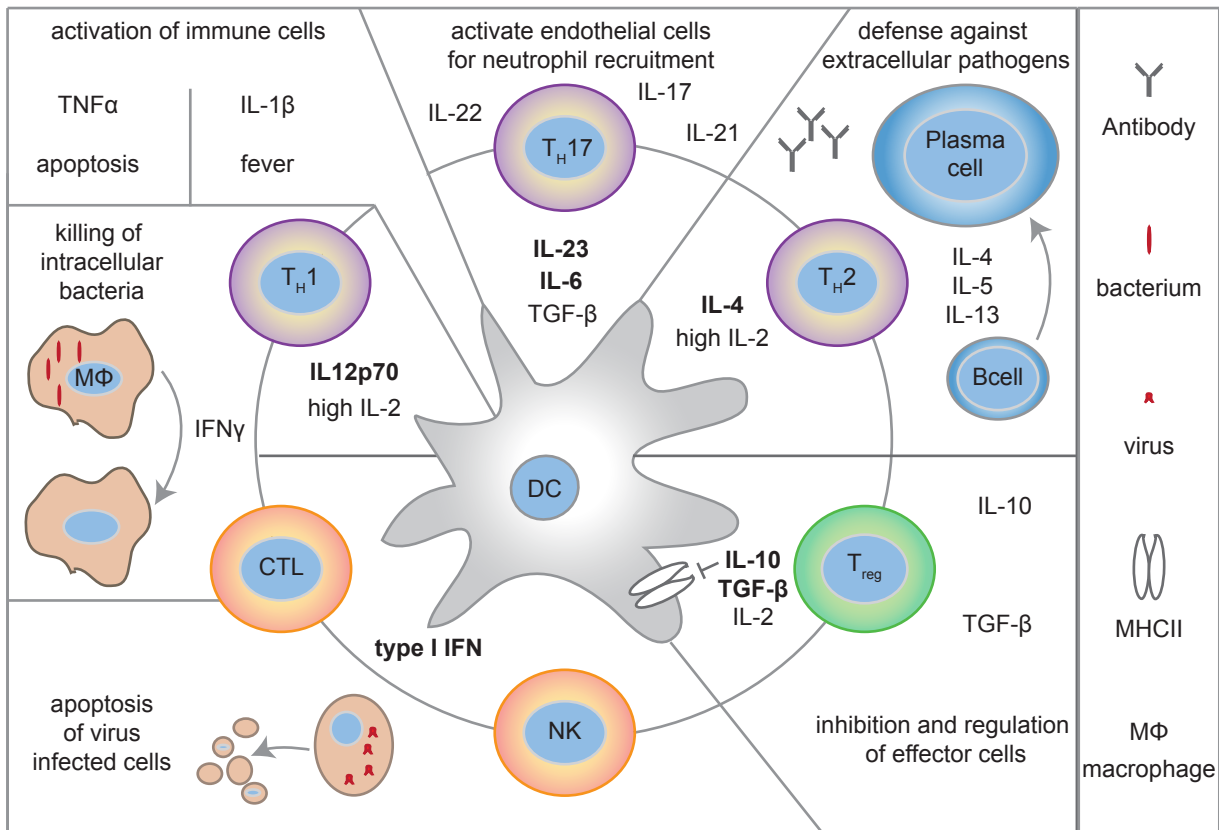


**Figure 8: DC cytokines in activation of innate and adaptive immune cells.** Cytokines released by DCs lead to differentiation and activation of T cells as well as NK cell induction. Cytokines in bold are the canonical inducers of indicated cells. IL-10 negatively regulates MHCII surface expression. T helper cell (T<sub>H</sub>), regulatory T cell (T<sub>reg</sub>), cytotoxic T cell (CTL), macrophage (MΦ). Adapted from Pulendran *et al.*, 2010 and Tussiwand and Gautier 2015.

The classes of DCs are specialised to respond to different pathogens infecting the host. Intracellular pathogens are mainly encountered by the cDC1 population. The release of IL-12p70 by cDC1s induces T<sub>H</sub>1 development (Hsieh *et al.*, 1993, Heufler *et al.*, 1996). This cytokine also plays a role in cytotoxic T cell (CTL) development (Schmidt and Mescher 2002, Kieper *et al.*, 2001). IFN $\gamma$ , produced by CTL and T<sub>H</sub>1, leads to activation of macrophages for killing of intracellular bacteria, as for example mycobacteria species (Cooper *et al.*, 1993, Tascon *et al.*, 1998).

Immune defence against multicellular parasites is mediated by IL-4 release by cDC2s leading to T<sub>H</sub>2 development (Le Gros *et al.*, 1990, Hsieh *et al.*, 1992, Silva-Filho *et al.*, 2014). The subsequent release of IL-4, IL-5, IL-9 and IL-13 by T<sub>H</sub>2 leads to activation of additional cell. Proliferation and immunoglobulin class-switching are induced in B cells, the numbers of granulocytes and goblet cells increase, macrophages become activated and smooth muscle cells contract (Walker and McKenzie 2018). Extracellular bacteria and fungi are also targets of cDC2s. The cDC2s release IL-23, IL-6 and transforming growth factor  $\beta$  (TGF $\beta$ ) upon activation. These cytokines lead to polarisation of T cells towards T<sub>H</sub>17 and survival of these (Bettelli

*et al.*, 2006, Veldhoen *et al.*, 2006). In turn, T<sub>H</sub>17 cells produce IL-17, IL-21 and IL-22, which induce chemokine secretion by epithelial cells for neutrophil recruitment and IgG antibody production in B cells (Ouyang *et al.*, 2008, Mitsdoerffer *et al.*, 2010).

Plasmacytoid DCs release high amounts of type I IFNs after recognition of foreign nucleic acids. Type I IFNs are comprised of IFN- $\alpha$ , IFN- $\beta$ , IFN- $\kappa$ , IFN- $\delta$ , IFN- $\epsilon$ , IFN- $\tau$ , IFN- $\omega$  and IFN- $\zeta$ . By release of type I IFNs, pDCs play a major role in viral, but also bacterial immunity (Hanabuchi and Liu 2011). Type I IFNs activate CTLs and virus-specific NK cells (Swiecki *et al.*, 2010).

IL-2, IL-10 and TGF $\beta$  induce development of regulatory T cells (T<sub>reg</sub>s; Hoeppli *et al.*, 2015, Workman *et al.*, 2009). However, also DC-T cell contact without costimulatory molecules leads to T<sub>reg</sub> development (Belkaid and Oldenhove 2008, Reis e Sousa 2006).

Besides cDCs and pDCs, which develop under steady-state conditions, monocytes can also give rise to moDCs during inflammation. This DC population can release IL-12p70 and thereby induce T<sub>H</sub>1 development (León *et al.*, 2007, Flores-Langarica Adriana *et al.*, 2011).

#### 1.4.4 Modulations of immune responses by cytokines

Cytokines secreted by DCs have functions beyond activation of T cells. Two important pro-inflammatory cytokines are TNF $\alpha$  and IL-1 $\beta$ . TNF $\alpha$  is associated with general activation of immune cells, tissue degeneration and regulated cell death, called apoptosis (Kalliolias and Ivashkiv 2016). TNF $\alpha$  as well as IL-1 $\beta$  and IL-6 induce systemic inflammation, also referred to as acute phase response. Release of proteins from the complement system is increased during acute phase reaction. The complement system proteins opsonise pathogens, which can in turn be sensed by phagocytic immune cells leading to resolution of the infection (Cray *et al.*, 2009).

Besides acute phase protein release, IL-1 $\beta$  induces fever and leukocyte recruitment by epithelial cells. Furthermore, it has survival and effector functions on neutrophils and monocytes (Garlanda *et al.*, 2013, Dinarello 2009). IL-1 $\beta$  can also regulate T<sub>H</sub>17 response and influence adaptive immunity (Zielinski *et al.*, 2012).

IL-1 $\beta$  is expressed as a pro-form, that is proteolysed by a multimeric protein complex, called the inflammasome. The canonical inflammasome contains the protease caspase 1 with a sensor molecule of the nucleotide-binding oligomerization domain-like receptors (NLR) family and the adaptor protein apoptosis-associated speck-like protein containing a caspase recruitment domain (ASC). Induction of the inflammasome is a two-step process where the first signal leads to increased expression of the sensor molecule and pro-IL-1 $\beta$  and a second signal to proteolytic activation of the inflammasome. Ligation of a PRR serves as first signal, while various triggers are known for the second signal (Latz *et al.*, 2013). Among these second signals

is the recognition of intracellular produced reactive oxygen species (ROS) or sensing of extracellular adenosine triphosphate (ATP) with the P2X receptor, which is released by DCs or macrophages (see figure 7, Gombault *et al.*, 2012, Pelegrin and Surprenant 2006, Perregaux and Gabel 1994).

In contrast to  $\text{TNF}\alpha$  and  $\text{IL-1}\beta$ ,  $\text{IL-10}$  serves as an anti-inflammatory cytokine and prevents tissue damage (Couper *et al.*, 2008).  $\text{IL-10}$  sensing by immune cells leads to reduced expression of pro-inflammatory cytokines, as for example  $\text{IL-1}\beta$ ,  $\text{IL-6}$ ,  $\text{IL-12}$  and  $\text{TNF}\alpha$ . Furthermore,  $\text{IL-10}$  leads to reduced expression of leukocyte attractant chemokines. Moreover,  $\text{IL-10}$  can inhibit activation of immune cells and suppress proper MHCII-peptide loading and trafficking to the plasma membrane (Mittal and Roche 2015).

$\text{IL-2}$  can also serve as anti-inflammatory cytokine in a dose-dependent manner. At low doses it induces  $T_{\text{reg}}$  development, survival and functions, but no effector T cells (Ye *et al.*, 2018). At higher concentrations,  $\text{IL-2}$  is known to promote  $T_{\text{H1}}$  and  $T_{\text{H2}}$  differentiation, but to inhibit  $T_{\text{H17}}$  development. It plays an important role in NK cell proliferation and function and CTL development (Liao *et al.*, 2013).

The  $\text{IL-12}$  family cytokines are special as they form homo- or heterodimers of an alpha chain (p19, p28 or p35) and a beta chain (p40 or Ebi3; Vignali and Kuchroo 2012). The best characterised members are  $\text{IL-12p70}$ , formed by p35 and p40 as well as  $\text{IL-23}$ , composed of p19 and p40.  $\text{IL-12p70}$  and  $\text{IL-23}$  have pro-inflammatory functions by induction of T cell differentiation, as described above. Furthermore, the p40 subunit can form homodimers ( $\text{IL-12p80}$ ) and antagonise the function of  $\text{IL-12p70}$  and  $\text{IL-23}$  by binding to their receptors without induction of signal cascades (Vignali and Kuchroo 2012). Contrary to that,  $\text{IL-12p80}$  also attracts macrophages and induces DC migration. Furthermore, a protective role of  $\text{IL-12p80}$  in mycobacteria infections has been implicated (Cooper and Khader 2007).

### 1.5 The role of SPPL2a in human patients

SPPL2a deficiency is also described in humans. A microdeletion in chromosome 15 affecting the *SPPL2A* gene was observed in patients with a neurodevelopmental brain disorder. This deletion leads to a lack of the SPPL2a protein, in addition to the neuronal adaptor protein complex-4 (Moreno-De-Luca *et al.*, 2011, Schneppenheim *et al.*, 2014a). The absence of the adaptor protein complex-4 is causative for the neurological disease. However, the deficiency of SPPL2a leads to an accumulation of the CD74 NTF in immortalised B cells derived from these patients (Schneppenheim *et al.*, 2014a). Unfortunately, no data about immune cell numbers are available from these patients. Very recently, SPPL2a deficiency was also discovered in three patients with Mendelian susceptibility to mycobacterial disease (Kong *et al.*, 2018).

### 1.5.1 Mendelian susceptibility to mycobacterial disease in SPPL2a-deficient patients

Mendelian susceptibility to mycobacterial disease (MSMD) describes the disseminated and recurrent infection with weakly virulent mycobacteria. This rare disorder can occur following disposition to the tuberculosis vaccination strain BCG or non-tuberculous environmental mycobacteria. MSMD patients are also susceptible to salmonellosis, candidiasis, tuberculosis and other intramacrophagic pathogens. Infections with weakly virulent mycobacteria are the most common clinical manifestation in MSMD patients. Gene defects in the IL-12-IFN $\gamma$  axis account for the disease in about half of the patients (Bustamante *et al.*, 2014).

Recently, the group of Dr. Casanova (The Rockefeller University, New York, USA) discovered mutations in the *SPPL2A* gene by a genetic screen in three MSMD patients of two unrelated families (Kong *et al.*, 2018). These mutations lead to a premature stop codon and truncated variants of the SPPL2a protein, lacking catalytic activity. The NTF of CD74 accumulates in immortalised B cells, peripheral blood monocytes or fibroblasts derived from these patients. Interestingly, no severe alterations in B cell populations or B cell function were observed in patients. Instead, they show a significant reduction of the cDC2 subpopulation. Other DC subpopulations showed only slight reduction (cDC1) or normal frequencies (pDC). Even though numbers of different T cell populations were normal in these patients, a mycobacterium-specific T cell subpopulation produces less IFN $\gamma$  than T cells from healthy controls upon BCG co-culture. The loss of DCs, possibly in conjunction with altered function of the mycobacterium-specific T cell subpopulation, is the reason for higher susceptibility to infection with weakly virulent BCG mycobacteria in SPPL2a-deficient MSMD patients (Kong *et al.*, 2018).

### 1.6 Aim of the study

B cells of SPPL2a-deficient mice display a strong phenotype comprising developmental and functional defects (Schneppenheim *et al.*, 2013, Bergmann *et al.*, 2013, Beisner *et al.*, 2013, Hüttl *et al.*, 2015). Due to accumulation of the CD74 NTF, which strictly requires SPPL2a for its proteolytical turnover, B cell development is blocked at splenic transitional stage 1 (T1) in *SPPL2a*<sup>-/-</sup> mice and remaining B cells show decreased B cell receptor (BCR or IgM) cell surface expression as well as subsequent BCR signalling. In humans, SPPL2a deficiency leads to normal development of B cells, but decreased frequencies of the conventional dendritic cell 2 (cDC2) population. This reduction causes mendelian susceptibility to mycobacterial disease (MSMD), which is characterised by high susceptibility to infections with weakly virulent mycobacteria (Kong *et al.*, 2018).

Since in humans DCs are the cell type most heavily affected by SPPL2a-deficiency, it was aimed to get further insight into the role of the intramembrane protease SPPL2a in DC development and function. As the accumulation of the SPPL2a substrate CD74 led to the described B cell phenotype in mice, its likely role in DCs should be addressed here. To investigate, if mice display the same defect in DC populations as observed in SPPL2a-deficient humans, the development of DCs in *SPPL2a*<sup>-/-</sup> mice were intended to be analysed. For functional studies, an *in vitro* culture system of bone marrow-derived DCs (BMDCs) will be established. A potential impact of SPPL2a-deficiency on DC differentiation in this system should be assessed first. Systematic assessment of the responses towards pattern recognition receptor (PRR) stimulations at the level of signalling pathway activation as well as cytokine induction and release will be measured. As representatives of two major PRR families, in particular the C-type lectin receptor Dectin-1 and the Toll-like receptor 4 will be studied. Based on the reduction of BCR surface expression in B cells, it was planned to explore the cellular distribution, especially the surface abundance, of these PRRs. Finally, with regard to the human disease, the impact of SPPL2a on mycobacterial recognition by DCs should be evaluated. The obtained insights to the physiological role of SPPL2a in DC function should be correlated with the clinical phenotype of SPPL2a-deficient patients.



## 2 Material & Methods

### 2.1 Material

#### 2.1.1 Chemicals

Chemicals were obtained from Carl Roth (Karlsruhe, Germany) or Merck (Darmstadt, Germany), if not stated otherwise. The purity grade was *pro analysi*.

#### 2.1.2 Animals

C57BL/6N *wild type* (*wt*), *SPPL2a*<sup>-/-</sup>, *CD74*<sup>-/-</sup> and *SPPL2a*<sup>-/-</sup>*CD74*<sup>-/-</sup> knockout mice were bred in the Victor–Hensen–Haus of the Christian–Albrechts–University of Kiel. Mice were housed pathogen free in individually ventilated cages. Animal care and handling were strictly performed according to local and national guidelines.

Originally, *wt* mice were obtained from Charles River and *CD74*<sup>-/-</sup> mice from The Jackson Laboratory (B6.129S-Cd74tm1Liz/J). *CatS*<sup>-/-</sup> mice were kindly provided by Prof. Dr. Diana Dudziak (Department of Dermatology, University Hospital of Erlangen, Germany). The generation of *SPPL2a*<sup>-/-</sup> and *SPPL2a*<sup>-/-</sup>*CD74*<sup>-/-</sup> mice (Schneppenheim *et al.*, 2013), *CD74*<sup>-/-</sup> mice (Bikoff *et al.*, 1993) and *CatS*<sup>-/-</sup> mice (Shi *et al.*, 1999) was described before. All mice were backcrossed for ten generations on a C57BL/6N background. Mice within experimental groups were matched for sex and age. They were asphyxiated with CO<sub>2</sub> followed by cervical dislocation.

#### 2.1.3 Antibodies

Primary and secondary antibodies listed below were used for indirect immunofluorescence (IF, section 2.2.1.5), Western Blotting (WB, section 2.2.2.7) and flow cytometry (FC, sections 2.2.1.1 and 2.2.1.6). Antibodies against Dectin–1 and SPPL2a were generated by Pineda antibody-service (Berlin, Germany). For generation of polyclonal antibodies against the N-terminus of Dectin–1, a peptide of the sequence *KYHSHIENLDEDGYTQLDFC* (amino acids 2–20 of Dectin–1) was used for immunisation of rabbits. A peptide of SPPL2a luminal domain of the sequence *HLSDIPPDGIRNKAVVVH* (amino acids 77–94 of SPPL2a) was used for immunisation of rabbits to obtain polyclonal antibodies against the protease. Antibodies were isolated from sera by affinity purification.

## MATERIAL & METHODS

**Table 5: List of primary antibodies.** WB: Western Blot; IF immunofluorescence; FC: flow cytometry; Sigma–Aldrich (Missouri, United States); eBioscience, now Thermo Fisher Scientific (Massachusetts, USA); BD Bioscience (California, USA); BioLegend (California, USA); Cell Signaling (Massachusetts, United States); Pineda antibody–service (Berlin, Germany).

Antigen	Conjugation	Clone/ Epitope	Host	Isotype	Company	Application
Actin		polyclonal	rabbit		Sigma–Aldrich	WB 1:5000
B220	Pe-Cy5.5	RA3-6B2	rat	IgG2a $\kappa$	eBioscience	FC 1:800
CD103	FITC	2E7	hamster	IgG	BioLegend	FC 1:100
CD115	Biotin	AFS98	rat	IgG2a $\kappa$	eBioscience	FC 1:500
CD117	BV605	2B8	rat	IgG2b $\kappa$	BD	FC 1:200
CD11b	AF700	RM4-5	rat	IgG2a $\kappa$	BD	FC 1:400
CD11b	PE-Cy7	M1/70	rat	IgG2b $\kappa$	eBioscience	FC 1:300
CD11c	FITC	N418	hamster	IgG	eBioscience	FC 1:100
CD11c	PE	N418	hamster	IgG	eBioscience	FC 1:100
CD11c	PECF594	HL3	hamster	IgG1	BD	FC 1:400
CD135	Pe-Cy5	A2F10	rat	IgG2a $\kappa$	BioLegend	FC 1:100
CD161b/c	BUV395	PK136	mouse	IgG2a $\kappa$	BD	FC 1:400
CD19	PerCP-Cy5.5	1D3	rat	IgG2a $\kappa$	eBioscience	FC 1:200
CD317	BV650	927	rat	IgG2b, $\kappa$	BioLegend	FC 1:400
CD34	BV421	MEC14.7	rat	IgG2a $\kappa$	BioLegend	FC 1:200
CD3e	FITC	145-2C11	hamster	IgG1	BD	FC 1:400
CD3e	PE	145-2C11	hamster	IgG1	BD	FC 1:400
CD74		In-1	rat	IgG2b $\kappa$	BD Bioscience	WB 1:5000 IF 1:200
CD86	BV605	GL-1	rat	IgG2a $\kappa$	BioLegend	FC 1:800
CD8a	APC	53-6.7	rat	IgG2a $\kappa$	eBioscience	FC 1:400
Cofilin		D3F9	rabbit	IgG	Cell Signaling	WB 1:1000
CX3CR1	BV711	SA011F11	mouse	IgG2a $\kappa$	BioLegend	FC 1:400
Dectin-1		polyclonal aa 2–20	rabbit		Pineda	WB 1:2000 IF 1:200
Dectin–1	PE	bg1fpj	rat	IgG2a $\kappa$	eBioscience	FC 1:100
Ly6C	APC-e780	HK1.4	rat	IgG2c $\kappa$	eBioscience	FC 1:200
Ly6G	BV570	1A8	rat	IgG2a $\kappa$	BioLegend	FC 1:200
Ly6G	FITC	1A8	rat	IgG2a $\kappa$	BD	FC 1:400
Ly6G	V450	1A8	rat	IgG2a $\kappa$	BD	FC 1:400
MerTK	PE-Cy7	DS5MMER	rat	IgG2a $\kappa$	eBioscience	FC 1:800
MHCII	APC	M5/114.15.2	rat	IgG2b $\kappa$	BioLegend	FC 1:300
MHCII	V500	M5/114.15.2	rat	IgG2b $\kappa$	BD	FC 1:200
pERK1/2		D13.14.4E	rabbit	IgG	Cell Signaling	WB 1:1000

Table 5 continued from previous page

Antigen	Conjugation	Clone/ Epitope	Host	Isotype	Company	Application
(T202/Y204)						
pSyk		C87C1	rabbit	IgG	Cell Signaling	WB 1:1000
(Y519/Y520)						
Sca-1	AF647	E13-161.7	rat	IgG2a $\kappa$	BioLegend	FC 1:800
SiglecH	PE	551	rat	IgG1 $\kappa$	BioLegend	FC 1:400
SPPL2a		polyclonal aa 77-94	rabbit		Pineda	WB 1:2000
tERK1/2		137F5	rabbit	IgG	Cell Signaling	WB 1:1000
TLR4		D8L5W	rabbit	IgG	Cell Signaling	WB 1:1000
tSyk		D3Z1E	rabbit	IgG	Cell Signaling	WB 1:1000
undirected	PE	eBR2a	rat	IgG2a $\kappa$	eBioscience	FC 1:100
$\beta$ -TCR	BV570	H57-597	hamster	IgG	BioLegend	FC 1:400

**Table 6: List of secondary antibodies.** HRP: horseradish peroxidase; WB: Western Blot; IF immunofluorescence. Dianova (Hamburg, Germany), Life Technologies, now Thermo Fisher Scientific.

Antibody	Conjugation	Host	Company	Application
Anti-rabbit IgG	HRP	goat	Dianova	WB 1:15000
Anti-rat IgG	HRP	goat	Dianova	WB 1:15000
Anti-rabbit IgG	Alexa Fluor 488	goat	Life Technologies	IF 1:300
Anti-rat IgG	Alexa Fluor 594	goat	Life Technologies	IF 1:300

### 2.1.4 Pattern recognition receptor ligands

Ligands for different pattern recognition receptors (PRR) from C-type-lectin (CLEC) and Toll-like receptor (TLR) families were used to activate immune cells.

**Table 7: Pattern recognition receptor ligands** Lipoarrabinomannan and Mannan were coated on bottom of plates. Toll-like receptor (TLR), C-type lectin-like receptors (CTLR), Mannose Receptor (MR). Invivogen (Toulouse, France), Nacalai Tesque (Kyoto, Japan), Sigma-Aldrich (Sigma).

Ligand	Solvent/ resuspended in	Stock concentration	Final quantity/ concentration	Company
Depleted Zymosan (dZym)	endotoxin-free water (Invivogen)	1 mg/mL	50 µg/mL	Invivogen
Heat-killed <i>M. tuberculosis</i> (HKMT)	endotoxin-free water (Invivogen)	10 mg/mL	250 µg/mL	Invivogen
Lipoarrabinomannan (LAM)	water (delivered solved)	1 mg/mL	200 ng/ 1.86 cm <sup>2</sup>	Nacalai Tesque
Lipopolysaccharides (LPS) O26:B06	water ≤ 1 EU/mL endotoxin (Sigma)	1 mg/mL	500 ng/mL	Sigma
Mannan	water ≤ 1 EU/mL endotoxin (Sigma)	10 mg/mL	10 µg/ 1.86 cm <sup>2</sup>	Sigma
Zymosan	endotoxin-free water (Invivogen)	10 mg/mL	50 µg/mL	Invivogen

## 2.2 Methods

### 2.2.1 Cell biological methods

#### 2.2.1.1 Analysis of DC populations in mice

**Table 8: Buffers for DC analysis in mice.** FACS: fluorescence-activated cell sorting; HBSS, PBS and RPMI were from Thermo Fisher Scientific or Sigma-Aldrich; Fetal calf serum (FCS) from Biochrom (Cambridge, United Kingdom), Collagenase IV from Worthington (New Jersey, USA), DNase I from Roche (Basel, Switzerland).

Buffer	Ingredients
Digestion buffer	1x HBSS + 2% FCS, 50 µg/mL DNase I + 75 IU/mL Collagenase IV
ACK solution	155 mM NH <sub>4</sub> Cl, 10 mM KHCO <sub>3</sub> , 0.1 mM EDTA; pH 7.4; filtered sterile
RPMI <sup>+</sup>	RPMI + 2% FCS
FACS buffer	PBS + 2% FCS

DC subsets were analysed in different murine organs in cooperation with Christian Lehmann (AG Dudziak, Department of Dermatology, University Hospital of Erlangen, Germany). Minced spleen, thymus and lymph nodes from mice were incubated in digestion buffer for 30 min at 37°C. Bone marrow was flushed from tibia and femur of mice hind legs with RPMI<sup>+</sup>. Cells from all sources were passed through a 100 µm cell strainer (BD Bioscience). Cells were sedimented for 10 min at 713 g and 4°C and were resuspended in ACK solution, if lysis of erythrocytes was necessary. The reaction was stopped by addition of RPMI<sup>+</sup> after five minutes at room temperature. In all cases, cells were rinsed through a 40 µm cell strainer (BD Bioscience) with RPMI<sup>+</sup>. Cell numbers were determined after three washes with RPMI<sup>+</sup>. Up to 10<sup>6</sup> cells were used for antibody labelling. All further steps were performed in the dark at 4°C. Biotin-coupled anti-CD115 diluted in FACS buffer was incubated on cells for 30 min first. Labelling of cells with directly fluorophore coupled antibodies and streptavidin-Pe-Cy7 (BioLegend, 1:1000) was performed in FACS buffer for 30 min as second staining step (see table 5 and 6). Cells were washed twice after each staining step and resuspended in FACS buffer supplemented with DAPI prior to flow cytometric analysis with a LSR Fortessa (BD Bioscience) cell analyser. FlowJo software (Tree Star, Inc., Ashland, OR, USA) was used for data evaluation.

The evaluation of cell populations in organs was performed by Christian Lehmann. Doublets of cells were excluded by side-scattered light area (SSC-A) and forward-scattered light width (FSC-W). DAPI positive cells were excluded in a SSC-A to DAPI dot plot. Cells were selected in FSC-A to SSC-A dot plot. Cells other than DCs were excluded. DCs were defined as CD3<sup>-</sup>/Ly6G<sup>-</sup>CD11b<sup>low</sup>CD161<sup>-</sup>. Conventional and plasmacytoid DCs (cDCs and pDCs) were defined by a CD11c to PDCA-1 plot. While pDCs showed high PDCA-1 and intermediate CD11c surface expression (PDCA-1<sup>high</sup>CD11c<sup>int</sup>), cDCs were PDCA-1<sup>int</sup>CD11c<sup>high</sup>. Further subdivi-

sion of cDCs was performed in a CD11b to Ly6C dot plot. Two population were defined as CD8<sup>+</sup> (cDC1) and CD11b<sup>+</sup> (cDC2).

### 2.2.1.2 Generation of bone marrow–derived immune cells

**Table 9: Cell culture media.** RPMI 1640 and Dulbecco's modified Eagle Medium (DMEM; Thermo Fisher Scientific, Waltham, Massachusetts, United States), fetal calf serum (FCS; Biochrom), penicillin and streptomycin (Sigma–Aldrich).

Medium	Ingredients
BMDC medium	RPMI 1640 + 10% (v/v) FCS + 50 mM $\beta$ -mercaptoethanol + 100 U/mL penicillin + 100 $\mu$ g/mL streptomycin
BMDM medium	DMEM + 20% (v/v) FCS + 100 U/mL penicillin + 100 $\mu$ g/mL streptomycin

Hind legs of mice were kept on ice in phosphate buffered saline (PBS; Sigma–Aldrich, endotoxin tested) until preparation. Legs were handled wearing Vasco<sup>®</sup> OP sensitive single use surgical gloves (B Braun, Melsungen, Germany) underneath a laminar flow work bench. Connective tissue was removed from bones using sterile gauze swabs (Lohmann & Rauscher, Regensdorf, Germany). Tibia and femur were cut open on both sides. Single–use forceps (Servopax GmbH, Wesel, Germany) were used for holding and single–use scalpels (B Braun, Tuttlingen, Germany) were used for cutting per mouse leg pair. Bone marrow was flushed into a petri dish with 5–10 mL of BMDC medium using a 27G x 3/4" cannula (Henke Sass Wolf, Tuttlingen, Germany). Cells were separated by flushing through a 23G x 1 1/4" cannula (Henke Sass Wolf). The resulting suspension was passed through a 100  $\mu$ m cell strainer (BD Bioscience) into a 50 mL tube and kept on ice. An aliquot of suspension was diluted 1:5 and then mixed 1:2 with trypan blue (0.4%, Life technologies) to stain dead cells. Numbers of viable cells were determined by counting in a C-Chip Neubauer Improved Disposable Hemocytometer (NanoEnTek Inc, Seoul, Korea) and calculation according to the manufacturer's instructions.

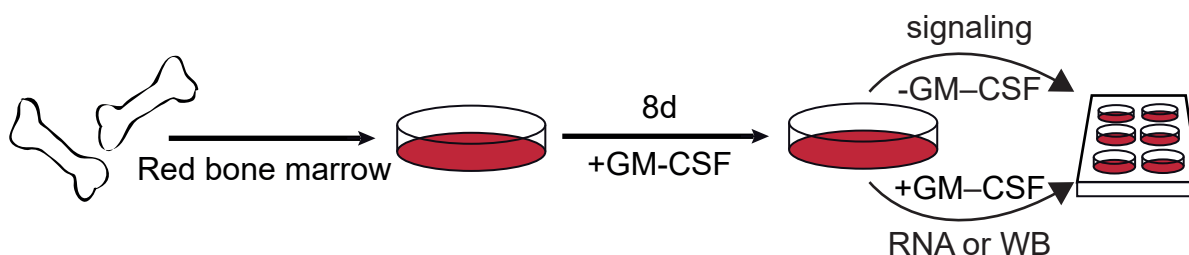


**Figure 9: Scheme of BMDC generation.** Bone marrow was obtained from murine tibia and femur by flushing. Cells were cultured in DC medium supplemented with the growth factor GM–CSF for eight days. Afterwards, suspension and adherent cells were collected. For signalling analysis by Western Blot cells were re–seeded without growth factor. For longer cultivation periods, as for stimulation experiments for mRNA isolation or enzyme–linked immunosorbent assay (ELISA) analysis, GM–CSF was added.

Generation of bone marrow–derived DCs (BMDCs) based on the protocol by Lutz *et al.*, 1999 with minor changes.  $5 \times 10^6$  cells were seeded within 10 mL BMDC medium supplemented with 20 ng/mL recombinant murine GM–CSF (Immunotools, Friesoythe, Germany) into a 10 cm petri dish (Sarstedt). Cells were cultured at 37 °C, 5% CO<sub>2</sub> under humidified air conditions. After three days, 10 mL BMDC medium supplemented with 20 ng/mL GM–CSF were added. After another three days, 10 mL of culture were centrifuged for 10 min at 210 g and room temperature (RT). The sedimented cells were resuspended in 10 mL BMDC medium supplemented with 10 ng/mL GM–CSF and added back to the culture. Suspension and adherent cells were used for experiments or direct analysis after a total culture period of eight days. Suspension cells were collected in a 50 mL tube. The dish was rinsed with PBS, which was collected as well. Adherent cells were detached with Accutase (Thermo Fisher Scientific) for 10 min at 37 °C. The cells were washed off the dish and added to the collected cells into the 50 mL tube. Cells were sedimented for 10 min at 210 g at RT and resuspended in BMDC medium. Counting of cell number was performed as described above using trypan blue to exclude dead cells. BMDCs were seeded out for experiments as described in table 10.

**Table 10: Overview of BMDC seeding for experiments.** Penicillin (Pen) streptomycin (Strep)

Assay	Plate format	Medium	GM–CSF	Volume	Cells/mL
ELISA	24–well	BMDC medium	10 ng/mL	1 mL	$0.5 \times 10^6$ cells/mL
ELISA of BCG co-culture	24–well	BMDC medium without Pen/Strep	10 ng/mL	1 mL	$0.5 \times 10^6$ cells/mL
RNA expression analysis	6–well	BMDC medium	10 ng/mL	1 mL	$1.5 \times 10^6$ cells/mL
RNA expression analysis of BCG co-culture	6–well	BMDC medium without Pen/Strep	10 ng/mL	1 mL	$1.5 \times 10^6$ cells/mL
Western Blot protein expression analysis	6–well	BMDC medium	10 ng/mL	1 mL	$1.5 \times 10^6$ cells/mL
Western Blot signalling analysis	6–well	RPMI medium without additions	-	1 mL	$1.5 \times 10^6$ cells/mL

Bone marrow–derived macrophages (BMDMs) were generated as described for BMDCs with modifications, according to a protocol based on Zhang *et al.*, 2008. Front legs were included to obtain additional bone marrow. Bones were flushed with BMDM medium.  $3 \times 10^7$  cells were seeded in 10 mL BMDM medium supplemented with 50 ng/mL recombinant murine Macrophage colony–stimulating factor (M–CSF, Immunotools). Three days later, 5 mL BMDM medium containing 50 ng/mL M–CSF were added. Only adherent cells were used for experiments after a total culture period of seven days. Per well of a 24–well plate,  $0.5 \times 10^6$  cells in 1 mL BMDM medium supplemented with 50 ng/mL M–CSF were seeded out for subsequent ELISA analysis.

### 2.2.1.3 Co-culture of BMDCs with *Mycobacterium bovis* Bacille Calmette–Guérin

**Table 11: BCG medium.** Oleic albumin dextrose catalase (OADC)

Component	Concentration	Company		
Middlebrook-7H9-Bouillon	0.47% (w/v)	BD Bioscience	autoclaved	filtered sterile
Tween 80	0.045% (v/v)	Sigma–Aldrich		
Middlebrook OADC	10% (v/v)	Sigma–Aldrich		

*Mycobacterium bovis* Bacille Calmette–Guérin (BCG; Pasteur ATCC 35734) was obtained from Prof. Dr. Ullrich Schaible (Research center Borstel, Germany). Bacteria were stored at -80 °C in 1 mL Middlebrook 7H9 medium supplemented with albumin dextrose catalase (Difco Labs, Detroit, MI, USA) containing 30% glycerol. Two aliquots were thawed and added to 13 mL BCG medium (Table 11). Bacteria were cultured in a upright standing 25 cm<sup>2</sup> tissue culture flask with a ventilation cap at 37 °C shaking at 150–200 rpm for two weeks. Cultures were split 1:5 all two to three days.

Live BCGs were prepared as follows for co-culture with BMDCs. Bacteria were sedimented for 10 min at 3452 g and 4 °C and washed once with PBS (Sigma–Aldrich, endotoxin tested). The mycobacteria were resuspended in 1 mL PBS by pipetting five times through a 27G x 3/4" cannula (Henke Sass Wolf). A 1:10 dilution of the bacterial culture was prepared in 4% paraformaldehyde (PFA) for determination of bacterial cell number. The optical density (OD) was measured at 595 nm with a GeneQuant Pro photometer (Biochrom). An OD of 0.1 corresponded to 5 × 10<sup>6</sup> bacteria/mL in this dilution. Bacteria were diluted in BMDC medium without penicillin and streptomycin and added to BMDC culture in a multiplicity of infection (MOI) of 10.

### 2.2.1.4 Stimulation of immune cells with different PRR ligands

Stimulation of BMDCs and BMDMs with different ligands (Table 7) was performed for indicated durations. In untreated samples (-) an equivalent volume of the respective solvent was added. For subsequent ELISA analysis, treatment was performed in technical duplicates.

The ligands Mannan and LAM were coated on the well-plate bottom before BMDCs were seeded on top. The respective amount of ligand was added to 250 µL water (endotoxin ≤ 1 EU/mL; Sigma–Aldrich) within one well of a 24-well plate. Wells with 250 µL water (endotoxin ≤ 1 EU/mL; Sigma–Aldrich), but without ligand, served as untreated controls (-). The plate was left to dry without lid within the fume hood over night at RT.



LEAF™ Purified anti–mouse IL–10 (BioLegend; clone JES5–2A5) and LEAF™ Purified Rat IgG1,  $\kappa$  (BioLegend; clone RTK2071) were used at 10 ng/mL to block IL–10 in supernatants from BMDCs in indicated experiments.

ATP (Sigma–Aldrich) was added in indicated experiments to activate the inflammasome (Perregaux and Gabel 1994). After 4 h of stimulation with 250  $\mu$ g/mL HKMT, 5 mM ATP were added for 30 min.

### 2.2.1.5 Indirect immunofluorescence

Cover slips (CS) were coated with 100  $\mu$ g/mL poly–L–lysine (Sigma–Aldrich) in 6–well plates over night at room temperature (RT). Afterwards, CS were rinsed with water (endotoxin  $\leq$  1 EU/mL; Sigma–Aldrich) three times for one hour. BMDCs were collected as described in section 2.2.1.2 and  $1.5 \times 10^5$  cells were seeded in 1 mL RPMI medium without any additions per well of the 6–well plate. Cells were left to adhere to the poly–L–lysine coated CS for two hours at 37°C, 5% CO<sub>2</sub> and humidified air conditions.

**Table 12: Indirect immunofluorescence buffers.** Sigma: Sigma–Aldrich

Buffer	Ingredients
PBS pH 7.4	137 mM NaCl, 2.7 mM KCl, 10 mM Na <sub>2</sub> HPO <sub>4</sub> , 1.8 mM KH <sub>2</sub> PO <sub>4</sub>
Permeabilization buffer	0.2% (w/v) saponine in PBS
Quenching buffer	0.12% (w/v) glycine + 0.2% (w/v) saponine in PBS
Blocking buffer	10% (v/v) FCS + 0.2% (w/v) saponine in PBS
Embedding buffer	17% (w/v) Mowiol 4-88 (EMD Millipore) + 33% (v/v) glycerol + 20 mg/mL DABCO (Sigma) + 1 $\mu$ g/mL DAPI (Sigma) in PBS

For indirect immunofluorescence, CS were rinsed three times with PBS (see Table 12). Cells were fixed with 4% PFA in PBS for 20 min at RT. After three washes with PBS, cells were incubated in permeabilization buffer for 5 min at RT. Free aldehyde groups were blocked with quenching buffer for 10 min at RT. After one washing step with permeabilization buffer, CS were incubated in blocking buffer for at least one hour at RT. Primary and secondary antibodies (Tables 5 & 6) were diluted in blocking buffer. A volume of 50  $\mu$ L antibody solution was used per CS. Staining with the primary antibodies was performed in a wet chamber over night at 4°C. The next day, CS were rinsed five times in permeabilization buffer. CS were incubated with secondary antibody solution in a wet chamber for one hour at RT. CS were rinsed five times in permeabilization buffer and two times in distilled water. Cover slips were mounted in embedding buffer on glass slides and dried at 4°C prior to microscopic analysis. Pictures were acquired with a FV1000 confocal laser scanning microscope (Olympus) equipped with an U Pan S Apo 100 x oil immersion objective (N.A. 1.40) and the Olympus Fluoview Software.

### 2.2.1.6 Flow cytometric analysis of BMDCs

**Table 13: Buffer for flow cytometry.** BSA: bovine serum albumin

Buffer	Ingredients
MACS buffer	BSA (Albumin fraction V) 0.5% (w/v) EDTA 2 mM in PBS pH 7.4

Suspension and adherent BMDCs were collected as described in section 2.2.1.2. Cells were fixed and permeabilized using the BD Cytofix/Cytoperm™ kit (BD Bioscience) according to manufacturer's protocol for subsequent staining of total protein. Cells were not pre-treated for staining of cell-surface antigens. Antibodies were diluted in BD Perm/wash™ buffer from the fix/perm kit for total protein staining or in magnetic activated cell sorting (MACS) buffer for surface protein staining (Table 5).  $1 \times 10^4$  cells were incubated with antibody solution in the dark for 30 min on ice. After washing and resuspension in MACS buffer, cells were subjected to flow cytometric analysis using a FACSCanto II flow cytometer (BD Bioscience). Flow cytometry data were analysed with FlowJo software (Tree Star). Cell populations were gated according to their expression of CD11c, MHCII and CD11b as described in detail in section 3.1.3. Subsequent calculations were performed in Excel (Microsoft). Graphs were plotted and statistical analysis was performed with GraphPad Prism software.

## 2.2.2 Biochemical methods

### 2.2.2.1 Preparation of protein extracts

**Table 14: Buffers for protein extract preparation.**

Buffer	Ingredients
PBS complete	PBS pH 7.4 4 mM EDTA, pH 8 1x Complete protease inhibitor cocktail (Roche)
Lysis buffer	50 mM Tris-HCl, pH 7.4 150 mM NaCl 1% (w/v) Triton X-100 0.1% (w/v) SDS 1x Complete protease inhibitor cocktail 4 mM Pefabloc® SC Protease Inhibitor (Carl Roth) 0.5 µg/mL Pepstatin A (Sigma-Aldrich) 4 mM EDTA

Table 14 continued from previous page

Buffer	Ingredients
Lysis buffer with phosphatase inhibitors	Lysis buffer 20 mM $\beta$ -glycerophosphate 4 mM sodiumorthovanadate 20 mM NaF 1x phosphatase inhibitor mix (Roche)
5x SDS–PAGE loading buffer	625 mM Tris-HCl, pH 6.8 500 mM DTT 50% (v/v) glycerol 5% (w/v) SDS Bromphenol blue
4x Tricine–PAGE loading buffer	150 mM Tris-HCl, pH 6.8 40 mM DTT 40% glycerol 4% (w/v) SDS 0.05% (w/v) Coomassie Blue G-250

Suspension BMDCs were transferred to a 1.5 mL tube and centrifuged for 10 min at 210 g and 4°C. Adherent cells were scraped off in PBS complete. Already collected suspension cells and adherent cells were combined and sedimented as described before. Adherent BMDMs were washed once with PBS pH 7.4 and then harvested by scraping into PBS complete. Cells were centrifuged at 210 g for 10 min at 4°C. Cells were lysed in lysis buffer with or without phosphatase inhibitors by pipetting. Lysis was performed on ice for one hour or 30 min for analysis of phosphorylated proteins. During this incubation, samples were sonicated at level 4 for 20 sec at 4°C using Branson Sonifier 450 (Emerson Industrial Automation, Danbury, Connecticut). Afterwards, samples were centrifuged for 10 min at 17,000 x g and 4°C. Suspension was transferred into a fresh 1.5 mL tube. 5  $\mu$ L lysate was used for measurement of protein concentration. The appropriate volume of 5x sodium dodecyl sulfate–polyacrylamide gel electrophoresis (SDS–PAGE) loading buffer was added to the remaining sample. 4x Tricine–SDS loading buffer was added instead for Western blot detection of CD74. Samples were denaturated for 5 min at 56°C or 95°C depending on proteins detected afterwards.

### 2.2.2.2 Determination of protein concentration

Protein concentrations of cell lysates were measured in a 96-well plate using Pierce™ bicinchoninic acid (BCA) Protein Assay Kit (Thermo Fisher Scientific, Waltham, MA, USA) according to manufacturer's protocol. In brief, samples were diluted 1:10 in water in a total volume of 25  $\mu$ L. A bovine serum albumin (BSA) standard curve ranging from 2  $\mu$ g/mL to 0  $\mu$ g/mL was used. BCA solution was prepared by mixing solution A and B in a ratio of 1:50. To each measurement 200  $\mu$ L BCA solution were added and incubated for 30 min at 37°C. Absorbance was measured at 562 nm using the Synergy HT multi detection reader (BioTek, Winooski, VT, USA). Afterwards, concentrations were calculated by use of the linear standard curve in Excel (Microsoft).

### 2.2.2.3 Biotinylation of BMDC surface proteins

**Table 15:** Buffers for biotinylation of surface proteins.

Buffer	Ingredients
PBS-CM	0.1 mM CaCl <sub>2</sub> + 1 mM MgCl <sub>2</sub> in PBS, pH 8
Biotin solution	1 mg/mL Sulfo-NHS-SS-Biotin (Thermo Fischer Scientific) in PBS-CM
Quenching buffer	50 mM Tris-HCl in PBS, pH 8
Pulldown buffer	50 mM Tris-HCl, pH 7.4 150 mM NaCl 1% (w/v) Triton X-100 0.1% (w/v) SDS 1x Complete protease inhibitor cocktail 4 mM EDTA, pH 8.0

Suspension and adherent cells from 10 cm dishes were recovered as described above (section 2.2.1.2). BMDCs were centrifuged for 10 min at 210 g and 4°C. Cells were washed twice with PBS-CM to adjust the pH and remove proteins derived from the cell culture media. Suspension cells were split equally. One half of cells was resuspended in biotin solution (+biotin). PBS-CM was added to the other half of the cells as a control (-biotin). Active biotin bound to primary amines of surface proteins during incubation of 30 min on ice. Cells were sedimented and resuspended in quenching buffer, containing primary amines, to stop the biotinylation reaction for 10 min on ice. Two washing steps were performed with PBS-CM. Cells were lysed in 600  $\mu$ L pulldown buffer for one hour on ice. Samples were sonicated and protein concentrations were determined as described above (Sections 2.2.2.1 & 2.2.2.2). Sample concentrations were adjusted to lowest concentrated sample by addition of pulldown buffer.

Per sample, 100  $\mu$ L immobilized streptavidin beads (Thermo Fischer Scientific) were equilibrated. Therefore, beads were sedimented for 1 min at 6000 rpm and 4°C and resuspended in 1 mL pulldown buffer. Beads were washed three times on a rotating wheel for 5 min at 4°C. 500  $\mu$ L sample were added to dry beads. Beads and sample were incubated on a rotating wheel to ensure proper binding of biotinylated proteins to streptavidin at the beads for one hour at 4°C. Appropriate volumes of 5x SDS–PAGE loading buffer were added to the remaining cell lysates (input). After incubation, beads were centrifuged. The supernatant, containing proteins which did not bind to the streptavidin–beads, was added to 5x SDS–PAGE loading buffer (unbound). The beads were washed five times in pulldown buffer to remove unbound proteins. 100  $\mu$ L 1x SDS–PAGE loading buffer was added to the dry beads (bound). All three probes (input, unbound & bound) per sample were denatured for 5 min at 95°C or 56°C and afterwards for 15 min at 37°C.

#### 2.2.2.4 Glycine–SDS PAGE

**Table 16: Buffers for Tris–Glycine–SDS gel electrophoresis.**

Buffer	Ingredients
Stacking gel buffer	0.5 M Tris-HCl, pH 6.8 0.4% (w/v) SDS
Separating gel buffer	1.5 M Tris-HCl, pH 8.8 0.4% (w/v) SDS
Electrophoresis buffer	0.193 M Glycine 25 mM Tris 0.1% (w/v) SDS

Electrophoretic separation of proteins was performed using Glycine–SDS–PAGE (also called Laemmli–SDS–PAGE), if not indicated otherwise. The system based on an discontinuous Tris–glycine buffer system, according to Laemmli 1970. Gels of 1.5 mm thickness containing 10% or 12.5% acrylamide in their separating gel were cast, depending on the molecular weight of the protein of interest. Used buffers are listed in table 16. The pipetting scheme is shown in table 17. The separation gel was prepared with 7.5 mL (5.5 cm height of gel) of the respective separating gel mixture. The casting chamber was filled with the stacking gel mixture after polymerisation of separating gel. Each gel contained ten pockets for loading of 20  $\mu$ g protein. 10–20  $\mu$ L of bound fraction from biotinylation of surface proteins were used (Section 2.2.2.3). PageRuler Plus Prestained Protein Ladder (Thermo Fisher Scientific) was applied for size determination of proteins. Electrophoresis was performed in a Mini-PROTEAN® Electrophoresis System (BioRad) in electrophoresis buffer at 80–120 V for 2–3 hours.

**Table 17: Pipetting scheme for Tris–Glycine–SDS gels.** Buffer compositions are listed in table 16.

<b>Solution</b>	<b>5.25% Stacking gel</b>	<b>10% Separating gel</b>	<b>12,5% Separating gel</b>
Stacking gel buffer	1.35 mL	0 mL	0 mL
Separating gel buffer	0 mL	2.6 mL	2.6 mL
30% acrylamide/bisacrylamide (Roti-phores <sup>®</sup> Gel 30 [37,5:1])	1.75 mL	3.3 mL	4.2 mL
ddH <sub>2</sub> O	6.85 mL	4 mL	3.1 mL
10% (w/v) APS	60 $\mu$ L	60 $\mu$ L	60 $\mu$ L
TEMED	30 $\mu$ L	30 $\mu$ L	30 $\mu$ L

### 2.2.2.5 Tricine–SDS PAGE

**Table 18: Buffers for Tris–Tricine–SDS gel electrophoresis.**

<b>Buffer</b>	<b>Ingredients</b>
3x Gel buffer	3 M Tris–HCl, pH 8.45 0.3% (w/v) SDS
Anode buffer	200 mM Tris–HCl, pH 8.9
Cathode buffer	100 mM Tris–HCl, pH 8.25 100 mM Tricine 0.1% (w/v) SDS

Separation of proteins smaller than 30 kDa, as it is the case for the CD74 NTF, was performed using Tricine–SDS–PAGE (Schägger and Jagow 1987, Schägger 2006). Gels of 1.5 mm thickness were cast using the solutions listed in tables 18 and 19. Separating gel (16% acrylamide) was cast 4.5 cm high (5.7 mL) and covered directly with 1 cm (1.3 mL) of intermediate gel (10% acrylamide). Casting chamber was filled with stacking gel (4% acrylamide) after intermediate and separating gel polymerised. Gels contained ten pockets for loading of 20  $\mu$ g protein or Spectra Multicolor Low Range Protein Ladder (Thermo Fisher Scientific) for size determination of proteins. Gels were run in a Mini-PROTEAN<sup>®</sup> Electrophoresis System (BioRad). Two different buffers were used at anode and cathode for electrophoresis at 30–80 V for approximate 6 hours (Table 18).

**Table 19: Pipetting scheme for Tris–Tricine–SDS gels.** Buffer ingredients are described in table 18.

<b>Solution</b>	<b>Stacking gel (4%)</b>	<b>Intermediate gel (10%)</b>	<b>Separating gel (16%)</b>
50% acrylamide/ bisacrylamide (16.6:1, Applichem)	0 mL	0 mL	3.29 mL
30% acrylamide/ bisacrylamide (37.5:1)	1.37 mL	3.18 mL	0 mL
2% biscacrylamide	91 µL	261 µL	338 µL
3x Gel buffer	2.5 mL	3.33 mL	3.33 mL
Urea			3.6 g
ddH <sub>2</sub> O	ad 10 mL	ad 10 mL	ad 10 mL
10% (w/v) APS	75 µL	50 µL	33.3 µL
TEMED	7.5 µL	10 µL	10 µL

### 2.2.2.6 Western Blotting

**Table 20: Buffers for Western Blotting.**

<b>Buffer</b>	<b>Ingredients</b>
Semidry transfer buffer	192 mM glycine 25 mM Tris 20% (v/v) Methanol
Electrode buffer	300 mM Tris, pH 8.6 100 mM acetic acid

Proteins were transferred from gels onto nitrocellulose membranes (Whatman<sup>®</sup> Protran<sup>®</sup> nitrocellulose membrane, 0.2 µm pore size, Whatman GmbH, Dassel, Germany). Blotting filter papers (Whatman<sup>®</sup> gel blotting paper, Whatman GmbH) and the nitrocellulose membranes were equilibrated with semidry transfer buffer (Table 20) after Tris–Glycine–SDS PAGE. A sandwich comprising of two blotting filter papers, the membrane, the gel and another two blotting filter papers was assembled from anode to cathode in a Trans-Blot (R) SD Semi-Dry Transfer Cell (BioRad). Proteins were transferred at constant current of 65 mA per blot for two hours at room temperature. Transfer from Tris–Tricine–SDS gels was performed using Electrode buffer for moistening of blotting filter papers and membranes. Current was set constant to 20 mA for 16 h at 4°C.

### 2.2.2.7 Immunodetection

**Table 21: Buffers for immunodetection of proteins.**

Buffer	Ingredients
TBS–T	137 mM NaCl 25 mM Tris-HCl, pH 7.4 2.7 mM KCl 0.1% (v/v) Tween 20
Milk in TBS–T	5% (w/v) milk powder in TBS–T
BSA in TBS–T	5% (w/v) BSA in TBS–T
ECL	50 $\mu$ L Lumigen ECL Ultra Solution A (Lumigen, Michigan, USA) 50 $\mu$ L Lumigen ECL Ultra Solution B (Lumigen) 1 mL 1.4 mM Luminol in 0.1 M Tris-HCl, pH 8.8 100 $\mu$ L 6.7 mM p-coumaric-acid in DMSO 3 $\mu$ L 30% H <sub>2</sub> O <sub>2</sub>

Binding sites on membranes were blocked with milk in tris buffered saline with 0.1% Tween 20 (TBS–T) after protein transfer. BSA in TBS–T was used instead when phosphorylated proteins were detected. Primary antibodies were diluted in BSA in TBS–T when phosphorylated proteins were detected, otherwise milk in TBS–T was used. Antibody dilutions were applied to the membranes over night at 4 °C. The next day, membranes were washed quickly three times with TBS–T and then over 30 min in TBS–T at RT. The respective horseradish peroxidase (HRP)–conjugated secondary antibody diluted in milk or BSA in TBS–T was applied to the membranes for 1 h at RT. After washing as described before, membranes were incubated in ECL solution. Chemiluminescent signals were detected using the ImageQuant™ LAS4000 (GE Healthcare, Little Chalfont, UK). Signal intensities were measured with ImageJ software. Calculations were performed in Excel (Microsoft). Graphs were plotted and statistical analysis was performed with GraphPad Prism software.

### 2.2.2.8 Measurement of secreted cytokines in conditioned media by ELISA

For harvesting of conditioned media, cell culture plates were cooled on ice. Medium was transferred into 1.5 mL reaction tubes to harvest cytokine–containing supernatants. Remaining cells within the medium were removed by centrifugation for 10 min at 210 g and 4 °C. Supernatants were transferred into a new 1.5 mL reaction tube. Cell debris was sedimented at 17,000 x g



for 10 min at 4°C. Supernatants were recovered and either stored at -20°C or directly used for cytokine measurements.

Samples were directly used for cytokine measurement with the Proteome Profiler™ Mouse XL Cytokine Array Kit (R&D systems, Bio–techne, Minneapolis, Minnesota, USA) according to manufacturer’s protocol. Technical replicates were combined from supernatants of dZym treated *wt* or *SPPL2a*<sup>-/-</sup> BMDCs and used for one membrane of the array. Chemiluminescent signals were detected with the ImageQuant™ LAS4000. Signal intensities were measured with ImageJ software using the Protein Array Analyzer tool. Calculations were performed in Excel (Microsoft). Graphs were plotted with GraphPad Prism software.

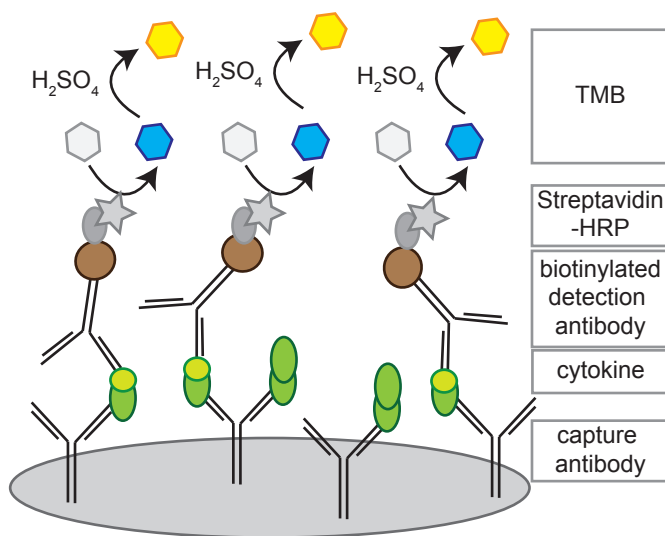


**Figure 10: Composition of the Duo Set ELISA.** The capture antibody adheres to high binding ELISA plates before recognition of a specific epitope at a certain cytokine. The biotinylated detection antibody is directed against another epitope of the cytokine. This is of special importance to distinguish IL–12 family members and to exclude false signals. HRP–coupled streptavidin attaches to biotin. The enzyme catalyses colorless 3,3',5,5'-Tetramethylbenzidine (TMB) into a blue coloured diimine. The addition of sulphuric acid stops the reaction and leads to a yellow color, which absorbance can be measured at 450 nm.

Enzyme–linked–immunosorbent assays (ELISAs) were performed according to manufacturer’s protocol (Due Set, R&D systems), but with half of the volumes indicated (Scheme see figure 10). High–binding ELISA plates (Sarstedt) were coated with capture antibodies solved in PBS (Sigma–Aldrich) over night at RT. Remaining binding sites were blocked with 1% (w/v) BSA in PBS for at least one hour at RT after three washes with 0.05% (v/v) Tween in PBS. Conditioned media was either used directly or diluted in respective culture medium. Serial dilution of respective recombinant cytokine of known concentration was prepared in culture medium and served as standard control. Conditioned media and standard were incubated on plates for two hours at RT. The capture antibody binds the targeted cytokine during that time. Unbound cytokines and medium were washed off, as described before. Biotin–conjugated detection antibody was diluted in 1% BSA in PBS (0.1% BSA with 0.05% Tween in TBS for IL–2 ELISA) and let bind to captured cytokines for two hours at RT. Excessive antibody was washed off, as described before. HRP–coupled streptavidin was diluted in 1% BSA in PBS (0.1% BSA with 0.05% Tween in TBS for IL–2 ELISA) and incubated for 20 min on plates at RT. The biotin from the detection antibodies couple to the HRP enzyme by binding to streptavidin. After three washing steps,

substrate solution BM blue POD substrate, soluble (Roche) was added to each well. It contains colorless 3,3',5,5'-Tetramethylbenzidin (TMB) and H<sub>2</sub>O<sub>2</sub>. HRP reduces hydrogen peroxide and oxidises thereby TMB, which becomes a blue color thereby. The addition of acid like 1 M H<sub>2</sub>SO<sub>4</sub> after 20–40 min stops the reaction and the solution turns yellow. Absorbance was measured at 450 nm and 690 nm as control reference with the Synergy HT multi detection reader. Standard curves and concentrations of samples were calculated with Excel (Microsoft). Graphs were plotted and statistical analysis was performed with GraphPad Prism software.

### 2.2.2.9 Lactate dehydrogenase cytotoxicity assay

Damaged cells release cytosolic proteins as lactate dehydrogenase (LDH). The activity of this enzyme can be measured by a coupled enzymatic test. LDH catalyses the conversion of lactate to pyruvate and reduces thereby the coenzyme NAD<sup>+</sup> to NADH. The latter donates electrons for the diaphorase mediated conversion of the yellow tetrazolium salt into a red formazan product. The latter absorbance can be measured at 490 nm.

BMDCs were seeded in 96–well round bottom plates at a density of 1.5x10<sup>6</sup> cells/mL in 200 µL per well. They were treated in technical duplicates with 250 µg/mL HKMT for 24 h or left untreated. In addition, cells were lysed with lysis solution from the Pierce LDH Cytotoxicity Assay (Thermo Fischer Scientific) for 30 min prior to LDH cytotoxicity assay and served as positive control. Supernatants were transferred as technical triplicates á 50 µL to a 96–well flat bottom plate. Medium was used as blank. The assay was performed according to manufacturer's protocol. Absorbance was measured at 490 nm and at a reference value of 680 nm with the Synergy HT multi detection reader. Calculations were performed with Excel (Microsoft). Graphs were plotted and statistical analysis was performed with GraphPad Prism software.

### 2.2.3 Molecular biology methods

#### 2.2.3.1 Genotyping of *SPPL2a*<sup>-/-</sup> and *CD74*<sup>-/-</sup> mice

Mice tail biopsies were digested in DirectPCR<sup>®</sup> Tail (Peqlab Biotechnologie GmbH, Erlangen, Germany) supplemented with 200 µg/mL proteinase K (Roche) shaking at 750 rpm at 56 °C over night. Subsequently, the enzyme was inactivated by heating the samples for 45 min at 85 °C. Samples were centrifuged for one minute at 17,000 x g to remove debris and hair particles. Oligonucleotides (primer) listed in table 22 were used for determination of mice genotypes. A polymerase chain reaction (PCR) using two primers spanning exon 2 of *SPPL2a* served for genotyping of *SPPL2a*–deficient mice. A PCR comprising three primers was used for determination of *CD74*–deficient mice. A typical pipetting scheme is shown in table 23.

**Table 22: Primers for mouse genotyping.** Primers were ordered at Sigma–Aldrich; ko: knockout; Fw: forward; Rv: reverse.

Gene	Primer	Sequence 5' to 3'	wt product	ko product
<i>SPPL2a</i>	mSPPL2a-Exon2-Fw	AAACTCATTGAAGGACTTGCTC	242 bp	1323 bp
	mSPPL2a-Exon2-Rv	TTTCTAGGGAAGTTGGAAGTC		
<i>CD74</i>	mCD74-Geno-Fw	GGCTAGGTCCCAGTGTAGGC	1100 bp	1400 bp
	mCD74-wt-Rv	AATCAGCGCTCAAGGTCACT		
	mCD74-ko-Rv	CGCTGACAGCCGGAACACGG		

**Table 23: Genotyping pipetting scheme.** Components from Thermo Fisher Scientific.

Solution	Volume
2 mM dNTPs	2.5 µL
DMSO	1.25 µL
10x DreamTaq Buffer	2.5 µL
Forward primer	1 µL
Reverse primer(s)	1 µL
DreamTaq DNA polymerase	0.25 µL
Template	1 µL
ddH <sub>2</sub> O	ad 25 µL

Polymerase chain reaction was performed to amplify genomic deoxyribonucleic acid (DNA) in a thermo cycler (protocols shown in table 24).

**Table 24: PCR protocols for genotyping.**

Step	CD74 PCR			SPPL2a PCR		
	Duration	Temp.	Cycles	Duration	Temp.	Cycles
Initial denaturation	3 min	94 °C	35	5 min	95 °C	40
Denaturation	30 sec	94 °C		15 sec	95 °C	
Annealing	1 min	66 °C		30 sec	55 °C	
Elongation	1.5 min	72 °C		3 min	72 °C	
Final elongation	2 min	72 °C		3 min	72 °C	
Pause	∞	10 °C		∞	10 °C	

### 2.2.3.2 Agarose gel electrophoresis

Agarose gel electrophoresis was performed to separate and visualise PCR products from genotyping (section 2.2.3.1). Agarose gels of 2% were prepared by melting 8 g agarose (Biozym Scientific GmbH, Hess. Oldendorf, Germany) in 400 mL TAE buffer (Table 25). After boiling, ethidiumbromide (Roth) was added and the solution was poured into the casting form. Appropriate volumes of 6x DNA loading dye (Thermo Fisher Scientific) were added to PCR samples prior to loading on the agarose gel. GeneRuler 1 kb or 100 bp Plus DNA Ladder (Thermo Fisher

Scientific) were used to determine the approximate size of PCR products. After electrophoresis at 120 V for 20–30 min, PCR products were visualized using Gel Jet Imager (Intas, Göttingen, Germany) at a wavelength of 312 nm.

**Table 25: Buffer for agarose gel electrophoresis.**

Buffer	Ingredients
TAE buffer	40 mM Tris 19.2 mM acetic acid 1 mM EDTA pH 8.0

### 2.2.3.3 RNA isolation

NucleoSpin RNA Plus Kit (Machery-Nagel, Düren, Germany) was applied to isolate RNA from BMDCs. Suspension cells were centrifuged for 10 min at 210 g and RT. Adherent cells were lysed directly in culture dish in LBP–buffer from the kit without prior detachment. Lysed adherent cells were added to sedimented suspension cells. Lysates were either shock frozen in liquid nitrogen and stored at -80°C or directly processed for RNA isolation according to the manufacturer’s protocol. Isolated RNA was stored at -80°C.

### 2.2.3.4 Complementary DNA synthesis

RevertAid First Strand cDNA Synthesis Kit (Thermo Fisher Scientific) was used for generation of complementary DNA (cDNA). Concentration and purity of prepared RNA samples were quantified photometric at absorbance wavelength of 260 nm with 320 nm as reference and 280 nm to determine phenol contamination (260/280 ratio should be 2 for no contamination) with Synergy HT multi detection reader (BioTek, Winooski, Vermont). Up to 1 µg RNA were used for cDNA synthesis. Equal RNA amounts were used within each experiment. RNA aliquots were mixed with 1 µL Random Hexamer Primers and adjusted with ddH<sub>2</sub>O to a total volume of 12 µL. Samples were incubated for 5 min at 65°C. Subsequently, 4 µl Reaction buffer, 1 µl RiboLock RNase inhibitor, 2 µl 10 mM dNTP and 1 µl RevertAid reverse Transcriptase were added as a master mix to each reaction. Synthesis of cDNA was performed for 60 min at 45°C. Reaction was terminated by incubation for 5 min at 70°C. Samples were stored at -20°C or directly used for gene expression analysis.

### 2.2.3.5 Expression analysis by quantitative real–time PCR

Expression of target genes was addressed by quantitative real–time PCR (qRT-PCR) using the Universal ProbeLibrary System Technology from Roche. Primers for genes of interest were designed by use of universal hydrolysis probe library assay design center (Roche, table 26).

**Table 26:** Primer pairs for gene expression analysis.

Gene	Forward primer	Reverse primer	Probe
<i>CD11b</i>	CAATAGCCAGCCTCAGTGC	GAGCCCAGGGGAGAAGTG	76
<i>CD11c</i>	GGAGCCTCAAGACAGGACAT	GGATCTGGGATGCTGAAATC	20
<i>Dectin-1</i>	AGAGTGAAGGGCCATGGTT	TGCATTTCTGACTTGAAACGA	88
<i>HPRT1</i>	CCTCCTCAGACCGCTTTTT	AACCTGGTTCATCATCGCTAA	95
<i>IL-1<math>\beta</math></i>	TTGACGGACCCCAAAAGAT	GAAGCTGGATGCTCTCATCTG	26
<i>IL-2</i>	GCTGTTGATGGACCTACAGGA	TTCAATTCTGTGGCCTGCTT	15
<i>IL-10</i>	CAGAGCCACATGCTCCTAGA	TGTCCAGCTGGTCCTTTGTT	41
<i>IL-12p19</i>	TCCCTACTAGGACTCAGCCAAC	AGAACTCAGGCTGGGCATC	19
<i>IL-12p35</i>	TCAGAATCACAACCATCAGCA	CGCCATTATGATTCAGAGACTG	49
<i>IL-12p40</i>	TTGCTGGTGTCTCCACTCAT	GGGAGTCCAGTCCACCTCTAC	78
<i>SDHa</i>	TGTTTCAGTTCCACCCACA	TCTCCACGACACCCTTCTG	71
<i>TLR4</i>	CTGATCCATGCATTGGTAGGT	GACTCTGATCATGGCACTG	2
<i>TNF<math>\alpha</math></i>	CTGTAGCCCACGTCGTAGC	TTGAGATCCATGCCGTTG	25
<i>Tub1a</i>	CTGGAACCCACGGTCATC	GTGGCCACGAGCATAGTTATT	88

High specificity of the assay is achieved by the use of universal hydrolysis probe library set mouse (Roche). The probe is labelled at the 5' end with the reporter fluorescein amidite (FAM) and at the 3' end with a dark quencher dye. When incorporated into a PCR product, the reporter gets cleaved off the probe due to the 5'-3'-exonuclease activity of the applied polymerase and the FAM fluorescence can be detected (Figure 11).

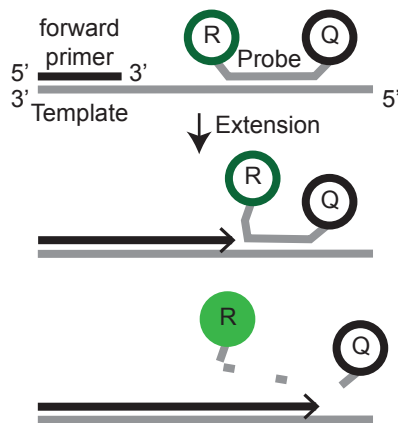


**Figure 11: Principle of Roche's Universal ProbeLibrary System qRT-PCR.** Intensity of fluorescein (FAM) signal is used for determination of mRNA quantity. In addition to specific primers, a probe of 8–9 nucleotides bind to the mRNA. The probes 5' end carries the reporter fluorescein (FAM, R) and at its 3' end a quencher (Q) inhibiting fluorescence of FAM. During elongation of the new synthesized strand, the FastStart Taq DNA Polymerase cleaves the probe, separating the reporter from the quencher. The fluorescence of the released FAM reporter is detected by the LightCycler 480 Instrument II with excitation filter of 465 nm and emission filter of 510 nm.

For each reaction, 4.5  $\mu$ L LightCycler 480 Probes Master (Roche), containing buffer, nucleotides and FastStart Taq DNA Polymerase, were mixed with 0.5  $\mu$ L cDNA. 5  $\mu$ L of primer mix containing 0.2  $\mu$ M of the respective hydrolysis probe and 0.6  $\mu$ M of forward and 0.6  $\mu$ M of reverse primer were added to the cDNA in Probes Master. A serial dilution of samples was performed for each gene of interest (GOI) to evaluate primer efficiency (E). Reactions were performed in technical duplicates with a LightCycler 480 Instrument II (Roche). Filter of 465 nm was applied for excitation and an emission filter of 510 nm for signal detection.

The  $C_p$  value was calculated according to a threshold of signal intensity. The geometric mean of the  $C_p$  of housekeeping genes *tubulin (tub1a)*, *succinate dehydrogenase (SDH)* and *hypoxanthine–guanine phosphoribosyltransferase (HPRT)* was determined. The  $\Delta C_p$  of each GOI was calculated by subtraction of the geometric mean  $C_p$  of the housekeepers from the GOI  $C_p$ . From each GOI the slope of serial dilution ( $m$ ) was used to calculate the primer efficiency  $E=10^{-1/m}$ . The  $\Delta\Delta C_p$  was calculated by  $\Delta\Delta C_p=E^{-\Delta C_p}$ . For better comparison between samples  $\Delta\Delta C_p$  were normalised to mean of untreated *wt*  $\Delta\Delta C_p$ .

### 3 Results

#### 3.1 Absence of SPPL2a leads to reduced DC numbers *in vivo*, but not *in vitro*

##### 3.1.1 Conventional DC2 population is reduced in spleens of *SPPL2a*<sup>-/-</sup> mice

Based on observations made in EMU generated *SPPL2a*<sup>mut/mut</sup> mice and *SPPL2a*-deficient patients (Kong *et al.*, 2018, Beisner *et al.*, 2013, Bergmann *et al.*, 2013), DC populations in spleens of our targeted mutated *SPPL2a*<sup>-/-</sup> mice were analysed in cooperation with Christian Lehmann (AG Dudziak, Department of Dermatology, University Hospital of Erlangen, Germany). The role of the *SPPL2a* substrate CD74 in our murine model system was addressed by including *SPPL2a*<sup>-/-</sup>*CD74*<sup>-/-</sup> mice. *CD74*<sup>-/-</sup> mice served as a control to be able to define possible effects caused by the absence of this protein. Splenocytes were isolated from *wt*, *SPPL2a*<sup>-/-</sup>, *CD74*<sup>-/-</sup> and *SPPL2a*<sup>-/-</sup>*CD74*<sup>-/-</sup> mice. Cells were stained for surface markers and the abundance of DC populations were analysed by flow cytometry as described in chapter 3.1.1 (Figure 12).

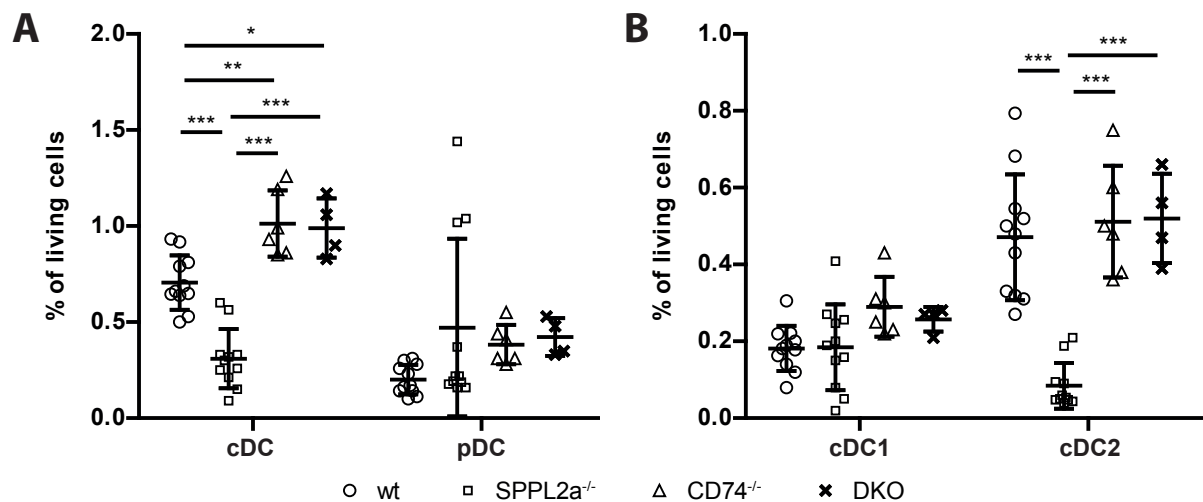


**Figure 12: Reduced cDC2 population in spleens of *SPPL2a*<sup>-/-</sup> mice.** Isolated splenocytes from *wt*, *SPPL2a*<sup>-/-</sup>, *CD74*<sup>-/-</sup> and *SPPL2a*<sup>-/-</sup>*CD74*<sup>-/-</sup> mice were stained for and defined by surface markers as described in chapter 3.1.1. According to their expression of PDCA-1 and CD11c, conventional DCs (cDCs) and plasmacytoid DCs (pDCs) were selected. The cDC population was further subdivided into CD8<sup>+</sup> cDC1 and CD11b<sup>+</sup> cDC2. Single values are shown with mean ± SD. A one-way Anova with a post-hoc-Tukey's testing was performed per population. \*  $p < 0.05$ , \*\*  $p < 0.01$ , \*\*\*  $p < 0.001$ ;  $n=4-11$

The frequency of DCs in spleen was low in general, as expected, with pDC population being smaller than cDC population. The pDC population is important for immune recognition and defence against viral infections (Durai and Murphy 2016). No significant difference of pDC abundance was observed between all genotypes analysed. The percentage of pDC showed high variance between analysed spleens from *SPPL2a*<sup>-/-</sup> mice. The frequency of cDCs was significantly reduced in *SPPL2a*<sup>-/-</sup> spleens to less than half of *wt* values. The additional ablation of

## RESULTS

CD74 rescued this effect. Furthermore, the *CD74*<sup>-/-</sup> and *SPPL2a*<sup>-/-</sup>*CD74*<sup>-/-</sup> spleens contained a 1.4-fold increased cDC population than *wt* spleens. This difference was statistically significant. The population of cDCs can be further subdivided into cDC1 and cDC2 (Macri *et al.*, 2017). The major task of cDC1 is induction of immune defence against intracellular pathogens, while cDC2 induce immune defence against extracellular pathogens (Durai and Murphy 2016). Interestingly, the cDC1 population was unaffected by the lack of SPPL2a. Only cDC2 population was significantly reduced in spleens from *SPPL2a*<sup>-/-</sup> mice compared to the three other genotypes. This raises the question, if the absence of SPPL2a does also have an effect on function of remaining DCs.

### 3.1.2 BMDCs as a model system for functional analysis

The analysis of function of DCs requires comparable populations. Direct isolation of DCs from mice led to a low yield of cells (data not shown and percentage indicated in figure 12) and isolation of specific subpopulations is elaborate. Furthermore, it cannot be excluded that the isolation process affects already functionality of the cells. Therefore an *in vitro* system was explored to generate DC from bone marrow. *In vitro* differentiation of DCs was analysed to answer the question, whether it is affected by the absence of the protease SPPL2a as it was the case *in vivo*. Furthermore, the expression of the protease and its substrate in this model system was addressed. Bone marrow cells of *wt* and *SPPL2a*<sup>-/-</sup> mice were cultured in the presence of the growth factor GM-CSF over eight days in order to obtain bone marrow-derived DCs (BMDCs, detailed protocol in chapter 2.2.1.2).

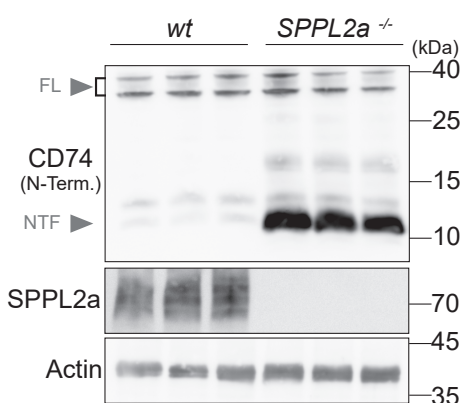


**Figure 13: The CD74 NTF accumulates in *SPPL2a*<sup>-/-</sup> BMDCs.** After eight days of GM-CSF culture, BMDCs were subjected to Western Blot analysis. CD74 was detected with an antibody recognizing an epitope at the N-terminus of CD74. Full length (FL) CD74 and CD74 N-terminal fragment (NTF) are indicated with arrowheads. SPPL2a was only detected in *wt* lanes. The membrane was reprobbed for actin as loading control. Three biological replicates per genotype.

BMDCs were then subjected to Western Blot analysis to validate the expression of SPPL2a and CD74 in this culture system. Full length CD74 was detected in comparable amounts in both genotypes. As expected, the CD74 NTF strongly accumulated in *SPPL2a*<sup>-/-</sup> BMDCs, while only a faint band was observed in *wt* cells (Figure 13). SPPL2a could only be detected in *wt* cells. These were prerequisites for the GM-CSF BMDC culture system to be used for functional assays.



### 3.1.3 Analysis of cell marker surface expression reveals comparable differentiation of *wt* and *SPPL2a*<sup>-/-</sup> BMDCs

The analysis of DCs in mice revealed reductions in distinct DC populations in *SPPL2a*<sup>-/-</sup> mice compared to *wt* mice (see chapter 3.1.1). The reduction of the cDC2 subset could be due to differentiation defects in *SPPL2a*<sup>-/-</sup> precursors. Thus, differentiation of BMDCs with regards to possible differences between *wt* and *SPPL2a*<sup>-/-</sup> cells were examined by flow cytometry. Cells were stained for DC markers CD11c, MHCII and CD11b. CD11c & MHCII double positive cells (CD11c<sup>+</sup>MHCII<sup>+</sup>) were defined as DCs (Figure 14 A). Detailed analysis of several experiments revealed a significant but mild reduction of the CD11c<sup>+</sup>MHCII<sup>+</sup> population in *SPPL2a*<sup>-/-</sup> BMDCs compared to *wt*. Double positive cells were further characterized by MHCII surface expression into intermediate MHCII (MHCII<sup>int</sup>) and high MHCII (MHCII<sup>high</sup>, as described by Helft *et al.*, 2015, Figure 14 B). Abundance of MHCII<sup>high</sup> and MHCII<sup>int</sup> populations was comparable between both genotypes (Figure 14 B & C).

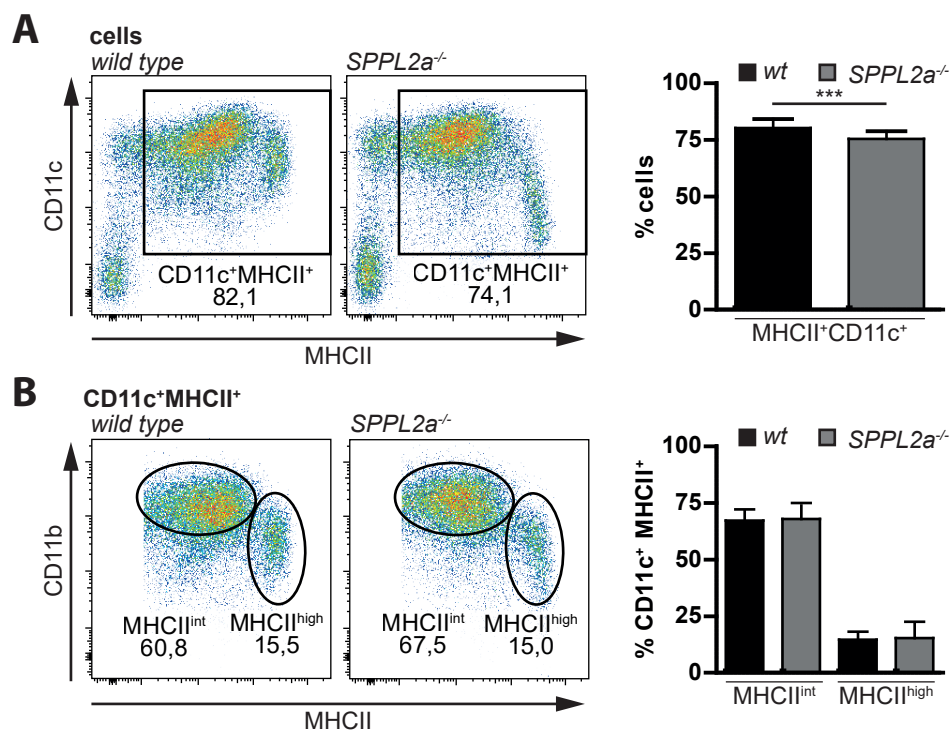


**Figure 14: Flow cytometric analysis of BMDC differentiation.** BMDCs from *wt* and *SPPL2a*<sup>-/-</sup> mice were stained with fluorescently labelled antibodies against CD11c, CD11b and MHCII. Fluorescence intensities were measured by flow cytometry. Cells were gated based on FSC, SSC (not shown). **A** Cells positive for CD11c and MHCII (CD11c<sup>+</sup>MHCII<sup>+</sup>) were quantified. **B** Double positive cells were plotted for CD11b and MHCII. MHCII<sup>int</sup> and MHCII<sup>high</sup> populations were gated for intermediate and high MHCII surface expression, respectively. Bar diagrams show evaluations of seven independent experiments as mean ± SD. An unpaired, two-tailed Student's *t*-test was performed. \*\*\* *p* < 0.001; *n*=21

*SPPL2a*<sup>-/-</sup> BMDCs, expressing large amounts of MHCII at their cell surface, had lower CD11c surface expression than *wt* BMDCs (Figure 14, A left & middle). Thus, surface expression of the single markers was evaluated to reveal possible alterations. Therefore, mean fluorescence

## RESULTS

intensities (MFI) of CD11c, CD11b and MHCII were examined in CD11c<sup>+</sup>MHCII<sup>+</sup> cells. Surface expression of CD11c was significantly reduced in *SPPL2a*<sup>-/-</sup> BMDCs (Figure 15 A). The reduction was mild as *SPPL2a*<sup>-/-</sup> BMDCs still expressed 88% of CD11c on their surface compared to *wt*. *SPPL2a*<sup>-/-</sup> BMDCs showed a significant but slight increase in CD11b surface expression with 1.1–fold of *wt* (Figure 15 C). No alterations in MHCII surface expression were observed between BMDCs of both genotypes (Figure 15 B).

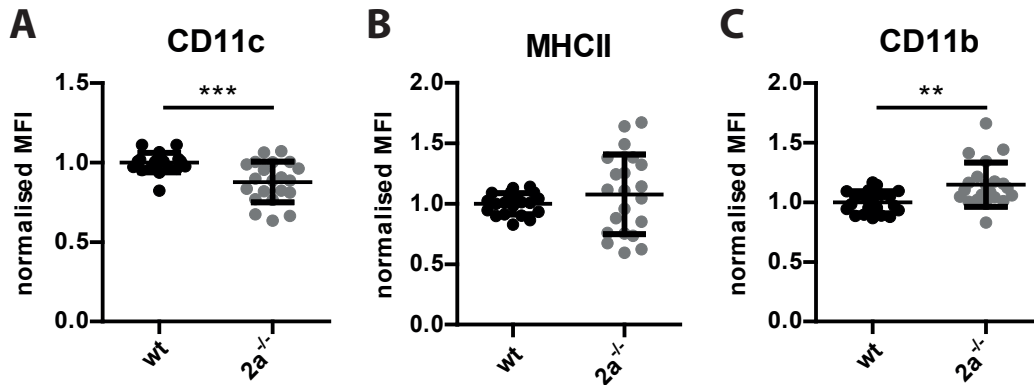


**Figure 15: Surface expressions of CD11c and CD11b are slightly altered in *SPPL2a*<sup>-/-</sup> BMDCs.** CD11c<sup>+</sup>MHCII<sup>+</sup> *wt* and *SPPL2a*<sup>-/-</sup> (*2a*<sup>-/-</sup>) BMDCs were analysed for median fluorescence intensities (MFIs) of **A** CD11c, **B** MHCII and **C** CD11b. The MFI values were normalised to median of *wt* MFI values per experiment. Single values of seven independent experiments are shown with mean  $\pm$  SD. An unpaired, two-tailed Student's *t*-test was performed. \*\*  $p < 0.01$ , \*\*\*  $p < 0.001$ ;  $n=21$

The observed alterations in surface markers could possibly be explained by changes in transcription, transport to or stability of the protein at the cell surface. Transcription of *CD11c* and *CD11b* was compared between *wt* and *SPPL2a*<sup>-/-</sup> BMDCs by qRT-PCR analysis. The analysis revealed equal expression of *CD11c* and *CD11b* in both genotypes (Figure 16 A & B). Thus, the altered surface expression of CD11c and CD11b as observed by flow cytometry cannot be attributed to reduced protein expression.

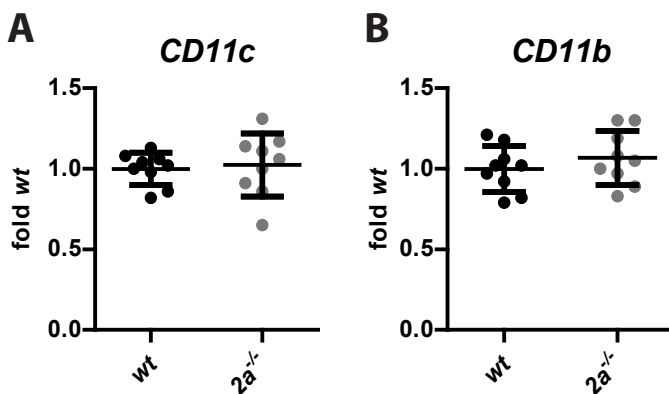


**Figure 16: Comparable expression of *CD11c* and *CD11b* between *wt* and *SPPL2a*<sup>-/-</sup> BMDCs.** After eight days of differentiation, *wt* and *SPPL2a*<sup>-/-</sup> (*2a*<sup>-/-</sup>) BMDCs were lysed for RNA isolation. The synthesised cDNA was used for quantitative real time PCR (qRT-PCR) with primers specific for **A** *CD11c* and **B** *CD11b*. Single values of three independent experiments are shown with mean  $\pm$  SD. An unpaired, two-tailed Student's *t*-test was performed;  $n=9$ .

*In vitro* differentiation of DCs was not affected to a relevant degree in the absence of *SPPL2a*. Thus, BMDCs represent a valid system to analyse the impact of *SPPL2a* deficiency on DC function.

## 3.2 Functional analysis of *in vitro* differentiated DCs in response to pattern recognition receptor stimuli

### 3.2.1 Altered response to Dectin–1 stimulation in *SPPL2a*<sup>-/-</sup> BMDCs

After proving comparable differentiation of *in vitro* generated DCs, the effect of the absence of SPPL2a on BMDC function was investigated. This was addressed by measurement of cytokine secretion responses towards pattern recognition receptor (PRR) stimulation. The PRR C-type lectin receptor (CLEC) Dectin–1 was chosen, because it activates the kinase Syk upon ligand binding. In *SPPL2a*<sup>-/-</sup> B cells the Syk-coupled BCR showed reduced signalling capacity (Hüttl *et al.*, 2015). Thus, it was hypothesised that also other Syk-coupled receptors could be affected by the absence of SPPL2a. Depleted Zymosan (dZym) was chosen as a specific ligand for Dectin–1 (Gantner *et al.*, 2003).

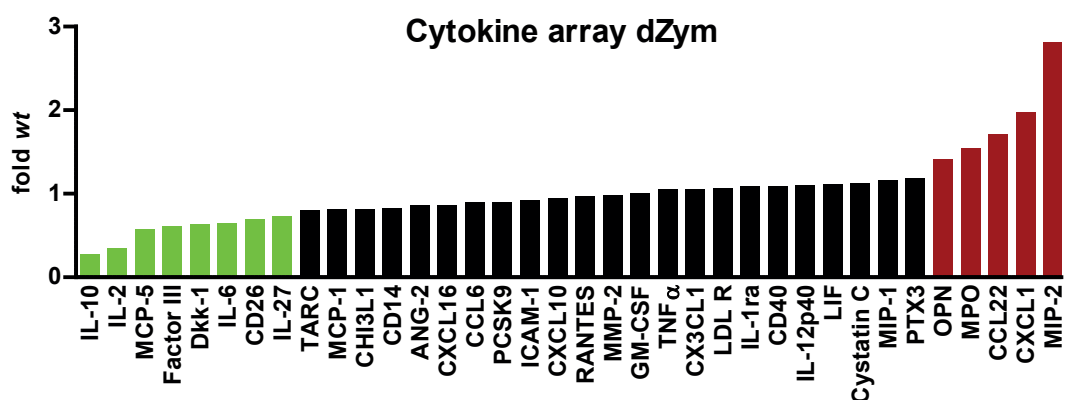


**Figure 17: No general functional deficiency in *SPPL2a*<sup>-/-</sup> DCs.** Supernatants from *wt* or *SPPL2a*<sup>-/-</sup> BMDCs treated with depleted Zymosan (dZym) for 24 h were measured for chemokine and cytokine secretion by a membrane-based sandwich immunoassay. Chemiluminescence intensities were detected. 36 chemokines and cytokines were selected by a threshold of signal intensity and normalized to *wt*. Chemokines and cytokines with a relative increase or reduction in supernatants of *SPPL2a*<sup>-/-</sup> BMDCs compared to *wt* are depicted in red or green, respectively. n=1.

A cytokine array was performed in order to obtain a general idea of the responsiveness and possible differences between *wt* and *SPPL2a*<sup>-/-</sup> BMDCs. The array was applied to examine possible cytokine secretion differences between *wt* and *SPPL2a*<sup>-/-</sup> BMDCs. Cells were stimulated with the Dectin–1 specific ligand depleted Zymosan (dZym) for 24 h and supernatants were subjected to the cytokine array. 36 chemokines and cytokines were selected by a threshold of signal intensity and normalized to *wt* values (Figure 17). Most chemokines and cytokines were detected to comparable amounts in supernatants from BMDCs of both genotypes. TNF $\alpha$  was one of the cytokines secreted equally by *wt* and *SPPL2a*<sup>-/-</sup> BMDCs. Macrophage inflammatory protein 2 (MIP–2), CXCL1, CCL22, myeloperoxidase (MPO) and osteopontin (OPN) were increased in supernatants from dZym treated *SPPL2a*<sup>-/-</sup> BMDCs. IL–10, IL–2, monocyte chemoattractant protein 5 (MCP–5), dickkopf–1 (Dkk-1), CD26 and IL-27 were reduced in supernatants from dZym treated *SPPL2a*<sup>-/-</sup> BMDCs.

## RESULTS

Expression differences of key cytokines were validated by ELISA. MIP-2, IL-10, IL-2 and TNF $\alpha$  were chosen from the array in addition to IL-1 $\beta$  (Figure 18). The increase of MIP-2 secretion by absence of SPPL2a could not be addressed due to technical problems of the ELISA. In contrast to *wt* BMDCs, *SPPL2a*<sup>-/-</sup> BMDCs released significantly less IL-10 upon dZym treatment. A trend towards reduced IL-2 secretion by *SPPL2a*<sup>-/-</sup> BMDCs was observed. The cytokines IL-1 $\beta$  and TNF $\alpha$  were released to comparable amounts by *wt* and *SPPL2a*<sup>-/-</sup> BMDCs when treated with dZym. Overall, this is in line with the cytokine array data.

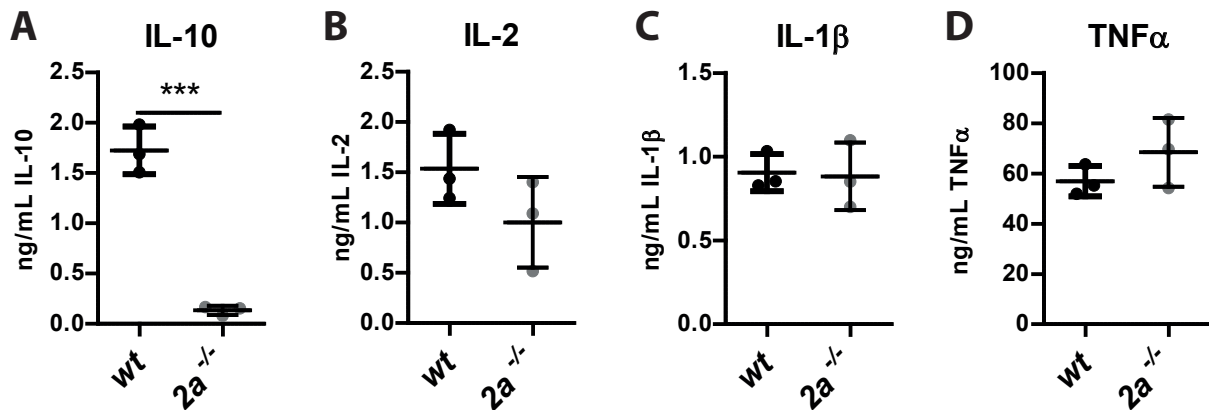


**Figure 18: Reduced IL-10 secretion in depleted Zymosan treated *SPPL2a*<sup>-/-</sup> DCs.** *Wt* and *SPPL2a*<sup>-/-</sup> (*2a*<sup>-/-</sup>) BMDCs were treated with 50  $\mu$ g/mL depleted Zymosan (dZym) for 24 h. Supernatants were measured for **A** IL-10, **B** IL-2, **C** IL-1 $\beta$  or **D** TNF $\alpha$  by ELISA. Single values are shown with mean  $\pm$  SD. An unpaired, two-tailed Student's *t*-test was performed. \*\*\*  $p < 0.001$ . Representative measurements of five independent experiments with three biological replicates per genotype ( $n=3$ ).

Transcription and release of cytokines are preceding steps before cytokine concentrations can be measured in conditioned media by ELISA. Alterations in these steps could explain reduced IL-10 and slightly decreased IL-2 concentrations in cell culture supernatants of dZym treated *SPPL2a*<sup>-/-</sup> BMDCs compared to *wt*. Cytokine expression was addressed by qRT-PCR. BMDCs were stimulated for three, six or nine hours with dZym or left untreated and mRNA levels of *IL-10*, *IL-2*, *IL-1 $\beta$*  and *TNF $\alpha$*  were quantified (Figure 19). The expression of *IL-10* in *wt* BMDCs increased up to 800-fold of untreated *wt* and reached a plateau after six hours. In contrast to that, *IL-10* transcription was significantly lower in *SPPL2a*<sup>-/-</sup> BMDCs with a maximum at 90-fold of untreated *wt*. Expression of *IL-2* peaked at three hours of dZym administration in both genotypes with the transcription being eight-fold lower in *SPPL2a*<sup>-/-</sup> compared to *wt* BMDCs. After six hours of Dectin-1 activation, *IL-2* transcription was still 4.6-fold lower in *SPPL2a*<sup>-/-</sup> than in *wt* BMDCs. The difference between genotypes was significant at both time points. *IL-1 $\beta$*  and *TNF $\alpha$*  were expressed without significant differences between *wt* and *SPPL2a*<sup>-/-</sup> BMDCs. Transcription of both cytokines showed strongest increase from untreated at three hours of dZym treatment. Afterwards, *IL-1 $\beta$*  expression slightly increased further, while *TNF $\alpha$*  expression declined.

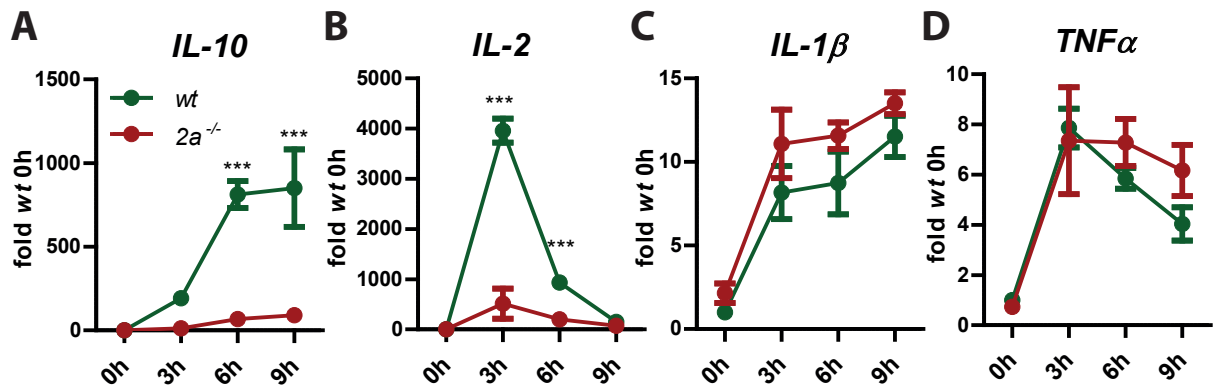


**Figure 19: Decreased IL–10 and IL–2 expression in *SPPL2a*<sup>-/-</sup> BMDCs upon stimulation with depleted Zymosan.** BMDCs from *wt* and *SPPL2a*<sup>-/-</sup> (*2a*<sup>-/-</sup>) mice were treated with dZym for 3, 6 or 9 h or left untreated. After RNA isolation, cDNA was synthesised. Transcription of **A** *IL–10*, **B** *IL–2*, **C** *IL–1β* and **D** *TNFα* were determined by qRT–PCR. Means of normalised expression ± SD are shown. A two–way Anova with a post–hoc–Bonferroni testing was performed. \*\*\* *p* < 0.001; Representative graphs from five (*IL–10*, *IL–2* & *IL–1β*) or three (*TNFα*) independent experiments with three biological replicates per genotype (*n*=3).

Taking together, stimulation of Dectin–1 by dZym emerged with only partial alterations in composition of chemokines and cytokines in *SPPL2a*<sup>-/-</sup> compared to *wt* BMDCs as shown by a cytokine array. Thus, function of *SPPL2a*<sup>-/-</sup> BMDCs was not completely modified. A clear reduction of IL–10 and a slight decrease of IL–2 secretion in the absence of SPPL2a was confirmed by ELISA. These cytokines were already massively reduced on transcription level in *SPPL2a*<sup>-/-</sup> compared to *wt* BMDCs. Thus, the reason for altered cytokine release lies between pathogen contact and mRNA expression in *SPPL2a*<sup>-/-</sup> BMDCs.

### 3.2.2 Increased TLR response in the absence of SPPL2a

Responses towards Toll–like receptor (TLR) stimulation were investigated to reveal if alterations in cytokines were restricted to Syk–coupled receptors, like Dectin–1, or a more general effect of SPPL2a deficiency. BMDCs from *wt* and *SPPL2a*<sup>-/-</sup> mice were stimulated with LPS, a specific ligand for TLR4, for 24 h (Poltorak *et al.*, 1998). Supernatants were harvested and cytokine concentrations were measured by ELISA.

Based on observations concerning Dectin–1 activation (section 3.2.1), IL–10, IL–2, IL–1β and TNFα were chosen as representative cytokines. While IL–10 and IL–2 were hardly detectable by ELISA after BMDC stimulation with LPS, release of IL–1β and TNFα could be measured (Figure 20). The absence of SPPL2a led to an increase of IL–1β in cell culture supernatants by a factor of three compared to *wt*. Observed TNFα concentrations in supernatants of *SPPL2a*<sup>-/-</sup> BMDCs stimulated with LPS showed a tendency towards an increased release compared to *wt*, which was not significant.

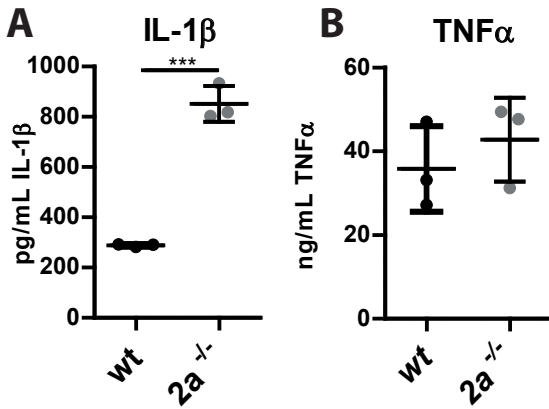


**Figure 20: Toll like receptor 4 activation leads to increased IL-1 $\beta$  release by *SPPL2a*<sup>-/-</sup> BMDCs.** BMDCs differentiated from *wt* and *SPPL2a*<sup>-/-</sup> (*2a*<sup>-/-</sup>) mice were stimulated for 24 h with 500 ng/mL LPS. Supernatants were harvested and cytokine concentrations of **A** IL-1 $\beta$  and **B** TNF $\alpha$  were measured by ELISA. Single values are shown with mean  $\pm$  SD. An unpaired, two-tailed Student's *t*-test was performed. \*\*\*  $p < 0.001$ . Representative measurements of six (IL-1 $\beta$ ) or five (TNF $\alpha$ ) independent experiments with three biological replicates per genotype ( $n=3$ ).

Expression of cytokines was quantified to investigate possible reasons for increased IL-1 $\beta$  release measured by ELISA. BMDCs differentiated from *wt* and *SPPL2a*<sup>-/-</sup> mice were treated for three to nine hours with LPS or left unstimulated. Levels of mRNA were measured by qRT-PCR (Figure 21). In contrast to ELISA measurements, *IL-10* and *IL-2* expression was detectable by qRT-PCR. As shown in figure 21, BMDCs from *wt* and *SPPL2a*<sup>-/-</sup> mice produced increasing *IL-10* mRNA over time of stimulation. *Wt* BMDCs expressed slightly more *IL-10* than *SPPL2a*<sup>-/-</sup> BMDCs with significant difference after nine hours of LPS treatment. At that time point, *IL-10* transcription by *SPPL2a*<sup>-/-</sup> BMDCs was reduced to 80% of *wt* BMDCs. Compared to *IL-10*, *IL-1 $\beta$*  showed a slightly different expression pattern. Transcription of *IL-1 $\beta$*  strongest increase from untreated to three hours of BMDC treatment with LPS. Expression slightly rose from three to six hours and then decreased again. The detected mean mRNA levels of *IL-1 $\beta$*  were 1.6- to 1.3-fold higher in *SPPL2a*<sup>-/-</sup> BMDCs compared to *wt* BMDCs for all treatment time points, which did not reach statistical significance. *IL-2* and *TNF $\alpha$*  showed a rather similar expression kinetics with a maximal expression after three hours of LPS application followed by a strong decrease. At three hours, *SPPL2a*<sup>-/-</sup> BMDCs expressed 1.7-fold less *IL-2* than *wt* BMDCs. Only minor amounts of *IL-2* mRNA were detectable at six and nine hours of LPS treatment without significant differences between genotypes. In contrast to that, transcription of *TNF $\alpha$*  was elevated in *SPPL2a*<sup>-/-</sup> BMDCs in comparison to *wt* BMDCs. A significant difference was detected after three hours of LPS treatment. *TNF $\alpha$*  transcription was 1.7-fold higher in *SPPL2a*<sup>-/-</sup> BMDCs than in *wt* BMDCs at that time point.

Overall, BMDCs lacking *SPPL2a* released slightly more TNF $\alpha$  and significantly higher amounts of IL-1 $\beta$  than *wt* BMDCs after TLR4 activation. This elevation was already detectable at mRNA level. Thus, reasons for altered cytokine response of *SPPL2a*<sup>-/-</sup> BMDCs appear to locate between LPS recognition and induction of expression.

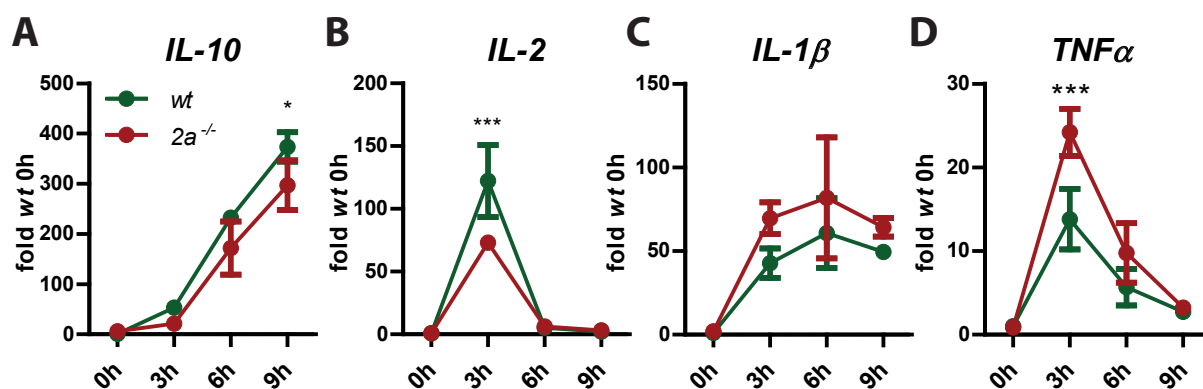


**Figure 21: Increased  $IL-1\beta$  and  $TNF\alpha$  expression in  $SPPL2a^{-/-}$  BMDCs upon LPS administration.** Cytokine expression in *wt* and  $SPPL2a^{-/-}$  ( $2a^{-/-}$ ) BMDCs was induced by 500 ng/mL LPS. RNA was extracted after three, six or nine hours of treatment as well as from untreated cells. After cDNA synthesis, qRT-PCR was performed with primers for **A**  $IL-10$ , **B**  $IL-2$ , **C**  $IL-1\beta$  and **D**  $TNF\alpha$ . Means of normalised expression  $\pm$  SD are shown. A two-way Anova with a post-hoc-Bonferroni testing was performed. \*  $p < 0.05$ , \*\*\*  $p < 0.001$ ; Representative graphs from two ( $IL-10$  &  $IL-2$ ) or three ( $IL-1\beta$  &  $TNF\alpha$ ) independent experiments with three biological replicates per genotype ( $n=3$ ).

### 3.3 Cytokine response towards mycobacteria in $SPPL2a^{-/-}$ immune cells

#### 3.3.1 Analysis of cytokine response of BMDCs to heat-killed *Mycobacterium tuberculosis*

Stimulation of single pattern-recognition receptors is rare in the course of immune reactions, since most pathogens lead to activation of different families and family-members of pattern-recognition receptors. Accordingly, the response of *wt* and  $SPPL2a^{-/-}$  BMDCs towards a complex ligand was analysed. For this purpose, heat-killed *Mycobacterium tuberculosis* (HKMT) was chosen. This ligand stimulates especially Mincle and TLR2, but also Dectin-1, Dectin-2 and other receptors (Ishikawa *et al.*, 2009, Underhill *et al.*, 1999, Yonekawa *et al.*, 2014, Yadav and Schorey 2006, Schlesinger 1993, Tailleux *et al.*, 2003). The mycobacterial ligand was chosen for an additional reason. Mutations in the  $SPPL2a$  gene were found in patients with mendelian susceptibility to mycobacterial disease (MSMD; Kong *et al.*, 2018). Therefore, it was aimed to analyse if an altered response of DCs towards mycobacteria could be a reason for the disease in  $SPPL2a$ -deficient patients.

DCs differentiated from bone marrow of *wt* and  $SPPL2a^{-/-}$  mice were treated with HKMT for 24 h. Supernatants were collected and used for measurement of the cytokines  $IL-10$ ,  $IL-2$ ,  $IL-1\beta$  and  $TNF\alpha$  by ELISA (Figure 22). In conditioned medium of *wt* BMDCs 1.4 ng/mL  $IL-10$  were measured. This cytokine concentration was significantly reduced by three-fold in  $SPPL2a^{-/-}$  BMDCs.  $IL-2$  was secreted at low amounts with 120 pg/mL in *wt* BMDCs and 50 pg/mL in  $SPPL2a^{-/-}$  BMDCs. This decrease of  $IL-2$  concentration in supernatants from

## RESULTS

*SPPL2a*<sup>-/-</sup> BMDCs was not significant. In contrast to IL-10 and IL-2, release of IL-1 $\beta$  and TNF $\alpha$  was significantly higher in the absence of SPPL2a. *SPPL2a*<sup>-/-</sup> BMDCs released two-fold more IL-1 $\beta$  and 1.4-fold more TNF $\alpha$  than *wt* BMDCs.

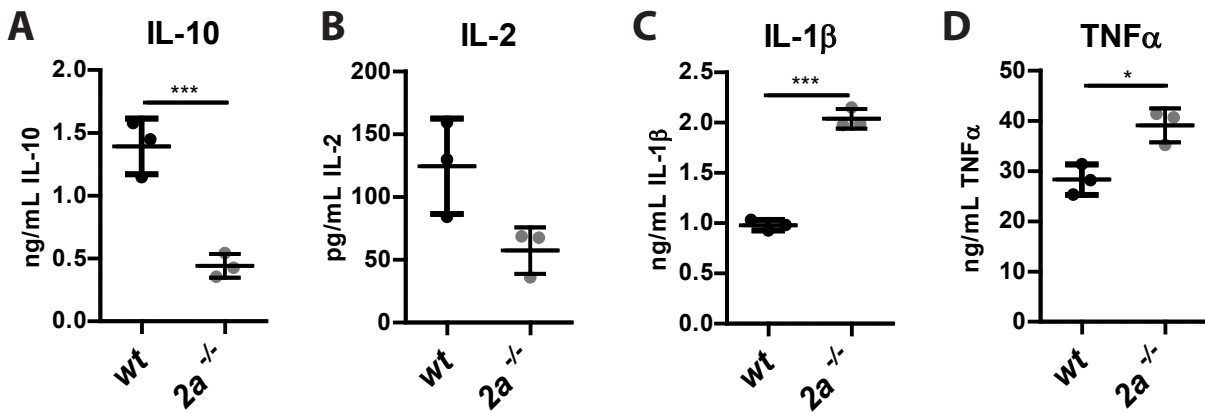


**Figure 22: Reduced IL-2 and IL-10, but increased IL-1 $\beta$  and TNF $\alpha$  release in *SPPL2a*<sup>-/-</sup> BMDCs upon HKMT treatment.** *Wt* and *SPPL2a*<sup>-/-</sup> (*2a*<sup>-/-</sup>) BMDCs were stimulated with 250  $\mu$ g/mL HKMT for 24 h. Supernatants were harvested. Cytokine concentrations of **A** IL-10, **B** IL-2, **C** IL-1 $\beta$  or **D** TNF $\alpha$  were measured by ELISA. Single values are shown with mean  $\pm$  SD. An unpaired, two-tailed Student's *t*-test was performed. \*  $p < 0.05$ , \*\*\*  $p < 0.001$ . Representative measurements of six (IL-10 & IL-2), five (IL-1 $\beta$ ) or seven (TNF $\alpha$ ) independent experiments with three biological replicates per genotype ( $n=3$ ).

Expression of the cytokines measured by ELISA was monitored as possible reason for altered cytokine release. Therefore, RNA was isolated from untreated and from three, six or nine hours HKMT treated BMDCs. Expression analysis of *IL-10*, *IL-2*, *IL-1 $\beta$*  and *TNF $\alpha$*  was performed by qRT-PCR (Figure 23). Transcription of *IL-10* increased steadily over the course of HKMT treatment (Figure 23 A). Amounts of *IL-10* mRNA were significantly decreased in *SPPL2a*<sup>-/-</sup> BMDCs compared to *wt* BMDCs at all time points of treatment. After nine hours, expression of *IL-10* in *SPPL2a*<sup>-/-</sup> BMDCs was as low as 26% of *wt*. *IL-2* expression reached a maximum at three hours HKMT treatment followed by a decrease in both genotypes (Figure 23 B). After three hours, *SPPL2a*<sup>-/-</sup> BMDCs showed a significant reduction in IL-2 transcription by five-fold. At the other treatment time points, *IL-2* mRNA was already as low as in untreated cells. Transcription of *IL-1 $\beta$*  in *wt* BMDCs reached a maximum after three hours of HKMT treatment (Figure 23 C). Then, expression of *IL-1 $\beta$*  decreased in *wt* BMDCs. In contrast, *IL-1 $\beta$*  expression was stable in *SPPL2a*<sup>-/-</sup> BMDCs at all time points of treatment measured. *IL-1 $\beta$*  expression was increased about two-fold in *SPPL2a*<sup>-/-</sup> BMDCs compared to *wt* BMDCs at all treatment time points. This difference was significant at six and nine hours of HKMT treatment. Expression of *TNF $\alpha$*  increased in BMDCs from both genotypes to the same degree after three hours of HKMT treatment (Figure 23 D). While expression of *TNF $\alpha$*  decreased afterwards in *wt* BMDCs, it stayed stable in *SPPL2a*<sup>-/-</sup> BMDCs from three to six hours of treatment with HKMT and decreased then. Mean values of *TNF $\alpha$*  transcription were increased significantly 2.3-fold



and 2.1–fold in *SPPL2a*<sup>-/-</sup> BMDCs compared to *wt* BMDCs after six or nine hours of treatment with HKMT, respectively.

In contrast to dZym and LPS, HKMT activates a number of different receptors. The observed changes in cytokine profiles could thus be a combination of what was observed for Dectin-1 and TLR4 activation alone.

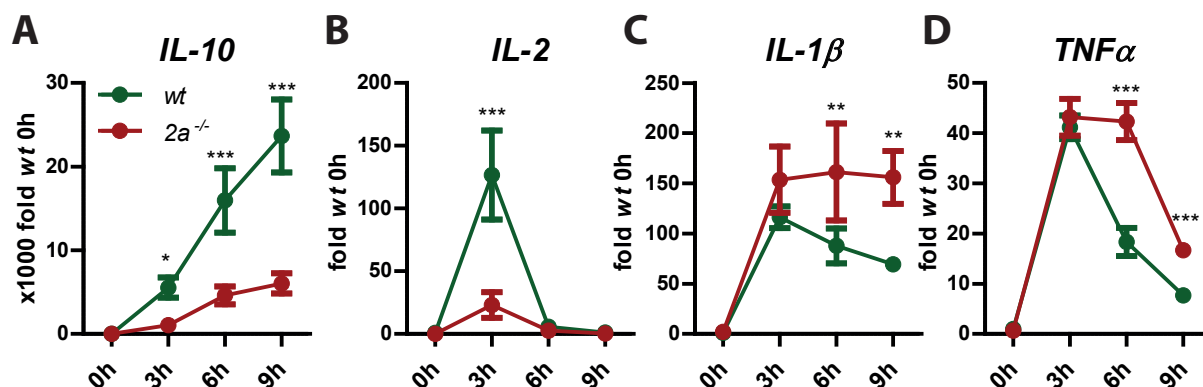


**Figure 23: Altered cytokine expression in HKMT treated *SPPL2a*<sup>-/-</sup> BMDCs.** *In vitro* differentiated DCs from *wt* and *SPPL2a*<sup>-/-</sup> (*2a*<sup>-/-</sup>) mice were stimulated with 250 µg/mL HKMT for three, six or nine hours or left untreated. Isolated RNA was used for cDNA synthesis. Subsequently, expression of **A** *IL-10*, **B** *IL-2*, **C** *IL-1β* and **D** *TNFα* was analysed by qRT-PCR. Means of normalised expression ± SD are shown. A two-way Anova with a post-hoc-Bonferroni testing was performed. \*  $p < 0.05$ , \*\*  $p < 0.01$  \*\*\*  $p < 0.001$ ; Representative graphs from six (*IL-10*), four (& *IL-2*) or five (*IL-1β* & *TNFα*) independent experiments with three biological replicates per genotype ( $n=3$ ).

### 3.3.2 Alterations in *IL-1β* expression and release are direct effects of *SPPL2a* deficiency

The release of *IL-1β* is tightly regulated (Latz *et al.*, 2013). First, pro-*IL-1β* expression and inflammasome assembly are induced. Second, the inflammasome is activated in order to cleave pro-*IL-1β* into its biologically active form. The first signal for this activation is derived by a pathogen-associated signal, as for example HKMT. The second signal is derived by a broad range of signals, mainly danger-associated signals, as for example ATP (Pelegrin and Surprenant 2006).

Increased *IL-1β* concentrations were measured in medium from *SPPL2a*<sup>-/-</sup> BMDCs compared to medium taken from *wt* BMDCs after 24 h stimulation with HKMT (Section 3.3.1). After six hours of stimulation of BMDCs with HKMT, an increased expression of *IL-1β* was observed in *SPPL2a*<sup>-/-</sup> BMDCs (see figure 23). These alterations could be induced due to secondary effects, which were analysed further. Increased activation of the inflammasome in *SPPL2a*<sup>-/-</sup> BMDCs could contribute to elevated *IL-1β* cytokine secretion from *SPPL2a*<sup>-/-</sup> BMDCs compared to *wt*. The activity of inflammasomes in *wt* and *SPPL2a*<sup>-/-</sup> BMDCs in response to HKMT treatment was studied. A short time point of stimulation with HKMT was chosen to exclude transcriptional differences between BMDCs from *wt* and *SPPL2a*<sup>-/-</sup> mice. The treatment of BMDCs

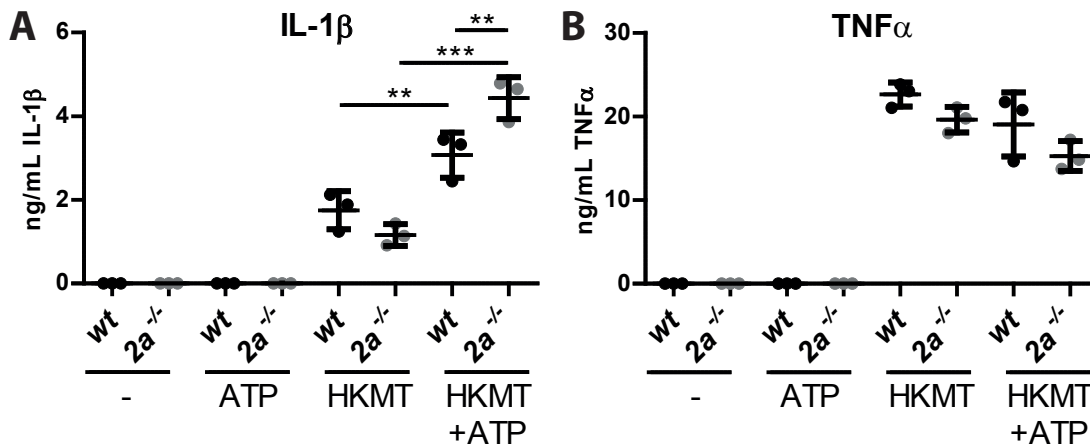


**Figure 24: The absence of SPPL2a does not lead to increased inflammasome activity.** DCs differentiated *in vitro* from bone marrow of *wt* and *SPPL2a*<sup>-/-</sup> (*2a*<sup>-/-</sup>) mice were stimulated for 4.5 h with 250 µg/mL HKMT. In the last 30 min, 5 mM ATP was added. Untreated (-), ATP alone or HKMT alone treated samples were included as controls. Supernatants were harvested and **A** IL-1β and **B** TNFα were measured by ELISA. Single values are shown with mean ± SD. A one-way Anova with a post-hoc-Tukey's testing was performed. \*\* p < 0.01 \*\*\* p < 0.001; Representative graphs from three independent experiments are shown with three biological replicates per genotype (n=3).

with HKMT served as a first signal for assembly of the inflammasome and *IL-1β* expression. Addition of ATP served as a second signal to fully activate the inflammasome. If assembly and activation of the inflammasome in *SPPL2a*<sup>-/-</sup> BMDCs was accelerated in comparison to *wt* BMDCs, the addition of ATP should lead to a higher increase of *IL-1β* in the supernatants of *wt* BMDCs than in supernatants of *SPPL2a*<sup>-/-</sup> BMDCs. *In vitro* differentiated DCs were stimulated with HKMT for four hours. ATP was added for additional 30 min to fully activate the inflammasome. Supernatants were harvested and subjected to cytokine measurements (Figure 24). No *IL-1β* was detected in supernatants of untreated or ATP treated BMDCs (Figure 24 A). Secretion of *IL-1β* by *SPPL2a*<sup>-/-</sup> BMDCs was slightly but not significantly reduced compared to *wt* after 4.5 h of HKMT treatment. The addition of ATP to HKMT treated BMDCs led to increased *IL-1β* release by 1.8-fold in *wt* and by 3.8-fold in *SPPL2a*<sup>-/-</sup> BMDCs. Hence, this does not support the theory of increased inflammasome activity in *SPPL2a*<sup>-/-</sup> BMDCs compared to *wt* BMDCs. Concentrations of TNFα in cell supernatants were determined to exclude activation of cytokine expression by ATP alone (Figure 24 B). Release of TNFα was comparable between genotypes and was not increased upon addition of ATP to HKMT stimulated BMDCs indicating no activation of cytokine expression by ATP.

Increased measurements of *IL-1β* by *SPPL2a*<sup>-/-</sup> BMDCs upon stimulation with HKMT can also be mediated by enhanced cell death. Cytoplasmic proteins are released when plasma membranes are damaged, among them uncleaved, biologically inactive pro-*IL-1β* and the enzyme lactate dehydrogenase (LDH; Korzeniewski and Callewaert 1983, Afonina *et al.*, 2015). The applied ELISA for *IL-1β* concentration measurement cannot discriminate between cleaved *IL-1β*

and the uncleaved pro-IL-1 $\beta$ . This allows the measurement of elevated IL-1 $\beta$ , if *SPPL2a*<sup>-/-</sup> BMDCs were more prone to cell death upon HKMT treatment than *wt* BMDCs. Cell death is measured by determining LDH activity using a colorimetric assay (see section 2.2.2.9). BMDCs from *wt* and *SPPL2a*<sup>-/-</sup> mice were stimulated for 24 h with HKMT. The OD measured within the assay reflects released LDH and correlates with cell death. The OD values were comparable between samples from *wt* and *SPPL2a*<sup>-/-</sup> BMDCs in both cases, untreated or HKMT stimulated (Figure 25). The treatment of BMDCs with HKMT led to a slight increase in OD values compared to untreated samples. The treatment with HKMT led to comparable rate of cell death in *wt* and *SPPL2a*<sup>-/-</sup> BMDCs. If pro-IL-1 $\beta$  is measured by the ELISA, same levels were detected in supernatants from HKMT treated BMDCs of both genotypes.

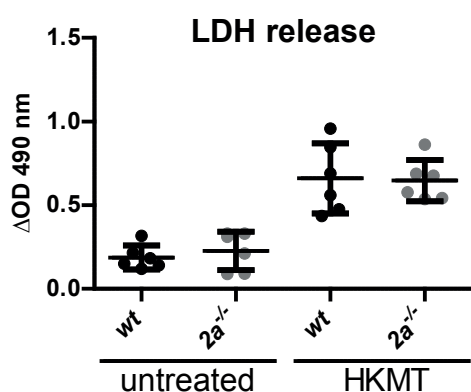


**Figure 25: Comparable cell death in *wt* and *SPPL2a*<sup>-/-</sup> BMDCs upon HKMT treatment.** *Wt* and *SPPL2a*<sup>-/-</sup> (*2a*<sup>-/-</sup>) BMDCs were treated with 250  $\mu$ g/mL HKMT for 24 h or left untreated. Medium was transferred to a 96-well plate and mixed 1:2 with the LDH kit reaction buffer. The reaction was stopped after 1 h and absorption was measured at 490 nm and 680 nm. The  $\Delta$  OD was calculated by absorbance at 490 nm minus absorbance at 680 nm. Single values from three biological replicates with two technical replicates are shown with mean  $\pm$  SD. An unpaired, two-tailed Student's *t*-test was performed. Assay was performed once (n=3).

The difference in IL-1 $\beta$  release and expression between *wt* and *SPPL2a*<sup>-/-</sup> BMDCs did not occur directly, but only after about six hours of treatment with HKMT. Therefore, we hypothesised that IL-1 $\beta$  expression might be regulated by cytokines, which are differentially released by *wt* and *SPPL2a*<sup>-/-</sup> BMDCs directly at the beginning of HKMT treatment. If this holds true, effects on IL-1 $\beta$  would be indirect and not direct due to the absence of SPPL2a in BMDCs. We focused on the anti-inflammatory cytokine IL-10, since it has been shown to negatively regulate IL-1 $\beta$  expression in monocytes (Waal Malefyt *et al.*, 1991). Furthermore, a reduction of IL-10 release was observed in *SPPL2a*<sup>-/-</sup> BMDCs (see chapter 3.3.1), which could lead to increased IL-1 $\beta$  transcription and release. For disabling potential negative regulatory functions of IL-10 on IL-1 $\beta$  it was neutralised in cell supernatants by anti-IL-10 antibodies. Accordingly, BMDCs were treated with HKMT for 24 h in the presence of the anti-IL-10 antibodies or undirected control antibodies (isotype). Supernatants were harvested and subjected to ELISA measurements (Figure 26). Release of IL-1 $\beta$  was increased by three-fold in HKMT treated *SPPL2a*<sup>-/-</sup> BMDCs compared to *wt* BMDCs in all three conditions (-, isotype and anti-IL-10, figure 26 A). The addition of the neutralising IL-10 antibodies did not alter IL-1 $\beta$  release in BMDCs. IL-12p70 cytokine concentrations were measured in conditioned media as a positive control for

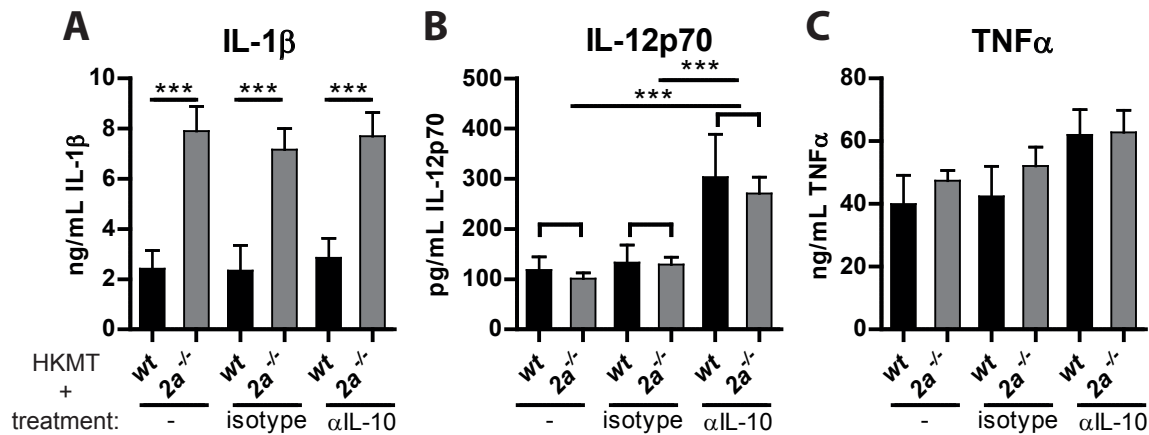


**Figure 26: IL-10 secretion does not influence IL-1 $\beta$  production.** BMDCs from *wt* and *SPPL2a*<sup>-/-</sup> (*2a*<sup>-/-</sup>) mice were incubated with 250  $\mu$ g/mL HKMT alone (-) or in addition to 10  $\mu$ g/mL undirected antibody (isotype) or neutralising IL-10 antibody ( $\alpha$ IL-10). Supernatants were harvested and measured for concentrations of **A** IL-1 $\beta$ , **B** IL-12p70 and **C** TNF $\alpha$ . Means  $\pm$  SDs are shown. A one-way Anova with a post-hoc-Tukey's testing was performed. \*\*\*  $p < 0.001$ ; Representative graphs from three independent experiments are shown with three biological replicates per genotype ( $n=3$ ).

the IL-10 blocking. Secretion of IL-12p70 has been reported to increase after addition of the anti-IL-10 antibodies (Meyaard *et al.*, 1996). The measured IL-12p70 concentration in media was increased in presence of the neutralising antibodies in both genotypes by three-fold (figure 26 B). Thus, functionality of the assay could be ensured. For excluding the activation of cells by the presence of antibodies, the concentration of TNF $\alpha$  was measured in supernatants of BMDCs. As shown in figure 26 C, the addition of the isotype did not alter TNF $\alpha$  release compared to HKMT only treated cells. The treatment of HKMT and anti-IL-10 antibodies together led to a slight but not significant increase of TNF $\alpha$  compared to HKMT treatment alone. Taken together, no evidence for relevant roles of secondary effects on the release and measurement of IL-1 $\beta$  was found.

### 3.3.3 IL-12 cytokine release from *wt* and *SPPL2a*<sup>-/-</sup> BMDCs

After exclusion of secondary effects on IL-1 $\beta$  release, we focused on cytokine responses of BMDCs towards HKMT administration. As shown in chapter 3.3.1, *SPPL2a*<sup>-/-</sup> BMDCs released decreased amounts of the anti-inflammatory IL-10 and increased amounts of the pro-inflammatory IL-1 $\beta$  after treatment with HKMT. This imbalance of anti- and pro-inflammatory cytokines could lead to an increased uncontrolled initial immune response towards mycobacteria in a *SPPL2a*<sup>-/-</sup> immune system. Furthermore, three *SPPL2a*-deficient patients developed MSMD, a disease in which the clearance of bacteria is disturbed (Kong *et al.*, 2018). A potential mechanism to explain the impaired bacterial clearance are changes in IL-12 production, which is important for activation of T<sub>H</sub>1 cells and subsequent intracellular killing of mycobacteria infected macrophages. Therefore, HKMT mediated IL-12 release by BMDCs was addressed by ELISA.

*Wt* and *SPPL2a*<sup>-/-</sup> BMDCs were stimulated with HKMT for 24 h prior to measurements of released cytokines of the IL-12 family by ELISA (Figure 27). For IL-23, IL-12p40 as well as IL-12p70 no significant difference between *wt* and *SPPL2a*<sup>-/-</sup> BMDCs was observed. However, a general tendency towards reduced release of all three cytokines from *SPPL2a*<sup>-/-</sup> compared to *wt* BMDCs was observed.

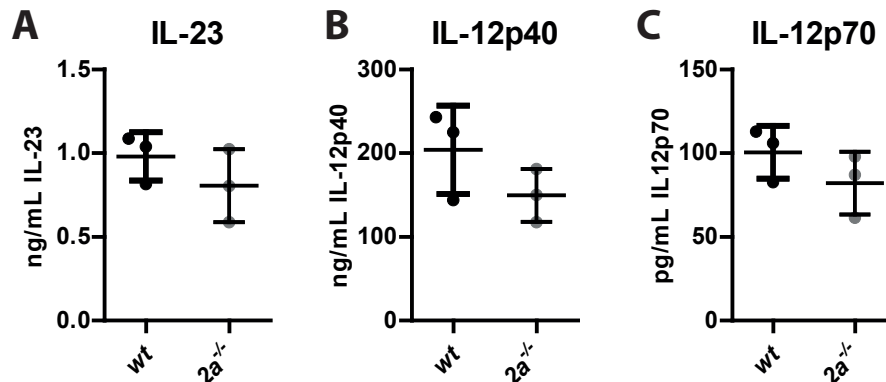


**Figure 27: Release of IL-12 family members from BMDCs after stimulation with HKMT.** Conditioned media from *wt* and *SPPL2a*<sup>-/-</sup> (*2a*<sup>-/-</sup>) BMDCs treated with 250 µg/mL HKMT for 24 h were harvested. Cytokine release of **A** IL-23, **B** IL-12p40 and **C** IL-12p70 was measured. Single values are shown with mean ± SD. An unpaired, two-tailed Student's *t*-test was performed. Representative measurements of three (IL-12p70), four (IL-12p40) or five (IL-23) independent experiments with three biological replicates per genotype (n=3).

The observed lack of a significant reduction of IL-12 release in *SPPL2a*<sup>-/-</sup> BMDCs is surprising in context of data published by Friedmann *et al.*, 2006. They showed that the inhibition of SPPL activity in human monocyte-derived DCs leads to four-fold reduced IL-12 release compared to not inhibited cells when stimulated with LPS. Furthermore, they could show that SPPL2a is necessary for IL-12 production by knockdown of SPPL2a in human monocyte-derived DCs. Therefore, conditioned media from LPS or dZym stimulated *wt* and *SPPL2a*<sup>-/-</sup> BMDCs were re-probed for IL-12 to rule out effects by HKMT-mediated activation of multiple receptors at once on IL-12 release (Figure 28). However, no differences in secretion of IL-23, IL-12p40 or IL-12p70 were observed between *wt* and *SPPL2a*<sup>-/-</sup> BMDCs after LPS treatment. Activation of BMDCs by dZym led to a mild decrease in IL-23 and IL-12p40 release by *SPPL2a*<sup>-/-</sup> BMDCs compared to *wt*, which did not reach statistical significance. IL-12p70 could not be detected in supernatants from dZym treated BMDCs.

Taken together, secretion of IL-12 family members by *SPPL2a*<sup>-/-</sup> BMDCs was not altered in response to the TLR4 ligand LPS. The stimulation of BMDCs with the Dectin-1 ligand dZym or the complex ligand HKMT led to slight reductions in release of these cytokines by *SPPL2a*<sup>-/-</sup> BMDCs compared to *wt*. Thus, SPPL2a deficiency did not affect IL-12 release to a major degree under the conditions tested.

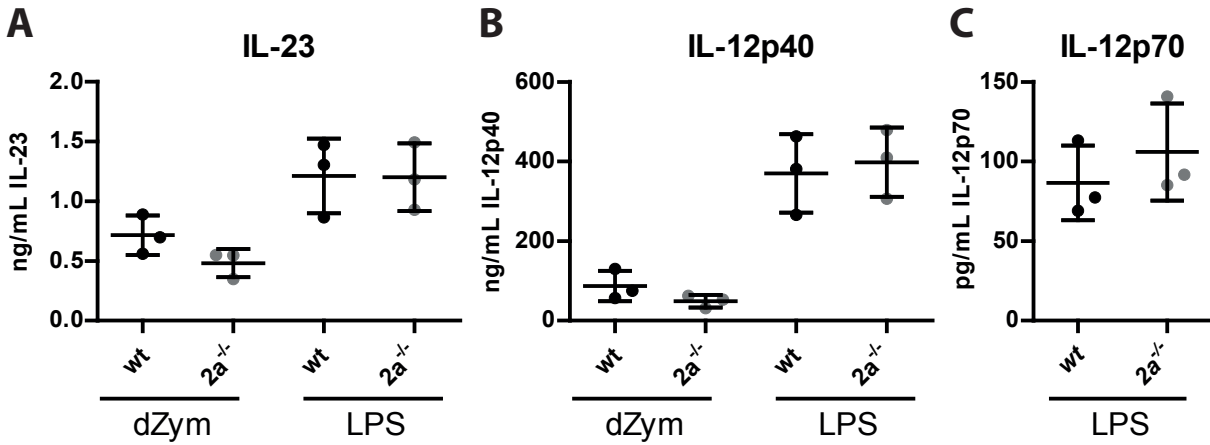


**Figure 28: IL-12 family members are released without significant difference between *wt* and *SPPL2a*<sup>-/-</sup> BMDCs upon dZym or LPS treatment.** Supernatants from *wt* and *SPPL2a*<sup>-/-</sup> (*2a*<sup>-/-</sup>) BMDCs treated with 50 µg/mL dZym, 250 µg/mL HKMT or 500 ng/mL LPS for 24 h were harvested. Cytokine concentrations of **A** IL-23 and **B** IL-12p40 were measured for all treatment conditions in media. IL-12p40 was measured in supernatants from BMDCs treated with **C** HKMT or **D** LPS. Single values are shown with mean ± SD. An unpaired, two-tailed Student's *t*-test was performed. Representative measurements of three (IL-12p70 HKMT, IL-12p70 LPS, IL-12p40 dZym & IL-12p40 LPS), four (IL-12p40 HKMT, IL-23 dZym & IL-23 LPS) or five (IL-23 HKMT) independent experiments with three biological replicates per genotype (n=3).

### 3.3.4 Analysis of BMDC cytokine responses upon BCG co-culture

As shown in chapter 3.3.1, the stimulation of *SPPL2a*<sup>-/-</sup> BMDCs with HKMT led to a significant reduction of IL-10 and a slight reduction of IL-2 release compared to *wt* BMDCs. Furthermore, a significant increased production of IL-1β and a slightly increased production of TNFα was observed in *SPPL2a*<sup>-/-</sup> BMDCs in comparison to *wt* BMDCs. These alterations were detected on transcriptional and secretory level. In contrast to that, the release of IL-12 family members was only mildly affected by SPPL2a deficiency. However, heat-killed bacteria such as HKMT display ligands for PRR differently than intact bacteria. Furthermore, SPPL2a-deficient patients with MSMD suffer from infection with BCG. This is a live bacterium with reduced virulence compared to *Mycobacterium tuberculosis*. It was intended to explore cytokine release of *wt* and *SPPL2a*<sup>-/-</sup> BMDCs upon co-culture with intact BCG.

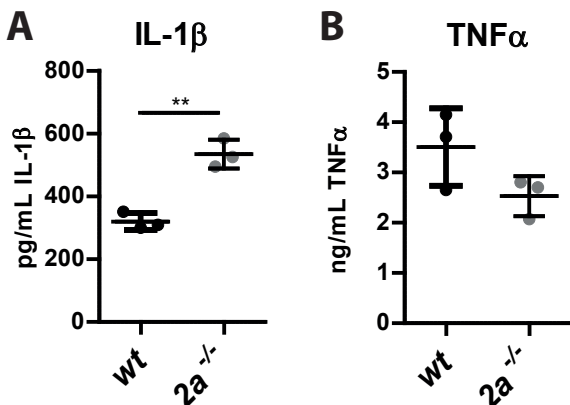


**Figure 29: Increased IL-1β release by *SPPL2a*<sup>-/-</sup> BMDCs in BCG co-culture.** 1.5x10<sup>6</sup> *wt* and *SPPL2a*<sup>-/-</sup> (*2a*<sup>-/-</sup>) BMDCs were co-cultured with 15x10<sup>6</sup> BCG (Multiplicity of infection=10) for 24 h. Conditioned media were harvested and measured for **A** IL-1β and **B** TNFα concentrations by ELISA. Single values are shown with mean ± SD. An unpaired, two-tailed Student's *t*-test was performed. \*\* *p* < 0.01. Representative measurements of two independent experiments with three biological replicates per genotype are shown (n=3).

Cell supernatants were harvested after co-culture of *wt* and *SPPL2a*<sup>-/-</sup> BMDCs with BCG for 24 h. Cytokine concentrations of IL-2, IL-10, IL-1 $\beta$  and TNF $\alpha$  were determined by ELISA. The incubation of BMDCs with BCG did not lead to detectable secretion of IL-2 and IL-10 by this method. Comparable to HKMT treatment (see figure 22), *SPPL2a*<sup>-/-</sup> BMDCs secreted significantly more IL-1 $\beta$  than *wt* BMDCs when co-cultured with BCG (Figure 29 A). The release was increased by 1.7-fold in *SPPL2a*<sup>-/-</sup> BMDCs compared to *wt*. In contrast to that, the concentration of TNF $\alpha$  in conditioned media was not significantly different between both genotypes (Figure 29 B). To address reasons for the increased IL-1 $\beta$  release, the expression of cytokines was measured by qRT-PCR. *In vitro* differentiated DCs were co-cultured for three or six hours with BCG or left untreated. The expression of *IL-10*, *IL-2*, *IL-1 $\beta$*  and *TNF $\alpha$*  was monitored by qRT-PCR. *IL-2* was not detectable by this method.

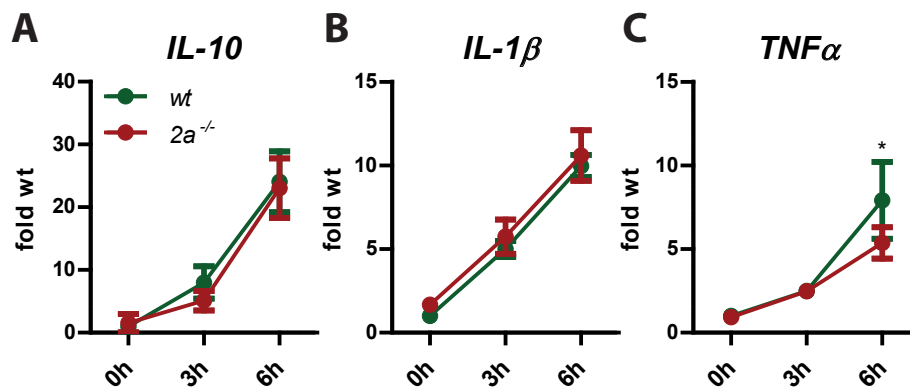


**Figure 30: Comparable expression of *IL-10*, *IL-1 $\beta$*  and *TNF $\alpha$*  in *wt* and *SPPL2a*<sup>-/-</sup> BMDCs after six hours of BCG co-culture.** *Wt* and *SPPL2a*<sup>-/-</sup> (*2a*<sup>-/-</sup>) BMDCs were incubated with ten-fold more BCG cells (MOI=10). RNA was extracted and used as template for cDNA synthesis after three or six hours of BCG co-culture or from untreated cells. Transcription of **A** *IL-10*, **B** *IL-1 $\beta$*  and **C** *TNF $\alpha$*  was determined by qRT-PCR. Means of normalised expression  $\pm$  SD are shown. A two-way Anova with a post-hoc-Bonferroni testing was performed. Representative graphs from two independent experiments with three biological replicates per genotype are shown (n=3).

Expression of *IL-10* increased to 25-fold of untreated *wt* in both genotypes at six hours of BCG co-culture (Figure 30 A). *IL-1 $\beta$*  transcription rose to 10-fold of untreated *wt* at six hours of BCG treatment without differences between *wt* and *SPPL2a*<sup>-/-</sup> BMDCs (Figure 30 B). The treatment of BMDCs with BCG led to increased *TNF $\alpha$*  expression in *wt* BMDCs compared to *SPPL2a*<sup>-/-</sup> BMDCs (Figure 30 C). However, in a repetition of the experiment, *SPPL2a*<sup>-/-</sup> BMDCs expressed more *TNF $\alpha$*  than *wt* BMDCs. Overall, the expression of *IL-10*, *IL-1 $\beta$*  and *TNF $\alpha$*  was comparable after six hours of BCG co-culture, which might be different at later time points.

As described above, IL-12 family members are important for T<sub>H</sub>1 activation and thus induction of intracellular killing of infected macrophages. Therefore, we were again interested in the release of these cytokines. The secretion of the IL-12 family members by 24 h BCG infected BMDCs was measured by ELISA in conditioned media. While in media from *SPPL2a*<sup>-/-</sup> BMDCs almost no IL-23 was detectable, *wt* BMDCs secreted substantial amounts of IL-23. Release

## RESULTS

of IL-12p40 and IL-12p70 by *SPPL2a*<sup>-/-</sup> BMDCs was significantly decreased by seven and three-fold, respectively compared to *wt* BMDCs (Figure 31).

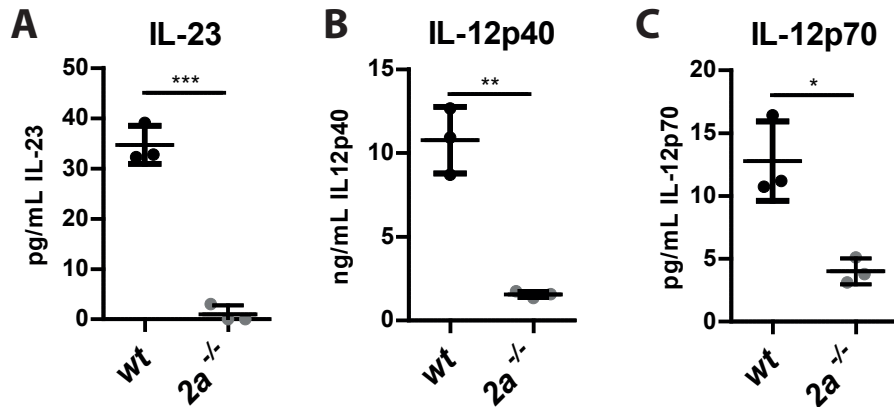


**Figure 31: SPPL2a deficiency impairs secretion of IL-12 family cytokines by BMDCs upon BCG co-culture.** *In vitro* differentiated DCs from *wt* and *SPPL2a*<sup>-/-</sup> (*2a*<sup>-/-</sup>) BMDCs were incubated with ten-fold more BCG cells (MOI=10) for 24 h. Supernatants were cleared from cells and used for cytokine measurement of **A** IL-23, **B** IL-12p40 and **C** IL-12p70 by ELISA. Single values are shown with mean ± SD. An unpaired, two-tailed Student's *t*-test was performed. \* *p* < 0.05; \*\* *p* < 0.01; \*\*\* *p* < 0.001. Representative measurements of two independent experiments with three biological replicates per genotype (*n*=3) are shown.

This reduced secretion of IL-12 family members could be due to reduced expression. Therefore, qRT-PCR analysis was performed as described above. Because IL-23 is a heterodimer formed by a p40 and a p19 subunit and IL-12p70 is comprised of p40 and p35, expression of *IL-12p19*, *IL-12p40* and *IL-12p35* was examined (Figure 32). *IL-12p19* mRNA amounts increased to the same degree in *wt* and *SPPL2a*<sup>-/-</sup> BMDCs three hours of BCG co-culture. From three to six hours, *IL-12p19* expression stayed stable in *wt* BMDCs, but slightly decreased in *SPPL2a*<sup>-/-</sup> BMDCs. Transcription of *IL-12p40* rose during the course of co-culture with BCG in *wt* and *SPPL2a*<sup>-/-</sup> BMDCs. After six hours of BCG infection, *SPPL2a*<sup>-/-</sup> BMDCs expressed significantly less *IL-12p40* than *wt* BMDCs with a reduction by 1.5-fold. For *IL-12p35* a tendency towards reduced expression in *SPPL2a*<sup>-/-</sup> BMDCs compared to *wt* BMDCs was observed after six hours of BCG infection.

It could be that reduction of *IL-12p40* expression alone accounted for reduced concentrations in conditioned media from *SPPL2a*<sup>-/-</sup> BMDCs of all three IL-12 family members. Nevertheless, the reduced release of IL-12 might play an important role in MSMD patients with *SPPL2a* deficiency.



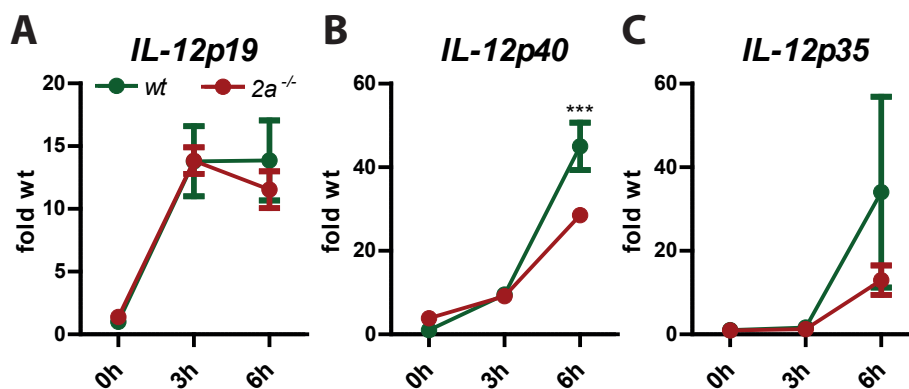


**Figure 32: Induction of IL-12 cytokine expression is reduced in *SPPL2a*<sup>-/-</sup> BMDCs in BCG co-culture.** DCs differentiated from bone marrow of *wt* and *SPPL2a*<sup>-/-</sup> (*2a*<sup>-/-</sup>) mice were treated with BCG at a multiplicity of infection of 10 (MOI=10) or left untreated. After extraction of RNA at indicated time points, cDNA was synthesised and used for qRT-PCR. Transcription of **A** *IL-12p19*, **B** *IL-12p40* and **C** *IL-12p35* were determined. Means of normalised expression  $\pm$  SD are shown. A two-way Anova with a post-hoc-Bonferroni testing was performed. Representative graphs from two independent experiments with three biological replicates per genotype are shown (n=3).

### 3.3.5 Macrophage responses to mycobacterial stimuli are not altered by *SPPL2a* deficiency

The pathways and receptors, which were investigated in DCs, do also play an important role in macrophages. Thus, it was aimed to explore responses of another immune cell type towards mycobacteria species. Bone marrow-derived macrophages (BMDMs) were incubated with HKMT for 24 h. Supernatants were harvested and subjected to cytokine measurements by ELISA. The lack of *SPPL2a* in BMDMs did not alter cytokine release upon HKMT administration (Figure 33). BMDMs from *wt* and *SPPL2a*<sup>-/-</sup> mice secreted comparable amounts of IL-10, IL-2, IL-1 $\beta$  and TNF $\alpha$ . Release of IL-12 family members was also not reduced (data not shown). This does not support a contribution of macrophages to MSMD in *SPPL2a*-deficient patients.

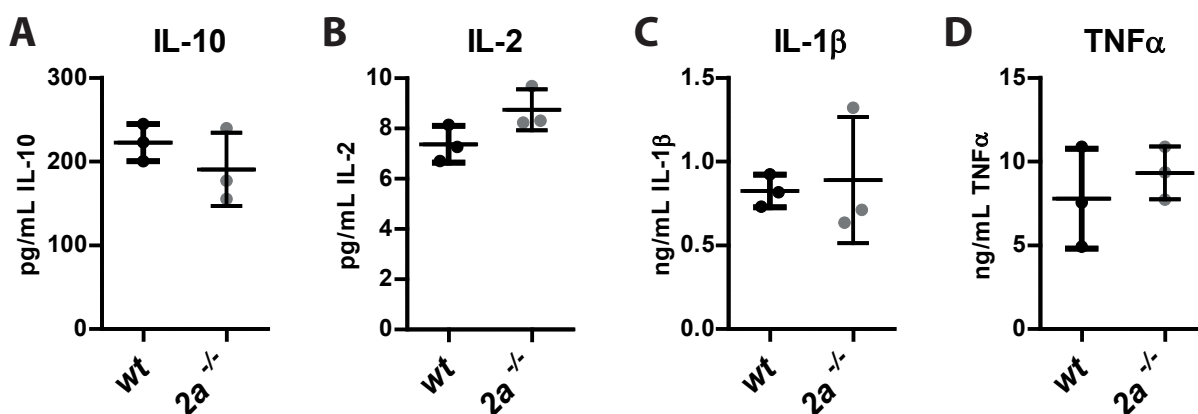


**Figure 33: Normal cytokine response of *SPPL2a*<sup>-/-</sup> macrophages towards heat-killed mycobacteria.** BMDMs from *wt* and *SPPL2a*<sup>-/-</sup> (*2a*<sup>-/-</sup>) mice were treated with 250  $\mu$ g/mL HKMT. Supernatants were harvested after 24 h. Concentrations of **A** IL-10, **B** IL-2, **C** IL-1 $\beta$  and **D** TNF $\alpha$  were determined by ELISA. Single values are shown with mean  $\pm$  SD. An unpaired, two-tailed Student's *t*-test was performed. Representative measurements of three (IL-10, IL-1 $\beta$  & TNF $\alpha$ ) independent experiments or the only measurement performed (IL-2) with three biological replicates per genotype (n=3).

### 3.4 CD74 protein abundance plays a major role in effects of SPPL2a knockout

#### 3.4.1 Lower CD74 protein levels and NTF accumulation in BMDMs compared to BMDCs

The described results raised the question, why the loss of SPPL2a affected DCs but not macrophage function. Accumulation of the SPPL2a substrate CD74 NTF led to functional defects in B cells (Hüttl *et al.*, 2015). The lack of SPPL2a led to accumulation of the CD74 NTF in BMDCs, as well (Figure 13). Macrophages and DCs both express SPPL2a and CD74 according to the transcription database BioGPS (<http://biogps.org>). One explanation might be differences of CD74 and SPPL2a protein levels or altered CD74 NTF degradation between both cell types.

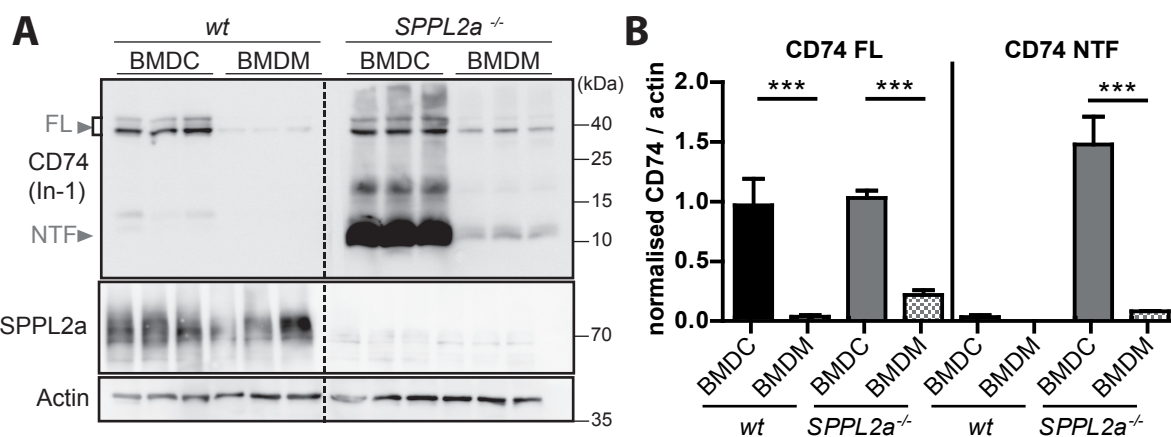


**Figure 34: Macrophages accumulate less CD74 NTF than DCs.** BMDCs and BMDMs were lysed and subjected to Western Blot analysis. **A** Western Blot analysis of CD74 and SPPL2a. CD74 was detected with an antibody directed against the N-terminus of the protein. The full length (FL) and N-terminal fragment (NTF) of CD74 are indicated with arrow heads. Actin was used as loading control. **B** CD74 FL and NTF as well as actin intensities were quantified using ImageJ. Measured intensity of the NTF or FL CD74 were divided by the intensity of actin. Means of ratios  $\pm$  SD are shown. A one-way Anova with a post-hoc-Tukey's testing was performed for the CD74 FL and the CD74 NTF. \*\*\*  $p < 0.001$ ;  $n=3$ .

Protein abundance of CD74 and SPPL2a were analysed in BMDMs to validate expression data obtained from BioGPS on protein level. In addition, BMDM protein levels were compared to BMDC protein levels. BMDMs and BMDCs from *wt* and *SPPL2a*<sup>-/-</sup> mice were lysed and subjected to Western Blot analysis (Figure 34 A). SPPL2a was observed in *wt* BMDCs as well as in *wt* BMDMs, whereby abundance was variable in BMDMs. As expected, SPPL2a was neither detectable in *SPPL2a*<sup>-/-</sup> BMDCs nor in BMDMs. Full length (FL) CD74 was detectable in *wt* BMDCs while only a weak band was visible in *wt* BMDMs. According to quantification of signal intensities, *wt* BMDMs expressed 60-fold less CD74 FL compared to *wt* BMDCs (Figure 34 B). The CD74 NTF highly accumulated in *SPPL2a*<sup>-/-</sup> BMDCs while in *SPPL2a*<sup>-/-</sup> BMDMs only minor amounts of the CD74 NTF were detected. Quantification of signal intensities revealed a significant 23-fold reduced expression of the CD74 NTF in *SPPL2a*<sup>-/-</sup> BMDMs compared

to *SPPL2a*<sup>-/-</sup> BMDCs. Accordingly, CD74 could be the trigger for the observed phenotype in BMDCs. Reduced CD74 protein levels in non-affected BMDMs compared to affected BMDCs are a first hint towards this theory.

### 3.4.2 Cathepsin S knockout BMDCs show milder phenotype than *SPPL2a*<sup>-/-</sup> BMDCs

For further validating the theory of accumulating CD74 NTF in *SPPL2a*<sup>-/-</sup> BMDCs as an important trigger for the observed phenotype, another CD74-related system was investigated. CD74 is cleaved by different endosomal proteases including cathepsin S (CatS) to generate the *SPPL2a* substrate CD74 NTF. As it was already shown that a CD74 fragment accumulates in *CatS*<sup>-/-</sup> B cells and DCs (Nakagawa *et al.*, 1999, Schneppenheim *et al.*, 2017), cytokine secretion in *CatS*<sup>-/-</sup> BMDCs was measured to examine the influence of another CD74 fragment on BMDC function.

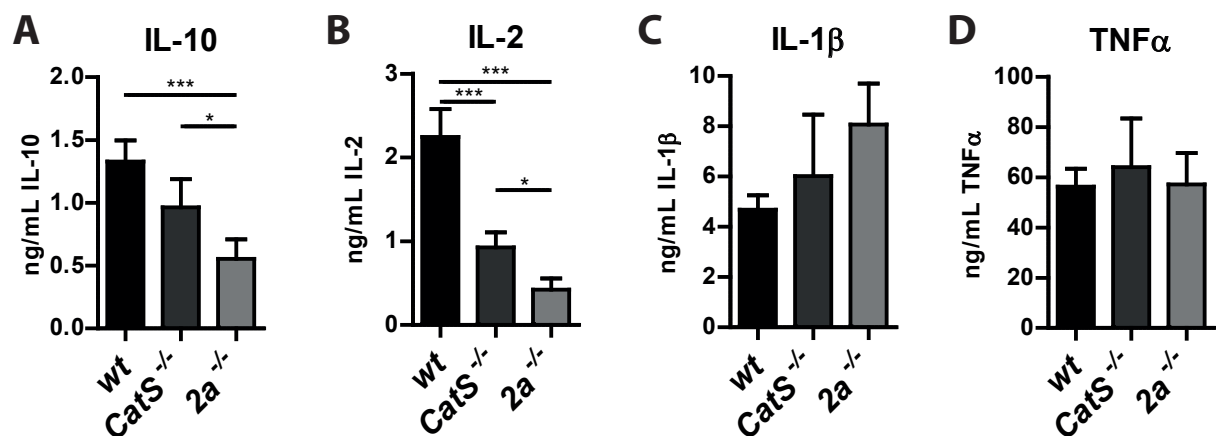


**Figure 35: *CatS*<sup>-/-</sup> BMDCs show similar but milder cytokine phenotype than *SPPL2a*<sup>-/-</sup> BMDCs.** BMDCs from *wt*, *CatS*<sup>-/-</sup> and *SPPL2a*<sup>-/-</sup> (*2a*<sup>-/-</sup>) mice were treated with 250 μg/mL HKMT for 24 h. Supernatants were harvested. Cytokine concentrations of **A** IL-10, **B** IL-2, **C** IL-1β and **D** TNFα were measured by ELISA. Mean ± SD are shown. A one-way Anova with a post-hoc-Tukey's testing was performed. \*  $p < 0.05$  \*\*\*  $p < 0.001$ ;  $n=4$

*In vitro* differentiated DCs from *wt*, *CatS*<sup>-/-</sup> and *SPPL2a*<sup>-/-</sup> mice were stimulated with HKMT for 24 h. Cell supernatants were collected and cytokine concentrations of IL-10, IL-2, IL-1β and TNFα were measured by ELISA (Figure 35). IL-10 secretion was highest in *wt* BMDCs and lowest in *SPPL2a*<sup>-/-</sup> BMDCs. *CatS*<sup>-/-</sup> BMDCs showed intermediate IL-10 release compared to *wt* and *SPPL2a*<sup>-/-</sup> BMDCs after stimulation with HKMT. Differences in IL-10 secretion were significant between *wt* and *SPPL2a*<sup>-/-</sup> BMDCs as well as between *CatS*<sup>-/-</sup> and *SPPL2a*<sup>-/-</sup> BMDCs. A similar pattern was observed for IL-2 release. The absence of CatS led to a significant reduction of IL-2 release of 2.1-fold compared to *wt*. Concentrations of IL-2 in conditioned media from *SPPL2a*<sup>-/-</sup> BMDCs were significantly reduced compared to *wt* and also compared

## RESULTS

to *CatS*<sup>-/-</sup> BMDCs. Again, *CatS*<sup>-/-</sup> BMDCs showed intermediate cytokine release compared to *wt* and *SPPL2a*<sup>-/-</sup> BMDCs upon HKMT treatment. In contrast to that, the mean concentration of IL-1 $\beta$  in conditioned media from HKMT stimulated *CatS*<sup>-/-</sup> BMDCs increased compared to *wt*. The highest IL-1 $\beta$  concentrations were measured in *SPPL2a*<sup>-/-</sup> BMDC supernatants. Differences were not significant. The release of TNF $\alpha$  was comparable between all genotypes. Overall, the accumulation of another CD74 fragment than in *SPPL2a*<sup>-/-</sup> BMDCs also led to altered cytokine release. However, the observed cytokine phenotype was milder in *CatS*<sup>-/-</sup> than in *SPPL2a*<sup>-/-</sup> BMDCs compared to *wt*.

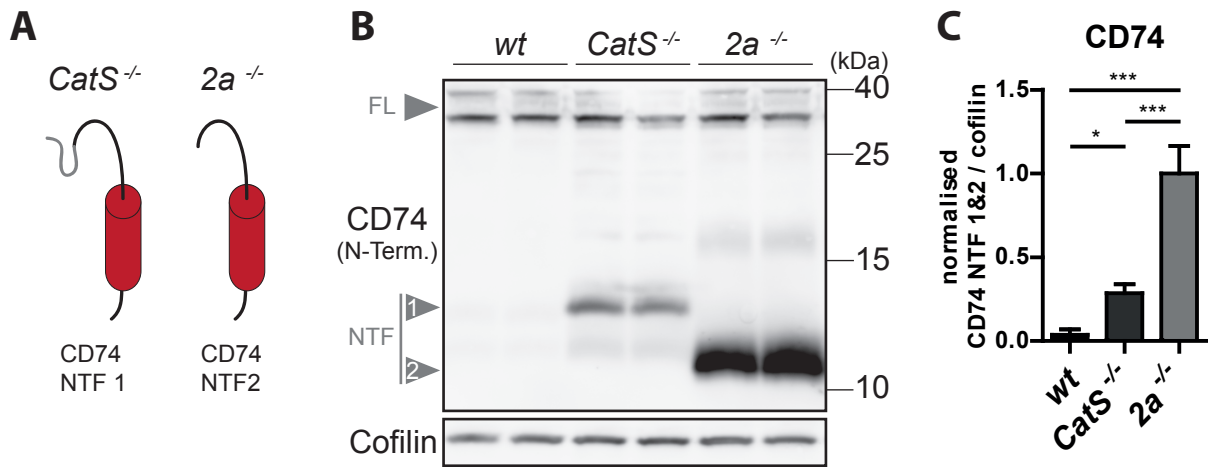


**Figure 36: *CatS*<sup>-/-</sup> BMDCs accumulate less CD74 NTF than *SPPL2a*<sup>-/-</sup> BMDCs.** Lysates from *wt*, *CatS*<sup>-/-</sup> and *SPPL2a*<sup>-/-</sup> (*2a*<sup>-/-</sup>) BMDCs were subjected to Western Blot analysis. **A** Illustration of CD74 fragments accumulating in *CatS*<sup>-/-</sup> and *SPPL2a*<sup>-/-</sup> cells **B** CD74 was detected with an antibody targeting the N-terminus of the protein. The full length (FL) and the two occurring N-terminal fragments (NTF1 & NTF2) are indicated with arrowheads. Cofilin served as loading control. **C** Intensities of signals derived from the CD74 NTF and cofilin were measured with ImageJ. An area including the size of both NTFs was selected in each lane for NTF intensity determination. A ratio of NTF intensity to cofilin intensity was calculated. Mean ratios  $\pm$  SD are shown. A one-way Anova with a post-hoc-Tukey's testing was performed. \*  $p < 0.05$  \*\*\*  $p < 0.001$ ;  $n=4-5$

Because differences between *SPPL2a*<sup>-/-</sup> and *CatS*<sup>-/-</sup> BMDCs regarding the CD74 NTF abundance could be a reason for the observed milder cytokine phenotype, protein levels of CD74 were determined in *wt*, *CatS*<sup>-/-</sup> and *SPPL2a*<sup>-/-</sup> BMDCs by Western Blot analysis. Lysates of *wt*, *CatS*<sup>-/-</sup> and *SPPL2a*<sup>-/-</sup> BMDCs were analysed for CD74 using an antibody targeting an N-terminal epitope (Figure 36 B). Full length CD74 was detected at comparable amounts in all three genotypes. The CD74 NTFs occurred in *CatS*<sup>-/-</sup> and *SPPL2a*<sup>-/-</sup> BMDCs but not in *wt* BMDCs. A larger CD74 NTF (NTF 1) was observed in *CatS*<sup>-/-</sup> BMDCs and a smaller one (NTF 2) in *SPPL2a*<sup>-/-</sup> BMDCs. A faint band of the CD74 NTF 2 was detected in *CatS*<sup>-/-</sup> BMDCs. The CD74 NTF abundance in *CatS*<sup>-/-</sup> BMDCs was reduced compared to *SPPL2a*<sup>-/-</sup> BMDCs. Analysis of NTF signal intensities revealed significant reduction of the CD74 NTF by 3.5-fold in *CatS*<sup>-/-</sup> BMDCs compared to *SPPL2a*<sup>-/-</sup> BMDCs (Figure 36 B).

Overall, the lack of Cathepsin S led to intermediate cytokine release upon HKMT administration compared to *wt* and *SPPL2a*<sup>-/-</sup> BMDCs in regard to IL-10, IL-2 and IL-1 $\beta$ . This was also observed for other ligands (data not shown). *CatS*<sup>-/-</sup> BMDCs accumulated less CD74 NTF and a larger fragment than *SPPL2a*<sup>-/-</sup> BMDCs. In macrophages CD74 expression was much lower than in DCs and they did not show altered cytokine response. Together, these observations pointed towards an important role of the CD74 NTF in functional alterations upon *SPPL2a* ablation in BMDCs.

### 3.4.3 Cytokine responses can be rescued by additional ablation of CD74

Data obtained from *SPPL2a*<sup>-/-</sup> BMDMs and *CatS*<sup>-/-</sup> BMDCs provided strong indications for a major role of CD74 in the cytokine expression phenotype observed in *SPPL2a*<sup>-/-</sup> BMDCs. Additional ablation of CD74 in *SPPL2a*<sup>-/-</sup> BMDCs would prevent the CD74 NTF accumulation and could thus clarify if a CD74 NTF accumulation is the reason for the observed alterations in immune responses in *SPPL2a*<sup>-/-</sup> BMDCs. Cytokine responses towards HKMT, LPS and dZym treatment were analysed including *CD74*<sup>-/-</sup> and *SPPL2a*<sup>-/-</sup>*CD74*<sup>-/-</sup> BMDCs. Cytokine measurements by ELISA of several independent experiments were normalized to concentrations secreted by *wt* BMDCs.

IL-10 release upon HKMT administration was significantly reduced in *SPPL2a*<sup>-/-</sup> BMDCs, as observed before (Figure 37 A). *SPPL2a*<sup>-/-</sup>*CD74*<sup>-/-</sup> BMDCs released IL-10 to a comparable amount than *wt* BMDCs upon HKMT treatment. The mild reduction of IL-2 concentrations in media from HKMT stimulated *SPPL2a*<sup>-/-</sup> BMDCs was lost in *SPPL2a*<sup>-/-</sup>*CD74*<sup>-/-</sup> BMDCs (Figure 37 B). Here, IL-2 release was even slightly increased in *SPPL2a*<sup>-/-</sup>*CD74*<sup>-/-</sup> BMDCs compared to *wt*. This rescue of IL-10 and IL-2 secretion in HKMT stimulated *SPPL2a*<sup>-/-</sup>*CD74*<sup>-/-</sup> compared to *SPPL2a*<sup>-/-</sup> BMDCs was also observed in supernatants from BMDCs after dZym treatment (Figure 37 E & F). Here, the increase of *SPPL2a*<sup>-/-</sup>*CD74*<sup>-/-</sup> IL-2 release compared to *wt* BMDCs was even significant. IL- $\beta$  cytokine concentration was increased upon HKMT or LPS treatment in conditioned medium from *SPPL2a*<sup>-/-</sup> BMDCs compared to *wt* (Figure 37 C & G). In both cases the additional ablation of CD74 led to IL- $\beta$  release comparable to the *wt* situation. Concentrations of IL- $\beta$  released by *SPPL2a*<sup>-/-</sup> BMDCs were significantly increased compared to all other genotypes investigated. The slight increase of TNF $\alpha$  release upon HKMT treatment in *SPPL2a*<sup>-/-</sup> BMDCs was significant compared to *wt* TNF $\alpha$  release (Figure 37 D). Concentrations of TNF $\alpha$  were significantly reduced in *SPPL2a*<sup>-/-</sup>*CD74*<sup>-/-</sup> BMDCs compared to *SPPL2a*<sup>-/-</sup> BMDCs after stimulation with HKMT. *SPPL2a*<sup>-/-</sup>*CD74*<sup>-/-</sup> BMDCs did even release less TNF $\alpha$  than *wt* BMDC, but so did the *CD74*<sup>-/-</sup> BMDCs.

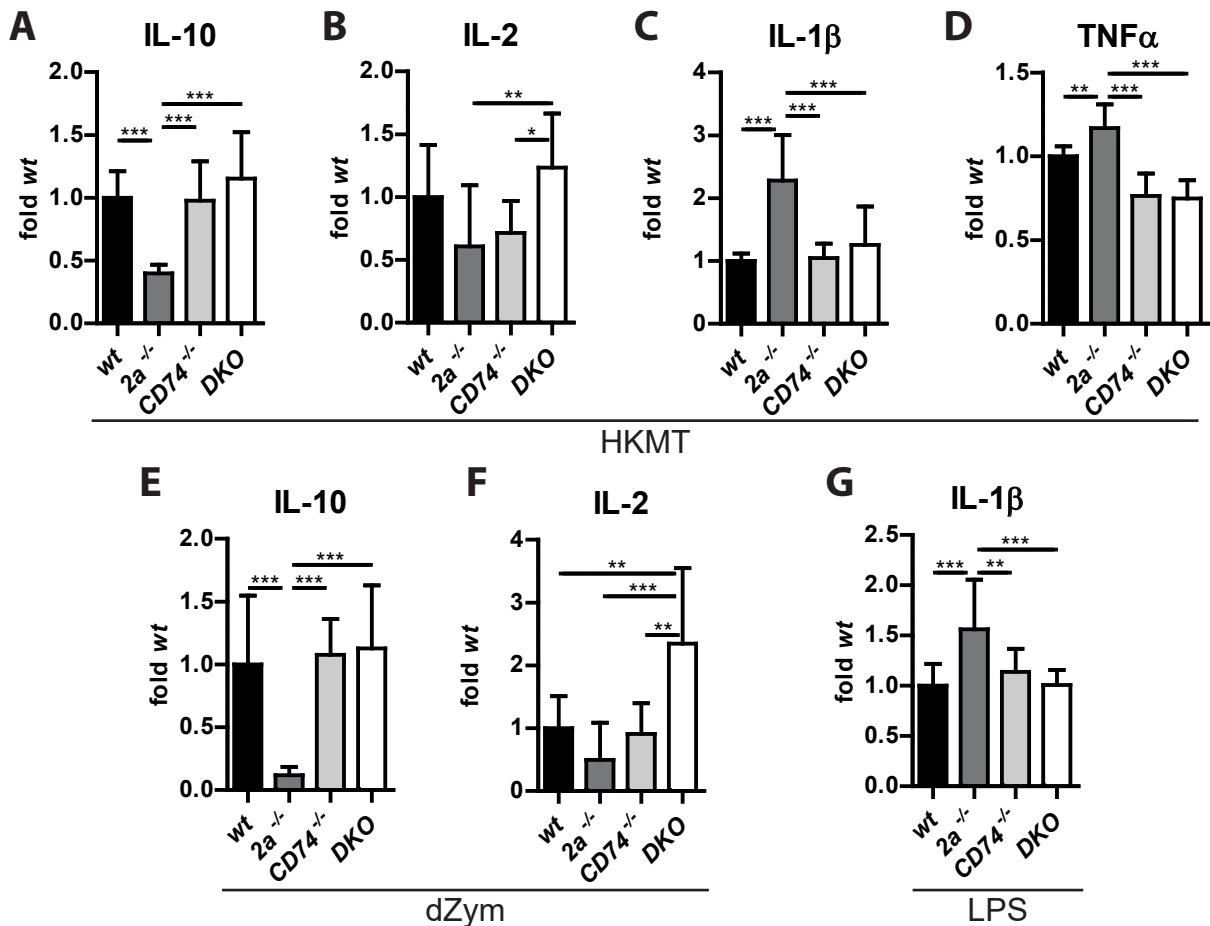


**Figure 37: Absence of CD74 in *SPPL2a*<sup>-/-</sup> BMDCs rescues cytokine phenotype.** *In vitro* differentiated DCs from *wt*, *SPPL2a*<sup>-/-</sup> (*2a*<sup>-/-</sup>), *CD74*<sup>-/-</sup> and *SPPL2a*<sup>-/-</sup>*CD74*<sup>-/-</sup> (DKO) mice were stimulated with 250 µg/mL HKMT, 50 µg/mL dZym or 500 ng/mL LPS. Supernatants were collected after treatment for 24 h. **A** IL-10, **B** IL-2, **C** IL-1β and **D** TNFα were measured by ELISA following HKMT application. **E** IL-10 and **F** IL-2 concentrations were determined in media from dZym treated cells. Concentrations of **G** IL-1β were analysed in conditioned media after LPS treatment. Data from several experiments were normalised to mean of respective *wt*. Mean of fold *wt* ± SD are shown. A one-way Anova with a post-hoc-Tukey’s testing was performed. \* *p* < 0.05, \*\* *p* < 0.01 \*\*\* *p* < 0.001; *n*=8–12 of three or four independent experiments.

It was also investigated, if the rescue of cytokine release in *SPPL2a*<sup>-/-</sup>*CD74*<sup>-/-</sup> BMDCs compared to *SPPL2a*<sup>-/-</sup> BMDCs was already observed at the transcription level. Thus, the expression of cytokines in response to dZym or HKMT treatment was analysed by pRT-PCR (Figure 38). *IL-10* expression upon dZym as well as HKMT stimulus was significantly higher in *wt*, *CD74*<sup>-/-</sup> and *SPPL2a*<sup>-/-</sup>*CD74*<sup>-/-</sup> BMDCs compared to *SPPL2a*<sup>-/-</sup> BMDCs after six hours of treatment. The same was observed for *IL-2* expression after three hours.

Summing up, cytokine secretion and expression in *SPPL2a*<sup>-/-</sup>*CD74*<sup>-/-</sup> BMDCs was mainly comparable to *wt* BMDCs, while *SPPL2a*<sup>-/-</sup> BMDCs showed alterations. The additional ablation of CD74 in *SPPL2a*<sup>-/-</sup> BMDCs rescued the observed cytokine release phenotype. Thus, it can be concluded that the accumulation of the CD74 NTF in *SPPL2a*<sup>-/-</sup> BMDCs caused the observed cytokine phenotype.

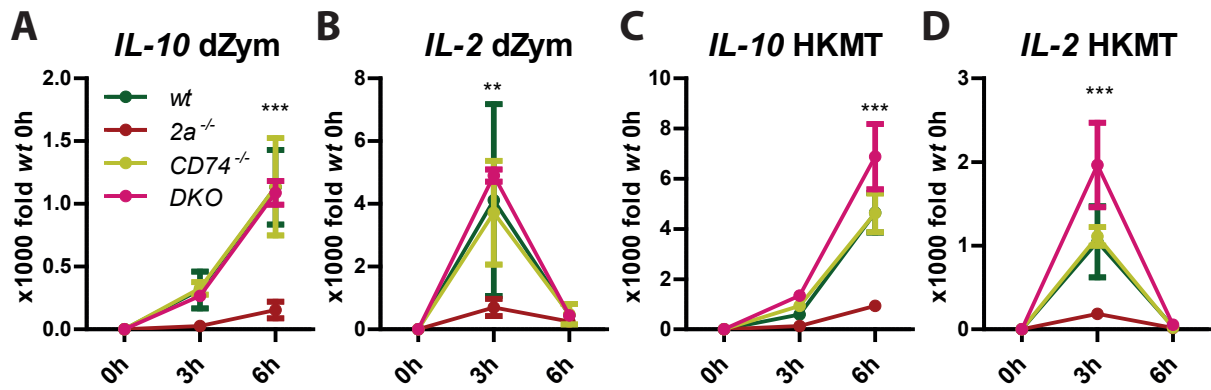


**Figure 38: Cytokine expression in *SPPL2a*<sup>-/-</sup>*CD74*<sup>-/-</sup> BMDCs is comparable to wt.** BMDCs from wt, *SPPL2a*<sup>-/-</sup> (*2a*<sup>-/-</sup>), *CD74*<sup>-/-</sup> and *SPPL2a*<sup>-/-</sup>*CD74*<sup>-/-</sup> (*DKO*) mice were stimulated with 50 µg/mL dZym or 250 µg/mL HKMT for three or six hours or left untreated. Extracted RNA was used for cDNA synthesis. Expression of **A** *IL-10* and **B** *IL-2* induced by dZym as well as **C** *IL-10* and **D** *IL-2* upon HKMT administration was analysed by qRT-PCR. Means of normalised expression ± SD are shown. A two-way Anova with a post-hoc-Bonferroni testing was performed. Significances account for wt, *CD74*<sup>-/-</sup> and *SPPL2a*<sup>-/-</sup>*CD74*<sup>-/-</sup> compared to *SPPL2a*<sup>-/-</sup> BMDC. \*\* p < 0.01 \*\*\* p < 0.001 Representative graphs from two (**D**) or three (**A-C**) independent experiments with three biological replicates per genotype are shown (n=3).

### 3.5 Altered receptor surface expression leads to differential cytokine response in *SPPL2a*<sup>-/-</sup> BMDCs

#### 3.5.1 Comparison of wt and *SPPL2a*<sup>-/-</sup> BMDC cytokine responses upon stimulation of different receptors

Since we could show that the CD74 NTF accumulation caused altered cytokine responses in *SPPL2a*<sup>-/-</sup> BMDCs, it was aimed to investigate possible reasons for the differences in cytokine expression and release. It was concluded from the experiments described before that the CD74 NTF influenced *SPPL2a*<sup>-/-</sup> BMDCs at stages of ligand recognition, signal transduction or induction of expression. For better defining receptors affected by the absence of SPPL2a, a large panel of ligands for different receptors was analysed. Therefore, cytokine responses of BMDCs towards three further pathogen-derived molecules were investigated and summarised (Table 27). As described above, Zymosan is a ligand for Dectin-1 and TLR2/6. LAM is a glycoprotein derived from from *Mycobacterium tuberculosis* cell wall, which activates TLR1/2, MR and Dectin-2 (Means *et al.*, 1999, Tapping and Tobias 2003, Schlesinger *et al.*, 1994, Yonekawa *et al.*, 2014). Mannan stimulates the MR as well and can also activate TLR4 (Stahl and Schlesinger 1980, Tada *et al.*, 2002).

When comparing the cytokine release between *SPPL2a*<sup>-/-</sup> BMDCs and wt BMDCs upon different stimuli mostly only slight or even no differences were observed. Thus, *SPPL2a*<sup>-/-</sup> BMDCs did not show a general defect in response towards different stimuli. However, reduction in IL-10 and IL-2 release and induction of IL-1β release by *SPPL2a*<sup>-/-</sup> BMDCs compared to wt were

## RESULTS

prominent throughout all stimulations. It is of note that the reduction in IL-10 and IL-2 was always detected with ligands for CTLRs, such as Dectin-1. The induction of IL-1 $\beta$  release by *SPPL2a*<sup>-/-</sup> BMDCs correlated with TLR stimulation.

**Table 27: Cytokine secretion of *SPPL2a*<sup>-/-</sup> compared to *wt* BMDCs.** Compilation of results from ELISA measurements of seven different cytokines from supernatants of *wt* and *SPPL2a*<sup>-/-</sup> BMDC, which were treated with one of the seven indicated ligands for 24 h. Comparable (=), reduced (-), increased (+) and tendencies towards reduced (=/-) or increased (=/+ ) cytokine release by *SPPL2a*<sup>-/-</sup> BMDCs compared to *wt* BMDCs are indicated. Some cytokines could not be detected (n.d.) by ELISA. MR abbreviates mannose receptor.

Ligand	dZym	HKMT	LPS	Zym	Mannan	LAM	BCG
<b>Receptor / Cytokine</b>	Dectin-1	TLR2 Mincle Dectin-1 Dectin-2 & others	TLR4	TLR2/6 Dectin-1	TLR4 Dectin-2/3, MR	TLR2/1 MR Dectin-2	TLR2 Mincle Dectin-1 Dectin-2 & others
<b>IL-10</b>	-	-	n.d.	-	-	-	n.d.
<b>IL-2</b>	-	=/-	n.d.	-	-	-	n.d.
<b>IL-1<math>\beta</math></b>	=	+	+	=	+	+	+
<b>TNF<math>\alpha</math></b>	=	=/+	=/+	=/+	=	=/+	=
<b>IL-23</b>	=/-	=/-	=	=	=	=	-
<b>IL-12p40</b>	=/-	=/-	=	=	=	=	-
<b>IL-12p70</b>	n.d.	=	=	=	n.d.	=/+	-

The observed differences in cytokine expression and release between *wt* and *SPPL2a*<sup>-/-</sup> BMDCs might be due to differences in the distribution of certain receptors or alterations in signalling pathways. Especially, stimulation with complex ligands such as HKMT or BCG showed cytokine alterations similar to what was observed for Dectin-1 or TLR4 stimulation alone.

### 3.5.2 Alterations of Dectin-1 receptor function and distribution in *SPPL2a*<sup>-/-</sup> BMDCs

The accumulation of the CD74 NTF in *SPPL2a*<sup>-/-</sup> BMDCs led to changes in cytokine transcription and release. Especially reduced IL-10 and IL-2 expression in *SPPL2a*<sup>-/-</sup> BMDCs upon Dectin-1 activation were observed (see chapter 3.2.1). Therefore, upstream events were explored for abnormalities to evaluate reasons for the altered cytokine responses in *SPPL2a*<sup>-/-</sup> BMDCs.

Dectin-1 signalling was explored by activation of kinases proximal and distal to the receptor upon ligand binding. *Wt*, *SPPL2a*<sup>-/-</sup>, *CD74*<sup>-/-</sup> and *SPPL2a*<sup>-/-</sup>*CD74*<sup>-/-</sup> BMDCs were stimulated with dZym for 15 min or left untreated. Cell lysates were subjected to Western Blot analysis. Amounts of phosphorylated as well as total protein levels of the kinases Syk and ERK were examined (Figure 39 A).



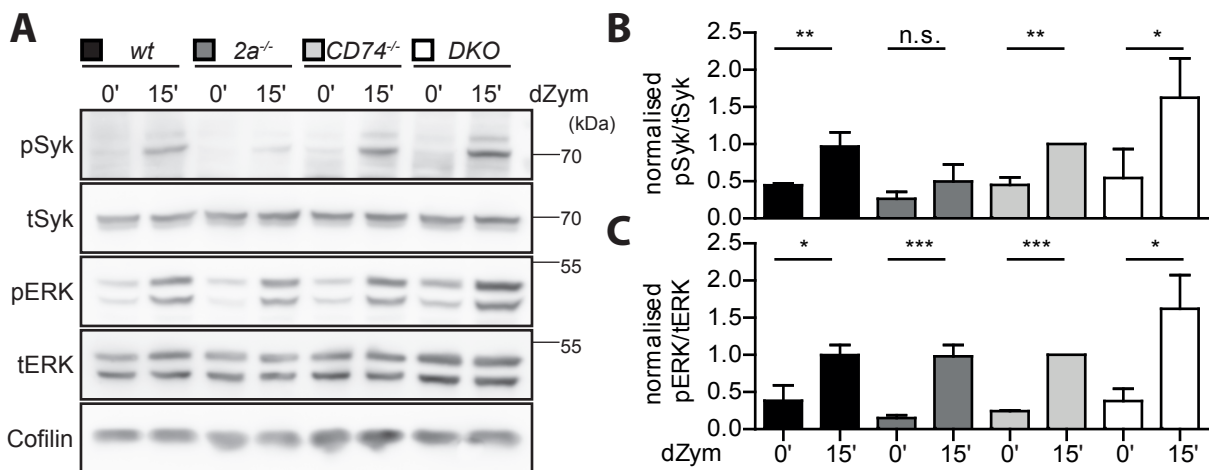


**Figure 39: Reduced Syk activation in *SPPL2a*<sup>-/-</sup> BMDCs upon Dectin–1 stimulation.** *Wt*, *SPPL2a*<sup>-/-</sup> (*2a*<sup>-/-</sup>), *CD74*<sup>-/-</sup> and *SPPL2a*<sup>-/-</sup>*CD74*<sup>-/-</sup> (DKO) BMDCs were stimulated for 15 min with 50  $\mu$ g/mL depleted Zymosan (dZym) or left untreated. **A** Cells were lysed and protein levels of phosphorylated (p) and total (t) Syk and ERK were determined by Western Blotting. Cofilin served as loading control. **B** Signal intensities of total and phosphorylated Syk were measured with ImageJ. A ratio of pSyk/tSyk was calculated and normalised to treated *CD74*<sup>-/-</sup> pSyk/tSyk ratio. **C** As described for B, a normalised pERK/tERK ratio was calculated. Mean  $\pm$  SD. An unpaired, two-tailed Student's *t*-test was performed. n.s. not significant; \*\*\*  $p < 0.001$  Three independent experiments were analysed  $n=3$ .

Abundance of total Syk and ERK were comparable between genotypes and time points of treatment. Syk was activated in *wt*, *CD74*<sup>-/-</sup> and *SPPL2a*<sup>-/-</sup>*CD74*<sup>-/-</sup> BMDCs after 15 min of dZym treatment as observed by increased phospho–Syk (pSyk) detection. BMDCs lacking *SPPL2a* showed reduced phosphorylation of Syk upon Dectin–1 stimulation compared to BMDCs of the other genotypes. Phosphorylation of ERK increased after dZym treatment in BMDCs of all genotypes. A ratio of signal intensities of phosphorylated to total Syk was calculated (Figure 39 B). The dZym treatment led to significant increase of pSyk/tSyk ratio in *wt*, *CD74*<sup>-/-</sup> and *SPPL2a*<sup>-/-</sup>*CD74*<sup>-/-</sup> BMDCs but not in *SPPL2a*<sup>-/-</sup> BMDCs. Analysis of the signal intensity ratio of pERK/tERK revealed a significant increase of ERK activation upon dZym administration in BMDCs of all genotypes (Figure 39 C).

The kinase Syk is phosphorylated directly at the receptor Dectin–1 and ERK is activated more distally (Drummond and Brown 2011, Brown and Crocker 2016). Therefore, surface expression of Dectin–1 was examined. Surface and total receptor expression were determined by flow cytometry. Intact or permeabilised *wt*, *SPPL2a*<sup>-/-</sup>, *CD74*<sup>-/-</sup> and *SPPL2a*<sup>-/-</sup>*CD74*<sup>-/-</sup> BMDCs were stained with a commercially available fluorophore–coupled antibody directed against the extracellular part of Dectin–1. Staining with an undirected fluorophore–conjugated antibody was performed as a control (isotype). Histograms of Dectin–1 stainings of *wt* and *SPPL2a*<sup>-/-</sup> BMDCs pointed towards reduced Dectin–1 surface expression in *SPPL2a*<sup>-/-</sup> BMDCs (Figure 40 A). Intensities of total Dectin–1 staining were increased compared to surface Dectin–1 stainings. Dectin–1 has an intracellular pool and is not only located at the cell surface. For quantifi-

## RESULTS

cation of the results Dectin–1 surface and total measurements of *wt*, *SPPL2a*<sup>-/-</sup>, *CD74*<sup>-/-</sup> and *SPPL2a*<sup>-/-</sup>*CD74*<sup>-/-</sup> BMDCs from independent experiments were normalised to *wt* surface expression and combined (Figure 40 B). This analysis showed a significant reduction of Dectin–1 surface expression on *SPPL2a*<sup>-/-</sup> BMDCs to 0.5–fold of *wt*. Surface expression of Dectin–1 on *CD74*<sup>-/-</sup> and *SPPL2a*<sup>-/-</sup>*CD74*<sup>-/-</sup> BMDCs was comparable to *wt*. Amounts of total Dectin–1 were not significantly different between all genotypes. *Wt* BMDCs expressed 1.6–fold more Dectin–1 in total than they display at their surface, but total amounts of Dectin–1 showed high variability. Total Dectin–1 was 1.3–fold of *wt* surface levels in *SPPL2a*<sup>-/-</sup> BMDCs and 1.2–fold of *wt* surface levels in *CD74*<sup>-/-</sup> as well as *SPPL2a*<sup>-/-</sup>*CD74*<sup>-/-</sup> BMDCs. The data obtained by flow cytometric Dectin–1 measurement revealed reduced surface Dectin–1 expression on *SPPL2a*<sup>-/-</sup> BMDCs, but no decrease in total Dectin–1 protein levels.

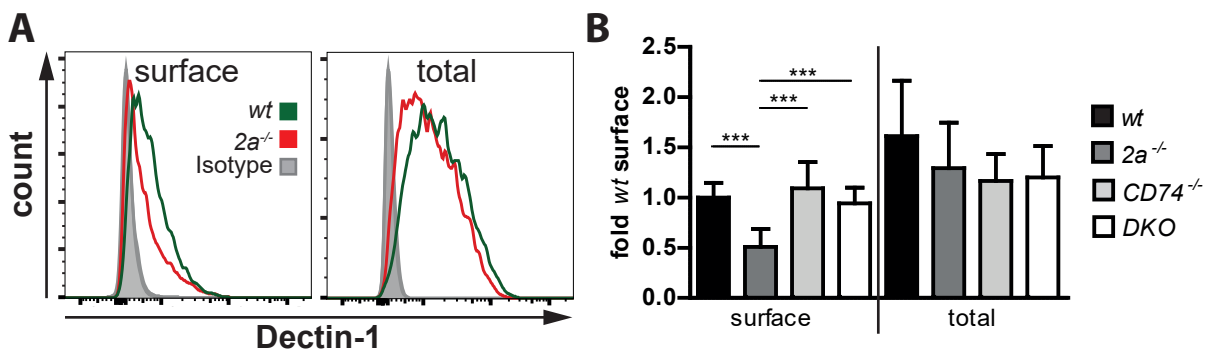


**Figure 40: Reduced Dectin–1 surface expression in *SPPL2a*<sup>-/-</sup> BMDCs measured by flow cytometry.** Intact or permeabilised *wt*, *SPPL2a*<sup>-/-</sup> (*2a*<sup>-/-</sup>), *CD74*<sup>-/-</sup> and *SPPL2a*<sup>-/-</sup>*CD74*<sup>-/-</sup> (*DKO*) BMDCs were stained for surface or total Dectin–1, respectively. The used antibody recognises an extracellular epitope of Dectin–1 and was directly fluorophore –conjugated. As a control the respective isotype was used. Intensities of stainings were detected by flow cytometry. **A** Histograms of surface or total isotype (gray filled) and Dectin–1 staining of *wt* (green line) and *SPPL2a*<sup>-/-</sup> (red line) BMDCs. **B** Mean fluorescence intensities were normalised to *wt* surface Dectin–1 for surface and total stainings. Mean of fold *wt* surface  $\pm$  SD are shown. A one–way Anova with a post–hoc–Tukey’s testing was performed. \*\*\*  $p < 0.001$ ;  $n=9-15$  of 3-5 independent experiments.

This reduction was validated by another method. For this purpose, biotinylation of surface proteins was performed. Intact *wt*, *SPPL2a*<sup>-/-</sup>, *CD74*<sup>-/-</sup> and *SPPL2a*<sup>-/-</sup>*CD74*<sup>-/-</sup> BMDCs were incubated with non cell–permeable biotin containing an active group, which binds to proteins at the cell surface. Biotinylated proteins were extracted with streptavidin–beads after cell lysis. Proteins bound to the beads (bound fraction) and total lysates (input) of biotinylated BMDCs were analysed by Western Blot (Figure 41). The cytosolic protein cofilin was used as a loading control of the input and quality control of the method, as it should not be biotinylated and thus not detectable in bound fraction. Indeed, cofilin was only detectable in the input at comparable levels, but not detectable in the bound fraction. Dectin–1 was detected with an antibody directed against the intracellular N–terminus of the protein. No differences for Dectin–1 FL

protein were observed in total lysates. Dectin-1 FL protein was reduced in *SPPL2a*<sup>-/-</sup> BMDCs compared to the other genotypes within the bound surface expressed fraction. Thus, CD74-dependent reduction of Dectin-1 surface expression in *SPPL2a*<sup>-/-</sup> BMDCs was confirmed by two independent methods.

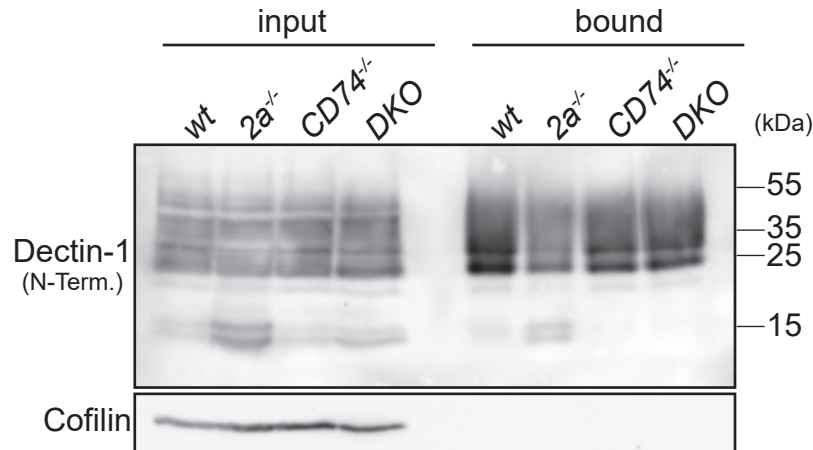


**Figure 41: Biotinylation of cell surface proteins reveals reduced Dectin-1 on *SPPL2a*<sup>-/-</sup> BMDCs.** *Wt*, *SPPL2a*<sup>-/-</sup> (*2a*<sup>-/-</sup>), *CD74*<sup>-/-</sup> and *SPPL2a*<sup>-/-</sup>*CD74*<sup>-/-</sup> (DKO) BMDCs were incubated with activated sulfo-NHS-SS-biotin. Cells were washed and biotinylation was stopped. Lysates were made. An aliquot was kept as input. Biotinylated proteins were isolated from lysates using streptavidin-coupled agarose beads (bound). Input and bound fraction were subjected to Western Blot analysis. Dectin-1 was detected with an antibody directed towards an epitope at the N-terminus. Blot was re-probed for Cofilin. Representative blot of three independent experiments.

As shown in figure 41, an additional Dectin-1 band of approximately 15 kDa accumulated in *SPPL2a*<sup>-/-</sup> BMDCs. This fragment has to be an N-terminal fragment (NTF) as the Dectin-1 antibody was directed against the N-terminus. The NTF was reduced in total lysates of *SPPL2a*<sup>-/-</sup>*CD74*<sup>-/-</sup> BMDCs compared to *SPPL2a*<sup>-/-</sup> BMDCs. A Dectin-1 NTF occurred in the bound fraction of *SPPL2a*<sup>-/-</sup> BMDCs, but not in the bound fraction of *SPPL2a*<sup>-/-</sup>*CD74*<sup>-/-</sup> BMDCs. This accumulation of the Dectin-1 NTF in *SPPL2a*<sup>-/-</sup> BMDCs was further analysed. BMDCs were stimulated with the Dectin-1 ligand Zymosan to provoke degradation of the receptor. Cell lysates of untreated or two hours Zymosan treated *wt*, *SPPL2a*<sup>-/-</sup>, *CD74*<sup>-/-</sup> and *SPPL2a*<sup>-/-</sup>*CD74*<sup>-/-</sup> BMDCs were used for Western Blot analysis. Dectin-1 was detected with an antibody directed against the N-terminal part of the protein (Figure 42 A). As expected, Dectin-1 FL protein decreased upon Zymosan treatment in BMDCs of all genotypes. The Dectin-1 NTF signal intensity increased in *SPPL2a*<sup>-/-</sup> and *SPPL2a*<sup>-/-</sup>*CD74*<sup>-/-</sup> BMDCs upon Zymosan treatment compared to NTF amounts in untreated BMDCs. For quantification purpose a ratio of Dectin-1 NTF to FL (NTF/FL) was calculated (Figure 42 B). This revealed a significant increase of the Dectin-1 NTF in untreated *SPPL2a*<sup>-/-</sup> BMDCs compared to the other genotypes. In Zymosan treated *SPPL2a*<sup>-/-</sup> BMDCs the NTF/FL ratio was also significantly increased compared to *wt* and *CD74*<sup>-/-</sup> BMDCs. The Dectin-1 NTF accumulation in *SPPL2a*<sup>-/-</sup> BMDCs

## RESULTS

was reduced by additional depletion of CD74. This observation led to the conclusion that the accumulation of the CD74 NTF disturbed the degradation of Dectin-1.

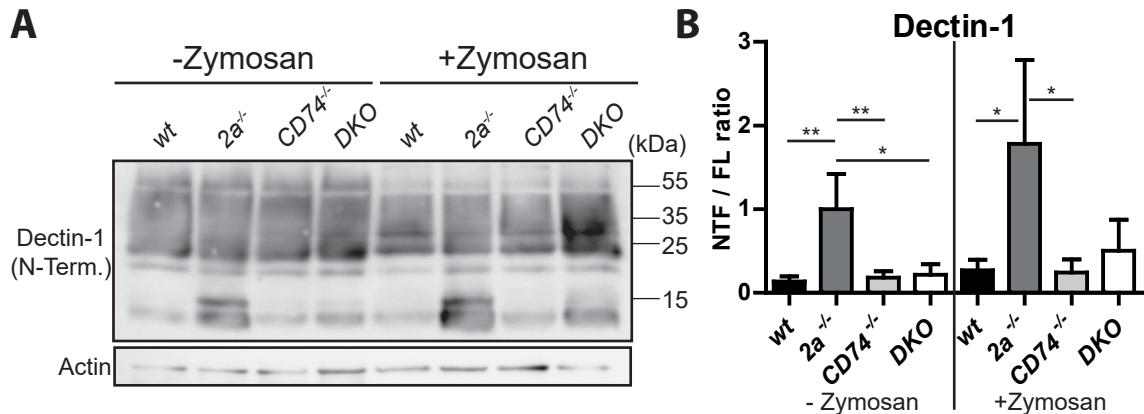


**Figure 42: Dectin-1 NTF accumulates in *SPPL2a*<sup>-/-</sup> BMDCs.** BMDCs from *wt*, *SPPL2a*<sup>-/-</sup> (*2a*<sup>-/-</sup>), *CD74*<sup>-/-</sup> and *SPPL2a*<sup>-/-</sup>*CD74*<sup>-/-</sup> (DKO) mice were treated with 50 µg/mL Zymosan for two hours or left untreated. Cell lysates were subjected to Western Blot analysis. **A** Immunodetection of Dectin-1 with an antibody directed against the N-terminus of the protein. Actin served as loading control. **B** Signal intensities of Dectin-1 N-terminal fragment (NTF) and full length (FL) were quantified with ImageJ and a ratio was calculated. Means of NTF/FL ratio ± SD are shown. A one-way Anova with a post-hoc-Tukey's testing was performed for either untreated or Zymosan stimulated samples. \*  $p < 0.05$ ; \*\*  $p < 0.01$ ;  $n=3$ .

Total Dectin-1 amounts were comparable between *wt* and *SPPL2a*<sup>-/-</sup> BMDCs. Influence of protein transcription on surface Dectin-1 expression was unlikely. Nevertheless, expression of *Dectin-1* was measured by qRT-PCR to validate this. RNA from *wt*, *SPPL2a*<sup>-/-</sup>, *CD74*<sup>-/-</sup> and *SPPL2a*<sup>-/-</sup>*CD74*<sup>-/-</sup> BMDCs were subjected to qRT-PCR analysis of *Dectin-1* (Figure 43). Transcription was normalised to *wt*. All four genotypes expressed similar amounts of *Dectin-1*. The mRNA levels of other CTLRs were also equal between all genotypes (data not shown).

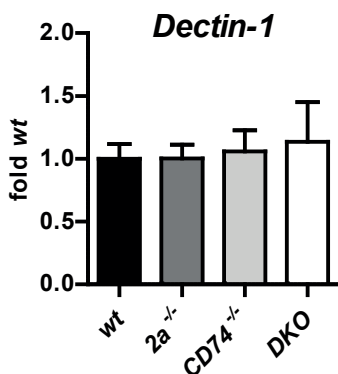


**Figure 43: *Dectin-1* expression is comparable between *wt*, *SPPL2a*<sup>-/-</sup>, *CD74*<sup>-/-</sup> and *SPPL2a*<sup>-/-</sup>*CD74*<sup>-/-</sup> BMDCs.** RNA was isolated from *wt*, *SPPL2a*<sup>-/-</sup> (*2a*<sup>-/-</sup>), *CD74*<sup>-/-</sup> and *SPPL2a*<sup>-/-</sup>*CD74*<sup>-/-</sup> (DKO) BMDCs. It was used as a template for cDNA synthesis. Expression of *Dectin-1* was determined by qRT-PCR. Means of normalised expression ± SD are shown. A one-way Anova with a post-hoc-Tukey's testing was performed.  $n=5-12$  of 2-4 independent experiments.

Total amounts of Dectin-1 were comparable between *wt* and *SPPL2a*<sup>-/-</sup> BMDCs while surface expression was reduced in the latter. This suggested an altered distribution of Dectin-1 in *SPPL2a*<sup>-/-</sup> BMDCs. Thus, the localisation of Dectin-1 in *SPPL2a*<sup>-/-</sup> BMDCs was investigated. Since the accumulation of the CD74 NTF appeared to play a major role in the decrease of

Dectin-1 surface expression an indirect immunofluorescence staining was performed to examine, if Dectin-1 localised in CD74 positive compartments. Labelling of endogenous proteins in BMDCs was performed with antibodies directed against the N-termini of CD74 and Dectin-1 for confocal fluorescence microscopy (Figure 44). Dectin-1 was detectable at the cell border and within the cell in *wt* BMDCs. *SPPL2a* knockout led to Dectin-1 staining mainly localised approximate to the cell nucleus. Dectin-1 staining in *SPPL2a*<sup>-/-</sup> BMDCs showed ring-like structures and Dectin-1 partially co-localised with CD74.

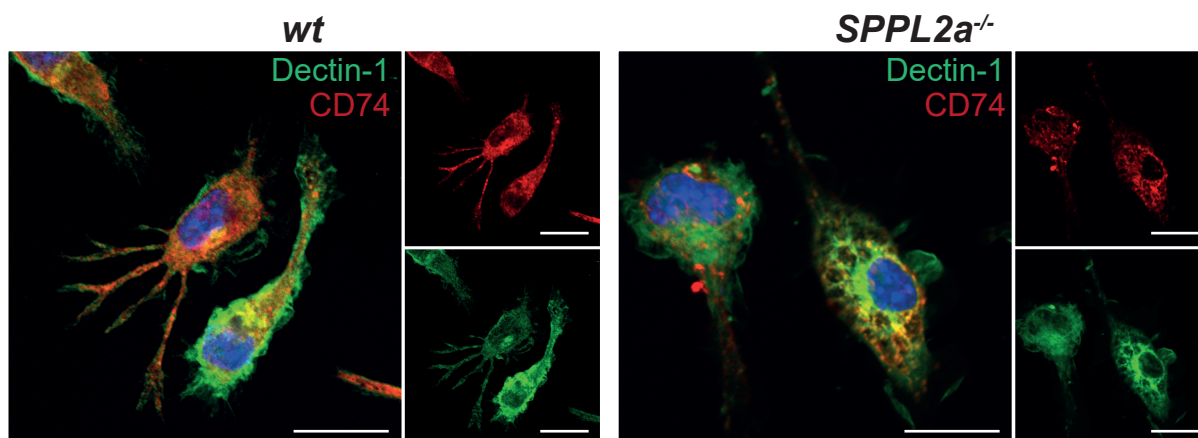


**Figure 44: Dectin-1 re-localises to CD74-positive compartments in *SPPL2a*-deficient BMDCs.** Visualisation of endogenous CD74 (red) and Dectin-1 (green) in *wt* and *SPPL2a*<sup>-/-</sup> BMDCs by indirect immunofluorescence. Cells adhered to poly-L-lysine coated cover slips prior to fixation and permeabilisation. Primary antibodies were directed against the N-termini of CD74 and Dectin-1. Secondary antibodies were fluorescently labelled with Alexa Fluor 488 (AF488) for Dectin-1 or AF647 for CD74 visualisation. Bars=20  $\mu$ m.

### 3.5.3 Increase of TLR4 surface levels and expression in *SPPL2a*<sup>-/-</sup> BMDCs

It was aimed to investigate, if the reduced Dectin-1 surface levels in *SPPL2a*<sup>-/-</sup> BMDCs is a receptor specific or a general effect. Therefore, surface abundance of another pattern recognition receptor was addressed. Since IL-1 $\beta$  and TNF $\alpha$  release was increased by *SPPL2a*<sup>-/-</sup> BMDCs compared to *wt* when stimulated with the TLR4 ligand LPS this receptor was chosen for experimental analysis.

Flow cytometric detection of TLR4 failed due to lack of a functional antibody. Biotinylation of surface proteins was performed, as described before, to examine surface abundance of TLR4. Cells without addition of biotin served as a control. As shown in figure 45, TLR4 was detected to comparable amounts in input of biotinylated *wt*, *CD74*<sup>-/-</sup> and *SPPL2a*<sup>-/-</sup>*CD74*<sup>-/-</sup> BMDC samples, while slightly more TLR4 was observed in *SPPL2a*<sup>-/-</sup> BMDCs. No TLR4 was detected in bound fraction when cells were not incubated with biotin prior to lysis. This indicates that the beads do not unspecifically bind TLR4. *SPPL2a*<sup>-/-</sup> BMDCs showed increased TLR4

RESULTS

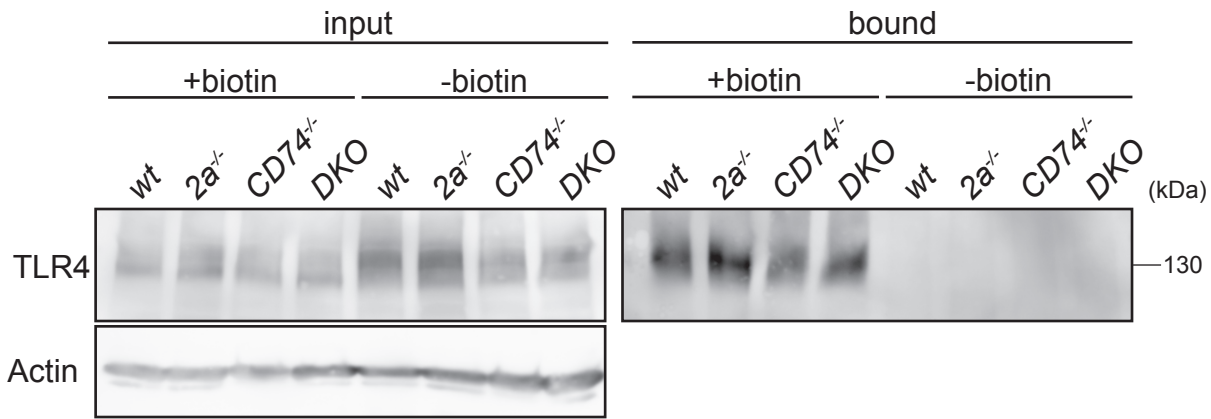


**Figure 45: TLR4 surface expression is increased upon ablation of SPPL2a.** *Wt*, *SPPL2a*<sup>-/-</sup> (*2a*<sup>-/-</sup>), *CD74*<sup>-/-</sup> and *SPPL2a*<sup>-/-</sup>*CD74*<sup>-/-</sup> (DKO) BMDCs were incubated with activated biotin or with buffer only as a control. Cells were lysed and an aliquot was taken (input). Streptavidin-coupled beads were added to the remaining lysate. After washing, beads were eluted with SDS-PAGE-sample buffer (bound). Samples were subjected to Western Blot analysis of TLR4. Actin was used as loading control. Representative blot from two independent experiments is shown.

staining compared to *wt*, *CD74*<sup>-/-</sup> and *SPPL2a*<sup>-/-</sup>*CD74*<sup>-/-</sup> BMDCs in bound fraction when biotin was added. This indicates increased surface abundance of TLR4 in *SPPL2a*<sup>-/-</sup> BMDCs.

Increased expression could explain increased total and surface TLR4 protein levels. Transcription of *TLR4* was quantified in *wt*, *SPPL2a*<sup>-/-</sup>, *CD74*<sup>-/-</sup> and *SPPL2a*<sup>-/-</sup>*CD74*<sup>-/-</sup> BMDCs by qRT-PCR. Transcript levels were normalised to *wt* (Figure 46). Expression of *TLR4* was significantly increased by 1.3-fold in *SPPL2a*<sup>-/-</sup> BMDCs compared to *wt* and *SPPL2a*<sup>-/-</sup>*CD74*<sup>-/-</sup> BMDCs. In contrast to that, expression of other TLRs was not different between genotypes (data not shown).

Thus, increased IL-1 $\beta$  and TNF $\alpha$  secretion in *SPPL2a*<sup>-/-</sup> BMDCs could be at least partially explained by increased surface expression of TLR4.

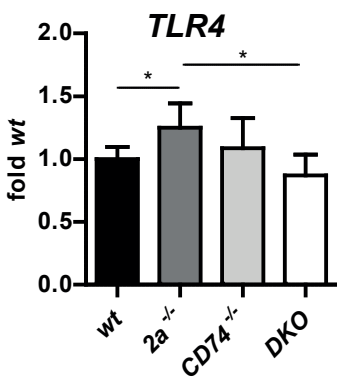


**Figure 46: TLR4 expression is slightly increased in SPPL2a<sup>-/-</sup> BMDCs.** Transcription of *TLR4* was measured in *wt*, *SPPL2a*<sup>-/-</sup> (*2a*<sup>-/-</sup>), *CD74*<sup>-/-</sup> and *SPPL2a*<sup>-/-</sup>*CD74*<sup>-/-</sup> (DKO) BMDCs by qRT-PCR after extraction of RNA and cDNA synthesis. Means of normalised expression  $\pm$  SD are shown. A one-way Anova with a post-hoc-Tukey's testing was performed. \*  $p < 0.05$ ;  $n=3-9$  of 1-3 independent experiments.

## 4 Discussion

The intramembrane protease SPPL2a plays an important role in the homeostasis and function of the immune system as displayed by B cell defects in SPPL2a-deficient mice (Schneppenheim *et al.*, 2013, Beisner *et al.*, 2013, Bergmann *et al.*, 2013, Hüttl *et al.*, 2015). In humans, the absence of the protease is described in patients with MSMD (Kong *et al.*, 2018). Interestingly, these patients harbour normal B cell numbers, but a reduction in the cDC2 population. To further elucidate the role of SPPL2a in DC development and function, a *SPPL2a*<sup>-/-</sup> mouse model system was used. While the frequencies of DCs were analysed directly within spleens of mice, an *in vitro* differentiation system was applied for functional studies. In B cells, the accumulation of the SPPL2a substrate CD74 was causative for the observed phenotype. Therefore, *CD74*<sup>-/-</sup> and *SPPL2a*<sup>-/-</sup>*CD74*<sup>-/-</sup> mice were included in this study to explore the effect of this substrate in the DC system. DCs connect the innate and the adaptive immune system (Macri *et al.*, 2017). They detect foreign antigens with their PRRs and induce differentiation and maintenance of effector and regulatory T cells thereafter. DCs induce clearance of infections, but also lead to regulation of immune response (Macri *et al.*, 2017). The different DC subtypes possess specialised tasks within the immune system. The pDC subset is important for defence against viral infections, cDC1s are mediators for immunity against intracellular pathogens and the cDC2 subpopulation sense extracellular parasites and bacteria (Durai and Murphy 2016). Thus, deregulation of composition of DC subsets as well as alterations in the response of DCs towards pathogens can lead to recurrent infections as well as tissue damage.

This DC network was disturbed in the absence of the intramembrane protease SPPL2a in mice. The cDC2 subpopulation was reduced in *SPPL2a*<sup>-/-</sup> mice compared to *wt*, while cDC1 and pDC populations were detected to comparable amounts. Key findings of the functional analysis of BMDCs are summarised in figure 47. The absence of SPPL2a led to accumulation of its substrate, the CD74 NTF, in BMDCs. These cells showed altered surface levels of different PRRs, which was reflected by altered responses towards different PRR ligands. Especially, the release and expression of the cytokines IL-10 and IL-2 were reduced upon CTLR ligation and IL-1 $\beta$  expression and release was increased when TLRs were activated. The CTLR Dectin-1 was localised in CD74 positive vesicular structures and thus reduced at the cell surface while the TLR4 surface levels were increased on *SPPL2a*<sup>-/-</sup> BMDCs compared to *wt*. The altered receptor surface levels and cytokine responses in *SPPL2a*<sup>-/-</sup> BMDCs led to the assumption that CTLR-response pathways could be hampered while TLR-response pathways might be enhanced by the accumulation of the SPPL2a substrate CD74 NTF.

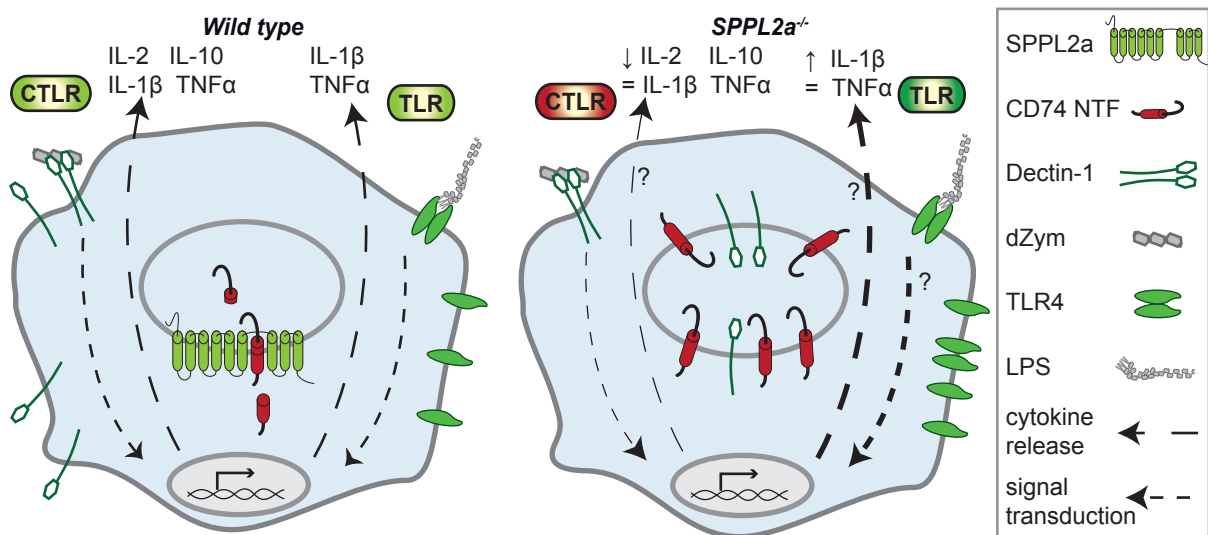


**Figure 47: Schematic summary of *SPPL2a*<sup>-/-</sup> BMDC phenotype.** The ligation of the CTLR Dectin-1 with depleted Zymosan (dZym) as well as the ligation of the TLR4 with LPS on BMDCs led to activation of signalling cascades, transcription and release of cytokines. The ablation of *SPPL2a* leads to the accumulation of the CD74 NTF in the endosomal system. The surface Dectin-1 levels were reduced in *SPPL2a*<sup>-/-</sup> BMDCs and the receptor relocated to CD74 positive compartments. The subsequent signalling was reduced and less IL-10 and IL-2 were transcribed and released. The surface expression of TLR4 was increased in *SPPL2a*<sup>-/-</sup> BMDCs as well as the release of IL-1 $\beta$ .

#### 4.1 The CD74 NTF accumulation is causative for altered *SPPL2a*<sup>-/-</sup> DC development *in vivo* and *SPPL2a*<sup>-/-</sup> BMDC function *in vitro*

The important role of the intramembrane protease *SPPL2a* in DC differentiation *in vivo* and function *in vitro* was demonstrated in this study, as described above. Since *SPPL2a* is an intramembrane protease, this effects were likely mediated by the accumulation of a proteolytic substrate. Increased amounts of the *SPPL2a* substrate CD74 NTF were observed in *SPPL2a*<sup>-/-</sup> BMDCs and are causative for B cell defects already described in *SPPL2a*-deficient mice (Schneppenheim *et al.*, 2013, Beisner *et al.*, 2013, Bergmann *et al.*, 2013, Hüttl *et al.*, 2015).

Further findings supported the assumption that the CD74 NTF accumulation led to the described DC phenotype. Only minor amounts of the CD74 NTF were detectable in *SPPL2a*<sup>-/-</sup> BMDMs, which had no obvious functional defect. Cytokine responses of *SPPL2a*<sup>-/-</sup> BMDMs were comparable to *wt* BMDMs in BCG-co-cultures. When evaluating the CD74 levels of BMDMs and comparing it to BMDCs, a significant difference was observed. *Wt* BMDMs expressed much less CD74 FL protein and *SPPL2a*<sup>-/-</sup> BMDMs accumulated significantly reduced amounts of the CD74 NTF compared to BMDCs of the respective genotype. Such a difference of CD74 expression between macrophages and dendritic cells was also observed by others in cells directly isolated from mice, strengthen our observations (Stables *et al.*, 2011).



For further analysis of the role of CD74 in the observed DC phenotype, a *CatS* knockout model also accumulating CD74 fragments was applied (Schneppenheim *et al.*, 2017). *CatS* is the protease which generates the SPPL2a substrate, the CD74 NTF. *CatS*<sup>-/-</sup> BMDCs released IL-1 $\beta$ , IL-10 and IL-2 in concentrations, which lay between concentrations measured in conditioned media from *wt* and *SPPL2a*<sup>-/-</sup> BMDCs upon HKMT treatment. Thus, *CatS*<sup>-/-</sup> BMDCs displayed a milder phenotype than *SPPL2a*<sup>-/-</sup> BMDCs. The analysis of the CD74 NTF protein levels revealed that the accumulating fragment was less abundant in *CatS*<sup>-/-</sup> BMDCs than in *SPPL2a*<sup>-/-</sup> BMDCs, pointing towards a dose dependent effect of CD74 accumulation. Such a dose dependency was already observed in B cells from *SPPL2a*<sup>-/-</sup> and *CatS*<sup>-/-</sup> mice (Schneppenheim *et al.*, 2017). The impact of CD74 fragment accumulation on DC function is displayed by reduced migration capacity of *CatS*<sup>-/-</sup> DCs compared to *wt* DCs (Faure-André *et al.*, 2008). Migration of DCs from periphery towards lymph nodes is important for induction of T cell responses (Heuzé *et al.*, 2013). As *CD74*<sup>-/-</sup> DCs migrate faster than *wt* DCs, the increased levels of the CD74 fragment in *CatS*<sup>-/-</sup> DCs reduces the migration capacity of *CatS*<sup>-/-</sup> DCs (Faure-André *et al.*, 2008). In *SPPL2a*<sup>-/-</sup> BMDCs, increased amounts of the CD74 NTF accumulated compared to *CatS*<sup>-/-</sup> BMDCs. Therefore, it seems likely that *SPPL2a*<sup>-/-</sup> BMDCs migrate even slower than *CatS*<sup>-/-</sup> BMDCs.

The final proof of CD74 NTF causing differentiation and functional defects in DCs was the rescue of the *SPPL2a*<sup>-/-</sup> phenotypes in *SPPL2a*<sup>-/-</sup>*CD74*<sup>-/-</sup> double knockout mice and BMDCs. Cytokine release by *SPPL2a*<sup>-/-</sup>*CD74*<sup>-/-</sup> BMDCs as well as DC frequencies in *SPPL2a*<sup>-/-</sup>*CD74*<sup>-/-</sup> mice were comparable to *wt* BMDCs and mice, respectively. This proves that the CD74 NTF accumulation is causative for the *SPPL2a*<sup>-/-</sup> DC phenotype described here.

#### **4.2 Potential role of further *SPPL2a*<sup>-/-</sup> substrates in the *SPPL2a*<sup>-/-</sup> DC phenotype**

We cannot exclude that further substrates of SPPL2a could also influence DC differentiation and function. Another SPPL2a substrate known to be involved in immunity is TNF $\alpha$  (Fluhrer *et al.*, 2006, Friedmann *et al.*, 2006). Friedmann *et al.*, 2006 published that TNF $\alpha$  ICD, released upon SPPL2a and SPPL2b cleavage, would induce IL-12p70 expression. They use a chemical compound for inhibition of SPPL2a and SPPL2b activity and knockdown SPPL2a or SPPL2b in human monocyte-derived DCs. In all cases, cells release reduced amounts of IL-12p70 after stimulation with LPS compared to unaltered human monocyte-derived DCs. The overexpression of the TNF $\alpha$  ICD rescues this effect. The used inhibitor does also affect proteolytic activity of other SPP/SPPL proteases and the knockdown of SPPL2a as well as the inhibitor would also affect CD74 degradation. However, in our murine BMDC system we could not observe a general defect of IL-12p70 expression by *SPPL2a*<sup>-/-</sup> BMDCs, but only in the case of the BCG-co-culture. Furthermore, if accumulation of the SPPL2a substrate TNF $\alpha$  NTF had an

effect in our system, it should be preserved in the *SPPL2a*<sup>-/-</sup>*CD74*<sup>-/-</sup> BMDCs, which is not the case. Thus, it is unlikely that uncleaved TNF $\alpha$  has an effect on the explored DC function in our murine model system. One has to admit, that we did not investigate SPPL2b knockout BMDCs, where TNF $\alpha$  ICD release could play a role. Furthermore, Friedmann *et al.*, 2006 explored human cells, while murine cells are used in this study. All in all, other substrates from SPPL2a than the CD74 NTF might also affect DC function, but either to a minor degree or functions we did not address here. Thus, the CD74 NTF accumulation in *SPPL2a*<sup>-/-</sup> mice and BMDCs causes differentiation defects as well as functional alterations observed.

### 4.3 How could the CD74 NTF accumulation cause the observed DC phenotype?

The mechanism of the CD74 NTF accumulation causing *SPPL2a*<sup>-/-</sup> DC differentiation defects *in vivo* and altered receptor surface levels and cytokine response in *SPPL2a*<sup>-/-</sup> BMDCs *in vitro* remains elusive and can only be speculated at this moment. Possible mechanisms are depicted in figure 48. In the absence of the intramembrane protease SPPL2a the CD74 NTF cannot be cleaved. This lack of cleavage could either cause the observed alterations as an CD74 ICD cannot be released and thus is missing for possible transcriptional regulation or by the presence of the CD74 fragment itself. A major role of the ICD seems unlikely, as the *SPPL2a*<sup>-/-</sup>*CD74*<sup>-/-</sup> mice displayed normal frequencies of DC populations and receptor levels. Furthermore, Cytokine expression upon activation of *SPPL2a*<sup>-/-</sup>*CD74*<sup>-/-</sup> BMDCs was comparable to the *wt* situation. Thus, the high abundance of the CD74 NTF most likely caused the described DC phenotype.

CD74 can trimerise at the cell surface and serves as a receptor for the cytokine MIF (Schröder 2016). The accumulating CD74 NTFs could interfere with that function, since also truncated versions of CD74 are still capable to trimerise (Ashman and Miller 1999). On the one hand, the MIF-mediated signalling could be enhanced, as truncated CD74 could continue signalling. On the other hand, MIF-mediated signalling could be inhibited by the CD74 NTF, as it could interfere with the CD74 FL trimerisation or binding to co-factors. MIF knockout leads to reduced Dectin-1 expression, but also decreased TLR4 expression on macrophages as well as reduced IL-10, IL-2 and TNF $\alpha$  response upon co-culture of macrophages with mycobacteria (Das *et al.*, 2013, Roger *et al.*, 2001). Furthermore, *MIF*<sup>-/-</sup> mice suffer from more severe infections with intracellular parasites due to reduced IL-12 production and decreased maturation of DCs (Terrazas *et al.*, 2011). Thus, the MIF knockout displays some similarities with our SPPL2a knockout, but there are also differences like the reduced TLR4 expression, which is increased in *SPPL2a*<sup>-/-</sup> BMDCs. In the absence of CD74, MIF signalling would also be affected. Therefore the normal development and function of DCs from *SPPL2a*<sup>-/-</sup>*CD74*<sup>-/-</sup> mice argue against a predominant role of MIF signalling in our *SPPL2a*<sup>-/-</sup> system.

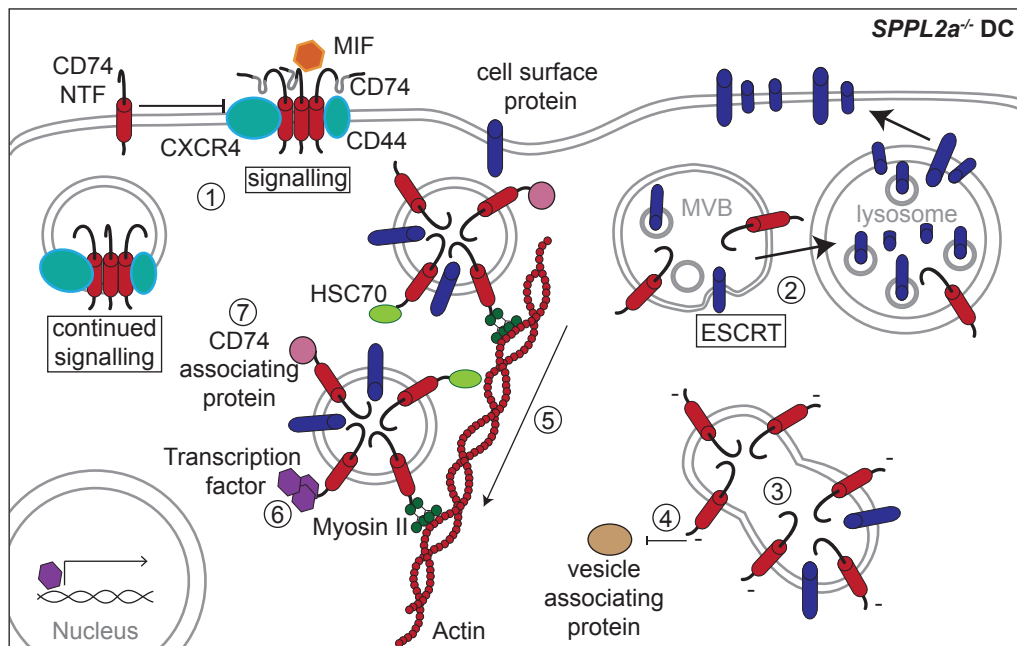


**Figure 48: Possible mechanisms of CD74 NTF influencing *SPPL2a*<sup>-/-</sup> DC functions.** ① CD74 homotrimer binds to the cytokine MIF at the cell surface. The subsequent signalling relies on the co-factors CD44 or CXCR4. Truncated intracellular CD74 NTFs could trimerise and continue signalling. The CD74 NTF could also inhibit MIF–signalling. ② The CD74 NTF could hinder membrane protein degradation via ESCRT. These undegraded or partially degraded proteins could recycle to the plasma membrane ③ Increased amounts of CD74 negative loaded cytoplasmic tail could lead to enhanced membrane fusion processes or ④ inhibit binding of proteins to vesicles. ⑤ CD74 interaction with proteins as Myosin II could be enhanced, leading to increased endocytosis. ⑥ CD74 interaction with transcription factors could hinder their nuclear translocation, thereby influencing transcription. ⑦ Interactions of the CD74 NTF with proteins not described so far are also possible. Scheme adapted and expanded from Hüttl 2015 and Schröder 2016.

In a CD74 NTF–dependent manner, degradation of Dectin–1 was hampered in *SPPL2a*<sup>-/-</sup> BMDCs as a Dectin–1 NTF accumulated. Upon ligand binding, Dectin–1 is internalised in a dynamin– and actin–dependent manner and delivered to lysosomal compartments (Goodridge *et al.*, 2012, Hernanz-Falcón *et al.*, 2009, Herre *et al.*, 2004). Lysosomal proteases degrade the full length receptor, which terminates also receptor signalling (Hernanz-Falcón *et al.*, 2009, Mansour *et al.*, 2013, McCann *et al.*, 2005). In general, membrane proteins can be degraded via the endosomal sorting complexes required for transport (ESCRT) pathway (Schmidt and Teis 2012, Piper and Katzmann 2007). The accumulating CD74 fragment in *SPPL2a*<sup>-/-</sup> BMDCs could have impaired the ESCRT pathway and thus degradation of membrane proteins. These proteins would then accumulate and they could modulate sorting of surface receptors, signalling or cytokine release and thus influence these pathways in *SPPL2a*<sup>-/-</sup> BMDCs.

The accumulating Dectin–1 fragment in *SPPL2a*<sup>-/-</sup> BMDCs is of special importance in regard to SPPL2a substrate determination. As the Dectin–1 fragment was reduced in *SPPL2a*<sup>-/-</sup> *CD74*<sup>-/-</sup> BMDCs compared to *SPPL2a*<sup>-/-</sup> BMDCs, it is not a SPPL2a substrate, even though it has the required type II orientation. The accumulating Dectin–1 fragment in *SPPL2a*<sup>-/-</sup> BMDCs showed that one has to be careful when searching for new SPPL2a substrates, as type II membrane

proteins can accumulate in *SPPL2a*<sup>-/-</sup> BMDCs, without being a substrate. Therefore analysis of *SPPL2a*<sup>-/-</sup>*CD74*<sup>-/-</sup> cells or mice should always be included in experiments using *SPPL2a*<sup>-/-</sup> cells or mice for SPPL2a substrate determination, to exclude CD74 NTF-mediated effects.

Based on the capability of CD74 to induce endosome fusion (Nordeng *et al.*, 2002), disturbed endosomal trafficking could also contribute to the observed *SPPL2a*<sup>-/-</sup> BMDC phenotype. The endosome fusion is mediated by the net negative charge in the CD74 cytoplasmic tail (Nordeng *et al.*, 2002), which is also present in the CD74 NTF. The increase in amount of the CD74 NTF could lead to increased membrane fusion processes and therefore affect intracellular pathways as for example receptor sorting. Alterations in membrane fusion processes are reflected by increased numbers of vesicles in *SPPL2a*<sup>-/-</sup> B cells (Schneppenheim *et al.*, 2013). However, no obvious morphological alterations of the endocytic system were observed in *SPPL2a*<sup>-/-</sup> BMDCs (Hüttl 2015). A more detailed analysis is required for membrane fusion processes and vesicle numbers including functions of this system in *SPPL2a*<sup>-/-</sup> BMDCs.

Furthermore, the increased amount of negatively charged CD74 NTF in *SPPL2a*<sup>-/-</sup> BMDCs could lead to an increased negative charge of the whole vesicle and thus hamper binding of cytosolic proteins to proteins within the vesicle membrane. To test this, the CD74 (D6R) mutant, in which the negative charged amino acid in the cytoplasmic tail is exchanged, could be expressed in *SPPL2a*<sup>-/-</sup>*CD74*<sup>-/-</sup> BMDCs and surface levels of Dectin-1 and TLR4 or cytokine response upon activation could be compared to *SPPL2a*<sup>-/-</sup> BMDCs. To determine which proteins are affected, CD74 positive vesicles could be isolated together with associated proteins from *wt* and *SPPL2a*<sup>-/-</sup> BMDCs. It could then be analysed which proteins are missing at vesicles from *SPPL2a*<sup>-/-</sup> BMDCs.

In contrast, it would also be possible that the high amount of the CD74 NTF in *SPPL2a*<sup>-/-</sup> BMDCs could lead to an enhanced recruitment of proteins binding to the CD74 cytosolic tail. Two proteins known to interact with CD74 are heat shock protein 70 (HSC70; Lagaudrière-Gesbert *et al.*, 2002) and Myosin II (Faure-André *et al.*, 2008, Vascotto *et al.*, 2007). It has been reported that overexpression of CD74 is responsible for formation of enlarged vesicles by recruitment of the uncoating ATPase of clathrin-coated vesicles HSC70 (Lagaudrière-Gesbert *et al.*, 2002). Myosin II is important for vesicle transport within B cells (Vascotto *et al.*, 2007). The CD74 NTF could also lead to such alterations in membrane and vesicle trafficking in our *SPPL2a*<sup>-/-</sup> BMDCs, thereby affecting surface levels of receptors, as observed for Dectin-1 and TLR4. Furthermore, CD74 was shown to be able to bind to transcription factors as p65 of the NF $\kappa$ B family and Runx1/3 (Gil-Yarom *et al.*, 2017). When the CD74 NTF could also sequester these transcription factors, it could thereby impact their translocation into the nucleus and thereby alter transcription, as observed for some cytokines and TLR4 in *SPPL2a*<sup>-/-</sup> BMDCs.

To further elucidate the pathological function of the CD74 NTF, known CD74 FL interaction partners should be also validated for the CD74 NTF. Furthermore, new CD74 NTF interacting proteins could be explored. Immunoprecipitation (IP) of the CD74 NTF from *SPPL2a*<sup>-/-</sup> BMDCs, where the fragment was observed in high abundance, could be performed followed by mass spectrometry. These data then would require validation by endogenous IP or by the use of overexpression systems, depending on availability of antibodies against possible CD74 NTF interaction partners. Validation of the possible influence of known and newly identified CD74 interaction partners on BMDC function could be performed with BMDC cultures from respective knockout mice in combination with inhibition of SPPL2a activity. Prerequisite of this method would be that these knockout mice are viable and that the SPPL2a inhibition is sufficient to mimic the SPPL2a knockout BMDC phenotype. An investigation of the CD74 NTF interaction partners in participation of the observed *SPPL2a*<sup>-/-</sup> BMDC phenotype could also be performed by modulating interaction partners with small interfering RNA (siRNA)-mediated knockdown in our *SPPL2a*<sup>-/-</sup> BMDCs followed by analysis of surface receptor abundance or cytokine responses.

#### **4.3.1 Possible CD74-dependent mechanisms for altered Dectin-1 and TLR4 surface levels**

Further elucidation of the mechanism causing the altered Dectin-1 and TLR4 surface levels on *SPPL2a*<sup>-/-</sup> BMDCs would also help to understand how the CD74 NTF accumulation leads to the DC phenotype. Possible mechanisms are summarised in figure 49. Since mRNA levels of Dectin-1 were comparable between *SPPL2a*<sup>-/-</sup> and *wt* BMDCs, altered expression is unlikely to account for reduced Dectin-1 surface levels. The increased surface abundance of TLR4 on *SPPL2a*<sup>-/-</sup> BMDCs was reflected by increased *TLR4* mRNA levels compared to *wt*. Several transcription factors positively and negatively regulate *TLR4* transcription, among them PU.1 and IRF family members (Rehli *et al.*, 2000, Roger *et al.*, 2005). For further investigation of the mechanism behind enhanced *TLR4* transcription, the transcription factors affected by SPPL2a deficiency need to be determined. Therefore, a method called proteomics of isolated chromatin segments (PICh) could be applied (Déjardin and Kingston 2009). Specific nucleic acid probes against TLR regulatory regions would be used to isolate genomic DNA with the associated transcription factors, which can be identified by mass spectrometric analysis. Another approach would be isolation of nuclei followed by Western Blot analysis of transcription factor abundance. In both cases *wt* BMDCs would serve as a control.

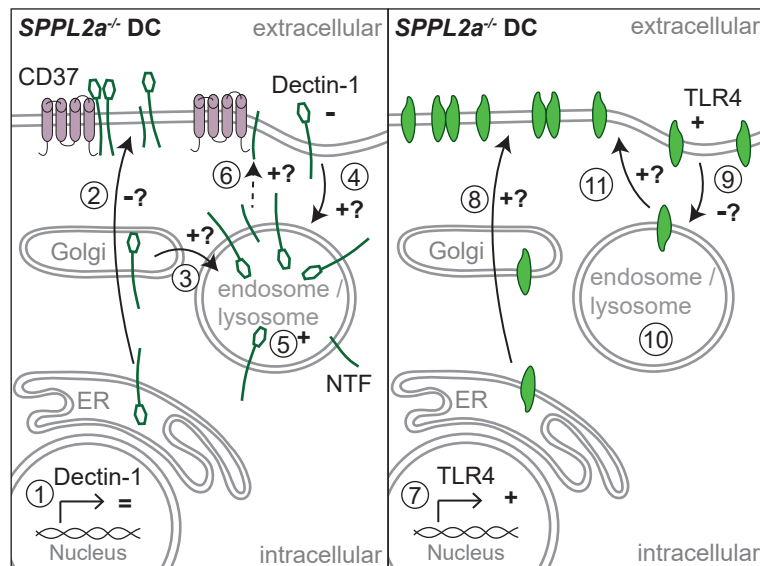


**Figure 49: Possible mechanisms for altered Dectin-1 and TLR4 surface levels on *SPPL2a*<sup>-/-</sup> BMDCs.** This scheme shows a theoretical model how the surface abundance of Dectin-1 and TLR4 could be influenced in *SPPL2a*<sup>-/-</sup> BMDCs. Pathways which might be enhanced (+), reduced (-) or unaffected (=) are marked. ①–⑥ Possible reasons for reduced Dectin-1 surface levels: ① Dectin-1 expression was unaffected in *SPPL2a*<sup>-/-</sup> BMDCs. ② Transport of Dectin-1 towards the plasma membrane could be hindered. ③ Increased translocation of Dectin-1 from the Golgi to the endolysosomal compartment could be possible. ④ Enhanced internalisation of Dectin-1 might play a role, maybe due to reduced association with other surface proteins like CD37. ⑤ Increased amounts of Dectin-1 were found within intracellular vesicles. ⑥ A Dectin-1 NTF might recycle from the endolysosomal compartment to the plasma membrane, where it could interfere with full length Dectin-1 to hamper Dectin-1–protein–interaction. ⑦–⑪ Possible reasons for elevated TLR4 surface levels: ⑦ Enhanced expression of TLR4 was detected. ⑧ TLR4 could be transported to the plasma membrane more rapidly. ⑨ Internalisation of TLR4 might be reduced. ⑩ Degradation of TLR4 could be reduced. ⑪ Recycling of TLR4 to the plasma membrane may be enhanced.

The elevated expression solely could explain the increased TLR4 surface abundance. However, stability of the receptor at the cell surface could also be enhanced in *SPPL2a*<sup>-/-</sup> BMDCs. At least after ligand binding, TLR4 internalisation is calcium-dependent (Chiang *et al.*, 2012). *SPPL2a*<sup>-/-</sup> B cells display reduced calcium influx upon BCR activation (Hüttl *et al.*, 2015). It is possible that *SPPL2a*<sup>-/-</sup> BMDCs also exhibit altered calcium homeostasis, which could affect TLR4 internalisation. Furthermore, TLR4 can be recycled from endosomes back to the plasma membrane (Liaunardy-Jopeace and Gay 2014). As discussed above, degradation of membrane bound proteins could be affected by *SPPL2a*-deficiency, thereby leading to increased TLR4 levels, which reach the membrane causing enhanced TLR4 surface abundance. Further elucidation of these processes in *SPPL2a*<sup>-/-</sup> BMDCs are required to determine if these processes could interfere with TLR4 surface levels.

Disturbance of correct surface expression was also observed for Dectin-1, which was reduced on *SPPL2a*<sup>-/-</sup> BMDCs compared to *wt* BMDCs. The general mechanisms of the CD74 NTF causing alterations in sorting of membrane proteins are described in detail above. An NTF of

Dectin-1 was observed at the cell surface of *SPPL2a*<sup>-/-</sup> BMDCs. Full length Dectin-1 does not recycle to the plasma membrane once it is internalised (Esteban *et al.*, 2011). Thus, surface abundance of the Dectin-1 fragment could display another result from disturbed membrane protein trafficking. The Dectin-1 fragment at the cell surface could have influenced Dectin-1 surface stability, for example by interfering with Dectin-1 interaction with other surface proteins. One known Dectin-1 interacting protein is the tetraspanin CD37 (Meyer-Wentrup *et al.*, 2007). CD37 stabilises Dectin-1 at cell surface, as macrophages of CD37 knockout mice display increased internalisation of Dectin-1 (Meyer-Wentrup *et al.*, 2007). Increased internalisation of surface proteins in *SPPL2a*<sup>-/-</sup> cells is already known for the BCR on B cells (Hüttl *et al.*, 2015). Besides surface stability, routes towards the plasma membrane could be disturbed, leading to reduced arrival of Dectin-1. Dynamics of Dectin-1 surface levels but also of other surface proteins in general could be addressed similar to experiments performed for the BCR, for example by labelling surface proteins with a biotinylated antibody. Since we had problems with detecting endogenous TLR4 by flow cytometry, immunofluorescence or biotinylation of surface proteins could be applied in combination with a time course of LPS treatment of *wt* and *SPPL2a*<sup>-/-</sup> BMDCs to determine TLR4 dynamics. The applied LPS should induce TLR4 internalisation (Zanoni *et al.*, 2011). In general, immunofluorescence could help to analyse distribution and localisation of surface proteins in *SPPL2a*<sup>-/-</sup> BMDCs when combined with stainings for organelle markers.

Taken together, several mechanisms are possible for the CD74 NTF affecting sorting of membrane proteins as well as intracellular processes as signal transduction or protein expression. It could well be that not a single mechanism, but several play together to cause the observed *SPPL2a*<sup>-/-</sup> DC phenotype.

#### 4.4 The role of SPPL2a in DC development *in vivo* and differentiation *in vitro*

A significant reduction in the cDC2 population was observed in spleens of *SPPL2a*<sup>-/-</sup> mice, while cDC1 and pDC frequencies were comparable to *wt*. Furthermore, the DC populations of *SPPL2a*<sup>-/-</sup>*CD74*<sup>-/-</sup> mice were comparable to *wt*. These observations fit to previous work analysing DC populations in *SPPL2a*<sup>mut/mut</sup> mice (Beisner *et al.*, 2013, Bergmann *et al.*, 2013). Thus, independent mouse models for SPPL2a deficiency could show the importance of the protease and CD74 in differentiation of cDC2s. Lately, in human patients with MSMD, mutations in the *SPPL2A* gene were described, leading to proteolytical inactive SPPL2a protein (Kong *et al.*, 2018). Interestingly, these patients displayed no overt alterations in B cell abundance, but reduced numbers of cDC2s (Kong *et al.*, 2018). Thus, SPPL2a deficiency leads to reduced cDC2 population in mice and man.

Why was only this specific DC subpopulation affected by the absence of SPPL2a? As the additional ablation of CD74 in SPPL2a-deficient mice led to normal cDC2 frequencies in this study and in the one of Beisner *et al.*, 2013, the abundance of CD74 in the DC populations could play a role. The idea of reduced CD74 levels in pDCs as compared to cDCs is supported by the observation that human pDCs have the lowest MHCII protein level of DCs (Nizzoli *et al.*, 2013). As CD74 has more functions besides serving as chaperone for MHCII, the abundance of MHCII is only an indirect indication for CD74 protein levels. Therefore, direct analysis of CD74 protein abundance in the different DC populations is required. Interestingly, human peripheral blood monocyte-derived cDC2 accumulate highest levels of CD74 compared to B cells, pDCs and cDC1s when SPPL2a is inhibited by a chemical compound (Kong *et al.*, 2018). Therefore, different CD74 protein levels are possible in the DC populations, explaining why only the cDC2 population was affected by SPPL2a deficiency. In humans, early DC precursor populations, giving rise to cDC2s, are reduced at a stage, when MHCII expression is initiated (Kong *et al.*, 2018). Whether this is also the case in our murine system needs to be evaluated.

How the CD74 NTF accumulation leads to reductions in the cDC2 populations remains elusive. The accumulating CD74 NTF could induce apoptosis. However, when splenic DC population in our mice were analysed by flow cytometry, no alterations in dead cell staining by DAPI could be observed (data not shown). This does not exclude apoptosis, as the cells may already be dead at the time point of analysis or die before they reach the examined organ, as already speculated for B cells (Hüttl *et al.*, 2015).

#### 4.4.1 Known factors in DC differentiation and homeostasis

So far, no mechanism behind reduced numbers of the cDC2 population in SPPL2a-deficient mice is known. In literature several factors are described to be important for DC development. As we observed altered surface abundance of Dectin-1 and TLR-4 on *SPPL2a*<sup>-/-</sup> BMDCs, it could be possible that the surface expression of receptors for survival and growth factors was reduced on *SPPL2a*<sup>-/-</sup> DCs and DC precursors. Reduced surface levels are known for the BCR on B cells, which leads to reduced survival signalling (Hüttl *et al.*, 2015).

One example for a receptor with a critical function on DC development is signal regulatory protein  $\alpha$  (SIRP $\alpha$ ; Saito *et al.*, 2010, Washio *et al.*, 2015). Its ligand CD47 is broadly expressed and as SIRP $\alpha$  is an inhibitory receptor for phagocytosis, ligation prevents host cell destruction (Barclay and Berg 2014). The underlying mechanism of SIRP $\alpha$  influencing DC development remains unknown ((Saito *et al.*, 2010, Washio *et al.*, 2015). *SIRP $\alpha$* <sup>-/-</sup> mice display reduced frequencies of the cDC2 population (Saito *et al.*, 2010, Washio *et al.*, 2015), similar to our *SPPL2a*<sup>-/-</sup> mice. The same population is missing in Epstein—Barr virus-induced gene 2 (EBI2)-deficient mice (Yi and Cyster 2013). The receptor EBI2 plays an important role in



mediating DC migration, which might affect DC numbers (Yi and Cyster 2013, Barington *et al.*, 2018). As discussed above, reduced migration capacity of *SPPL2a*<sup>-/-</sup> DCs could be possible. This could then also affect DC numbers in spleen in our *SPPL2a*<sup>-/-</sup> mice.

Factors on other cells could also influence DC frequencies. The lymphotoxin  $\beta$  (LT $\beta$ ) / LT $\beta$  receptor (LT $\beta$ R) axis is also known to ensure correct DC frequencies and localisation within organs (Wu *et al.*, 1999). While the LT $\beta$ R is expressed on DCs, B cells harbour LT $\beta$  at their cell surface (Wang *et al.*, 2005, Tumanov *et al.*, 2002). *SPPL2a*-deficient mice lack mature B cells (Schneppenheim *et al.*, 2013, Beisner *et al.*, 2013, Bergmann *et al.*, 2013). This could influence the numbers of DCs in spleens. However, humans with *SPPL2a* deficiency do not display altered B cell frequencies, but a reduction in the cDC2 population (Kong *et al.*, 2018), arguing against a contribution of B cells to the DC phenotype.

Apart from altered surface receptors, differences in transcription factor expression or nuclear translocation of transcription factors due to *SPPL2a*-deficiency, as discussed before, could have influenced DC differentiation. transcription factors of the IRF family play a pivotal role not only in DC but also in B cell, T cell, monocyte, granulocyte and NK cell differentiation (Tamura *et al.*, 2008). IRF8 deficiency leads to reductions in both the pDC and cDC populations (Tsuji-mura *et al.*, 2003b, Tsujimura *et al.*, 2003a, Aliberti *et al.*, 2003). Thus, this transcription factor might not be of major relevance in our *SPPL2a*<sup>-/-</sup> mice, as the pDC and cDC1 development was not affected. IRF4- and IRF2-deficient mice display a defect in cDC2 development (Suzuki *et al.*, 2004, Gabriele *et al.*, 2006), reflecting a similar situation of DCs in *SPPL2a*<sup>-/-</sup> mice. Nuclear localisation of IRF transcription factors in early DC developmental stages in *SPPL2a*<sup>-/-</sup> mice and further analysis of *SPPL2a*<sup>-/-</sup> BMDCs would be interesting.

Defects in IRF transcription factors could only play a minor role in our studies due to a major difference to the differentiation of DCs from IRF-8 and IRF-4 knockout mice. *In vitro* *SPPL2a*<sup>-/-</sup> BMDC development was comparable to *wt* BMDCs in our study but development of IRF4 or IRF8-deficient BMDCs is impaired (Suzuki *et al.*, 2004, Tsujimura *et al.*, 2003a). A difference between *in vivo* and *in vitro* DC differentiation is not novel. Even though their *in vivo* DC differentiation is affected, normal *in vitro* DC differentiation is observed in BMDCs derived from LT $\beta$ R-deficient and SIRP $\alpha$ -deficient mice (Abe *et al.*, 2003, Saito *et al.*, 2010). Furthermore, *in vitro* DC differentiation from human donor stem cells was not affected by the addition of a chemical compound for *SPPL2a* activity inhibition (Kong *et al.*, 2018). However, commercial available inhibitors have limitations in their capacity to block *SPPL2a*-activity. Though, the *in vitro* culture system does not reflect the *in vivo* differentiation, it serves as a good system for functionality studies of DCs. These may be confirmed in DC populations directly isolated from mice.

#### 4.5 Can the altered Dectin-1 and TLR4 surface levels and Dectin-1 signalling explain cytokine differences between *wt* and *SPPL2a*<sup>-/-</sup> BMDCs?

The examination of the *SPPL2a*<sup>-/-</sup> BMDC functionality was performed by cytokine secretion measurements upon activation of cells with different pathogen-derived ligands for several PRRs. Reduced IL-10 and IL-2 concentrations were measured in supernatants of *SPPL2a*<sup>-/-</sup> BMDCs compared to *wt* following stimulation with CTLR ligands, including the Dectin-1 ligand dZym and the complex ligand HKMT, which activates several CTLR and TLR. Increased IL-1 $\beta$  concentrations were measured in supernatants of *SPPL2a*<sup>-/-</sup> BMDCs compared to *wt* when stimulated with TLR ligands, including LPS and HKMT. These differences in cytokines released were already observable at the mRNA expression level. Therefore, SPPL2a deficiency mainly affects stages of ligand recognition, signal transduction and induction of cytokine expression. Even though, effects of SPPL2a knockout on cytokine secretion processes cannot be excluded and have not been analysed so far.

The altered surface abundances of Dectin-1 and TLR4 observed on *SPPL2a*<sup>-/-</sup> BMDCs could have influenced the cytokine response. Increased surface receptor levels of TLR4 were detected by biotinylation of surface proteins on *SPPL2a*<sup>-/-</sup> BMDCs compared to *wt* BMDCs. Murase *et al.*, 2018 and Chiang *et al.*, 2012 showed that, when TLR4 internalisation is inhibited, LPS activated BMDCs express enhanced levels of TNF $\alpha$ . TNF $\alpha$  release was not significantly enhanced in *SPPL2a*<sup>-/-</sup> BMDCs compared to *wt* BMDCs, but its expression after three hours was significantly increased. In *SPPL2a*<sup>-/-</sup> BMDCs the expression and release of IL-1 $\beta$  was enhanced by ablation of SPPL2a. Murase *et al.*, 2018 did not measure IL-1 $\beta$  expression. However, increased TLR4 surface levels could explain increased IL-1 $\beta$  expression by *SPPL2a*<sup>-/-</sup> BMDCs compared to *wt* but it does not explain why release of other cytokines, as IL-12p70, was not altered upon TLR4 activation. To further explore this difference in expression of certain cytokines, signalling pathways should be analysed.

Dectin-1 surface expression was reduced in *SPPL2a*<sup>-/-</sup> BMDCs compared to *wt* as well as *CD74*<sup>-/-</sup> and *SPPL2a*<sup>-/-</sup>*CD74*<sup>-/-</sup> BMDCs. BMDCs, derived from Dectin-1 knockout mice, release reduced amounts of IL-10 and IL-2, while TNF $\alpha$  expression is comparable to *wt* BMDCs, when treated with Zymosan (Robinson *et al.*, 2009). This corresponds to observations made for *SPPL2a*<sup>-/-</sup> BMDCs when treated with dZym. But different ligands for Dectin-1 were used in these two studies. Zymosan is a preparation from *Saccharomyces cerevisiae* yeast cell wall and activates Dectin-1 as well as the TLR2/6 (Underhill *et al.*, 1999, Ozinsky *et al.*, 2000, Brown and Gordon 2001). The affinity of Zymosan to TLR2/6 can be eliminated by treating Zymosan with hot alkali (dZym; Gantner *et al.*, 2003). Thus, in the *SPPL2a*<sup>-/-</sup> BMDCs treated with dZym

no TLR should participate in activation of cytokine production and release. However, we could not control if dZym solely activated Dectin-1 in our experimental settings. Zymosan and dZym can also be detected by Dectin-2 (Robinson *et al.*, 2009, Rosas *et al.*, 2011). Thus, surface expression of this CTLR should be investigated in *SPPL2a*<sup>-/-</sup> BMDCs. Furthermore, we cannot exclude involvement of complement receptors, as the used FCS was not heat-inactivated. Complement factors are part of the innate immune system (Nesargikar *et al.*, 2012). They coat foreign carbohydrate patterns and target them to complement receptors, as for example, on DCs (Nesargikar *et al.*, 2012).

Apart from altered surface receptor levels, subsequent signalling pathways could be influenced by *SPPL2a* deficiency in BMDCs as depicted in figure 50. A reduction of phosphorylated and thus active kinase Syk was observed in *SPPL2a*<sup>-/-</sup> BMDCs after treatment with dZym. Syk knockout BMDCs release almost no IL-10 or IL-2 after Zymosan treatment, while IL-12p70 is detected at normal levels in conditioned media (Rogers *et al.*, 2005). This fits to cytokine releases observed in *SPPL2a*<sup>-/-</sup> BMDCs after dZym treatment. Therefore, the reduced activation of Syk could have led to reduced IL-10 and IL-2 release in the *SPPL2a*<sup>-/-</sup> BMDCs. Again, the stimulant was slightly different between the studies.

The accumulating fragment of Dectin-1 at the cell surface of *SPPL2a*<sup>-/-</sup> BMDCs could interfere with initiation of the signalling cascade. This could be tested by overexpression of the Dectin-1 NTF in a cell line, that harbours endogenous Dectin-1, and evaluation of Syk activation after Dectin-1 stimulation in comparison to a control without Dectin-1 NTF overexpression. Another possibility for reduced Syk phosphorylation could be an enhanced activity of phosphatases dephosphorylating Syk in *SPPL2a*<sup>-/-</sup> BMDCs. SHP-1 and SHP-2 are such phosphatases (Maeda *et al.*, 1999, Dustin *et al.*, 1999, Okazaki *et al.*, 2001). By Western Blot analysis their activation status could be investigated in *SPPL2a*<sup>-/-</sup> BMDCs and compared to *wt*, as they are also phosphorylated. Reduced activation of Syk was already observed in *SPPL2a*<sup>-/-</sup> B cells after BCR stimulation (Hüttl *et al.*, 2015). Surface levels of the BCR were also reduced in the *SPPL2a*<sup>-/-</sup> B cells. Thus decreased activity of Syk could be caused by the reduced receptor levels or by a more general Syk affecting mechanism. To answer this question a Syk-coupled receptor with normal surface abundance needs to be identified and signalling cascade needs to be investigated.

Besides Syk, further kinases are activated upon Dectin-1 ligation. Dectin-1 can signal via the kinase Raf-1 in a Syk-independent manner (Gringhuis *et al.*, 2009). Furthermore, Raf-1 activates NF $\kappa$ B-mediated transcription of cytokines (Gringhuis *et al.*, 2009). This could explain why some cytokines are still released to normal levels in *SPPL2a*<sup>-/-</sup> BMDCs even though Syk is less activated. To validate this theory, the activation status of Raf-1 has to be investigated.

IL-10 and IL-2 release is also regulated by ERK activation (Slack *et al.*, 2007). This kinase was phosphorylated and thus active in comparable amounts in *SPPL2a*<sup>-/-</sup> and *wt* BMDCs after dZym treatment. Thus, ERK does not lead to normal IL-10 and IL-2 release in our experimental setup. However, the normal ERK activity could explain why cytokines like TNF $\alpha$  are released in comparable amounts by *SPPL2a*<sup>-/-</sup> and *wt* BMDCs after dZym treatment. How is it possible that ERK is activated normally, when the Dectin-1 receptor surface levels were reduced as well as activation of the receptor proximal kinase Syk in *SPPL2a*<sup>-/-</sup> BMDCs compared to *wt*? Normal activation of ERK by reduced Syk phosphorylation was already observed in B cells, when the BCR was activated (Hüttl *et al.*, 2015). ERK might be activated by signalling cascades derived from other receptors activated upon dZym treatment, as described above. As in B cells the BCR was activated with antibodies directed against it, receptors for antibodies on B cells could have been stimulated in that experimental approach (Hüttl *et al.*, 2015), thereby inducing ERK phosphorylation. However, B cells only express one receptor for antibodies, which has inhibitory functions and does not activate ERK (Nimmerjahn and Ravetch 2008). Thus, more likely, the CD74 NTF could interfere with signalling cascade transduction in DCs and in B cells, thereby inducing ERK. That CD74 overexpression can induce ERK activation has been shown in human embryonic kidney cells (Liu *et al.*, 2008).

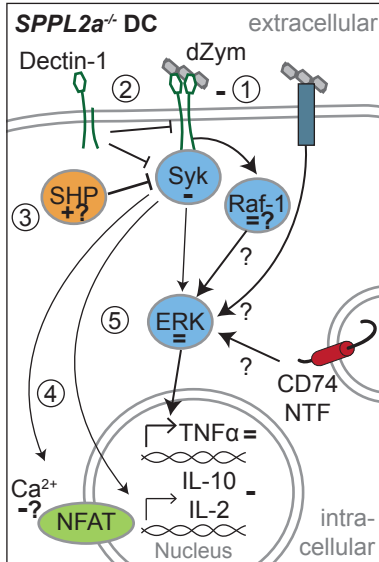


**Figure 50: Possible mechanisms for dZym-induced signalling and cytokine response alterations in *SPPL2a*<sup>-/-</sup> BMDCs.** Theoretical model how signalling and cytokine responses of dZym treated *SPPL2a*<sup>-/-</sup> BMDCs are affected. Pathways which might be enhanced (+), reduced (-) or unaffected (=) are marked. ① The reduced Dectin-1 surface level could lead to the reduced Syk activation. ② The Dectin-1 NTF could influence Dectin-1 mediated Syk-signalling. ③ Enhanced activity of SHP phosphatases could lead to reduced Syk activity. ④ Reduced Syk could lead to reduced induction of NFAT-dependent or -independent IL-10 and IL-2 transcription. ⑤ ERK was as activated as in *wt* BMDCs. This could have been mediated by Raf-1, further dZym detecting receptors or influence of signalling cascades by the CD74 NTF. The normal activation of ERK could have led to normal TNF $\alpha$  transcription.

Despite reduced input from Syk, the expression of cytokines could be affected by *SPPL2a* deficiency downstream of signalling. The expression of IL-10 and IL-2 is mediated by activation of transcription factors of the NFAT family (Goodridge *et al.*, 2007). The activation of NFAT is Ca<sup>2+</sup>-dependent. The calcium homeostasis in *SPPL2a*<sup>-/-</sup> BMDCs might be altered, as it was observed in *SPPL2a*<sup>-/-</sup> B cells (Hüttl *et al.*, 2015). Translocation of NFAT in stimulated *SPPL2a*<sup>-/-</sup> BMDCs was intended to measure by nuclear extraction, however results were inconclusive (data not shown). Thus, further analysis of nuclear localisation of transcription factors

for cytokines are required. The normal ERK activation indicates further signalling cascades and regulations being involved in our experimental setup.

#### 4.5.1 The impact of altered PRR levels on Mycobacteria detection

We were interested in the role of SPPL2a deficiency in DC function with regard to mycobacteria recognition and induction of immunity against the bacteria, as patients with MSMD harbour mutation within the *SPPL2A* gene. Alterations of surface abundance of receptors in *SPPL2a*<sup>-/-</sup> BMDCs could indicate functional deficiencies of these cells to detect mycobacteria.

Could the observed decreased Dectin-1 surface levels on *SPPL2a*<sup>-/-</sup> BMDCs account for altered cytokine responses towards HKMT and in BCG co-cultures? Dectin-1 is required for TNF $\alpha$  release, when BMDMs are co-cultured with BCG but not with *Mycobacterium tuberculosis* (Yadav and Schorey 2006). To block Dectin-1, Yadav and Schorey 2006 either used a specific antibody against the receptor or laminarin, a soluble  $\beta$ -glucan that binds but does not activate Dectin-1 and thereby blocks the receptor. In our studies with BMDCs, TNF $\alpha$  release was comparable between *SPPL2a*<sup>-/-</sup> and *wt* BMDCs in BCG co-cultures. This could be explained by the different immune cell types used in the studies. Furthermore, on *SPPL2a*<sup>-/-</sup> BMDCs other TNF $\alpha$  release-activating receptors might be increased, as observed for TLR4. Laminarin-mediated inhibition of Dectin-1 on DCs, isolated from spleens of *wt* mice, causes reduced release of IL-12p40 and IL-12p70 in co-cultures with *Mycobacterium tuberculosis* (Rothfuchs *et al.*, 2007). Furthermore, splenic DCs from Dectin-1-deficient mice secrete decreased levels of IL-12p40 in *Mycobacterium tuberculosis* and BCG co-cultures (Rothfuchs *et al.*, 2007). This cytokine was also reduced in conditioned media from *SPPL2a*<sup>-/-</sup> BMDCs either treated with HKMT or when co-cultured with BCG. IL-12p70 was also decreased in *SPPL2a*<sup>-/-</sup> BMDC co-cultures with BCG. These alterations in cytokine release from *SPPL2a*<sup>-/-</sup> BMDCs upon mycobacterial stimulation could derive from reduced Dectin-1 surface levels. In an *in vivo* infection model of *wt* and Dectin-1-deficient mice with *Mycobacterium tuberculosis* no difference in histology of infected organs or survival of mice is observed (Marakalala *et al.*, 2011). However, Dectin-1-deficient mice display reduced bacterial burden in comparison to the *wt* mice, which could have a significant influence on disease outcome (Marakalala *et al.*, 2011). Thus, Dectin-1 has a role in mycobacteria detection and reduced Dectin-1 surface levels on *SPPL2a*<sup>-/-</sup> BMDCs could have influenced cytokine responses towards mycobacteria species.

The increased surface receptor levels of TLR4 on *SPPL2a*<sup>-/-</sup> BMDCs could also influence responses in BCG co-cultures or HKMT treatment. An involvement of TLR4 in mycobacteria recognition is discussed controversial in literature. On the one hand, *TLR4*<sup>-/-</sup> mice suffer from

more severe infection with *Mycobacterium tuberculosis* and even die in contrast to *wt* mice (Abel *et al.*, 2002). On the other hand, studies of Reiling *et al.*, 2002 show that *TLR4*<sup>-/-</sup> mice can clear *Mycobacterium tuberculosis* infections as sufficient as the *wt* controls. The dosis of the bacteria were differed between the studies and could explain the discrepancy. Thus, increased TLR4 receptor surface levels in *SPPL2a*<sup>-/-</sup> BMDCs could play a role for mycobacteria recognition under certain conditions.

Other important receptors for mycobacteria recognition are TLR2 and the CTLR Mincle (Basu *et al.*, 2012, Matsunaga and Moody 2009). Both receptors have even a pivotal role of BCG clearance *in vivo* (Heldwein *et al.*, 2003, Behler *et al.*, 2012 Behler *et al.*, 2015). In *SPPL2a*<sup>-/-</sup> BMDCs the mRNA levels of TLR2 and Mincle were not altered compared to *wt*. However, as seen for Dectin-1, this does not exclude a change in surface abundance. Therefore, surface levels of these receptors should be analysed. The functionality of TLR2-mediated responses was tested with the mycobacteria-derived ligand LAM ( Means *et al.*, 1999, Tapping and Tobias 2003). As for TLR4 activation, enhanced IL-1 $\beta$  release was detected in *SPPL2a*<sup>-/-</sup> BMDCs compared to *wt*. More specifically for TLR2 would be the synthetic triacylated lipoprotein Pam3CSK4 (Aliprantis *et al.*, 1999, Ozinsky *et al.*, 2000). This could be applied to test TLR2 response more defined. The functionality of Mincle on *SPPL2a*<sup>-/-</sup> BMDCs could be adressed by treatment of BMDCs with the mycobacterial glycolipid trehalose-6,6'-dimycolate (TDM; cord factor) or its synthetic form trehalose-6,6-dibehenate (TDB; Matsunaga and Moody 2009).

#### **4.6 The physiological relevance of SPPL2a deficiency in infections**

Having discussed the receptors in detail, the question raises what the observed alterations in *SPPL2a*<sup>-/-</sup> mice and *SPPL2a*<sup>-/-</sup> BMDCs would mean for a mycobacterial infection in general. In the MSMD patients with SPPL2a deficiency, the lack of the cDC2 subset causes the disease, as they are the main producers of IL-12p70, the cytokine inducing the required T cell response (Kong *et al.*, 2018, Nizzoli *et al.*, 2013). The same DC subset is missing in the *SPPL2a*<sup>-/-</sup> mice (Bergmann *et al.*, 2013 and section 3.1.1). SPPL2a-deficient mice are also more susceptible to BCG infections (Kong *et al.*, 2018). However, in contrast to the human situation, in mice the cDC1 population is the main source of IL-12p70 (Hochrein *et al.*, 2001). This DC subpopulation was unaffected in *SPPL2a*<sup>-/-</sup> mice. At least in mice, the reduced frequency of a DC population cannot solely explain why SPPL2a deficiency causes increased susceptibility for mycobacterial infections.

SPPL2a-deficient mice cannot give rise to mature B cells and remaining B cells display functional defects (Schneppenheim *et al.*, 2013, Bergmann *et al.*, 2013, Beisner *et al.*, 2013, Hüttl *et al.*, 2015). As B cells are involved in clearance of mycobacteria infections (Achkar *et al.*,

2015), this could contribute to reduced BCG clearance in the *SPPL2a*<sup>-/-</sup> mice. Contribution of B cells could be excluded by transfer of sorted *wt* B cells into *SPPL2a*<sup>-/-</sup> mice prior to BCG infection. In a similar approach, cDC2s from either *wt* or *SPPL2a*<sup>-/-</sup> mice could be sorted and transferred into *SPPL2a*<sup>-/-</sup> mice. Thereby the question could be addressed, if reduced numbers of DCs in *SPPL2a*<sup>-/-</sup> mice or also altered functionality of *SPPL2a*<sup>-/-</sup> DCs affect course of disease and BCG clearance *in vivo*.

Reduced capability of macrophages to clear mycobacterial infection could contribute to increased susceptibility to mycobacterial infections in *SPPL2a*-deficient mice and man. Killing capacities of BMDMs against mycobacteria were examined in cooperation with Maïke Burmeister (AG Schaible, Research center Borstel, Germany). This analysis revealed that killing capacities against BCG and *Mycobacterium tuberculosis* are comparable between BMDMs derived from *wt* or *SPPL2a*<sup>-/-</sup> mice (data not shown). Together with normal cytokine responses by *SPPL2a*<sup>-/-</sup> BMDMs, these findings indicate that DC abundance and function play an important role in mycobacterial infections of *SPPL2a*-deficient mice and man.

When *SPPL2a*<sup>-/-</sup> BMDCs were co-cultured with BCG, they released significantly decreased amounts of the IL-12 family members IL-12p70, IL-12p40 and IL-23. The importance of IL-12p70 in mycobacterial infections is known, as it induces the required T<sub>H</sub>1 differentiation for bacterial clearance in *SPPL2a*<sup>-/-</sup> BMDCs (Hsieh *et al.*, 1993, Heufler *et al.*, 1996, Méndez-Samperio 2010). Not only IL-12p70, but also IL-23 plays an important role in defence against mycobacteria (Cooper *et al.*, 2002). Furthermore, reduced IL-12p40 in media of BCG co-cultured *SPPL2a*<sup>-/-</sup> BMDCs compared to *wt*, could negatively influence bacterial removal. Although IL-12p40 is thought to inhibit IL-12p70 and IL-23 functions, it plays an important role of induction of DC migration and T cell differentiation (Khader *et al.*, 2006). A general protective role of IL-12p40 is shown in BCG infections of mice (Hölscher *et al.*, 2001). Furthermore, the lack of the IL-12p40 receptor is a common genetic feature in MSMD (Bustamante *et al.*, 2014). Thus, the reduction of IL-12 family member release observed in *SPPL2a*<sup>-/-</sup> BMDCs could account for the reduced clearance of BCG in *SPPL2a*-deficient mice and man, as T cells cannot be activated to an appropriate degree.

Besides the IL-12 family members other cytokines are also of importance for the induction of immunity against BCG. IL-1 $\beta$  can induce IFN $\gamma$  release from T cells, which is required for activation of intracellular killing in infected macrophages (Tominaga *et al.*, 2000). IL-1 $\beta$  is also protective in the early phase of mycobacterial infections (Yamada *et al.*, 2000). *SPPL2a*<sup>-/-</sup> BMDCs released significantly increased amounts of this cytokine in BCG co-cultures. One can speculate that the concentrations released by *SPPL2a*<sup>-/-</sup> DCs are too high, leading to increased tissue damage and unregulated immune response and thus are not protective any longer. This

assumption is underlined by several studies. In humans, polymorphisms in IL-1 $\beta$  expression regulation are known and patients with the polymorphism leading to higher IL-1 $\beta$  expression are also the patients with a more severe course of tuberculosis (Zhang *et al.*, 2014). Mice deficient for negative regulation of IL- $\beta$ -mediated signalling and IL- $\beta$  expression display increased liver necrosis and mortality rate compared to *wt* mice when infected with *Mycobacterium tuberculosis* (Garlanda *et al.*, 2007).

In BMDC-BCG co-cultures no IL-10 release was detectable and IL-10 expression at measured time points was comparable between *SPPL2a*<sup>-/-</sup> and *wt* BMDCs. However, HKMT treated *SPPL2a*<sup>-/-</sup> BMDCs released decreased IL-10 amounts compared to *wt*. Induction of IL-10 release is an immune evasion mechanism of mycobacteria (Redford *et al.*, 2011) and it inhibits the intracellular killing by infected macrophages (Gazzinelli *et al.*, 1992). IL-10 also inhibits production of the destructive ROS and protects from tissue damage in general (Gazzinelli *et al.*, 1992, Couper *et al.*, 2008). On the one hand, the decreased release of IL-10 in HKMT treated *SPPL2a*<sup>-/-</sup> BMDCs could lead to a better clearance of mycobacterial infections. On the other hand, the reduced anti-inflammatory and tissue-protective function could cause enhanced tissue damage and create an environment for better mycobacteria survival. After BCG infection, IL-10-deficient mice can clear the infection better than *wt* mice, when analysed after a short time of less than 80 days after infection (Murray and Young 1999, Jacobs *et al.*, 2000). However, when IL-10-deficient mice are infected with a low dose of *Mycobacterium tuberculosis*, they display increased inflammation, represented by enhanced TNF $\alpha$  serum levels, compared to *wt* mice after 185 days of infection (Higgins *et al.*, 2009).

*SPPL2a* deficiency could lead to an enhanced general immune activation upon mycobacteria infection with destructive outcome and reduced mycobacterial clearance, as cytokines for appropriate T cell induction are decreased. Thus, the altered cytokine response of *SPPL2a*<sup>-/-</sup> DCs could, together with reduced DC frequencies, cause the increased susceptibility to mycobacterial infections. The observed alterations in released cytokines and surface receptor levels of *SPPL2a*<sup>-/-</sup> BMDCs could also influence other diseases than infections with mycobacteria species only. Reductions of Dectin-1 abundance are associated with increased susceptibility for fungal infections in mice and man (Taylor *et al.*, 2007, Ferwerda *et al.*, 2009). Defects in IL-10 expression and IL-10 mediated signalling are found in patients with inflammatory bowel disease (Glocker *et al.*, 2011). Furthermore, deficiency of IL-2 release or receptor signalling are associated with severe combined immunodeficiency (SCID; Weinberg and Parkman 1990, Gilmour *et al.*, 2001). *SPPL2a* deficiency causing SCID in mice and man is unlikely, as the *SPPL2a*<sup>-/-</sup> mice, are not conspicuous ill and *SPPL2a*-deficient patients do not suffer from severe infections. To address the susceptibility of *SPPL2a*<sup>-/-</sup> mice towards inflammations within



the bowel or fungal infections, appropriate mouse models could be applied. Colitis could be induced by application of the chemical product dextran sulfate sodium (DSS) and severity of disease could be compared between *wt* and *SPPL2a*<sup>-/-</sup> mice (Manicassamy and Manoharan 2014). *SPPL2a*<sup>-/-</sup> and *wt* mice could be infected with *Candida albicans* and bacterial burden in organs and survival could be analysed (Conti *et al.*, 2014). Based on the observed cytokine alterations in *SPPL2a*<sup>-/-</sup> BMDCs, it is tempting to speculate that patients with SPPL2a deficiency would also suffer from other diseases than MSMD. However, this was not reported yet.

Within this study, we focused on DCs and their function. The above described diseases are caused by global defects, not only affecting DCs. However, it could be possible that SPPL2a deficiency in these contexts are not described yet, as it was not tested in patients. Therefore, human SPPL2a-deficiency could be searched for in patients, for example with inflammatory bowel diseases, to further elucidate the (patho-)physiological role of SPPL2a.

#### 4.7 Outlook

SPPL2a-deficiency affects DC development and function in a CD74-dependent manner with important consequences on their ability to clear mycobacterial infections. Due to its potential to block development of B cells and DCs, SPPL2a is discussed as therapeutic target for autoimmunity (Velcicky *et al.*, 2018, Mentrup *et al.*, 2017b). The observed altered differentiation *in vivo* and functionality *in vitro* of DCs, as reflected by changes in surface receptor levels and cytokine responses, could have serious consequences besides increased susceptibility towards infections with weakly virulent mycobacteria, when SPPL2a would be inhibited in patients. To be aware of and eventually counteract adverse effects of SPPL2a inhibitors, mechanistically exploration of the consequences of SPPL2a inhibition require further investigation, as discussed with potential approaches in detail above. First, the reasons for reduced cDC2 frequencies in *SPPL2a*<sup>-/-</sup> mice requires further exploration. Since the CD74 NTF accumulation caused the described *SPPL2a*<sup>-/-</sup> DC phenotype, the focus should lie on the precise molecular role of this substrate. To further elucidate the function of the CD74 NTF, interaction partners need to be identified, validated and evaluated for their contribution to the *SPPL2a*<sup>-/-</sup> DC phenotype. The molecular mechanism of the CD74 NTF affecting degradation of membrane proteins should be investigated, as well as the potential role of the negatively charged CD74 cytoplasmic tail. Further elucidation of the mechanism behind the altered Dectin-1 and TLR4 surface levels on *SPPL2a*<sup>-/-</sup> BMDCs would also help to better understand how the CD74 NTF accumulation causes the DC phenotype. Thereby, the analysis of their endosomal trafficking would be of major interest. Surface levels of additional receptors should be addressed in an unbiased approach. In regard to mycobacterial defence, especially TLR2 and Mincle require further at-

## DISCUSSION

---

tention. Finally, the impact of the functional defect of *SPPL2a*<sup>-/-</sup> DCs affecting immune defence against mycobacterial infections should also be assessed in the context of other diseases, in particular those caused by intracellular bacteria. Therefore, suitable infection or disease models should be applied.

## 5 Summary

Deficiency of the intramembrane protease SPPL2a is known to affect B cell development and function in murine model systems. In contrast, in SPPL2a-deficient patients B cell frequencies measured in peripheral blood are normal. Instead, they display a reduction of the conventional DC 2 (cDC2) population, causing mendelian susceptibility to mycobacterial disease (MSMD). Therefore, it was aimed to further elucidate the role of SPPL2a in DC development and function, especially in regard to responses towards mycobacterial infections. Furthermore, due to its critical role for B cell defects in SPPL2a-deficient mice, the relevance of the SPPL2a substrate CD74 for possible DC alterations was studied. For this purpose, DCs from either *SPPL2a*<sup>-/-</sup> or *SPPL2a*<sup>-/-</sup>*CD74*<sup>-/-</sup> mice were analysed *in vivo* and *in vitro* by various cell biological methods. *SPPL2a*<sup>-/-</sup> mice displayed a reduction of the cDC2 population, which was CD74-dependent. *In vitro* differentiated *SPPL2a*<sup>-/-</sup> BMDCs were in general responsive towards different pattern recognition receptor (PRR) ligands with specific alterations in signalling and cytokine expression. Surface levels of the PRR Dectin-1 were reduced, while Toll-like receptor 4 (TLR4) surface expression was increased on *SPPL2a*<sup>-/-</sup> BMDCs. This may contribute to the observed reduced IL-10 and IL-2 expression following Dectin-1 activation and enhanced IL-1 $\beta$  release when TLR4 ligands were applied to *SPPL2a*<sup>-/-</sup> BMDCs. These alterations in cytokine responses were also observed when heat-killed *Mycobacterium tuberculosis* was used to activate *SPPL2a*<sup>-/-</sup> BMDCs. These effects were dependent on the CD74 NTF accumulation, as they were reversed in *SPPL2a*<sup>-/-</sup>*CD74*<sup>-/-</sup> BMDCs. Furthermore, upon co-culture with *Mycobacterium bovis* Bacille Calmette-Guérin (BCG), the pathogen to which SPPL2a-deficient patients show an increased susceptibility, *SPPL2a*<sup>-/-</sup> BMDCs released reduced amounts of IL-12 family cytokines, which are important to induce clearance of mycobacteria.

In summary, SPPL2a-deficiency affects DC development and function in a CD74-dependent manner with important consequences on their ability to clear mycobacterial infections. The altered surface abundance of PRR receptors and the disturbed cytokine response observed in *SPPL2a*<sup>-/-</sup> BMDCs possibly contributes to MSMD in SPPL2a-deficient patients. Reductions of the anti-inflammatory cytokine IL-10 together with enhanced IL-1 $\beta$  responses could lead to enhanced inflammatory responses with increased tissue damage, thereby creating an environment supporting the spreading of mycobacteria. Reduced release of IL-12 family members by *SPPL2a*<sup>-/-</sup> BMDCs could result in impaired induction of T helper cell type 1 responses, which are required for clearance of mycobacteria. Thus, the results from this thesis reveal that MSMD in SPPL2a-deficient humans is not only caused by the reduced frequency of cDC2 population, but also by a functional deficit of the remaining DCs.



## 6 Zusammenfassung

Eine Defizienz der Intramembranprotease SPPL2a beeinflusst die Entwicklung und Funktion von B-Zellen in murinen Modellsystemen. Im Gegensatz dazu sind bei SPPL2a-defizienten Patienten B-Zellzahlen im peripheren Blut im Normbereich. Stattdessen zeigen sie eine Reduktion in der Population der konventionellen dendritischen Zellen 2 (cDC2), was zu einer mendelschen Anfälligkeit für Erkrankungen durch Mykobakterien (MSMD) führt. Im Rahmen dieser Arbeit sollte daher die Rolle von SPPL2a bei der DC-Entwicklung und -Funktion geklärt werden, insbesondere im Hinblick auf Reaktionen auf mykobakterielle Infektionen. Darüber hinaus wurde aufgrund seiner kritischen Rolle in B-Zelldefekten bei SPPL2a-defizienten Mäusen die Relevanz des SPPL2a-Substrats CD74 für mögliche DC-Veränderungen untersucht. Zu diesem Zweck wurden DCs von *SPPL2a*<sup>-/-</sup> oder *SPPL2a*<sup>-/-</sup>*CD74*<sup>-/-</sup> Mäusen *in vivo* und *in vitro* mit verschiedenen zellbiologischen Methoden analysiert. *SPPL2a*<sup>-/-</sup> Mäuse zeigten eine CD74-abhängige Reduktion der cDC2-Population. *In vitro* differenzierte *SPPL2a*<sup>-/-</sup> BMDCs reagierten auf verschiedene Mustererkennungsrezeptor (PRR)-Liganden mit spezifischen Veränderungen in Signalwegen und der Zytokinexpression. Auf der Oberfläche von *SPPL2a*<sup>-/-</sup> BMDCs war der PRR Dectin-1 reduziert, der Toll-ähnlichen Rezeptor 4 (TLR4) erhöht. Dies könnte zu der beobachteten reduzierten IL-10- und IL-2-Expression nach der Aktivierung von Dectin-1 und einer verbesserten IL-1 $\beta$ -Freisetzung nach Aktivierung von TLR4 in *SPPL2a*<sup>-/-</sup> BMDCs beigetragen haben. Diese Veränderungen der Zytokinreaktionen wurden ebenfalls bei Verwendung von hitzeabgetötetem *Mycobacterium tuberculosis* zur Aktivierung von *SPPL2a*<sup>-/-</sup> BMDCs beobachtet. Diese Effekte waren abhängig von der CD74 NTF-Akkumulation, da sie sich in *SPPL2a*<sup>-/-</sup>*CD74*<sup>-/-</sup> BMDCs wieder vergleichbar zum Wildtypen darstellten. *SPPL2a*<sup>-/-</sup> BMDCs setzten reduzierte Mengen an Zytokinen der IL-12-Familie frei, die für die mykobakterielle Beseitigung wichtig sind, wenn sie mit *Mycobacterium bovis* Bacille Calmette-Guérin (BCG) ko-kultiviert wurden, dem Erreger, gegenüber dem SPPL2a-defiziente Patienten eine vermehrte Anfälligkeit zeigen.

Zusammenfassend lässt sich sagen, dass eine SPPL2a-Defizienz abhängig von CD74 die Entwicklung und Funktion dendritischer Zellen beeinflusst, mit Auswirkungen auf ihre Fähigkeit, mykobakterielle Infektionen zu erkennen und zu beseitigen. Die veränderte Oberflächenhäufigkeit der PRR-Rezeptoren und der gestörten Zytokinreaktion, die in *SPPL2a*<sup>-/-</sup> BMDCs beobachtet wurden, tragen möglicherweise zur MSMD bei SPPL2a-defizienten Patienten bei. Verminderte Freisetzung des entzündungshemmenden Zytokins IL-10 zusammen mit vermehrter IL-1 $\beta$ -Antwort könnte zu stärkeren Entzündungsreaktionen mit erhöhter Gewebeschädigung führen, wodurch eine Umgebung geschaffen wird, die die Verbreitung von Mykobakterien be-

günstigt. Reduzierte Freisetzung von IL-12-Familienmitgliedern durch *SPPL2a*<sup>-/-</sup> BMDCs können zu einer beeinträchtigten Induktion von Typ1-T-Helferzell-Antworten führen, die für die Beseitigung von Mykobakterien erforderlich sind. So zeigen die Ergebnisse dieser Arbeit, dass MSMD in *SPPL2a*-defizienten Patienten nicht nur durch die reduzierte Häufigkeit der cDC2-Population verursacht, sondern auch durch ein funktionelles Defizit der verbleibenden DCs beeinflusst werden kann.

## References

- Abe, K., Yarovinsky, F. O., Murakami, T., Shakhov, A. N., Tumanov, A. V., Ito, D., Drutskaya, L. N., Pfeffer, K., Kuprash, D. V., Komschlies, K. L., and Nedospasov, S. A. (2003). Distinct contributions of TNF and LT cytokines to the development of dendritic cells in vitro and their recruitment in vivo, *Blood*. **101**(4): 1477–1483.
- Abel, B., Thieblemont, N., Quesniaux, V. J. F., Brown, N., Mpagi, J., Miyake, K., Bihl, F., and Ryffel, B. (2002). Toll-like receptor 4 expression is required to control chronic Mycobacterium tuberculosis infection in mice, *J. Immunol.* **169**(6): 3155–3162.
- Achkar, J. M., Chan, J., and Casadevall, A. (2015). B cells and antibodies in the defense against Mycobacterium tuberculosis infection, *Immunol. Rev.* **264**(1): 167–181.
- Adrain, C., Strisovsky, K., Zettl, M., Hu, L., Lemberg, M. K., and Freeman, M. (2011). Mammalian EGF receptor activation by the rhomboid protease RHBDL2, *EMBO Rep.* **12**(5): 421–427.
- Afonina, I. S., Müller, C., Martin, S. J., and Beyaert, R. (2015). Proteolytic Processing of Interleukin-1 Family Cytokines: Variations on a Common Theme, *Immunity*. **42**(6): 991–1004.
- Akira, S. and Takeda, K. (2004). Toll-like receptor signalling, *Nat. Rev. Immunol.* **4**(7): 499–511.
- Aliberti, J., Schulz, O., Pennington, D. J., Tsujimura, H., Reis e Sousa, C., Ozato, K., and Sher, A. (2003). Essential role for ICSBP in the in vivo development of murine CD8alpha + dendritic cells, *Blood*. **101**(1): 305–310.
- Aliprantis, A. O., Yang, R. B., Mark, M. R., Suggett, S., Devaux, B., Radolf, J. D., Klimpel, G. R., Godowski, P., and Zychlinsky, A. (1999). Cell activation and apoptosis by bacterial lipoproteins through toll-like receptor-2, *Science*. **285**(5428): 736–739.
- Ashman, J. B. and Miller, J. (1999). A role for the transmembrane domain in the trimerization of the MHC class II-associated invariant chain, *J. Immunol.* **163**(5): 2704–2712.
- Avcı, D. and Lemberg, M. K. (2015). Clipping or Extracting: Two Ways to Membrane Protein Degradation, *Trends Cell Biol.* **25**(10): 611–622.
- Barclay, A. N. and Berg, T. K. v. d. (2014). The Interaction Between Signal Regulatory Protein Alpha (SIRP $\alpha$ ) and CD47: Structure, Function, and Therapeutic Target, *Annual Review of Immunology*. **32**(1): 25–50.
- Barrington, L., Wanke, F., Niss Arfelt, K., Holst, P. J., Kurschus, F. C., and Rosenkilde, M. M. (2018). EBI2 in splenic and local immune responses and in autoimmunity, *J. Leukoc. Biol.*
- Basu, J., Shin, D.-M., and Jo, E.-K. (2012). Mycobacterial signaling through toll-like receptors, *Front. Cell Infect. Microbiol.* **2**:
- Becker-Herman, S., Arie, G., Medvedovsky, H., Kerem, A., and Shachar, I. (2005). CD74 Is a Member of the Regulated Intramembrane Proteolysis-processed Protein Family, *Mol. Biol. Cell.* **16**(11): 5061–5069.
- Beel, A. J. and Sanders, C. R. (2008). Substrate specificity of gamma-secretase and other intramembrane proteases, *Cell. Mol. Life Sci.* **65**(9): 1311–1334.
- Beers, C., Burich, A., Kleijmeer, M. J., Griffith, J. M., Wong, P., and Rudensky, A. Y. (2005). Cathepsin S controls MHC class II-mediated antigen presentation by epithelial cells in vivo, *J. Immunol.* **174**(3): 1205–1212.
- Behler, F., Maus, R., Bohling, J., Knippenberg, S., Kirchhof, G., Nagata, M., Jonigk, D., Izykowski, N., Mägel, L., Welte, T., Yamasaki, S., and Maus, U. A. (2015). Macrophage-inducible C-type lectin

## REFERENCES

---

- Mincle-expressing dendritic cells contribute to control of splenic *Mycobacterium bovis* BCG infection in mice, *Infect. Immun.* **83**(1): 184–196.
- Behler, F., Steinwede, K., Balboa, L., Ueberberg, B., Maus, R., Kirchhof, G., Yamasaki, S., Welte, T., and Maus, U. A. (2012). Role of Mincle in alveolar macrophage-dependent innate immunity against mycobacterial infections in mice, *J. Immunol.* **189**(6): 3121–3129.
- Behnke, J., Schneppenheim, J., Koch-Nolte, F., Haag, F., Saftig, P., and Schröder, B. (2011). Signal-peptide-peptidase-like 2a (SPPL2a) is targeted to lysosomes/late endosomes by a tyrosine motif in its C-terminal tail, *FEBS Lett.* **585**(19): 2951–2957.
- Beisner, D. R., Langerak, P., Parker, A. E., Dahlberg, C., Otero, F. J., Sutton, S. E., Poirot, L., Barnes, W., Young, M. A., Niessen, S., Wiltshire, T., Bodendorf, U., Martoglio, B., Cravatt, B., and Cooke, M. P. (2013). The intramembrane protease Sppl2a is required for B cell and DC development and survival via cleavage of the invariant chain, *J. Exp. Med.* **210**(1): 23–30.
- Belkaid, Y. and Oldenhove, G. (2008). Tuning Microenvironments: Induction of Regulatory T Cells by Dendritic Cells, *Immunity.* **29**(3): 362–371.
- Bergbold, N. and Lemberg, M. K. (2013). Emerging role of rhomboid family proteins in mammalian biology and disease, *Biochim. Biophys. Acta, Biomembr.* **1828**(12): 2840–2848.
- Bergmann, H., Yabas, M., Short, A., Miosge, L., Barthel, N., Teh, C. E., Roots, C. M., Bull, K. R., Jeelall, Y., Horikawa, K., Whittle, B., Balakishnan, B., Sjollem, G., Bertram, E. M., Mackay, F., Rimmer, A. J., Cornall, R. J., Field, M. A., Andrews, T. D., Goodnow, C. C., and Enders, A. (2013). B cell survival, surface BCR and BAFFR expression, CD74 metabolism, and CD8- dendritic cells require the intramembrane endopeptidase SPPL2A, *J. Exp. Med.* **210**(1): 31–40.
- Bettelli, E., Carrier, Y., Gao, W., Korn, T., Strom, T. B., Oukka, M., Weiner, H. L., and Kuchroo, V. K. (2006). Reciprocal developmental pathways for the generation of pathogenic effector TH17 and regulatory T cells, *Nature.* **441**(7090): 235–238.
- Bijlmakers, M. J., Benaroch, P., and Ploegh, H. L. (1994). Mapping functional regions in the luminal domain of the class II-associated invariant chain. *J. Exp. Med.* **180**(2): 623–629.
- Bikoff, E. K., Huang, L. Y., Episkopou, V., Meerwijk, J. v., Germain, R. N., and Robertson, E. J. (1993). Defective major histocompatibility complex class II assembly, transport, peptide acquisition, and CD4+ T cell selection in mice lacking invariant chain expression. *J. Exp. Med.* **177**(6): 1699–1712.
- Binsky, I., Haran, M., Starlets, D., Gore, Y., Lantner, F., Harpaz, N., Leng, L., Goldenberg, D. M., Shvidel, L., Berrebi, A., Bucala, R., and Shachar, I. (2007). IL-8 secreted in a macrophage migration-inhibitory factor- and CD74-dependent manner regulates B cell chronic lymphocytic leukemia survival, *PNAS.* **104**(33): 13408–13413.
- Black, R. A., Rauch, C. T., Kozlosky, C. J., Peschon, J. J., Slack, J. L., Wolfson, M. F., Castner, B. J., Stocking, K. L., Reddy, P., Srinivasan, S., Nelson, N., Boiani, N., Schooley, K. A., Gerhart, M., Davis, R., Fitzner, J. N., Johnson, R. S., Paxton, R. J., March, C. J., and Cerretti, D. P. (1997). A metalloproteinase disintegrin that releases tumour-necrosis factor-alpha from cells, *Nature.* **385**(6618): 729–733.
- Boname, J. M., Bloor, S., Wandel, M. P., Nathan, J. A., Antrobus, R., Dingwell, K. S., Thurston, T. L., Smith, D. L., Smith, J. C., Randow, F., and Lehner, P. J. (2014). Cleavage by signal peptide peptidase is required for the degradation of selected tail-anchored proteins, *J. Cell Biol.* **205**(6): 847–862.
- Brady, O. A., Zhou, X., and Hu, F. (2014). Regulated Intramembrane Proteolysis of the Frontotemporal Lobar Degeneration Risk Factor, TMEM106B, by Signal Peptide Peptidase-like 2a (SPPL2a), *J. Biol. Chem.* **289**(28): 19670–19680.
- Brasel, K., De Smedt, T., Smith, J. L., and Maliszewski, C. R. (2000). Generation of murine dendritic cells from flt3-ligand-supplemented bone marrow cultures, *Blood.* **96**(9): 3029–3039.



- Broeke, T. ten, Wubbolts, R., and Stoorvogel, W. (2013). MHC Class II Antigen Presentation by Dendritic Cells Regulated through Endosomal Sorting, *Cold Spring Harb. Perspect. Biol.* **5**(12):
- Brown, G. D. and Gordon, S. (2001). Immune recognition. A new receptor for beta-glucans, *Nature*. **413**(6851): 36–37.
- Brown, G. D. and Crocker, P. R. (2016). Lectin Receptors Expressed on Myeloid Cells, *Microbiol. Spectr.* **4**(5):
- Bustamante, J., Boisson-Dupuis, S., Abel, L., and Casanova, J.-L. (2014). Mendelian susceptibility to mycobacterial disease: genetic, immunological, and clinical features of inborn errors of IFN-gamma immunity, *Semin. Immunol.* **26**(6): 454–470.
- Chiang, C.-Y., Veckman, V., Limmer, K., and David, M. (2012). Phospholipase Cgamma-2 and Intracellular Calcium Are Required for Lipopolysaccharide-induced Toll-like Receptor 4 (TLR4) Endocytosis and Interferon Regulatory Factor 3 (IRF3) Activation, *J. Biol. Chem.* **287**(6): 3704–3709.
- Conti, H. R., Huppler, A. R., Whibley, N., and Gaffen, S. L. (2014). Animal Models for Candidiasis, *Curr. Protoc. Immunol.* **105**: 19.6.1–19.6.17.
- Cooper, A. M., Dalton, D. K., Stewart, T. A., Griffin, J. P., Russell, D. G., and Orme, I. M. (1993). Disseminated tuberculosis in interferon gamma gene-disrupted mice, *J. Exp. Med.* **178**(6): 2243–2247.
- Cooper, A. M. and Khader, S. A. (2007). IL-12p40: an inherently agonistic cytokine, *Trends Immunol.* **28**(1): 33–38.
- Cooper, A. M., Kipnis, A., Turner, J., Magram, J., Ferrante, J., and Orme, I. M. (2002). Mice Lacking Bioactive IL-12 Can Generate Protective, Antigen-Specific Cellular Responses to Mycobacterial Infection Only if the IL-12 p40 Subunit Is Present, *J. Immunol.* **168**(3): 1322–1327.
- Couper, K. N., Blount, D. G., and Riley, E. M. (2008). IL-10: The Master Regulator of Immunity to Infection, *J. Immunol.* **180**(9): 5771–5777.
- Cray, C., Zaias, J., and Altman, N. H. (2009). Acute Phase Response in Animals: A Review, *Comp. Med.* **59**(6): 517–526.
- Dambuzza, I. M. and Brown, G. D. (2015). C-type lectins in immunity: recent developments, *Curr. Opin. Immunol.* **32**: 21–27.
- Das, R., Koo, M.-S., Kim, B. H., Jacob, S. T., Subbian, S., Yao, J., Leng, L., Levy, R., Murchison, C., Burman, W. J., Moore, C. C., Scheld, W. M., David, J. R., Kaplan, G., MacMicking, J. D., and Bucala, R. (2013). Macrophage migration inhibitory factor (MIF) is a critical mediator of the innate immune response to *Mycobacterium tuberculosis*, *Proc. Natl. Acad. Sci. U.S.A.* **110**(32): E2997–E3006.
- De Strooper, B., Annaert, W., Cupers, P., Saftig, P., Craessaerts, K., Mumm, J. S., Schroeter, E. H., Schrijvers, V., Wolfe, M. S., Ray, W. J., Goate, A., and Kopan, R. (1999). A presenilin-1-dependent gamma-secretase-like protease mediates release of Notch intracellular domain, *Nature*. **398**(6727): 518–522.
- Déjardin, J. and Kingston, R. E. (2009). Purification of proteins associated with specific genomic Loci, *Cell*. **136**(1): 175–186.
- Dinarello, C. A. (2009). Immunological and Inflammatory Functions of the Interleukin-1 Family, *Annu. Rev. Immunol.* **27**(1): 519–550.
- Driessen, C., Bryant, R. A., Lennon-Duménil, A. M., Villadangos, J. A., Bryant, P. W., Shi, G. P., Chapman, H. A., and Ploegh, H. L. (1999). Cathepsin S controls the trafficking and maturation of MHC class II molecules in dendritic cells, *J. Cell Biol.* **147**(4): 775–790.
- Drummond, R. A. and Brown, G. D. (2011). The role of Dectin-1 in the host defence against fungal infections, *Curr. Opin. Microbiol.* **14**(4): 392–399.

## REFERENCES

---

- Durai, V. and Murphy, K. M. (2016). Functions of Murine Dendritic Cells, *Immunity*. **45**(4): 719–736.
- Dustin, L. B., Plas, D. R., Wong, J., Hu, Y. T., Soto, C., Chan, A. C., and Thomas, M. L. (1999). Expression of dominant-negative src-homology domain 2-containing protein tyrosine phosphatase-1 results in increased Syk tyrosine kinase activity and B cell activation, *J. Immunol.* **162**(5): 2717–2724.
- Esteban, A., Popp, M. W., Vyas, V. K., Strijbis, K., Ploegh, H. L., and Fink, G. R. (2011). Fungal recognition is mediated by the association of dectin-1 and galectin-3 in macrophages, *Proc. Natl. Acad. Sci. U.S.A.* **108**(34): 14270–14275.
- Faure-André, G., Vargas, P., Yuseff, M.-I., Heuzé, M., Diaz, J., Lankar, D., Steri, V., Manry, J., Hugues, S., Vascotto, F., Boulanger, J., Raposo, G., Bono, M.-R., Roseblatt, M., Piel, M., and Lennon-Duménil, A.-M. (2008). Regulation of dendritic cell migration by CD74, the MHC class II-associated invariant chain, *Science*. **322**(5908): 1705–1710.
- Ferwerda, B., Ferwerda, G., Plantinga, T. S., Willment, J. A., Spriel, A. B. van, Venselaar, H., Elbers, C. C., Johnson, M. D., Cambi, A., Huysamen, C., Jacobs, L., Jansen, T., Verheijen, K., Masthoff, L., Morré, S. A., Vriend, G., Williams, D. L., Perfect, J. R., Joosten, L. A., Wijmenga, C., Meer, J. W. van der, Adema, G. J., Kullberg, B. J., Brown, G. D., and Netea, M. G. (2009). Human Dectin-1 Deficiency and Mucocutaneous Fungal Infections, *N. Engl. J. Med.* **361**(18): 1760–1767.
- Fleck, D., Voss, M., Brankatschk, B., Giudici, C., Hampel, H., Schwenk, B., Edbauer, D., Fukumori, A., Steiner, H., Kremmer, E., Haug-Kröper, M., Rossner, M. J., Fluhrer, R., Willem, M., and Haass, C. (2016). Proteolytic Processing of Neuregulin 1 Type III by Three Intramembrane-cleaving Proteases, *J. Biol. Chem.* **291**(1): 318–333.
- Flores-Langarica Adriana, Marshall Jennifer L., Bobat Saeeda, Mohr Elodie, Hitchcock Jessica, Ross Ewan A., Coughlan Ruth E., Khan Mahmood, Van Rooijen Nico, Henderson Ian R., MacLennan Ian C.M., and Cunningham Adam F. (2011). T-zone localized monocyte-derived dendritic cells promote Th1 priming to Salmonella, *Eur. J. Immunol.* **41**(9): 2654–2665.
- Fluhrer, R., Grammer, G., Israel, L., Condrón, M. M., Haffner, C., Friedmann, E., Böhland, C., Imhof, A., Martoglio, B., Teplow, D. B., and Haass, C. (2006). A gamma-secretase-like intramembrane cleavage of TNFalpha by the GxGD aspartyl protease SPPL2b, *Nat. Cell Biol.* **8**(8): 894–896.
- Francis, R., McGrath, G., Zhang, J., Ruddy, D. A., Sym, M., Apfeld, J., Nicoll, M., Maxwell, M., Hai, B., Ellis, M. C., Parks, A. L., Xu, W., Li, J., Gurney, M., Myers, R. L., Himes, C. S., Hiebsch, R., Ruble, C., Nye, J. S., and Curtis, D. (2002). *aph-1* and *pen-2* are required for Notch pathway signaling, gamma-secretase cleavage of betaAPP, and presenilin protein accumulation, *Dev. Cell.* **3**(1): 85–97.
- Freeman, M. (2008). Rhomboid Proteases and their Biological Functions, *Annu. Rev. Genet.* **42**(1): 191–210.
- Friedmann, E., Hauben, E., Maylandt, K., Schlegler, S., Vreugde, S., Lichtenthaler, S. F., Kuhn, P.-H., Stauffer, D., Rovelli, G., and Martoglio, B. (2006). SPPL2a and SPPL2b promote intramembrane proteolysis of TNFalpha in activated dendritic cells to trigger IL-12 production, *Nat. Cell Biol.* **8**(8): 843–848.
- Friedmann, E., Lemberg, M. K., Weihofen, A., Dev, K. K., Dengler, U., Rovelli, G., and Martoglio, B. (2004). Consensus Analysis of Signal Peptide Peptidase and Homologous Human Aspartic Proteases Reveals Opposite Topology of Catalytic Domains Compared with Presenilins, *J. Biol. Chem.* **279**(49): 50790–50798.
- Gabriele, L., Fragale, A., Borghi, P., Sestili, P., Stellacci, E., Venditti, M., Schiavoni, G., Sanchez, M., Belardelli, F., and Battistini, A. (2006). IRF-1 deficiency skews the differentiation of dendritic cells toward plasmacytoid and tolerogenic features, *J. Leukoc. Biol.* **80**(6): 1500–1511.

- Gantner, B. N., Simmons, R. M., Canavera, S. J., Akira, S., and Underhill, D. M. (2003). Collaborative induction of inflammatory responses by dectin-1 and Toll-like receptor 2, *J. Exp. Med.* **197**(9): 1107–1117.
- Garlanda, C., Di Liberto, D., Vecchi, A., La Manna, M. P., Buracchi, C., Caccamo, N., Salerno, A., Dieli, F., and Mantovani, A. (2007). Damping excessive inflammation and tissue damage in Mycobacterium tuberculosis infection by Toll IL-1 receptor 8/single Ig IL-1-related receptor, a negative regulator of IL-1/TLR signaling, *J. Immunol.* **179**(5): 3119–3125.
- Garlanda, C., Dinarello, C. A., and Mantovani, A. (2013). The Interleukin-1 Family: Back to the Future, *Immunity.* **39**(6): 1003–1018.
- Gazzinelli, R. T., Oswald, I. P., James, S. L., and Sher, A. (1992). IL-10 inhibits parasite killing and nitrogen oxide production by IFN-gamma-activated macrophages. *J. Immunol.* **148**(6): 1792–1796.
- Geissmann, F., Manz, M. G., Jung, S., Sieweke, M. H., Merad, M., and Ley, K. (2010). Development of Monocytes, Macrophages, and Dendritic Cells, *Science.* **327**(5966): 656–661.
- Gil-Yarom, N., Radomir, L., Sever, L., Kramer, M. P., Lewinsky, H., Bornstein, C., Blecher-Gonen, R., Barnett-Itzhaki, Z., Mirkin, V., Friedlander, G., Shvidel, L., Herishanu, Y., Lolis, E. J., Becker-Herman, S., Amit, I., and Shachar, I. (2017). CD74 is a novel transcription regulator, *PNAS.* **114**(3): 562–567.
- Gilmour, K. C., Fujii, H., Cranston, T., Davies, E. G., Kinnon, C., and Gaspar, H. B. (2001). Defective expression of the interleukin-2/interleukin-15 receptor beta subunit leads to a natural killer cell-deficient form of severe combined immunodeficiency, *Blood.* **98**(3): 877–879.
- Glocker, E.-O., Kotlarz, D., Klein, C., Shah, N., and Grimbacher, B. (2011). IL-10 and IL-10 receptor defects in humans, *Ann. N. Y. Acad. Sci.* **1246**: 102–107.
- Gombault, A., Baron, L., and Couillin, I. (2012). ATP release and purinergic signaling in NLRP3 inflammasome activation, *Front. Immunol.* **3**: 414.
- Goodridge, H. S., Simmons, R. M., and Underhill, D. M. (2007). Dectin-1 Stimulation by Candida albicans Yeast or Zymosan Triggers NFAT Activation in Macrophages and Dendritic Cells, *J. Immunol.* **178**(5): 3107–3115.
- Goodridge, H. S., Underhill, D. M., and Touret, N. (2012). Mechanisms of Fc receptor and dectin-1 activation for phagocytosis, *Traffic.* **13**(8): 1062–1071.
- Gore, Y., Starlets, D., Maharshak, N., Becker-Herman, S., Kaneyuki, U., Leng, L., Bucala, R., and Shachar, I. (2008). Macrophage Migration Inhibitory Factor Induces B Cell Survival by Activation of a CD74-CD44 Receptor Complex, *J. Biol. Chem.* **283**(5): 2784–2792.
- Grigorenko, A. P., Moliaka, Y. K., Korovaitseva, G. I., and Rogaev, E. I. (2002). Novel class of polytopic proteins with domains associated with putative protease activity, *Biochemistry Mosc.* **67**(7): 826–835.
- Gringhuis, S. I., Dunnen, J. den, Litjens, M., Vlist, M. van der, Wevers, B., Bruijns, S. C. M., and Geijtenbeek, T. B. H. (2009). Dectin-1 directs T helper cell differentiation by controlling noncanonical NF-kappaB activation through Raf-1 and Syk, *Nat. Immunol.* **10**(2): 203–213.
- Gu, Y., Chen, F., Sanjo, N., Kawarai, T., Hasegawa, H., Duthie, M., Li, W., Ruan, X., Luthra, A., Mount, H. T. J., Tandon, A., Fraser, P. E., and St George-Hyslop, P. (2003). APH-1 interacts with mature and immature forms of presenilins and nicastrin and may play a role in maturation of presenilin.nicastrin complexes, *J. Biol. Chem.* **278**(9): 7374–7380.
- Haapasalo, A. and Kovacs, D. M. (2011). The many substrates of presenilin/gamma-secretase, *J. Alzheimers Dis.* **25**(1): 3–28.
- Haass, C. and Steiner, H. (2002). Alzheimer disease gamma-secretase: a complex story of GxGD-type presenilin proteases, *Trends Cell Biol.* **12**(12): 556–562.

## REFERENCES

---

- Hampton, S. E., Dore, T. M., and Schmidt, W. K. (2018). Rce1: mechanism and inhibition, *Crit. Rev. Biochem. Mol. Biol.* **53**(2): 157–174.
- Hanabuchi, S. and Liu, Y.-J. (2011). In Vivo Role of pDCs in Regulating Adaptive Immunity, *Immunity*. **35**(6): 851–853.
- Heldwein, K. A., Liang, M. D., Andresen, T. K., Thomas, K. E., Marty, A. M., Cuesta, N., Vogel, S. N., and Fenton, M. J. (2003). TLR2 and TLR4 serve distinct roles in the host immune response against *Mycobacterium bovis* BCG, *J. Leukoc. Biol.* **74**(2): 277–286.
- Helft, J., Böttcher, J., Chakravarty, P., Zelenay, S., Huotari, J., Schraml, B. U., Goubau, D., and Reis e Sousa, C. (2015). GM-CSF Mouse Bone Marrow Cultures Comprise a Heterogeneous Population of CD11c(+)MHCII(+) Macrophages and Dendritic Cells, *Immunity*. **42**(6): 1197–1211.
- Hernanz-Falcón, P., Joffre, O., Williams, D. L., and Reis e Sousa, C. (2009). Internalization of Dectin-1 terminates induction of inflammatory responses, *Eur. J. Immunol.* **39**(2): 507–513.
- Herre, J., Marshall, A. S. J., Caron, E., Edwards, A. D., Williams, D. L., Schweighoffer, E., Tybulewicz, V., Sousa, C. R. e., Gordon, S., and Brown, G. D. (2004). Dectin-1 uses novel mechanisms for yeast phagocytosis in macrophages, *Blood*. **104**(13): 4038–4045.
- Heufler, C., Koch, F., Stanzl, U., Topar, G., Wysocka, M., Trinchieri, G., Enk, A., Steinman, R. M., Romani, N., and Schuler, G. (1996). Interleukin-12 is produced by dendritic cells and mediates T helper 1 development as well as interferon-gamma production by T helper 1 cells, *Eur. J. Immunol.* **26**(3): 659–668.
- Heuzé, M. L., Vargas, P., Chabaud, M., Le Berre, M., Liu, Y.-J., Collin, O., Solanes, P., Voituriez, R., Piel, M., and Lennon-Duménil, A.-M. (2013). Migration of dendritic cells: physical principles, molecular mechanisms, and functional implications, *Immunol. Rev.* **256**(1): 240–254.
- Higgins, D. M., Sanchez-Campillo, J., Rosas-Taraco, A. G., Lee, E. J., Orme, I. M., and Gonzalez-Juarrero, M. (2009). Lack of IL-10 alters inflammatory and immune responses during pulmonary *Mycobacterium tuberculosis* infection, *Tuberculosis (Edinb)*. **89**(2): 149–157.
- Hochrein, H., Shortman, K., Vremec, D., Scott, B., Hertzog, P., and O’Keefe, M. (2001). Differential production of IL-12, IFN-alpha, and IFN-gamma by mouse dendritic cell subsets, *J. Immunol.* **166**(9): 5448–5455.
- Hoepli, R. E., Wu, D., Cook, L., and Levings, M. K. (2015). The Environment of Regulatory T Cell Biology: Cytokines, Metabolites, and the Microbiome, *Front. Immunol.* **6**:
- Hölscher, C., Atkinson, R. A., Arendse, B., Brown, N., Myburgh, E., Alber, G., and Brombacher, F. (2001). A protective and agonistic function of IL-12p40 in mycobacterial infection, *J. Immunol.* **167**(12): 6957–6966.
- Hsieh, C. S., Heimberger, A. B., Gold, J. S., O’Garra, A., and Murphy, K. M. (1992). Differential regulation of T helper phenotype development by interleukins 4 and 10 in an alpha beta T-cell-receptor transgenic system, *Proc. Natl. Acad. Sci. U.S.A.* **89**(13): 6065–6069.
- Hsieh, C. S., Macatonia, S. E., Tripp, C. S., Wolf, S. F., O’Garra, A., and Murphy, K. M. (1993). Development of TH1 CD4+ T cells through IL-12 produced by *Listeria*-induced macrophages, *Science*. **260**(5107): 547–549.
- Hüttl, S. (2015). Dissertation Processing of CD74 by the intramembrane protease SPPL2a in B cells: Impact on endosomal trafficking and signaling:
- Hüttl, S., Kläsener, K., Schweizer, M., Schneppenheim, J., Oberg, H.-H., Kabelitz, D., Reth, M., Saftig, P., and Schröder, B. (2015). Processing of CD74 by the Intramembrane Protease SPPL2a Is Critical for B Cell Receptor Signaling in Transitional B Cells, *J. Immunol.* **195**(4): 1548–1563.

- Inaba, K., Inaba, M., Romani, N., Aya, H., Deguchi, M., Ikehara, S., Muramatsu, S., and Steinman, R. M. (1992). Generation of large numbers of dendritic cells from mouse bone marrow cultures supplemented with granulocyte/macrophage colony-stimulating factor, *J. Exp. Med.* **176**(6): 1693–1702.
- Ishikawa, E., Ishikawa, T., Morita, Y. S., Toyonaga, K., Yamada, H., Takeuchi, O., Kinoshita, T., Akira, S., Yoshikai, Y., and Yamasaki, S. (2009). Direct recognition of the mycobacterial glycolipid, trehalose dimycolate, by C-type lectin Mincle, *J. Exp. Med.* **206**(13): 2879–2888.
- Jacobs, M., Brown, N., Allie, N., Gulert, R., and Ryffel, B. (2000). Increased resistance to mycobacterial infection in the absence of interleukin-10, *Immunology.* **100**(4): 494–501.
- Jorissen, E. and De Strooper, B. (2010). Gamma-secretase and the intramembrane proteolysis of Notch, *Curr. Top. Dev. Biol.* **92**: 201–230.
- Jules, F., Sauvageau, E., Dumaresq-Doiron, K., Mazzaferri, J., Haug-Kröper, M., Fluhrer, R., Costantino, S., and Lefrancois, S. (2017). CLN5 is cleaved by members of the SPP/SPPL family to produce a mature soluble protein, *Exp. Cell Res.* **357**(1): 40–50.
- Kalliolias, G. D. and Ivashkiv, L. B. (2016). TNF biology, pathogenic mechanisms and emerging therapeutic strategies, *Nat. Rev. Rheumatol.* **12**(1): 49–62.
- Kerscher, B., Willment, J. A., and Brown, G. D. (2013). The Dectin-2 family of C-type lectin-like receptors: an update, *Int. Immunol.* **25**(5): 271–277.
- Khader, S. A., Partida-Sanchez, S., Bell, G., Jelley-Gibbs, D. M., Swain, S., Pearl, J. E., Ghilardi, N., Desauvage, F. J., Lund, F. E., and Cooper, A. M. (2006). Interleukin 12p40 is required for dendritic cell migration and T cell priming after Mycobacterium tuberculosis infection, *J. Exp. Med.* **203**(7): 1805–1815.
- Kieper, W. C., Prlc, M., Schmidt, C. S., Mescher, M. F., and Jameson, S. C. (2001). Il-12 enhances CD8 T cell homeostatic expansion, *J. Immunol.* **166**(9): 5515–5521.
- Kirkin, V., Cahuzac, N., Guardiola-Serrano, F., Huault, S., Lückcrath, K., Friedmann, E., Novac, N., Wels, W. S., Martoglio, B., Hueber, A.-O., and Zörnig, M. (2007). The Fas ligand intracellular domain is released by ADAM10 and SPPL2a cleavage in T-cells, *Cell Death Differ.* **14**(9): 1678–1687.
- Koch, N., Koch, S., and Hämmerling, G. J. (1982). Ia invariant chain detected on lymphocyte surfaces by monoclonal antibody, *Nature.* **299**(5884): 644–645.
- Kong, X.-F., Martinez-Barricarte, R., Kennedy, J., Mele, F., Lazarov, T., Deenick, E. K., Breton, G., ..., Bustamante, J., and Casanova, J.-L. (2018). Disruption of an anti-mycobacterial circuit between dendritic and T helper cells in humans with inherited SPPL2a deficiency, *Nat. Immunol. in revision.*
- Korzeniewski, C. and Callewaert, D. M. (1983). An enzyme-release assay for natural cytotoxicity, *J. Immunol. Methods.* **64**(3): 313–320.
- Krawitz, P., Haffner, C., Fluhrer, R., Steiner, H., Schmid, B., and Haass, C. (2005). Differential localization and identification of a critical aspartate suggest non-redundant proteolytic functions of the presenilin homologues SPPL2b and SPPL3, *J. Biol. Chem.* **280**(47): 39515–39523.
- Kuhn, P.-H., Voss, M., Haug-Kröper, M., Schröder, B., Schepers, U., Bräse, S., Haass, C., Lichtenthaler, S. F., and Fluhrer, R. (2015). Secretome analysis identifies novel signal Peptide peptidase-like 3 (Sppl3) substrates and reveals a role of Sppl3 in multiple Golgi glycosylation pathways, *Mol. Cell Proteomics.* **14**(6): 1584–1598.
- Laemmli, U. K. (1970). Cleavage of Structural Proteins during the Assembly of the Head of Bacteriophage T4, *Nature.* **227**(5259): 680–685.

## REFERENCES

---

- Lagaudrière-Gesbert, C., Newmyer, S. L., Gregers, T. F., Bakke, O., and Ploegh, H. L. (2002). Uncoating ATPase Hsc70 is recruited by invariant chain and controls the size of endocytic compartments, *PNAS*. **99**(3): 1515–1520.
- Lal, M. and Caplan, M. (2011). Regulated intramembrane proteolysis: signaling pathways and biological functions, *Physiology*. **26**(1): 34–44.
- Latz, E., Xiao, T. S., and Stutz, A. (2013). Activation and regulation of the inflammasomes, *Nat. Rev. Immunol.* **13**(6): 397–411.
- Laurent, S. A., Hoffmann, F. S., Kuhn, P.-H., Cheng, Q., Chu, Y., Schmidt-Suppran, M., Hauck, S. M., Schuh, E., Krumbholz, M., Rübsamen, H., Wanngren, J., Khademi, M., Olsson, T., Alexander, T., Hiepe, F., Pfister, H.-W., Weber, F., Jenne, D., Wekerle, H., Hohlfeld, R., Lichtenthaler, S. F., and Meinel, E. (2015). Gamma-Secretase directly sheds the survival receptor BCMA from plasma cells, *Nat. Commun.* **6**: 7333.
- Le Gros, G., Ben-Sasson, S. Z., Seder, R., Finkelman, F. D., and Paul, W. E. (1990). Generation of interleukin 4 (IL-4)-producing cells in vivo and in vitro: IL-2 and IL-4 are required for in vitro generation of IL-4-producing cells, *J. Exp. Med.* **172**(3): 921–929.
- Lee, S.-F., Shah, S., Li, H., Yu, C., Han, W., and Yu, G. (2002). Mammalian APH-1 Interacts with Presenilin and Nicastrin and Is Required for Intramembrane Proteolysis of Amyloid-beta Precursor Protein and Notch, *J. Biol. Chem.* **277**(47): 45013–45019.
- LeibundGut-Landmann, S., Gross, O., Robinson, M. J., Osorio, F., Slack, E. C., Tsoni, S. V., Schweighofer, E., Tybulewicz, V., Brown, G. D., Ruland, J., and Reis e Sousa, C. (2007). Syk- and CARD9-dependent coupling of innate immunity to the induction of T helper cells that produce interleukin 17, *Nat. Immunol.* **8**(6): 630–638.
- Leng, L., Metz, C. N., Fang, Y., Xu, J., Donnelly, S., Baugh, J., Delohery, T., Chen, Y., Mitchell, R. A., and Bucala, R. (2003). MIF Signal Transduction Initiated by Binding to CD74, *J. Exp. Med.* **197**(11): 1467–1476.
- León, B., López-Bravo, M., and Ardavín, C. (2007). Monocyte-Derived Dendritic Cells Formed at the Infection Site Control the Induction of Protective T Helper 1 Responses against Leishmania, *Immunity*. **26**(4): 519–531.
- Liao, W., Lin, J.-X., and Leonard, W. J. (2013). Interleukin-2 at the Crossroads of Effector Responses, Tolerance, and Immunotherapy, *Immunity*. **38**(1): 13–25.
- Liaunardy-Jopeace, A. and Gay, N. J. (2014). Molecular and Cellular Regulation of Toll-Like Receptor-4 Activity Induced by Lipopolysaccharide Ligands, *Front. Immunol.* **5**:
- Liu, Y.-H., Lin, C.-Y., Lin, W.-C., Tang, S.-W., Lai, M.-K., and Lin, J.-Y. (2008). Up-regulation of vascular endothelial growth factor-D expression in clear cell renal cell carcinoma by CD74: a critical role in cancer cell tumorigenesis, *J. Immunol.* **181**(9): 6584–6594.
- Lutz, M. B., Kukutsch, N., Ogilvie, A. L., Rössner, S., Koch, F., Romani, N., and Schuler, G. (1999). An advanced culture method for generating large quantities of highly pure dendritic cells from mouse bone marrow, *J. Immunol. Methods*. **223**(1): 77–92.
- Macri, C., Pang, E. S., Patton, T., and O’Keeffe, M. (2017). Dendritic cell subsets, *Semin. Cell Dev. Biol.*
- Maeda, A., Scharenberg, A. M., Tsukada, S., Bolen, J. B., Kinet, J. P., and Kurosaki, T. (1999). Paired immunoglobulin-like receptor B (PIR-B) inhibits BCR-induced activation of Syk and Btk by SHP-1, *Oncogene*. **18**(14): 2291–2297.
- Makowski, S. L., Wang, Z., and Pomerantz, J. L. (2015). A protease-independent function for SPPL3 in NFAT activation, *Mol. Cell. Biol.* **35**(2): 451–467.

- Manicassamy, S. and Manoharan, I. (2014). Mouse models of acute and chronic colitis, *Methods Mol. Biol.* **1194**: 437–448.
- Manolaridis, I., Kulkarni, K., Dodd, R. B., Ogasawara, S., Zhang, Z., Bineva, G., O'Reilly, N., Hanrahan, S. J., Thompson, A. J., Cronin, N., Iwata, S., and Barford, D. (2013). Mechanism of farnesylated CAAX protein processing by the intramembrane protease Rce1, *Nature*. **504**(7479): 301–305.
- Mansour, M. K., Tam, J. M., Khan, N. S., Seward, M., Davids, P. J., Puranam, S., Sokolovska, A., Sykes, D. B., Dagher, Z., Becker, C., Tanne, A., Reedy, J. L., Stuart, L. M., and Vyas, J. M. (2013). Dectin-1 activation controls maturation of  $\beta$ -1,3-glucan-containing phagosomes, *J. Biol. Chem.* **288**(22): 16043–16054.
- Marakalala, M. J., Guler, R., Matika, L., Murray, G., Jacobs, M., Brombacher, F., Rothfuchs, A. G., Sher, A., and Brown, G. D. (2011). The Syk/CARD9-coupled receptor Dectin-1 is not required for host resistance to *Mycobacterium tuberculosis* in mice, *Microbes Infect.* **13**(2): 198–201.
- Martin, L., Fluhrer, R., Reiss, K., Kremmer, E., Saftig, P., and Haass, C. (2008). Regulated intramembrane proteolysis of Bri2 (Itm2b) by ADAM10 and SPPL2a/SPPL2b, *J. Biol. Chem.* **283**(3): 1644–1652.
- Matsunaga, I. and Moody, D. B. (2009). Mincle is a long sought receptor for mycobacterial cord factor, *J. Exp. Med.* **206**(13): 2865–2868.
- Matza, D., Kerem, A., Medvedovsky, H., Lantner, F., and Shachar, I. (2002a). Invariant Chain-Induced B Cell Differentiation Requires Intramembrane Proteolytic Release of the Cytosolic Domain, *Immunity*. **17**(5): 549–560.
- Matza, D., Kerem, A., and Shachar, I. (2003). Invariant chain, a chain of command, *Trends Immunol.* **24**(5): 264–268.
- Matza, D., Lantner, F., Bogoch, Y., Flaishon, L., Hershkoviz, R., and Shachar, I. (2002b). Invariant chain induces B cell maturation in a process that is independent of its chaperonic activity, *PNAS*. **99**(5): 3018–3023.
- Matza, D., Wolstein, O., Dikstein, R., and Shachar, I. (2001). Invariant Chain Induces B Cell Maturation by Activating a TAFII105-NF-kappaB-dependent Transcription Program, *J. Biol. Chem.* **276**(29): 27203–27206.
- McCann, F., Carmona, E., Puri, V., Pagano, R. E., and Limper, A. H. (2005). Macrophage internalization of fungal beta-glucans is not necessary for initiation of related inflammatory responses, *Infect. Immun.* **73**(10): 6340–6349.
- McCarthy, A. J., Coleman-Vaughan, C., and McCarthy, J. V. (2017). Regulated intramembrane proteolysis: emergent role in cell signalling pathways, *Biochem. Soc. Trans.* **45**(6): 1185–1202.
- Means, T. K., Lien, E., Yoshimura, A., Wang, S., Golenbock, D. T., and Fenton, M. J. (1999). The CD14 ligands lipoarabinomannan and lipopolysaccharide differ in their requirement for Toll-like receptors, *J. Immunol.* **163**(12): 6748–6755.
- Méndez-Samperio, P. (2010). Role of interleukin-12 family cytokines in the cellular response to mycobacterial disease, *Int. J. Infect. Dis.* **14**(5): e366–e371.
- Mentrup, T. (2018). SPPL2-mediated intramembrane proteolysis controls pro-atherogenic signalling of the receptor LOX-1, *a*:
- Mentrup, T., Fluhrer, R., and Schröder, B. (2017a). Latest emerging functions of SPP/SPPL intramembrane proteases, *Eur. J. Cell Biol.* **96**(5): 372–382.
- Mentrup, T., Häsler, R., Fluhrer, R., Saftig, P., and Schröder, B. (2015). A Cell-Based Assay Reveals Nuclear Translocation of Intracellular Domains Released by SPPL Proteases, *Traffic*. **16**(8): 871–892.

## REFERENCES

---

- Mentrup, T., Loock, A.-C., Fluhrer, R., and Schröder, B. (2017b). Signal peptide peptidase and SPP-like proteases - Possible therapeutic targets?, *Biochim. Biophys. Acta.* **1864**(11 Pt B): 2169–2182.
- Merad, M., Sathe, P., Helft, J., Miller, J., and Mortha, A. (2013). The dendritic cell lineage: ontogeny and function of dendritic cells and their subsets in the steady state and the inflamed setting, *Annu. Rev. Immunol.* **31**: 563–604.
- Meyaard, L., Hovenkamp, E., Otto, S. A., and Miedema, F. (1996). IL-12-induced IL-10 production by human T cells as a negative feedback for IL-12-induced immune responses, *J. Immunol.* **156**(8): 2776–2782.
- Meyer-Wentrup, F., Figdor, C. G., Ansems, M., Brossart, P., Wright, M. D., Adema, G. J., and Spriell, A. B. v. (2007). Dectin-1 Interaction with Tetraspanin CD37 Inhibits IL-6 Production, *J. Immunol.* **178**(1): 154–162.
- Mitsdoerffer, M., Lee, Y., Jäger, A., Kim, H.-J., Korn, T., Kolls, J. K., Cantor, H., Bettelli, E., and Kuchroo, V. K. (2010). Proinflammatory T helper type 17 cells are effective B-cell helpers, *PNAS.* **107**(32): 14292–14297.
- Mittal, S. K. and Roche, P. A. (2015). Suppression of antigen presentation by IL-10, *Curr. Opin. Immunology.* **34**: 22–27.
- Momburg, F., Koch, N., Möller, P., Moldenhauer, G., Butcher, G. W., and Hämmerling, G. J. (1986). Differential expression of Ia and Ia-associated invariant chain in mouse tissues after in vivo treatment with IFN-gamma, *J. Immunol.* **136**(3): 940–948.
- Moreno-De-Luca, A., Helmers, S. L., Mao, H., Burns, T. G., Melton, A. M. A., Schmidt, K. R., Fernhoff, P. M., Ledbetter, D. H., and Martin, C. L. (2011). Adaptor protein complex-4 (AP-4) deficiency causes a novel autosomal recessive cerebral palsy syndrome with microcephaly and intellectual disability, *J. Med. Genet.* **48**(2): 141–144.
- Moss, M. L., Jin, S.-L. C., Milla, M. E., Burkhart, W., Carter, H. L., Chen, W.-J., Clay, W. C., Didsbury, J. R., Hassler, D., Hoffman, C. R., Kost, T. A., Lambert, M. H., Leesnitzer, M. A., McCauley, P., McGeehan, G., Mitchell, J., Moyer, M., Pahel, G., Rocque, W., Overton, L. K., Schoenen, F., Seaton, T., Su, J.-L., Warner, J., Willard, D., and Becherer, J. D. (1997). Cloning of a disintegrin metalloproteinase that processes precursor tumour-necrosis factor-alpha, *Nature.* **385**(6618): 733–736.
- Murase, M., Kawasaki, T., Hakozaki, R., Sueyoshi, T., Putri, D. D. P., Kitai, Y., Sato, S., Ikawa, M., and Kawai, T. (2018). Intravesicular Acidification Regulates Lipopolysaccharide Inflammation and Tolerance through TLR4 Trafficking, *J. Immunol.*
- Murray, P. J. and Young, R. A. (1999). Increased Antimycobacterial Immunity in Interleukin-10-Deficient Mice, *Infect. Immun.* **67**(6): 3087–3095.
- Naik, S. H., Proietto, A. I., Wilson, N. S., Dakic, A., Schnorrer, P., Fuchsberger, M., Lahoud, M. H., O’Keeffe, M., Shao, Q.-x., Chen, W.-f., Villadangos, J. A., Shortman, K., and Wu, L. (2005). Cutting edge: generation of splenic CD8+ and CD8- dendritic cell equivalents in Fms-like tyrosine kinase 3 ligand bone marrow cultures, *J. Immunol.* **174**(11): 6592–6597.
- Nakagawa, T. Y., Brissette, W. H., Lira, P. D., Griffiths, R. J., Petrushova, N., Stock, J., McNeish, J. D., Eastman, S. E., Howard, E. D., Clarke, S. R. M., Rosloniec, E. F., Elliott, E. A., and Rudensky, A. Y. (1999). Impaired Invariant Chain Degradation and Antigen Presentation and Diminished Collagen-Induced Arthritis in Cathepsin S Null Mice, *Immunity.* **10**(2): 207–217.
- Nesargikar, P. N., Spiller, B., and Chavez, R. (2012). The complement system: history, pathways, cascade and inhibitors, *Eur. J. Microbiol. Immunol. (Bp).* **2**(2): 103–111.
- Nimmerjahn, F. and Ravetch, J. V. (2008). Fcγ receptors as regulators of immune responses, *Nat. Rev. Immunol.* **8**(1): 34–47.



- Nizzoli, G., Krietsch, J., Weick, A., Steinfeldler, S., Facciotti, F., Gruarin, P., Bianco, A., Steckel, B., Moro, M., Crosti, M., Romagnani, C., Stölzel, K., Torretta, S., Pignataro, L., Scheibenbogen, C., Neddermann, P., Francesco, R. D., Abrignani, S., and Geginat, J. (2013). Human CD1c+ dendritic cells secrete high levels of IL-12 and potently prime cytotoxic T-cell responses, *Blood*. **122**(6): 932–942.
- Nordeng, T. W., Gregers, T. F., Kongsvik, T. L., Méresse, S., Gorvel, J.-P., Jourdan, F., Motta, A., and Bakke, O. (2002). The cytoplasmic tail of invariant chain regulates endosome fusion and morphology, *Mol. Biol. Cell*. **13**(6): 1846–1856.
- Nyborg, A. C., Kornilova, A. Y., Jansen, K., Ladd, T. B., Wolfe, M. S., and Golde, T. E. (2004). Signal peptide peptidase forms a homodimer that is labeled by an active site-directed gamma-secretase inhibitor, *J. Biol. Chem.* **279**(15): 15153–15160.
- O'Neill, L. A. J., Golenbock, D., and Bowie, A. G. (2013). The history of Toll-like receptors - redefining innate immunity, *Nat. Rev. Immunol.* **13**(6): 453–460.
- Okazaki, T., Maeda, A., Nishimura, H., Kurosaki, T., and Honjo, T. (2001). PD-1 immunoreceptor inhibits B cell receptor-mediated signaling by recruiting src homology 2-domain-containing tyrosine phosphatase 2 to phosphotyrosine, *Proc. Natl. Acad. Sci. U.S.A.* **98**(24): 13866–13871.
- Ouyang, W., Kolls, J. K., and Zheng, Y. (2008). The biological functions of T helper 17 cell effector cytokines in inflammation, *Immunity*. **28**(4): 454–467.
- Ozinsky, A., Underhill, D. M., Fontenot, J. D., Hajjar, A. M., Smith, K. D., Wilson, C. B., Schroeder, L., and Aderem, A. (2000). The repertoire for pattern recognition of pathogens by the innate immune system is defined by cooperation between toll-like receptors, *Proc. Natl. Acad. Sci. U.S.A.* **97**(25): 13766–13771.
- Patin, E. C., Orr, S. J., and Schaible, U. E. (2017). Macrophage Inducible C-Type Lectin As a Multifunctional Player in Immunity, *Front. Immunol.* **8**: 861.
- Pelegrin, P. and Surprenant, A. (2006). Pannexin-1 mediates large pore formation and interleukin-1beta release by the ATP-gated P2X7 receptor, *EMBO J.* **25**(21): 5071–5082.
- Perregaux, D. and Gabel, C. A. (1994). Interleukin-1 beta maturation and release in response to ATP and nigericin. Evidence that potassium depletion mediated by these agents is a necessary and common feature of their activity, *J. Biol. Chem.* **269**(21): 15195–15203.
- Piper, R. C. and Katzmann, D. J. (2007). Biogenesis and function of multivesicular bodies, *Annu. Rev. Cell Dev. Biol.* **23**: 519–547.
- Poltorak, A., He, X., Smirnova, I., Liu, M. Y., Van Huffel, C., Du, X., Birdwell, D., Alejos, E., Silva, M., Galanos, C., Freudenberg, M., Ricciardi-Castagnoli, P., Layton, B., and Beutler, B. (1998). Defective LPS signaling in C3H/HeJ and C57BL/10ScCr mice: mutations in Tlr4 gene, *Science*. **282**(5396): 2085–2088.
- Ponting, C. P., Hutton, M., Nyborg, A., Baker, M., Jansen, K., and Golde, T. E. (2002). Identification of a novel family of presenilin homologues, *Hum. Mol. Genet.* **11**(9): 1037–1044.
- Pulendran, B., Tang, H., and Manicassamy, S. (2010). Programming dendritic cells to induce T(H)2 and tolerogenic responses, *Nat. Immunol.* **11**(8): 647–655.
- Rawson, R. B., Zelenski, N. G., Nijhawan, D., Ye, J., Sakai, J., Hasan, M. T., Chang, T. Y., Brown, M. S., and Goldstein, J. L. (1997). Complementation cloning of S2P, a gene encoding a putative metalloprotease required for intramembrane cleavage of SREBPs, *Mol. Cell*. **1**(1): 47–57.
- Rawson, R. B. (2013). The site-2 protease, *Biochim. Biophys. Acta, Biomembr.* **1828**(12): 2801–2807.
- Redelinghuys, P. and Brown, G. D. (2011). Inhibitory C-type lectin receptors in myeloid cells, *Immunol. Lett.* **136**(1): 1–12.

## REFERENCES

---

- Redford, P. S., Murray, P. J., and O'Garra, A. (2011). The role of IL-10 in immune regulation during M. tuberculosis infection, *Mucosal Immunol.* **4**(3): 261–270.
- Rehli, M., Poltorak, A., Schwarzfischer, L., Krause, S. W., Andreesen, R., and Beutler, B. (2000). PU.1 and Interferon Consensus Sequence-binding Protein Regulate the Myeloid Expression of the Human Toll-like Receptor 4 Gene, *J. Biol. Chem.* **275**(13): 9773–9781.
- Reiling, N., Hölscher, C., Fehrenbach, A., Kröger, S., Kirschning, C. J., Goyert, S., and Ehlers, S. (2002). Cutting edge: Toll-like receptor (TLR)2- and TLR4-mediated pathogen recognition in resistance to airborne infection with Mycobacterium tuberculosis, *J. Immunol.* **169**(7): 3480–3484.
- Reis e Sousa, C. (2006). Dendritic cells in a mature age, *Nat. Rev. Immunol.* **6**(6): 476–483.
- Robinson, M. J., Osorio, F., Rosas, M., Freitas, R. P., Schweighoffer, E., Groß, O., Verbeek, J. S., Ruland, J., Tybulewicz, V., Brown, G. D., Moita, L. F., Taylor, P. R., and Reis e Sousa, C. (2009). Dectin-2 is a Syk-coupled pattern recognition receptor crucial for Th17 responses to fungal infection, *J. Exp. Med.* **206**(9): 2037–2051.
- Roger, T., David, J., Glauser, M. P., and Calandra, T. (2001). MIF regulates innate immune responses through modulation of Toll-like receptor 4, *Nature.* **414**(6866): 920–924.
- Roger, T., Miconnet, I., Schiesser, A.-L., Kai, H., Miyake, K., and Calandra, T. (2005). Critical role for Ets, AP-1 and GATA-like transcription factors in regulating mouse Toll-like receptor 4 (Tlr4) gene expression, *Biochem. J.* **387**(Pt 2): 355–365.
- Rogers, N. C., Slack, E. C., Edwards, A. D., Nolte, M. A., Schulz, O., Schweighoffer, E., Williams, D. L., Gordon, S., Tybulewicz, V. L., Brown, G. D., and Reis e Sousa, C. (2005). Syk-dependent cytokine induction by Dectin-1 reveals a novel pattern recognition pathway for C type lectins, *Immunity.* **22**(4): 507–517.
- Rogers, P. B., Driessnack, M. G., and Schwartz, E. H. (2017). Analysis of the developmental stages, kinetics, and phenotypes exhibited by myeloid cells driven by GM-CSF in vitro, *PLOS ONE.* **12**(7): e0181985.
- Rosas, M., Osorio, F., Robinson, M. J., Davies, L. C., Dierkes, N., Jones, S. A., Reis e Sousa, C., and Taylor, P. R. (2011). Hoxb8 conditionally immortalised macrophage lines model inflammatory monocytic cells with important similarity to dendritic cells, *Eur. J. Immunol.* **41**(2): 356–365.
- Rothfuchs, A. G., Bafica, A., Feng, C. G., Egen, J. G., Williams, D. L., Brown, G. D., and Sher, A. (2007). Dectin-1 interaction with Mycobacterium tuberculosis leads to enhanced IL-12p40 production by splenic dendritic cells, *J. Immunol.* **179**(6): 3463–3471.
- Saito, Y., Iwamura, H., Kaneko, T., Ohnishi, H., Murata, Y., Okazawa, H., Kanazawa, Y., Sato-Hashimoto, M., Kobayashi, H., Oldenborg, P.-A., Naito, M., Kaneko, Y., Nojima, Y., and Matozaki, T. (2010). Regulation by SIRPalpha of dendritic cell homeostasis in lymphoid tissues, *Blood.* **116**(18): 3517–3525.
- Sakai, J., Duncan, E. A., Rawson, R. B., Hua, X., Brown, M. S., and Goldstein, J. L. (1996). Sterol-regulated release of SREBP-2 from cell membranes requires two sequential cleavages, one within a transmembrane segment, *Cell.* **85**(7): 1037–1046.
- Sapozhnikov, A., Pewzner-Jung, Y., Kalchenko, V., Krauthgamer, R., Shachar, I., and Jung, S. (2008). Perivascular clusters of dendritic cells provide critical survival signals to B cells in bone marrow niches, *Nat. Immunol.* **9**(4): 388–395.
- Schägger, H. and Jagow, G. von (1987). Tricine-sodium dodecyl sulfate-polyacrylamide gel electrophoresis for the separation of proteins in the range from 1 to 100 kDa, *Anal. Biochem.* **166**(2): 368–379.
- Schägger, H. (2006). Tricine-SDS-PAGE, *Nat. Protoc.* **1**(1): 16–22.

- Scheicher, C., Mehlig, M., Zecher, R., and Reske, K. (1992). Dendritic cells from mouse bone marrow: in vitro differentiation using low doses of recombinant granulocyte-macrophage colony-stimulating factor, *J. Immunol. Methods*. **154**(2): 253–264.
- Schlesinger, L. S. (1993). Macrophage phagocytosis of virulent but not attenuated strains of *Mycobacterium tuberculosis* is mediated by mannose receptors in addition to complement receptors, *J. Immunol.* **150**(7): 2920–2930.
- Schlesinger, L. S., Hull, S. R., and Kaufman, T. M. (1994). Binding of the terminal mannosyl units of lipoarabinomannan from a virulent strain of *Mycobacterium tuberculosis* to human macrophages, *J. Immunol.* **152**(8): 4070–4079.
- Schmidt, C. S. and Mescher, M. F. (2002). Peptide antigen priming of naive, but not memory, CD8 T cells requires a third signal that can be provided by IL-12, *J. Immunol.* **168**(11): 5521–5529.
- Schmidt, O. and Teis, D. (2012). The ESCRT machinery, *Curr. Biol.* **22**(4): R116–R120.
- Schneppenheim, J., Dressel, R., Hüttl, S., Lüllmann-Rauch, R., Engelke, M., Dittmann, K., Wienands, J., Eskelinen, E.-L., Hermans-Borgmeyer, I., Fluhrer, R., Saftig, P., and Schröder, B. (2013). The intramembrane protease SPPL2a promotes B cell development and controls endosomal traffic by cleavage of the invariant chain, *J. Exp. Med.* **210**(1): 41–58.
- Schneppenheim, J., Hüttl, S., Kruchen, A., Fluhrer, R., Müller, I., Saftig, P., Schneppenheim, R., Martin, C. L., and Schröder, B. (2014a). Signal-peptide-peptidase-like 2a is required for CD74 intramembrane proteolysis in human B cells, *Biochem. Biophys. Res. Commun.* **451**(1): 48–53.
- Schneppenheim, J., Hüttl, S., Mentrup, T., Lüllmann-Rauch, R., Rothaug, M., Engelke, M., Dittmann, K., Dressel, R., Araki, M., Araki, K., Wienands, J., Fluhrer, R., Saftig, P., and Schröder, B. (2014b). The intramembrane proteases signal Peptide peptidase-like 2a and 2b have distinct functions in vivo, *Mol. Cell. Biol.* **34**(8): 1398–1411.
- Schneppenheim, J., Looock, A.-C., Hüttl, S., Schweizer, M., Lüllmann-Rauch, R., Oberg, H.-H., Arnold, P., Lehmann, C. H. K., Dudziak, D., Kabelitz, D., Lucius, R., Lennon-Duménil, A.-M., Saftig, P., and Schröder, B. (2017). The Influence of MHC Class II on B Cell Defects Induced by Invariant Chain/CD74 N-Terminal Fragments, *J. Immunol.* **199**(1): 172–185.
- Schröder, B. (2016). The multifaceted roles of the invariant chain CD74—More than just a chaperone, *Biochim. Biophys. Acta.* **1863**(6 Pt A): 1269–1281.
- Schröder, B., Wrocklage, C., Pan, C., Jäger, R., Kösters, B., Schäfer, H., Elsässer, H.-P., Mann, M., and Hasilik, A. (2007). Integral and associated lysosomal membrane proteins, *Traffic.* **8**(12): 1676–1686.
- Schulte, M., Reiss, K., Lettau, M., Marezky, T., Ludwig, A., Hartmann, D., Strooper, B. de, Janssen, O., and Saftig, P. (2007). ADAM10 regulates FasL cell surface expression and modulates FasL-induced cytotoxicity and activation-induced cell death, *Cell Death Differ.* **14**(5): 1040–1049.
- Schwartz, V., Lue, H., Kraemer, S., Korbiel, J., Krohn, R., Ohl, K., Bucala, R., Weber, C., and Bernhagen, J. (2009). A functional heteromeric MIF receptor formed by CD74 and CXCR4, *FEBS Letters.* **583**(17): 2749–2757.
- Segura, E. and Amigorena, S. (2013). Inflammatory dendritic cells in mice and humans, *Trends Immunol.* **34**(9): 440–445.
- Shachar, I. and Flavell, R. A. (1996). Requirement for Invariant Chain in B Cell Maturation and Function, *Science.* **274**(5284): 106–108.
- Shi, G. P., Villadangos, J. A., Dranoff, G., Small, C., Gu, L., Haley, K. J., Riese, R., Ploegh, H. L., and Chapman, H. A. (1999). Cathepsin S required for normal MHC class II peptide loading and germinal center development, *Immunity.* **10**(2): 197–206.

## REFERENCES

---

- Shi, X., Leng, L., Wang, T., Wang, W., Du, X., Li, J., McDonald, C., Chen, Z., Murphy, J. W., Lolis, E., Noble, P., Knudson, W., and Bucala, R. (2006). CD44 Is the Signaling Component of the Macrophage Migration Inhibitory Factor-CD74 Receptor Complex, *Immunity*. **25**(4): 595–606.
- Shortman, K., Sathe, P., Vremec, D., Naik, S., and O’Keeffe, M. (2013). Plasmacytoid dendritic cell development, *Adv. Immunol.* **120**: 105–126.
- Silva-Filho, J. L., Caruso-Neves, C., and Pinheiro, A. A. S. (2014). IL-4: an important cytokine in determining the fate of T cells, *Biophys. Rev.* **6**(1): 111–118.
- Slack, E. C., Robinson, M. J., Hernanz-Falcón, P., Brown, G. D., Williams, D. L., Schweighoffer, E., Tybulewicz, V. L., and Reis e Sousa, C. (2007). Syk-dependent ERK activation regulates IL-2 and IL-10 production by DC stimulated with zymosan, *Eur. J. Immunol.* **37**(6): 1600–1612.
- Stables, M. J., Shah, S., Camon, E. B., Lovering, R. C., Newson, J., Bystrom, J., Farrow, S., and Gilroy, D. W. (2011). Transcriptomic analyses of murine resolution-phase macrophages, *Blood*. **118**(26): e192–e208.
- Stahl, P. D. and Schlesinger, P. H. (1980). Receptor-mediated pinocytosis of mannose/N-acetylglucosamine-terminated glycoproteins and lysosomal enzymes by macrophages, *Trends Biochem. Sci.* **5**(7): 194–196.
- Steiner, H., Kostka, M., Romig, H., Basset, G., Pesold, B., Hardy, J., Capell, A., Meyn, L., Grim, M. L., Baumeister, R., Fichteler, K., and Haass, C. (2000). Glycine 384 is required for presenilin-1 function and is conserved in bacterial polytopic aspartyl proteases, *Nat. Cell Biol.* **2**(11): 848–851.
- Steinman, R. M. and Cohn, Z. A. (1973). Identification of a novel cell type in peripheral lymphoid organs of mice. I. Morphology, quantitation, tissue distribution, *J. Exp. Med.* **137**(5): 1142–1162.
- Suzuki, S., Honma, K., Matsuyama, T., Suzuki, K., Toriyama, K., Akitoyo, I., Yamamoto, K., Suematsu, T., Nakamura, M., Yui, K., and Kumatori, A. (2004). Critical roles of interferon regulatory factor 4 in CD11b<sup>high</sup>CD8 $\alpha$ - dendritic cell development, *Proc. Natl. Acad. Sci. U.S.A.* **101**(24): 8981–8986.
- Swiecki, M., Gilfillan, S., Vermi, W., Wang, Y., and Colonna, M. (2010). Plasmacytoid Dendritic Cell Ablation Impacts Early Interferon Responses and Antiviral NK and CD8<sup>+</sup> T Cell Accrual, *Immunity*. **33**(6): 955–966.
- Tada, H., Nemoto, E., Shimauchi, H., Watanabe, T., Mikami, T., Matsumoto, T., Ohno, N., Tamura, H., Shibata, K.-i., Akashi, S., Miyake, K., Sugawara, S., and Takada, H. (2002). Saccharomyces cerevisiae- and Candida albicans-derived mannan induced production of tumor necrosis factor alpha by human monocytes in a CD14- and Toll-like receptor 4-dependent manner, *Microbiol. Immunol.* **46**(7): 503–512.
- Tailleux, L., Schwartz, O., Herrmann, J.-L., Pivert, E., Jackson, M., Amara, A., Legres, L., Dreher, D., Nicod, L. P., Gluckman, J. C., Lagrange, P. H., Gicquel, B., and Neyrolles, O. (2003). DC-SIGN Is the Major Mycobacterium tuberculosis Receptor on Human Dendritic Cells, *J. Exp. Med.* **197**(1): 121–127.
- Tamura, T., Yanai, H., Savitsky, D., and Taniguchi, T. (2008). The IRF family transcription factors in immunity and oncogenesis, *Annu. Rev. Immunol.* **26**: 535–584.
- Tapping, R. I. and Tobias, P. S. (2003). Mycobacterial lipoarabinomannan mediates physical interactions between TLR1 and TLR2 to induce signaling, *J. Endotoxin Res.* **9**(4): 264–268.
- Tascon, R. E., Stavropoulos, E., Lukacs, K. V., and Colston, M. J. (1998). Protection against Mycobacterium tuberculosis infection by CD8<sup>+</sup> T cells requires the production of gamma interferon, *Infect. Immun.* **66**(2): 830–834.

- Taylor, P. R., Tsoni, S. V., Willment, J. A., Dennehy, K. M., Rosas, M., Findon, H., Haynes, K., Steele, C., Botto, M., Gordon, S., and Brown, G. D. (2007). Dectin-1 is required for beta-glucan recognition and control of fungal infection, *Nat. Immunol.* **8**(1): 31–38.
- Terrazas, C. A., Huitron, E., Vazquez, A., Juarez, I., Camacho, G. M., Calleja, E. A., and Rodriguez-Sosa, M. (2011). MIF synergizes with *Trypanosoma cruzi* antigens to promote efficient dendritic cell maturation and IL-12 production via p38 MAPK, *Int. J. Biol. Sci.* **7**(9): 1298–1310.
- Tominaga, K., Yoshimoto, T., Torigoe, K., Kurimoto, M., Matsui, K., Hada, T., Okamura, H., and Nakanishi, K. (2000). IL-12 synergizes with IL-18 or IL-1beta for IFN-gamma production from human T cells, *Int. Immunol.* **12**(2): 151–160.
- Tsujimura, H., Tamura, T., Gongora, C., Aliberti, J., Reis e Sousa, C., Sher, A., and Ozato, K. (2003a). ICSP/IRF-8 retrovirus transduction rescues dendritic cell development in vitro, *Blood.* **101**(3): 961–969.
- Tsujimura, H., Tamura, T., and Ozato, K. (2003b). Cutting edge: IFN consensus sequence binding protein/IFN regulatory factor 8 drives the development of type I IFN-producing plasmacytoid dendritic cells, *J. Immunol.* **170**(3): 1131–1135.
- Tumanov, A. V., Kuprash, D. V., Lagarkova, M. A., Grivennikov, S. I., Abe, K., Shakhov, A. N., Drutskaya, L. N., Stewart, C. L., Chervovsky, A. V., and Nedospasov, S. A. (2002). Distinct Role of Surface Lymphotoxin Expressed by B Cells in the Organization of Secondary Lymphoid Tissues, *Immunity.* **17**(3): 239–250.
- Tussiwand, R. and Gautier, E. L. (2015). Transcriptional Regulation of Mononuclear Phagocyte Development, *Front. Immunol.* **6**:
- Underhill, D. M., Ozinsky, A., Hajjar, A. M., Stevens, A., Wilson, C. B., Bassetti, M., and Aderem, A. (1999). The Toll-like receptor 2 is recruited to macrophage phagosomes and discriminates between pathogens, *Nature.* **401**(6755): 811–815.
- Urban, S. (2016). SnapShot: Cartography of Intramembrane Proteolysis, *Cell.* **167**(7): 1898–1898.e1.
- Vascotto, F., Lankar, D., Faure-André, G., Vargas, P., Diaz, J., Le Roux, D., Yuseff, M.-I., Sibarita, J.-B., Boes, M., Raposo, G., Mougneau, E., Glaichenhaus, N., Bonnerot, C., Manoury, B., and Lennon-Duménil, A.-M. (2007). The actin-based motor protein myosin II regulates MHC class II trafficking and BCR-driven antigen presentation, *J. Cell Biol.* **176**(7): 1007–1019.
- Velcicky, J., Bodendorf, U., Rigollier, P., Epple, R., Beisner, D. R., Guerini, D., Smith, P., Liu, B., Feifel, R., Wipfli, P., Aichholz, R., Couttet, P., Dix, I., Widmer, T., Wen, B., and Brandl, T. (2018). Discovery of the First Potent, Selective, and Orally Bioavailable Signal Peptide Peptidase-Like 2a (SPPL2a) Inhibitor Displaying Pronounced Immunomodulatory Effects In Vivo, *J. Med. Chem.* **61**(3): 865–880.
- Veldhoen, M., Hocking, R. J., Atkins, C. J., Locksley, R. M., and Stockinger, B. (2006). TGFbeta in the context of an inflammatory cytokine milieu supports de novo differentiation of IL-17-producing T cells, *Immunity.* **24**(2): 179–189.
- Vignali, D. A. A. and Kuchroo, V. K. (2012). IL-12 family cytokines: immunological playmakers, *Nat. Immunol.* **13**(8): 722–728.
- Voss, M., Fukumori, A., Kuhn, P.-H., Künzel, U., Klier, B., Grammer, G., Haug-Kröper, M., Kremmer, E., Lichtenthaler, S. F., Steiner, H., Schröder, B., Haass, C., and Fluhner, R. (2012). Foamy Virus Envelope Protein Is a Substrate for Signal Peptide Peptidase-like 3 (SPPL3), *J. Biol. Chem.* **287**(52): 43401–43409.
- Voss, M., Künzel, U., Higel, F., Kuhn, P.-H., Colombo, A., Fukumori, A., Haug-Kröper, M., Klier, B., Grammer, G., Seidl, A., Schröder, B., Obst, R., Steiner, H., Lichtenthaler, S. F., Haass, C., and Fluhner, R. (2014). Shedding of glycan-modifying enzymes by signal peptide peptidase-like 3 (SPPL3) regulates cellular N-glycosylation, *EMBO J.* **33**(24): 2890–2905.

## REFERENCES

---

- Voss, M., Schröder, B., and Fluhrer, R. (2013). Mechanism, specificity, and physiology of signal peptide peptidase (SPP) and SPP-like proteases, *Biochim. Biophys. Acta.* **1828**(12): 2828–2839.
- Waal Malefyt, R. de, Abrams, J., Bennett, B., Figdor, C. G., and Vries, J. E. de (1991). Interleukin 10(IL-10) inhibits cytokine synthesis by human monocytes: an autoregulatory role of IL-10 produced by monocytes, *J. Exp. Med.* **174**(5): 1209–1220.
- Walker, J. A. and McKenzie, A. N. J. (2018). TH2 cell development and function, *Nat. Rev. Immunol.* **18**(2): 121–133.
- Wang, Y.-G., Kim, K. D., Wang, J., Yu, P., and Fu, Y.-X. (2005). Stimulating lymphotoxin beta receptor on the dendritic cells is critical for their homeostasis and expansion, *J. Immunol.* **175**(10): 6997–7002.
- Washio, K., Kotani, T., Saito, Y., Respatika, D., Murata, Y., Kaneko, Y., Okazawa, H., Ohnishi, H., Fukunaga, A., Nishigori, C., and Matozaki, T. (2015). Dendritic cell SIRP $\alpha$  regulates homeostasis of dendritic cells in lymphoid organs, *Genes Cells.* **20**(6): 451–463.
- Weihofen, A., Binns, K., Lemberg, M. K., Ashman, K., and Martoglio, B. (2002). Identification of signal peptide peptidase, a presenilin-type aspartic protease, *Science.* **296**(5576): 2215–2218.
- Weihofen, A. and Martoglio, B. (2003). Intramembrane-cleaving proteases: controlled liberation of proteins and bioactive peptides, *Trends Cell Biol.* **13**(2): 71–78.
- Weinberg, K. and Parkman, R. (1990). Severe Combined Immunodeficiency Due to a Specific Defect in the Production of Interleukin-2, *N. Engl. J. Med.* **322**(24): 1718–1723.
- West, A. P., Koblansky, A. A., and Ghosh, S. (2006). Recognition and signaling by toll-like receptors, *Annu. Rev. Cell Dev. Biol.* **22**: 409–437.
- Wevers, B. A., Kaptein, T. M., Zijlstra-Willems, E. M., Theelen, B., Boekhout, T., Geijtenbeek, T. B. H., and Gringhuis, S. I. (2014). Fungal engagement of the C-type lectin mincle suppresses dectin-1-induced antifungal immunity, *Cell Host Microbe.* **15**(4): 494–505.
- Wolfe, M. S., De Los Angeles, J., Miller, D. D., Xia, W., and Selkoe, D. J. (1999). Are presenilins intramembrane-cleaving proteases? Implications for the molecular mechanism of Alzheimer's disease, *Biochemistry.* **38**(35): 11223–11230.
- Workman, C. J., Szymczak-Workman, A. L., Collison, L. W., Pillai, M. R., and Vignali, D. A. (2009). The Development and Function of Regulatory T Cells, *Cell. Mol. Life Sci.* **66**(16): 2603–2622.
- Wu, Q., Wang, Y., Wang, J., Hedgeman, E. O., Browning, J. L., and Fu, Y.-X. (1999). The Requirement of Membrane Lymphotoxin for the Presence of Dendritic Cells in Lymphoid Tissues, *J. Exp. Med.* **190**(5): 629–638.
- Xu, Y., Zhan, Y., Lew, A. M., Naik, S. H., and Kershaw, M. H. (2007). Differential Development of Murine Dendritic Cells by GM-CSF versus Flt3 Ligand Has Implications for Inflammation and Trafficking, *J. Immunol.* **179**(11): 7577–7584.
- Yadav, M. and Schorey, J. S. (2006). The beta-glucan receptor dectin-1 functions together with TLR2 to mediate macrophage activation by mycobacteria, *Blood.* **108**(9): 3168–3175.
- Yamada, A., Arakaki, R., Saito, M., Kudo, Y., and Ishimaru, N. (2017). Dual Role of Fas/FasL-Mediated Signal in Peripheral Immune Tolerance, *Front. Immunol.* **8**:
- Yamada, H., Mizumo, S., Horai, R., Iwakura, Y., and Sugawara, I. (2000). Protective role of interleukin-1 in mycobacterial infection in IL-1 alpha/beta double-knockout mice, *Lab. Invest.* **80**(5): 759–767.
- Yamasaki, A., Eimer, S., Okochi, M., Smialowska, A., Kaether, C., Baumeister, R., Haass, C., and Steiner, H. (2006). The GxGD motif of presenilin contributes to catalytic function and substrate identification of gamma-secretase, *J. Neurosci.* **26**(14): 3821–3828.

- Ye, C., Brand, D., and Zheng, S. G. (2018). Targeting IL-2: an unexpected effect in treating immunological diseases, *Signal Trans. Target. Therapy.* **3**(1): 2.
- Yi, T. and Cyster, J. G. (2013). EB12-mediated bridging channel positioning supports splenic dendritic cell homeostasis and particulate antigen capture, *Elife.* **2**: e00757.
- Yonekawa, A., Saijo, S., Hoshino, Y., Miyake, Y., Ishikawa, E., Suzukawa, M., Inoue, H., Tanaka, M., Yoneyama, M., Oh-Hora, M., Akashi, K., and Yamasaki, S. (2014). Dectin-2 is a direct receptor for mannose-capped lipoarabinomannan of mycobacteria, *Immunity.* **41**(3): 402–413.
- Zahn, C., Kaup, M., Fluhrer, R., and Fuchs (2013). The transferrin receptor-1 membrane stub undergoes intramembrane proteolysis by signal peptide peptidase-like 2b, *The FEBS Journal.* **280**(7): 1653–1663.
- Zanoni, I., Ostuni, R., Marek, L. R., Barresi, S., Barbalat, R., Barton, G. M., Granucci, F., and Kagan, J. C. (2011). CD14 controls the LPS-induced endocytosis of Toll-like Receptor 4, *Cell.* **147**(4): 868–880.
- Zhang, G., Zhou, B., Li, S., Yue, J., Yang, H., Wen, Y., Zhan, S., Wang, W., Liao, M., Zhang, M., Zeng, G., Feng, C. G., Sasseti, C. M., and Chen, X. (2014). Allele-Specific Induction of IL-1 $\beta$  Expression by C/EBP $\beta$  and PU.1 Contributes to Increased Tuberculosis Susceptibility, *PLoS Pathog.* **10**(10):
- Zhang, X., Goncalves, R., and Mosser, D. M. (2008). The Isolation and Characterization of Murine Macrophages, *Curr. Protoc. Immunol.* Unit–14.1.
- Zheng, Y., Saftig, P., Hartmann, D., and Blobel, C. (2004). Evaluation of the Contribution of Different ADAMs to Tumor Necrosis Factor alpha (TNFalpha) Shedding and of the Function of the TNFalpha Ectodomain in Ensuring Selective Stimulated Shedding by the TNFalpha Convertase (TACE/ADAM17), *J. Biol. Chem.* **279**(41): 42898–42906.
- Zielinski, C. E., Mele, F., Aschenbrenner, D., Jarrossay, D., Ronchi, F., Gattorno, M., Monticelli, S., Lanzavecchia, A., and Sallusto, F. (2012). Pathogen-induced human TH17 cells produce IFN-gamma or IL-10 and are regulated by IL-1beta, *Nature.* **484**(7395): 514–518.





## Supplement

### List of Figures

1	Scheme of regulated intramembrane proteolysis. . . . .	1
2	Subcellular localisation of I-CLiPs. . . . .	3
3	Comparison of aspartyl proteases. . . . .	4
4	CD74 in antigen presentation and MIF signalling. . . . .	8
5	Influence of the CD74 NTF accumulation on B cell development. . . . .	9
6	Development of DCs. . . . .	11
7	Signalling by receptors of the CTLR family. . . . .	14
8	DC cytokines in activation of innate and adaptive immune cells. . . . .	16
9	Scheme of BMDC generation. . . . .	26
10	Composition of the Duo Set ELISA. . . . .	37
11	Principle of Roches Universal ProbeLibrary System qRT-PCR. . . . .	41
12	Reduced cDC2 population in spleens of <i>SPPL2a</i> <sup>-/-</sup> mice. . . . .	43
13	The CD74 NTF accumulates in <i>SPPL2a</i> <sup>-/-</sup> BMDCs. . . . .	44
14	Flow cytometric analysis of BMDC differentiation. . . . .	45
15	Surface expressions of CD11c and CD11b are slightly altered in <i>SPPL2a</i> <sup>-/-</sup> BMDCs. . . . .	46
16	Comparable expression of <i>CD11c</i> and <i>CD11b</i> between <i>wt</i> and <i>SPPL2a</i> <sup>-/-</sup> BMDCs. . . . .	46
17	No general functional deficiency in <i>SPPL2a</i> <sup>-/-</sup> DCs. . . . .	47
18	Reduced IL-10 secretion in depleted Zymosan treated <i>SPPL2a</i> <sup>-/-</sup> DCs. . . . .	48
19	Decreased IL-10 and IL-2 expression in <i>SPPL2a</i> <sup>-/-</sup> BMDCs upon stimulation with depleted Zymosan. . . . .	49
20	Toll like receptor 4 activation leads to increased IL-1 $\beta$ release by <i>SPPL2a</i> <sup>-/-</sup> BMDCs. . . . .	50
21	Increased IL-1 $\beta$ and TNF $\alpha$ expression in <i>SPPL2a</i> <sup>-/-</sup> BMDCs upon LPS administration. . . . .	51
22	Reduced IL-2 and IL-10, but increased IL-1 $\beta$ and TNF $\alpha$ release in <i>SPPL2a</i> <sup>-/-</sup> BMDCs upon HKMT treatment. . . . .	52
23	Altered cytokine expression in HKMT treated <i>SPPL2a</i> <sup>-/-</sup> BMDCs. . . . .	53
24	The absence of SPPL2a does not lead to increased inflammasome activity. . . . .	54
25	Comparable cell death in <i>wt</i> and <i>SPPL2a</i> <sup>-/-</sup> BMDCs upon HKMT treatment. . . . .	55
26	IL-10 secretion does not influence IL-1 $\beta$ production. . . . .	56
27	Release of IL-12 family members from BMDCs after stimulation with HKMT. . . . .	57

LIST OF FIGURES

---

28	IL-12 family members are released without significant difference between <i>wt</i> and <i>SPPL2a</i> <sup>-/-</sup> BMDCs upon dZym or LPS treatment. . . . .	58
29	Increased IL-1 $\beta$ release by <i>SPPL2a</i> <sup>-/-</sup> BMDCs in BCG co-culture. . . . .	58
30	Comparable expression of <i>IL-10</i> , <i>IL-1<math>\beta</math></i> and <i>TNF<math>\alpha</math></i> in <i>wt</i> and <i>SPPL2a</i> <sup>-/-</sup> BMDCs after six hours of BCG co-culture. . . . .	59
31	SPPL2a deficiency impairs secretion of IL-12 family cytokines by BMDCs upon BCG co-culture. . . . .	60
32	Induction of IL-12 cytokine expression is reduced in <i>SPPL2a</i> <sup>-/-</sup> BMDCs in BCG co-culture. . . . .	61
33	Normal cytokine response of <i>SPPL2a</i> <sup>-/-</sup> macrophages towards heat-killed mycobacteria. . . . .	61
34	Macrophages accumulate less CD74 NTF than DCs. . . . .	62
35	<i>CatS</i> <sup>-/-</sup> BMDCs show similar but milder cytokine phenotype than <i>SPPL2a</i> <sup>-/-</sup> BMDCs. . . . .	63
36	<i>CatS</i> <sup>-/-</sup> BMDCs accumulate less CD74 NTF than <i>SPPL2a</i> <sup>-/-</sup> BMDCs. . . . .	64
37	Absence of CD74 in <i>SPPL2a</i> <sup>-/-</sup> BMDCs rescues cytokine phenotype. . . . .	66
38	Cytokine expression in <i>SPPL2a</i> <sup>-/-</sup> <i>CD74</i> <sup>-/-</sup> BMDCs is comparable to <i>wt</i> . . . . .	67
39	Reduced Syk activation in <i>SPPL2a</i> <sup>-/-</sup> BMDCs upon Dectin-1 stimulation. . . . .	69
40	Reduced Dectin-1 surface expression in <i>SPPL2a</i> <sup>-/-</sup> BMDCs measured by flow cytometry. . . . .	70
41	Biotinylation of cell surface proteins reveals reduced Dectin-1 on <i>SPPL2a</i> <sup>-/-</sup> BMDCs. . . . .	71
42	Dectin-1 NTF accumulates in <i>SPPL2a</i> <sup>-/-</sup> BMDCs. . . . .	72
43	<i>Dectin-1</i> expression is comparable between <i>wt</i> , <i>SPPL2a</i> <sup>-/-</sup> , <i>CD74</i> <sup>-/-</sup> and <i>SPPL2a</i> <sup>-/-</sup> <i>CD74</i> <sup>-/-</sup> BMDCs. . . . .	72
44	Dectin-1 re-localises to CD74-positive compartments in SPPL2a-deficient BMDCs. . . . .	73
45	TLR4 surface expression is increased upon ablation of SPPL2a. . . . .	74
46	<i>TLR4</i> expression is slightly increased in <i>SPPL2a</i> <sup>-/-</sup> BMDCs. . . . .	74
47	Schematic summary of <i>SPPL2a</i> <sup>-/-</sup> BMDC phenotype. . . . .	76
48	Possible mechanisms of CD74 NTF influencing <i>SPPL2a</i> <sup>-/-</sup> DC functions. . . . .	79
49	Possible mechanisms for altered Dectin-1 and TLR4 surface levels on <i>SPPL2a</i> <sup>-/-</sup> BMDCs. . . . .	82
50	Possible mechanisms for dZym-induced signalling and cytokine response alterations in <i>SPPL2a</i> <sup>-/-</sup> BMDCs. . . . .	88

**List of Tables**

2	Overview of intramembrane cleaving protease families. . . . .	2
3	SPPL family member substrates. . . . .	6
4	Markers defining DC populations. . . . .	11
5	List of primary antibodies. . . . .	22
6	List of secondary antibodies. . . . .	23
7	Pattern recognition receptor ligands . . . . .	24
8	Buffers for DC population analysis in mice. . . . .	25
9	Cell culture media. . . . .	26
10	Overview of BMDC seeding for experiments. . . . .	27
11	BCG medium. . . . .	28
12	Indirect immunofluorescence buffers. . . . .	29
13	Buffer for flow cytometric analysis of BMDCs. . . . .	30
14	Buffers for protein extract preparation. . . . .	30
15	Buffers for biotinylation of surface proteins. . . . .	32
16	Buffers for Tris–Glycine–SDS gel electrophoresis. . . . .	33
17	Pipetting scheme for Tris–Glycine–SDS gels. . . . .	34
18	Buffers for Tris–Tricine–SDS gel electrophoresis. . . . .	34
19	Pipetting scheme for Tris–Tricine–SDS gels. . . . .	35
20	Buffers for Western Blotting. . . . .	35
21	Buffers for immunodetection of proteins. . . . .	36
22	Primers for mouse genotyping. . . . .	39
23	Genotyping pipetting scheme. . . . .	39
24	PCR protocols for genotyping. . . . .	39
25	Buffer for agarose gel electrophoresis. . . . .	40
26	Primer pairs for gene expression analysis. . . . .	41
27	Cytokine secretion of <i>SPPL2a</i> <sup>-/-</sup> compared to <i>wt</i> BMDCs. . . . .	68



## List of publications

### Publications containing data not shown in this dissertation:

Dudeck J., Medyukhina A., Fröbel J., Svensson CM., Kotrba J., Gerlach M., **Gradtke AC.**, Schröder B., Speier S., Figge MT., Dudeck A. (2017) Mast cells acquire MHCII from dendritic cells during skin inflammation *J. Exp. Med.* 214(12):3791-3811

Own contribution: Experimental support with MHCII knockout mice

Mentrup T., **Loock AC.**, Fluhrer R., Schröder B. (2017) Signal peptide peptidase and SPP-like proteases - Possible therapeutic targets? *Biochim. Biophys. Acta.* 1864(11 Pt B):2169-2182.

Own contribution: Sections 5.1 and 5.2

Schneppenheim J., **Loock AC.**, Hüttl S., Schweizer M., Lüllmann-Rauch R., Oberg HH., Arnold P., Lehmann CHK., Dudziak D., Kabelitz D., Lucius R., Lennon-Duménil AM., Saftig P., Schröder B. (2017) The Influence of MHC Class II on B Cell Defects Induced by Invariant Chain/CD74 N-Terminal Fragments. *J. Immunol.* 199(1):172-185.

Own contribution: Figures 2 F—H, J; 3 A, B, E—H; 4 A, B, D, G, H, 6, flow cytometric sorting of B cells for electron microscopy

### Publication containing data not shown in this dissertation currently in revision:

Mentrup T., Theodorou K., Cabrera-Cabrera F., Happ K., **Gradtke AC.**, Rabe B., Fukumori A., Steiner H., Häsler R., Fluhrer R., Donners M. and Schröder B. (2018) SPPL2-mediated intramembrane proteolysis controls pro-atherogenic signalling of the receptor LOX-1 *J. Exp. Med.* *in revision*

Own contribution: Evaluation of TNF $\alpha$  antibody on DC lysates in Western Blot analysis; flow cytometric analysis of surface LOX-1 expression after ligand application

### Publication in preparation:

A Manuscript containing data presented in this thesis is currently in preparation.

**Further publication:** Schmidt F., Kunze M., **Loock AC.**, Dobbelstein M. (2015) Screening analysis of ubiquitin ligases reveals G2E3 as a potential target for chemosensitizing cancer cells. *Oncotarget* 20;6(2):617-32.



## Statutory Declaration

The data presented in this dissertation were generated at the Institute for Biochemistry of the Christian-Albrechts-Universität, Kiel under guidance of Prof. Dr. Paul Saftig and Prof. Dr. Bernd Schröder.

I hereby assure that:

- I have composed the content and design of the present dissertation, apart from the supervisor's guidance, independently.
- This thesis has not been wholly or partially submitted elsewhere as part of a doctoral degree or for scientific publication.
- I have produced my works according to the rules of Good Scientific Practice of the German Research Foundation.
- I have used no other appliances than indicated. Parts being gathered from other works according to wording or meaning I have indicated in every single case by declaration of source.

Date:

---

(Ann-Christine Gradtke)





## Acknowledgements

I would like to thank Prof. Dr. Bernd Schröder and Prof. Dr. Paul Saftig for the opportunity to work on this multifaceted project. I am grateful for all the time they spent with me in fruitful discussions of my data. In particular I would like to thank Prof. Dr. Bernd Schröder for his guidance throughout the project.

Furthermore, I want to thank Prof. Dr. Thomas Roeder for his willingness to take over the co-reference of this thesis.

Special thanks go to my cooperation partners, who kindly supported me in my experiments. I would like to thank Prof. Dr. Ulrich Schaible from the research center in Borstel, for providing the *Mycobacterium bovis* BCGs, and his doctoral student Dr. Maike Burmeister, for all her time with me in performing the initial co-culture experiments. I want to acknowledge the input of their expertise about mycobacterial infections. I thank Prof. Dr. Diana Dudziak from the University Hospital of Erlangen, for the supply of CatS knockout mice. In addition, my thanks go to her postdoctoral fellow Dr. Christian Lehmann for the DC analysis of our mice.

Many thanks go to our group members and members from AG Saftig! Thanks for all the ideas, help and of course fun! I thank Torben Mentrup for introducing me into special laboratory techniques at my start at the biochemical institute. All scientific and non-scientific discussions with him but also Florencia Cabrera Cabrera enriched the time and the work spent for this thesis. I did not only learn all anthems of the soccer teams Torben likes but also some Spanish! Muchas gracias por las lecciones de español también a David Massa López y Adriana González! I also appreciate the opportunity to guide Daniela Tenfelde throughout her laboratory training to become a technical assistant. I am very glad about all her help and hope that she will recover at some point from beating all the ELISA plates. I would like to thank Sebastian Held for his great technical support and willingness to come in the early morning to start experiments with me. Even though sometimes I had to buy him over with coffee. Furthermore, I thank my Bachelor student Melina Winkler for her accurate work not only during her thesis but also afterwards during her HiWi time. In addition to Melina, Lea Kählau and Sabrina Clemens were also great help for me, many thanks for that! I am especially grateful for getting to know Sandra Kissing and Sebastian Wetzel from AG Saftig, to whom I got friends with. Apart from scientific knowledge, we could share our interest in board games.

Finally, I thank my family and friends, who always supported me. I am happy to have all of you! Especially, my beloved mom Angelika Loock, my wonderful husband Gerrit Gradtke and my good friend Christin Döring gave me motivation whenever needed and endured all my scientific crisis.



## Scientific career

### Personal data

Name	Ann-Christine Gradtke
Name at birth	Looock
Date of birth	28th January 1990
Place of birth	Bremen, Germany
Nationality	German

### PhD studies

07/14 – present	PhD studies at the Institute for Biochemistry at the Christian–Albrechts–University Kiel in the group of PD Dr. Bernd Schröder within the department headed by Prof. Dr. Paul Saftig
-----------------	--

### Academic studies

09/12 – 05/14	Master of Science in Molecular Medicine at the University of Goettingen, Germany Final grade: 1.8 (1.0 max possible)
11/13 – 05/14	Master Thesis: "Investigating possible causes for COPD development in the miR–449 knock-out mouse", Molecular Oncology (Prof. Dr. Dobbelstein / Dr. Lizé), University of Goettingen, Germany
09/12 – 10/12	Research assistant at the department of Molecular Oncology (Prof. Dr. Dobbelstein), University of Goettingen, Germany
10/09 – 09/12	Bachelor of Science in Molecular Medicine at the University of Goettingen, Germany Final grade: 2.0 (1.0 max possible)
05/12 – 08/12	Bachelor Thesis: "Associations of the oncogenic ubiquitin ligase Mdm2", Molecular Oncology (Prof. Dr. Dobbelstein), University of Goettingen, Germany

### Education

09/06 – 06/09	Abitur (university entrance qualification) at the grammar school in Osterholz-Scharmbeck, Germany Final grade: 2.1 (1.0 max possible)
---------------	--

### Awards

09/17	Poster prize at the international symposium "Development of tissue- and pathogen-specific cellular innate immune response" in Freiburg, Germany for the poster "The intramembrane protease SPPL2a and its substrate CD74 influence differentiation and cytokine response of dendritic cells".
-------	---